THE EFFECTS OF A GREEN ROOIBOS EXTRACT ON THE REPRODUCTIVE FUNCTION OF OBESITY-INDUCED INSULIN RESISTANT OR HYPERTENSIVE MALE WISTAR RATS

by

Claudine Manirafasha

Dissertation presented for the degree of Doctor of Philosophy
in the Faculty of Medicine and Health Sciences at
Stellenbosch University

Supervisor: Prof SS du Plessis

Co-supervisors: Prof B Huisamen & Dr YG Aboua

December 2019

DECLARATION

By submitting this thesis electronically, I declare that the entirety of the work contained therein is my own, original work, that I am the sole author thereof (save to the extent explicitly otherwise stated), that reproduction and publication thereof by Stellenbosch University will not infringe any third party rights and that I have not previously in its entirety or in part submitted it for obtaining any qualification.

Claudine Manirafasha

December 2019

ABSTRACT

Diet-induced obesity (DIO) due to a high caloric diet (HCD) predisposes an individual to the development of diabetes and cardiovascular diseases, with high prevalence in young populations. Existing evidence supports the sentiment that insulin resistance and hypertension (HT) affect male reproduction. A greater understanding of the influence of insulin resistance and/or HT on male reproduction is required in order to prevent or treat male infertility. Due to the limitations of orthodox drugs, there is currently a strong movement towards and support for studies on phytomedicine. Rooibos *(Aspalathus linearis*) has been used in several studies and is known to have natural antioxidant effects and anti-obesogenic, antidiabetic, anti-hypertensive and anti-infertility activities. Currently, the company Afriplex (Pty) Ltd is producing an aspalathin-rich laboratory standardized extract prepared from green rooibos called Afriplex GRT^{TM} (GRT). However, there is very little knowledge regarding the use of GRT in obesity-related insulin resistance and/or HT, and specifically, its effects on male reproductive health.

Aim

This study aimed to explore the effect of GRT on the reproductive function in obesity-induced insulin resistant and hypertensive male Wistar rats.

Methods

A prospective randomized control and experimental animal study design was used. Two different diets were used to induce obesity-related insulin resistance with or without HT in male Wistar rats. Subsequently, the possible protective properties of GRT on the male reproductive system were evaluated. Animals (weighing 120 ±10 g, approximately 7 weeks old) were randomly assigned to seven groups with seven rats each. All rats had unrestricted access to their respective diets and water for 16 weeks. At baseline (week 0–10), we had three groups: 1) lean control (LC) – animals that received standard rat chow; 2) obese (OB) – animals that received a diet to induce obesity associated with insulin resistance; and 3) obese with hypertension (OBHT) – animals were placed on a slightly modified DIO and additionally developed HT.

From weeks 11 to 16, one LC, OB and OBHT group were each treated with GRT (prepared and supplied by Afriplex (Pty) Ltd) at 60 mg/kg/day as a dietary supplement in the form of jelly blocks. An additional group of OBHT animals was treated during the same period for 6 weeks with Captopril, an angiotensin-converting-enzyme (ACE) inhibitor (positive control for HT) at 60 mg/kg per day. Food and water intake were monitored on a daily basis. An oral glucose tolerance test was performed during the 10th week after the onset of the respective diets and during the 16th week, after which the

animals were sacrificed. Blood pressure measurements were taken once per week throughout the experimental period. After the 16-week period, animals were killed and blood, testis and epididymal tissue were harvested for further analysis. Body weight, intra-peritoneal fat, non-fasting glucose levels, IL-1β, IL-6, IL-12, IL-18 and TNFα, oxidative stress (OS) markers (superoxide dismutase and catalase activity, malondialdehyde), testosterone and estradiol, sperm concentration, viability, morphology, total motility, progressive motility and various velocity parameters were measured.

Results and conclusion

Both diets successfully induced insulin resistance with or without hypertension and demonstrated detrimental effects on male reproductive function as evidenced by OS and hormone dysregulation. Treatment with GRT reversed OS and balanced the androgens. This study provided insight into the pharmacological effects of GRT in the treatment of pathophysiological changes that occur in DIO associated with insulin resistance or HT. These findings will hopefully inspire further research into the clinical setting related to the GRT and could possibly lead to the development of new drugs from this compound.

OPSOMMING

Dieet-geïnduseerde vetsug (DGV) as gevolg van ’n hoë kalorie-dieet (HKD) maak individue vatbaar vir die ontwikkeling van diabetes en kardiovaskulêre siektes, met hoë voorkoms in jong populasies. Bestaande bewyse ondersteun die sentiment dat insulienweerstand en hipertensie (HT) manlike voortplanting beïnvloed. ’n Beter begrip van invloed van insulienweerstand en/of HT op manlike voortplanting is nodig om manlike onvrugbaarheid te voorkom of te behandel. As gevolg van die beperkings van ortodokse medisyne is daar tans ’n sterk beweging na en ondersteuning van die studie van fitomedisyne. Rooibos *(Aspalathus linearis*) is in verskillende studies gebruik en is bekend vir sy natuurlike antioksidant-effek en anti-obesogeniese, anti-diabetiese, anti-hipertensiewe en anti-onvrugbaarheidsaktiwiteite. Tans vervaardig die maatskappy Afriplex (Edms.) Bpk. ’n aspalatienryke laboratorium gestandaardiseerde ekstrak, wat uit groen rooibos ekstrak voorberei is, genaamd Afriplex GRT^{TM} (GRT) ekstrak. Daar is egter baie min kennis aangaande die gebruik van GRT-ekstrak in obesiteitverwante insulienweerstand en/of hipertensie en spesifiek wat die effek daarvan op manlike voorplantingsgesondheid is.

Doelstelling

Die doel van hierdie studie is om die effek van GRT-ekstrak op die voortplantingsfunksie van obesiteit-geïnduseerde insulienweerstandige en hipertensiewe manlike Wistar-rotte te ondersoek.

Metodes

Hierdie studie het ’n prospektiewe ewekansige kontrole en eksperimentele ontwerp. Twee verskillende diëte is gebruik om obesiteit-verwante insulienweerstandigheid en/of hipertensie in manlike Wistar-rotte te bewerkstellig. Vervolgens is die moontlike beskermende eienskappe van GRT-ekstrak op die manlike voortplantingstelsel geëvalueer. Diere (120 ± 10g gewig, ~ 7 weke oud) is lukraak toegewys aan sewe groepe en elke groep het sewe rotte bevat. Alle rotte het vir 16 weke onbeperkte toegang tot hul onderskeie diëte en water gehad. By aanvang (week 0–10) was daar drie groepe: 1) maer kontrole (LK) diere wat standaard rotvoer ontvang het; 2) obees (OB) rotte wat ’n dieet ontvang om vetsug te veroorsaak wat verband hou met insulienweerstandigheid; en 3) obees met hipertensie (OBHT) was diere wat op ’n aangepaste dieet geplaas is om sodoende ook HT te veroorsaak.

Van weke 11 tot 16 is een LK, OB- en OBHT-groep elk met 60 mg/kg/dag GRT-ekstrak (vervaardig en verskaf deur Afriplex (Edms.) Bpk.) as ’n dieetaanvulling in die vorm van jellie-GRT-blokke behandel. ’n Verdere groep OBHT-diere is gedurende dieselfde tydperk vir 6 weke daagliks behandel met 50 mg/kg Captopril, ’n ACE-inhibeerder (positiewe kontrole vir HT) (Huisamen *et al.*, 2013).

Voedsel- en waterinname is daagliks gemonitor. ’n Orale glukose-toleransietoets is gedurende die 10de week na die aanvang van die onderskeie diëte en gedurende die 16de week uitgevoer, waarna die diere doodgemaak is. Bloeddrukmetings is een keer per week tydens die eksperimentele periode geneem. Na die 16-week periode is die diere doodgemaak en is bloed, testis en epididimale weefsel geoes vir verdere analise. Liggaamsgewig, intraperitoneale vet, nie-vastende glukosevlakke, IL-1β, IL-6, IL-12, IL-18 en TNFα, superoksied dismutase en katalase aktiwiteit, malondialdehied, testosteroon en estradiol, spermkonsentrasie, lewensvatbaarheid, morfologie, totale motiliteit, progressiewe motiliteit en verskeie snelheidsparameters is gemeet.

Resultate en gevolgtrekking

Albei diëte was suksesvol in die bewerkstelling van insulienweerstandigheid met of sonder hipertensie en het nadelige uitwerkings op manlike voortplantingsfunksie, soos gesien in OS en hormoondisregulasie, veroorsaak. Behandeling met GRT-ekstrak het OS omgekeer en het androgeenvlakke gebalanseer. Hierdie studie het insig gebied in die farmakologiese effekte van GRT in die behandeling van patofisiologiese veranderinge wat voorkom gedurende DGV wat verband hou met insulienweerstandigheid of hipertensie. Die resultate sal hopelik verdere kliniese studies oor GRT-ekstrak inspireer en kan moontlik lei die ontwikkeling van nuwe medisyne gemaak van hierdie samestelling.

DEDICATION

This dissertation is dedicated to all members of my family.

ACKNOWLEDGEMENTS

I would like to thank the following persons who have actively contributed to the accomplishment of this research:

- My supervisors: Prof Stefan du Plessis, Prof Barbara Huisamen and Dr Guillaume Yapo Aboua. Their remarks, advice, guidance and enthusiasm enabled me to be well grounded in Medical Physiology
- My family members for their love and motivation
- All my colleagues in the Division of Medical Physiology for their assistance and friendship through the years, especially, Dr Shantal Windvogel, Dr Festus Kamau, Dr Sybrand Smit, Dr Mignon Van Vuuren, Sonja Alberts, Bongekile Skosana, Zimvo Maqeda, Zibele Ndlovu, Sibonginkosi Roselyn Mzezewa, Cebisa Bladula and Temidayo Omolaoyo
- The Division of Clinical Anatomy, Stellenbosch University and Tygerberg Hospital for helping me to perform histomorphometry analysis
- Afriplex (Pty) Ltd and the South African Medical Research Council (SAMRC) who have provided the GRT used in the experimental study
- Postgraduate Skills Development and the Division for Research Development, Stellenbosch University, especially the Language Centre and Writing Lab for providing various training opportunities on thesis/dissertation writing
- My sponsors, namely the Postgraduate Office, Department of Biomedical Sciences, Harry Crossley Foundation and Higher Education Council Rwanda

We also cannot forget to give thanks to the Almighty God for his grace and strength

TABLE OF CONTENTS

LIST OF ABBREVIATIONS

Ab	Antibody
ACE	Angiotensin converting enzyme
ADH	Antidiuretic hormone
ADP	Adenosine diphosphate
AGEs	Advanced glycation end-products
AHA	American Heart Association
AI	Aromatase inhibitors
AMP	Adenosine monophosphate
AMPK	Adenosine monophosphate-activated protein kinase
ANOVA	Analysis of variance
AOX	Antioxidants
ARBs	Angiotensin II receptor blockers
ARTs	Assisted reproductive technologies
ATI	Angiotensin I
ATII	Angiotensin II
ATP	Adenosine triphosphate
AUC	Area under the curve
BAT	Brown adipose tissue
BBs	Beta blockers
BCA	Bicinchoninic acid assay
BHT	Butylated hydroxytoluene
BMI	Body mass index
BP	Blood pressure
BPA	Bradford protein assay
BSA	Bovine serum albumin

BW	Body weight
cAMP	Cyclic adenosine monophosphate
Cap	Captopril
CASA	Computer-aided sperm analysis
CASMA	Computer-aided sperm morphometry analysis
CAT	Catalase
CCBs	Calcium channel blockers
CVD's	Cardiovascular diseases
Cu	Copper
DAG	Diacylglycerol
deiH$_2$O	Deionized water
DIO	Diet-induced obesity
DM	Diabetes mellitus
DNA	Deoxyribonucleic acid
DP	Diastolic pressure
DPX	Distyrene plasticizer xylene
DETAPAC	Diethylenetriaminepentaacetic acid
E	Oestrogen
E2	Estradiol
ECL	Enhanced chemiluminescence
EDTA	Ethylenediaminetetraacetic acid
EGTA	Ethylene glycol tetraacetic acid
ELISA	Enzyme-linked immunosorbent assay
FFAs	Free fatty acids
FPG	Fasting plasma glucose
GIFT	Gamete intra-fallopian transfer

GLUT	Glucose transporter
GRE	Green rooibos extracts
GRT	Afriplex GRT^{TM} /green rooibos extract from Afriplex (Pty) Ltd
H&E	Haematoxylin and eosin
H_2O	Water
H_2O_2	Hydrogen peroxides
HbA1c	Hemoglobin A1c
HCD	High caloric diet
HCl	Hydrochloric acid
HED	High-energy diets
$HO^{\bullet}$	Hydroxyl radicals
HOD	Hydroxydopamine
HPG	Hypothalamic-pituitary-gonadal
HPLC	High-performance liquid chromatography
HT	Hypertension
ICSI	Intra-cytoplasmic sperm injection
IL-1	Interleukin 1
IL-10	Interleukin 10
IL-12	Interleukin 12
IL-18	Interleukin 18
IL-6	Interleukin 6
IP	Intra-peritoneal
IR	Insulin receptor
IRS	Insulin receptor substrate
IVF	*In vitro* fertilization
KH_2PO_4	Potassium dihydrogenphosphate

LC	Lean control rats
LC+GRT	Lean control treated with Afriplex GRT^{TM} extract
LH	Luteinizing hormone
LPO	Lipid peroxidation
Ltd	Limited
MAP	Mean arterial pressures
MAPK	Mitogen-activated protein kinases
MCT4	Monocarboxylate transporter 4
MCP-1	Monocyte chemoattractant protein-1
MDA	Malondialdehyde
MetS	Metabolic syndrome
mTOR	Mammalian Target of Rapamycin
Na^+	Sodium ion
NaCl	Sodium chloride
NADPH	Nicotinamide adenine dinucleotide phosphate
Na_3VO_4	Sodium orthovanadate
nq	Not quantifiable
$O_2^{\bullet-}$	Superoxide ion
OB	Obese
OBHT	Obese associated with hypertension
OB+GRT	Obese treated with GRT
OBHT+GRT	Obese associated with hypertension and treated with GRT
OBHT+Cap	Obese associated with hypertension and treated with Captopril
OGTT	Oral glucose tolerance test
OS	Oxidative stress
P-AMPK	Phosphorylated AMPK

PBS	Phosphate buffered saline
PAGE	Polyacrylamide gel electrophoresis
PARP	Poly ADP ribose polymerase
PPAR	Peroxisome proliferator-activated receptor
pH	Potential of hydrogen
PI3K	Phosphoinositide 3-kinase
PKB	Protein kinase B
P-PKB	Phosphypryted PKB
PKC	Protein kinase C
PMSF	Phenylmethylsulfonyl fluoride
Pty	Proprietary Limited Company
PUFAs	Polyunsaturated fatty acids
PVDF	Polyvinylidene fluoride
RAAS	Renin-angiotensin-aldosterone system
RNS	Reactive nitrogen species
ROS	Reactive oxygen species
rRNA	Ribosomal ribonucleic acid
SA	South Africa
SEM	Standard error of the mean
SAMRC	South African Medical Research Council
SCA	Sperm Class Analyzer
SDS	Sodium dodecyl sulfate
SHBG	Sex hormone-binding globulin
SOD	Superoxide dismutase
SP	Systolic pressure
SURRG	Stellenbosch University Reproductive Research Group

T	TestosteroneT-AMPKTotal AMPK
T:E2	Ratio of testosterone and estradiol
TBA	Thiobarbituric Acid
TBARS	Thiobarbituric Acid Reactive Substance
TBS	Tris-buffered saline
TCA	Trichloroacetic acid
T1DM	Diabetes mellitus type 1
T2DM	Diabetes mellitus type 2
TGF-β	Transforming growth factor beta 1
TNF-α	Tumor necrosis factor alpha
™	Trade mark
T-PKB	Total PKB
TW	Testicular weight
TW:BW	Ratio of testicular weight to body weight
USA	United States of America
UV	Ultraviolet
VAP	Average path velocity
VCL	Curvilinear velocity
VPR	Volume pressure recording
VSL	Straight line velocity
WAT	White adipose tissue
WHO	World Health Organization
Zn	Zinc

LIST OF UNITS OF MEASUREMENTS

%	percentage	ml	millilitre
°C	degree celsius	mm	millimetre
µm	micrometer	mmHg	millimetres of mercury
µm²	square micrometer	mmol	millimole
10x	ten times	ng	nanogram
5x	five times	pg	picogram
dl	decilitre	rpm	revolutions per minute
fps	frames per second	sec	second
g	gram	v	volume
iu	international units	α	alpha
kda	kilo dalton	β	beta
kg	kilogram	γ	gamma
l	litre	µ	micro
m	metre	µl	microliter
m	molar	µmol	micromol
ma	milliampere	w/v	weight to volume
mg	milligram		
min	minute		

LIST OF FIGURES

LIST OF TABLES

CHAPTER ONE

INTRODUCTION

1.1 Background and problem statement

Factors that contribute to abnormalities in male reproductive function are diverse and not only cause infertility, but also aggravate existing reproductive problems (Alves *et al.*, 2013; Shi *et al.*, 2017). Infertility is characterized by the failure to achieve a clinical pregnancy after twelve months of regular unprotected sexual intercourse (Zegers-Hochschild *et al.*, 2017). This disease has been a major medical and social concern since the dawn of humanity (Verma & Baniya, 2016). Agarwal *et al.* (2015) have reported the global prevalence of 48.5 million infertile couples and 30 million infertile men, with the highest rates in Africa and Eastern Europe (Agarwal *et al.*, 2015). Furthermore, between 60–75% of male infertility cases are idiopathic, because the molecular mechanisms underlying the defects remain unknown (Filipponi & Feil, 2009; Hamada *et al.*, 2011; Mansour *et al.*, 2017).

Numerous literature reviews and scientific investigations have explored the pathophysiological conditions underlying causes and mechanisms of male reproductive disorders (Eladak *et al.*, 2018; Skakkebaek *et al.*, 2015). Testicular and epididymal disorders are mainly caused by genetic and anatomical abnormalities, physical injuries and physiological alterations. However, some of these conditions are caused by other underlying metabolic disorders such as cardiovascular diseases (CVDs) and diabetes mellitus (DM). CVDs and DM have also been proposed as possible contributors to idiopathic male infertility (Kasturi *et al.*, 2008).

In recent years, the incidence of CVDs and DM became a large-scale threat to human health as there has been a tremendous increase in the consumption of processed food in addition to sedentary lifestyle practices (World Health Organization, 2017). These diseases are accompanied by metabolic disorders such as high blood pressure, high blood sugar, excess body and abdominal fat and abnormal cholesterol or triglyceride levels, thereby affecting physiological homeostasis (Cheung & Li, 2012). These metabolic disorders are interlinked and generate a state of oxidative stress (OS), which is commonly known as aetiology of disease development. Furthermore, CVDs and DM comorbidity form key components of the metabolic syndrome (MetS), commonly as a sequel to obesity (Cheung & Li, 2012). CVDs are a group of disorders that affect the heart and blood vessels, thereby generating different medical conditions, including hypertension (Hermida *et al.*, 2018). During hypertensive conditions, the vasculature experience persistently raised pressure due to extra fluid in the blood and

blood vessels that are narrow, stiff or clogged (Medley & Wilson, 2016). This state is accompanied by many complications, including male reproductive disorders (Weissheimer *et al.*, 2012). It is speculated that hypertension could affect reproductive health through different mechanisms, including OS and alteration of endogenous hormones (Azu, 2015).

According to the American Diabetes Association (2010), DM is defined as a metabolic disorder due to abnormal function of the insulin hormone or inadequate insulin production by the pancreatic β cells and is characterized by hyperglycaemia. DM is classified into type-1 (T1DM) and type-2 (T2DM) respectively. T1DM is caused by the absence of insulin, while T2DM is characterized by insulin resistance (American Diabetes Association, 2010). Hyperglycaemia results in autoxidation, thereby generating free radicals which are harmful to organ function (Phaniendra *et al.*, 2015; Rolo & Palmeira, 2006). Moreover, patients often suffer from both diabetes and hypertension, necessitating pharmacological therapeutic treatment and further complicating the underlining cause of sexual dysfunction (Konzem *et al.*, 2002).

As mentioned previously, the MetS is a group of pathological conditions or diseases that attack individuals at the same time, and these conditions are capable of disturbing physiological homeostasis of the body by, among others, the onset of OS. OS is characterized by an imbalance in oxidants and antioxidants (AOX) due to overproduction of free radicals, including reactive oxygen species (ROS) and reactive nitrogen species (RNS) and the body's failing AOX defence mechanisms. It is also well documented that OS impacts upon androgen biosynthesis, spermatogenesis and sperm maturation in mammalians (Rani G *et al.*, 2016).

ROS and RNS are constitutively produced under physiological conditions; however, they may reach supraphysiological levels due to certain pathophysiological conditions (Di Meo *et al.*, 2016). The anatomy and physiology of the testes make them susceptible to OS because the testicular cells use mitochondrial respiration which can be a source of ROS. Furthermore, immature spermatozoa generate ROS (Agarwal *et al.*, 2014). Spermatozoa contain limited cytoplasmic AOX enzymes, while the plasma membrane consists mostly of polyunsaturated fatty acids (PUFAs), thereby making it highly susceptible to a free radical attack (Agarwal *et al.*, 2014). These free radicals can induce lipid peroxidation (LPO) and DNA fragmentation thereby not only impairing spermatogenesis, but also disturbing sperm quality (Agarwal *et al.*, 2014). The management of male fertility disorders includes medications, fertility counselling, and assisted reproductive technologies (ART) (Jungwirth *et al.*, 2012). However, these treatments are expensive and, in some instances, not available or accessible to all infertile couples (Inhorn & Patrizio, 2015). Furthermore, it has been indicated that some of these medications aggravate the root cause of OS (Tremellen, 2008).

Several investigations have proposed alternative medications, nutritional advice or derivatives of plant material to alleviate ROS-induced injury, as some plant extracts have biological properties which can scavenge ROS. The plant extracts upregulate AOX defence systems, thereby protecting the body against excessive free radical formation and attack (Mahajan & Gajare, 2012). Moreover, the supplementation or treatment with phytomedicine acts naturally or nonaggressive without interfering with the normal physiology, thereby rendering them safe in controlled dosages (Khan *et al.*, 2016; Kristanc & Kreft, 2016). Also, phytomedicine works together/synergistically with synthetic medication in order to highlight the significant effect of curative medication to target diseases (Van Vuuren & Viljoen, 2011; Wiesner *et al.*, 2002; Zhou *et al.*, 2016).

Rooibos (*Aspalathus linearis*) belongs to the *fabaceae* family of plants and is a very popular tea indigenous to South Africa (SA). It is mostly grown in the Cederberg mountain region of SA (Kanu *et al.*, 2014; Wyk & Gorelik, 2017). Traditionally, rooibos is used both as beverage and for medical purposes (Joubert & De Beer, 2011). Phytochemical screening of green rooibos extracts (GRE) has shown that it is extremely rich in polyphenolic compounds, especially aspalathin, while it does not contain any tannins (Joubert & De Beer, 2011). Various studies have investigated the role of GRE as a possible therapeutic agent, and to date it has shown great potential in promoting health properties (Awoniyi *et al.*, 2012; Joubert & De Beer, 2011; Muller *et al.*, 2018; Opuwari & Monsees, 2014).

1.2 Rationale of the study

Existing evidence supports the sentiment that diabetes and CVDs play a role in male infertility (Dias *et al.*, 2014; Guo *et al.*, 2017). It has been found that insulin resistance in men with unexplained infertility can be a possible cause of hypogonadism and oligozoospermia. Nevertheless, knowledge regarding the underlying molecular mechanisms concerning insulin resistance and male infertility is limited (Filipponi & Feil, 2009; Hamada *et al.*, 2011; Mansour *et al.*, 2017; Omolaoye & Du Plessis, 2018).

Hypertension is believed to be associated with erectile dysfunction, but the direct effects on other parts of the male reproductive system, if any, are not well understood (Guo *et al.*, 2017). Hypertension on its own (untreated) or the use of anti-hypertensive medications (treated) have been linked to impaired hormone regulation and semen parameters (Filipponi & Feil, 2009; Hamada *et al.*, 2011; Mansour *et al.*, 2017). Consequently, it becomes difficult to distinguish if there is a possible association between male infertility and HT or between male infertility and the treatment of HT. Further investigation is therefore needed to determine whether these associations are valid.

A greater understanding of underlying causative mechanisms between insulin resistance and/or hypertension and male reproduction is required in order to design target molecules to prevent or cure male infertility. Due to the limitations (side effects, availability and cost) of orthodox drugs, there is currently a strong movement towards and support for studies on phytomedicine (Mahomoodally, 2013; Muller *et al.*, 2018; Wyk & Gorelik, 2017). Sustained investigations into plants with antioxidant, anti-obesogenic, antidiabetic, anti-hypertensive and anti-infertility activities are necessary. GRE has been used in various studies and is known as a natural AOX with curative properties. Currently, the company Afriplex (Pty) Ltd is producing an aspalathin-rich laboratory standardized extract prepared from green rooibos called Afriplex GRT^{TM} (GRT). However, there is very little knowledge regarding the use of GRT in obesity-related insulin resistance and/or hypertension and specifically its effects on male reproductive health.

Considering the multiple benefits of rooibos, we hypothesize that GRT supplementation/treatment can ameliorate male reproductive complications developed due to obesity associated insulin resistance or hypertension. Therefore, this research project could potentially contribute towards the development of a treatment regime for men with fertility-related issues due to obesity and associated metabolic disorders.

1.3 Research questions

- Does a 16-week obesogenic diet cause insulin resistance and/or hypertension in male Wistar rats?
- Does an obesity-induced insulin resistant and/or hypertensive male Wistar rat develop OS that may impair reproductive function within 16 weeks?
- Can GRT supplementation of 6 weeks reverse OS and improve male reproductive function in insulin resistant and/or hypertensive Wistar rats?

1.4 Research aim and objectives

The aim of this study was to explore the effect of GRT on the reproductive function in obesity-induced insulin resistant and hypertensive male Wistar rats.

The study was driven by four objectives:

Objective 1: To evaluate the contribution of two different diets on the development of obesity associated with insulin resistance and/or hypertension in male Wistar rats, and a subsequent 6-week treatment period with GRT. This was assessed by determining the following parameters:

- Biometric changes in body weight and intraperitoneal fat weight
- Oral glucose tolerance test (OGTT)
- Blood pressure
- Pro-inflammatory cytokine levels: IL-1β, IL-6, IL-12, IL-18 and TNFα

Objective 2: To determine the effect of obesity-induced insulin resistance and hypertension as well as GRT on testicular tissue function parameters by evaluating:

- Histological and morphometrical changes of testicular tissue
- Testosterone and oestrogen levels

Objective 3: To determine a possible mechanistic link induced by insulin resistance and/or hypertension on testicular disorders by evaluating:

- The expression and activation of signalling intermediates of the insulin signalling pathway: protein kinase B (PKB) and adenosine monophosphate-activated protein kinase (AMPK)
- Apoptotic markers, including caspase 7 and cleaved poly Adenosine diphosphate (ADP) ribose polymerase (PARP)
- Oxidative stress (OS) parameters by means of the end product of lipid peroxidation (LPO); malondialdehyde (MDA), and antioxidant enzymes, including superoxide dismutase (SOD) and catalase (CAT)

Objective 4: To determine the effect of obesity-induced insulin resistance and/or hypertension as well as GRT treatment on epididymal sperm function by assessing motility, viability, morphology and concentration.

CHAPTER TWO

LITERATURE REVIEW

2.1 Introduction

Lifestyle factors, such as a high-energy diet and physical inactivity, are linked to the development of obesity and are associated with MetS features, including insulin resistance, hypertension and dyslipidaemia. The association between MetS with CVD and male infertility may be explained by overlapping disease pathways, including OS and chronic inflammation. In this context, treatments which target these pathways may decrease the cumulative risk for both conditions (Du Plessis *et al.*, 2010; Leisegang *et al.*, 2014; Palmer *et al.*, 2012).

Indeed, many pharmacological treatments for T2DM and hypertension are known to possess anti-inflammatory properties and combat OS. However, there is also interest in natural products, including GREs, which are rich in the AOX compound aspalathin, and which hold promise as a treatment for conditions associated with inflammation and OS.

In this chapter, an overview of the mechanistic link between MetS features (i.e. obesity, insulin resistance and hypertension) and male infertility is presented, with a focus on inflammation and OS. Emphasis is placed on the association of hypertension and insulin resistance with testicular and spermatogenic pathology. In addition, the potential role of GRE as a future treatment to improve male infertility is discussed.

2.2 Male infertility: sperm and testicular pathologies

There are multiple causes of infertility, including physiological (e.g. obesity, MetS) and environmental (e.g. unhealthy diet, low physical activity, drug use) (Durairajanayagam, 2018; Kasturi *et al.*, 2008). The etiology of impaired sperm production and function can be related to factors acting on pre-testicular, post-testicular or directly on the testicular level. Primary testicular failure accounts for about 75% of all male factor infertility (Krausz, 2011; Mittal *et al.*, 2017). Altered testicular function is reflected anatomically by various abnormalities in spermatogenesis, including spermatogenic arrest, which is often associated with germinal aplasia. There are several disorders that affect testicular structure and function, thereby leading to the incidence of testicular pathology. These include testicular torsion, varicocoele and testicular cancer as well as hypogonadism and hydrocele (Mittal *et al.*, 2017).

Primary testicular pathology should always be considered as a cause of altered testosterone biosynthesis and sperm production in infertile patients. Standardized protocols as described by the Word Health Organization (WHO) are routinely used in most andrology laboratories to perform sperm analysis in infertile males according to WHO criteria (Cooper *et al.*, 2009). Male infertility patients display azoospermia (absence of sperm in the ejaculate), oligozoospermia (low concentration of spermatozoa in the ejaculate, i.e. <15 million sperm per millilitre), asthenozoospermia (reduced percentage of motile sperm in the ejaculate, i.e. <40%) and teratozoospermia (reduced percentages of morphologically normal sperm in the ejaculate, i.e. <4%) (Cooper *et al.*, 2009) (Figure 2.1).

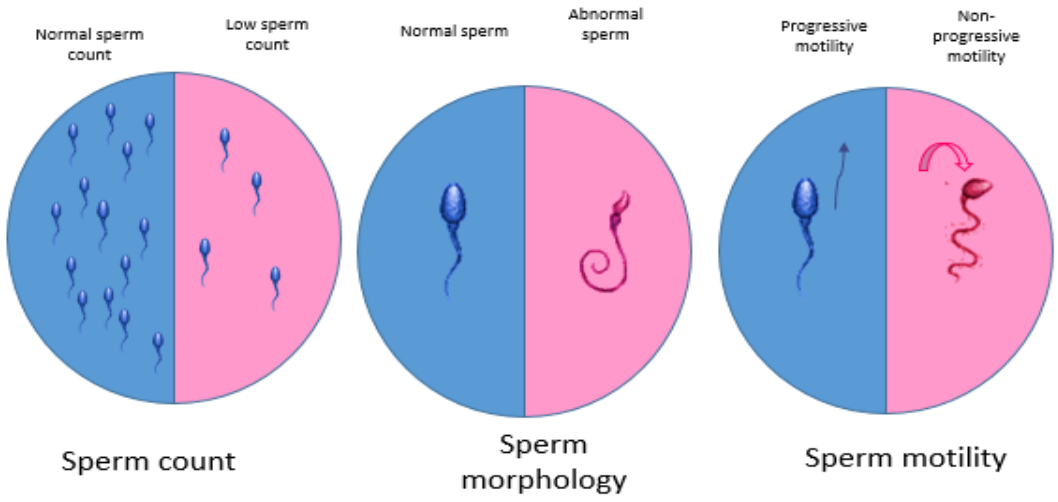

Figure 2.1: Sperm function parameters under physiological and pathophysiological conditions (Cooper *et al.*, 2009)

2.3 Obesity and etiological factors for diseases

2.3.1 Background on obesity

Obesity is a growing global health epidemic, and its prevalence has nearly tripled since 1975 (Smith, 2016). The high prevalence is caused by an absence of proper management of this epidemic, compounded by a western diet. Epidemiologically, it was predicted that 1 billion people worldwide will be obese by 2030 (Kelly *et al.*, 2008). This increase in obesity is observed not only in the middle-

aged population, but also increasingly in younger individuals. Obesity is therefore common among people of reproductive age (Hruby & Hu, 2016).

A hallmark of obesity is an excessive increase in body fat, attributable to a chronic intake of high-energy diets (HED), combined with a sedentary lifestyle (Hruby & Hu, 2016). The HED includes high levels of sugar and saturated fats, which in turn, favours the accumulation of white adipose tissue (WAT) (Paniagua, 2016). The condition of being overweight or obese is determined by calculating the ratio between weight and the square of the height (kg/m^2), i.e. body mass index (BMI) or body fat percentage (BF%) (Lin *et al.*, 2018). The WHO considers individuals overweight when their BMI is over 25 kg/m^2, and as obese when the BMI is over 30kg/m^2. Moreover, BMI is associated with lipid profiles, leptin and cytokines production levels. Severe health conditions, including T2DM, high blood pressure and male infertility, have been linked to adipose tissue metabolites (Paniagua, 2016).

2.3.2 Adipose tissue in the development of obesity: focus on male fertility

Adipose tissue includes brown adipose tissue (BAT), which generates body heat (Lidell *et al.*, 2014), and WAT, which stores energy (Lee *et al.*, 2015). These tissues are distributed in different parts of the body and their distribution depends on the species (Lee *et al.*, 2015). WAT is mostly distributed around visceral or intra-peritoneal organs (Lee *et al.*, 2015). It is not only a place where excess fats/triglycerides is stored, but is also an active endocrine organ which secretes adipokines/cytokines and chemokines (Kwok *et al.*, 2016). Hyperplasia and hypertrophy of WAT in obesity is accompanied by high formation of free fatty acids (FFAs) and upregulation of pro-inflammatory cytokines (TNF-α, mcp-1,TGF-β, IL-1, IL-6, IL-18, leptin, resistin and angiotensin) as well as downregulation of anti-inflammatory cytokines (Adiponection, IL-10) (Jung & Choi, 2014). This imbalance contributes to visceral obesity and its related metabolic disorders, including inflammation, hyperinsulinaemia, hyperglycaemia, hyperestrogenaemia, aromatization, hyperleptinaemia, sleep apnoea, dyslipidaemia, thermoregulation defects and scrotal lipomatosis. These conditions can overlap in the same individual, thereby resulting in MetS and subsequently affect male fertility. Most MetS components interact with the hypothalamus-pituitary-gonadal (HPG) axis, resulting in the alteration of energy homeostasis and the impairment of androgen biosynthesis and spermatogenesis (Craig *et al.*, 2017; Tsatsanis *et al.*, 2015). Likewise, hypogonadism, oligozoospermia and increased sperm DNA fragmentation have been observed in obese men (Craig *et al.*, 2017).

2.3.3 Adipose tissue and aromatization: testicular steroidogenesis

In the testis, the steroid hormones are produced from cholesterol substrate via a series of enzymatic reactions in Leydig cells during foetal and neonatal development (Dong & Hardy, 2003) (Figure 2.2). Steroids include testosterone (T) and oestrogen (E), which are normally produced at different levels. T levels are higher than that of E in men. The T influences physiological activities of men, including muscles and bone density, heart, brain and blood vessels. Furthermore, target tissues and cells to steroid are much more controlled by sex hormone-binding globulin (SHBG) (Anheim *et al.*, 2006). T has a higher affinity for SHBG than for albumin. Approximately 50–70% serum T binds to SHBG, 20–30% to albumin and less than 2% is free (Li *et al.*, 2016). The T bioavailability includes both free T and the fraction bound to albumin (Anheim *et al.*, 2006; Li *et al.*, 2016).

Circulating T in the body is the substrate for E, which is produced by aromatization in the liver, muscles, brain and the fat cells. Importantly, T production increases during male puberty and thereafter declines with age (Li *et al.*, 2016). Also, obesity and its metabolic disorders have been reported to reduce T and increase E (Katib, 2015). Therefore, low T with high E levels cause abnormal male reproductive function (Siegel *et al.*, 2008).

Metabolic disorders, including biometric parameters (e.g. body weight, BMI, blood circulation) and abnormalities in the enzymes involved in steroid synthesis (aromatase cytochrome P450 enzyme, 17β-hydroxysteroid dehydrogenases) affect T levels in men. These parameters interact with one another, for instance, overweight and high BMI are correlated with increased production of the aromatase cytochrome P450 enzyme (Hilborn *et al.*, 2015; Vihma *et al.*, 2017), thereby leading to increased aromatization of T to E (Figure 2.2). Aromatase enzymes are naturally secreted by adipose tissue, with production being proportional to the amount of adipose tissue. In obese men, high production of aromatase cytochrome P450 enzymes are positively correlated with elevated E levels (Katib, 2015). Hypersecretion of oestrogens results in inhibition of the HPG axis via kisspeptin neurons, and subsequently affects testosterone levels and impairs spermatogenesis. Subfertile men, with a significantly higher BMI (≥30) due to obesity, have shown reduced testicular volume, reduced semen quality and lower sperm count (oligozoospermia) as well as lower motility (asthenozoospermia) when compared to the general population (Eisenberg *et al.*, 2014; Hammiche *et al.*, 2012).

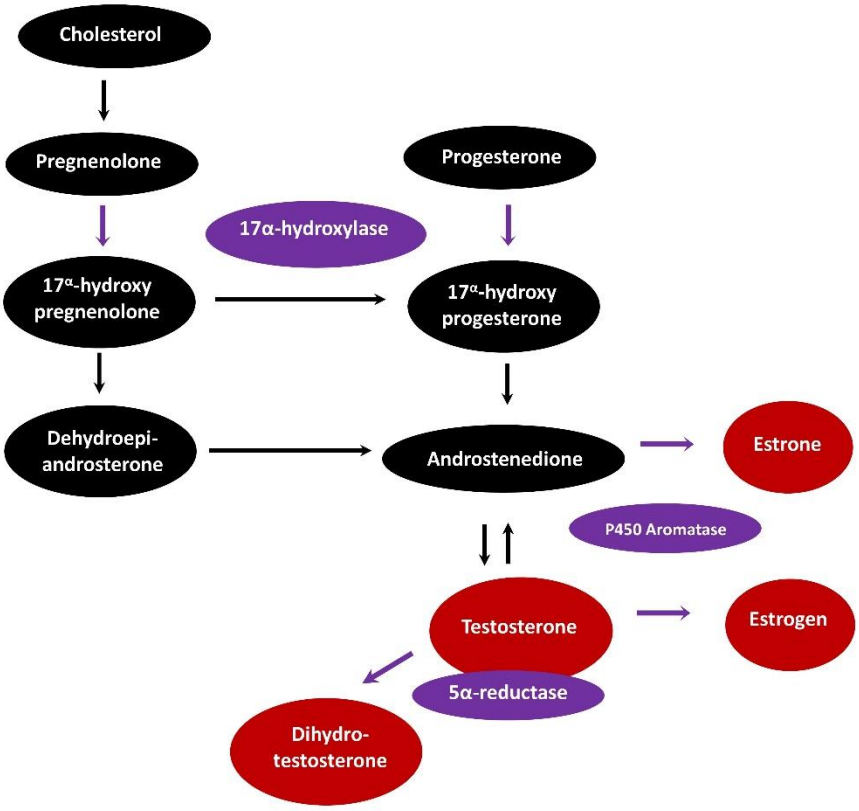

Figure 2.2: Testicular steroidogenesis

2.4 Insulin resistance and male infertility

2.4.1 Insulin and energy homeostasis

Insulin is an anabolic hormone secreted by the beta (β) cells of the pancreas. This hormone regulates blood glucose levels. Glucose is a source of energy used by bodily systems to perform specific functions, including male reproduction (Dupont *et al.*, 2014). Glucose is produced from digested or metabolized carbohydrate nutrients and is stored in liver cells and skeletal muscles as glycogen. However, glycogen stores are limited and excess glucose is converted into fats/triglycerides through lipogenesis. Triglycerides are stored in adipose tissues. When blood glucose concentrations are low, glycogen is mobilized and converted to glucose by glycogenolysis. Glucose is also produced from amino acids or fatty acids through the process of gluconeogenesis, especially during starvation and intense exercise. Hence, the body maintains plasma glucose concentration within a narrow range by balancing oxidative metabolism, glycogenesis, glycogenolysis and lipogenesis. Energy metabolism homeostasis is further controlled by molecular signalling pathways, including the insulin-dependent pathway (PI3K/AKT) and insulin-independent pathway (AMPK) (Berridge, 2014; Dupont *et al.*, 2014; Yu & Cui, 2016) (Figure 2.3).

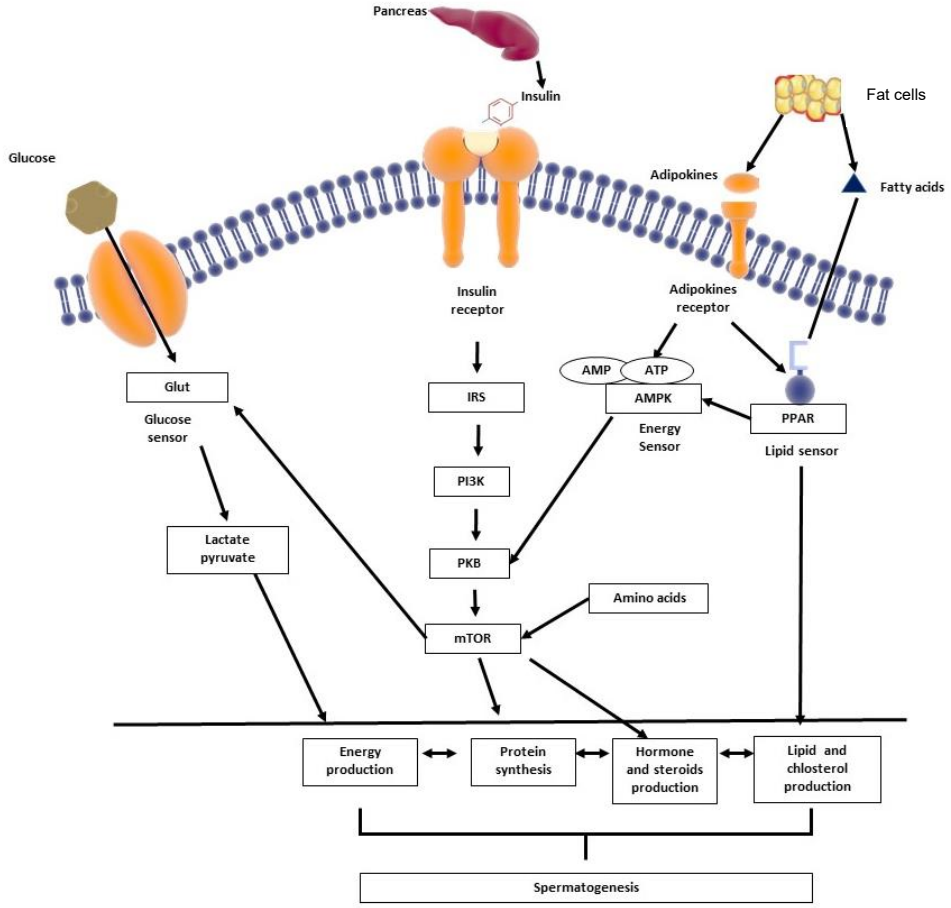

Figure 2.3: Insulin signalling and energy homeostasis involved in the regulation of testicular function (Dupont *et al.*, 2014)

GLUT: glucose transporter, IRS: insulin receptor substrate, PI3K: phosphatidylinositol 3-kinase, PKB: protein kinase B, mTOR: mammalian target of rapamycin, AMP: adenosine monophosphate, ATP: adenosine triphosphate, AMPK: adenosine monophosphate-activated protein kinase, PPAR: peroxisome proliferator-activated receptor

2.4.2 Insulin-dependent pathway

The male reproductive system requires balanced energy and metabolic signals for the modulation of testicular steroidogenesis, proliferation and survival of somatic testicular cells, as well as the maturation of spermatozoa (Nguyen, 2017). Insulin signalling is an important mechanism which maintains metabolic homeostasis and influences testicular physiology through insulin receptors (IRs), which are located on the hypothalamus, testicular cells (Leydig, Sertoli, peritubular/myoid cells) and spermatozoa (Alves *et al.*, 2013).

Insulin signalling encompasses different molecules which interact through phosphorylation (Berridge, 2014; Boura-Halfon & Zick, 2009). Attachment of insulin to its IRs causes transformative changes at both cellular and molecular levels. The IR has two external alpha (α) domains and two intracellular beta (β) domains. Attachment of insulin to the α-domains results in tyrosine kinase auto-phosphorylation of the β-domains. These β domains become active and recruit the insulin receptor substrates (IRS). IRS phosphorylation results in the activation of two different pathways, namely the Ras-Raf-MAPK and the PI3K/Akt pathway. The Ras-Raf-MAPK pathway controls cellular proliferation and gene regulation, while the PI3K/Akt pathway plays a role in glucose uptake and storage (Berridge, 2014; Yu & Cui, 2016).

Phosphorylated Akt/PKB stimulates translocation of glucose transporters to the cell membrane. The isoforms of glucose transporters (GLUT), responsible for mediating passive glucose transport (GLUT 1, 3 and 8), are expressed specifically in Sertoli cells (Dupont *et al.*, 2014). GLUT 1 and 3 are localized on the cell membrane and are able to carry glucose from the external milieu to the cytoplasm, while GLUT 8 is an internal glucose transporter and therefore glucose is converted into lactate within Sertoli cells. During translocation of GLUT to the cell membrane, the cell becomes permeable to glucose and this facilitates the cells to produce energy. Furthermore, PKB interacts with mammalian target of rapamycin (mTOR) to regulate protein synthesis and cell growth in response to growth factors, nutrients and increased energy levels (Figure 2.3).

2.4.3 Insulin-independent pathway

The AMPK pathway is an insulin-independent signalling pathway (Berridge, 2014). AMPK is the master energy regulating molecule, which is expressed in muscle and liver, but also in the ovaries and testes (Bertoldo *et al.*, 2015). AMPK detects and indicates cellular energy levels in the cell through biochemical and molecular mechanisms. When ATP production is inadequate, AMPK restores energy homeostasis by switching on catabolic pathways and switching off anabolic pathways. Catabolic pathways include glucose uptake, glycolysis, fatty acid oxidation, oxidative metabolism, mitochondrial biogenesis and autophagy that generate ATP. Anabolic pathways include fatty acid synthesis, triglyceride/phospholipid synthesis, steroid synthesis, glycogen synthesis, rRNA synthesis and protein synthesis that consume energy required for cell growth and proliferation (Galardo *et al.*, 2007; Hardie, 2017). AMPK can be activated by metabolic hormones (i.e. leptin, adiponectin and ghrelin) and natural substances such as polyphenols, as well as by antidiabetic medication (e.g. metformin) (Hardie, 2017; Rice *et al.*, 2013). Therefore, AMPK is considered an important potential therapeutic agent for the treatment of obesity, prediabetes and male factor infertility.

AMPK isoforms α1 and γ1, α2 and γ3 are expressed in testicular cells and spermatozoa (Nguyen, 2017; Ross *et al.*, 2016). The activation of AMPK α1 by toxic substances links to the mTOR signalling pathway and therefore both AMPK and mTOR signalling pathways are involved in the regulation of autophagy and apoptosis in Sertoli cells (Nguyen, 2017). AMPK activation leads to an increase in lactate production in response to an increase in glucose uptake, and accordingly results in increased levels of GLUT 1 and monocarboxylate transporter 4 (MCT4) (Galardo *et al.*, 2007).

2.4.4 Mechanisms of insulin resistance linked to male infertility

Insulin resistance refers to the perturbation of insulin signalling due to the dysfunction of insulin receptors and protein kinases of target cells (Berridge, 2014). Obesity is the main cause of insulin resistance where free fatty acids stimulate elevated IL-1, 6, 12, 18 and TNF-α levels, which inhibit or supress insulin signalling (Kwok *et al.*, 2016). The intracellular expression and activation of signalling proteins, including PKB and AMPK, are decreased (Berridge, 2014). Moreover, it has been reported that obesity-induced insulin resistance suppresses the action of luteinizing hormone (LH) in the testis, which significantly reduces circulating testosterone levels (Grossmann *et al.*, 2014).

Hyperinsulinaemia and hyperglycaemia occur when the target cell is unable to respond to insulin action and both insulin and glucose levels in the blood stream increase. This insulin resistance acts as a precursor for both prediabetes and T2DM (American Diabetes Association, 2010). When the blood sugar/glucose levels are slightly increased above the normal levels, this condition is called prediabetes. Over time, the blood glucose levels become high enough to be diagnosed as T2DM. Different tests can confirm prediabetes or diabetes in fasted and non-fasted blood samples by measuring glucose levels (American Diabetes Association, 2010) (Table 2.1).

Table 2.1: Diagnosis and classification of T2DM (American Diabetes Association, 2010)

Tests	Prediabetes	Diabetes
FPG (after 8 hours of fasting)	100–125 mg/dL 5.6 mmol/L–6.9 mmol/L	>125 mg/Dl >6.9 mmol/L
OGTT after fasting 8 hours and administrating 50–75 g of glucose	140 mg/dL–199 mg/dL 7.8 mmol/L–11 mmol/L	>199 mg/dL >11 mmol/L
HbA1c	5.7%–6.4%	>6.4%

T2DM: type 2 diabetes mellitus, HbA1c: hemoglobin A1c, OGTT: oral glucose tolerance test, FPG: fasting plasma glucose

2.4.4.1 Hyperglycaemia: oxidative stress (OS), inflammation and apoptosis in male infertility

OS, inflammation and apoptosis are closely interlinked in hyperglycaemic conditions and consequently cause histological damage to the testes, with a negative impact on hormone and sperm production. High glucose levels lead to an increased glycolysis and glucose autoxidation, which generate elevated levels of free radicals (Berdja *et al.*, 2016; Rolo & Palmeira, 2006). AXO defence mechanisms become weak due to the overwhelming free radicals and therefore contribute to OS. Likewise, protein kinase C (PKC) via diacylglycerol (DAG), the hexosamine pathway flux (N-acetylglucosanimine), advanced glycation end-products (AGE) and the polyol pathway flux (sorbitol, fructose) are activated and increased in their expression (Berdja *et al.*, 2016). Subsequently, this activation of biological mechanisms with alteration of their functionalities contribute to the development of male infertility (Berdja *et al.*, 2016; Rolo & Palmeira, 2006). Furthermore, high ROS production may accelerate the process of germ cell apoptosis, LPO, protein oxidation and DNA damage (Aprioku, 2013; Maneesh & Jayalekshmi, 2006). Therefore, it can lead to impaired and poor fertility outcome due to reduced sperm count, motility and viability (Agarwal *et al.*, 2014; Aprioku, 2013; Maneesh & Jayalekshmi, 2006) (Figure 2.4).

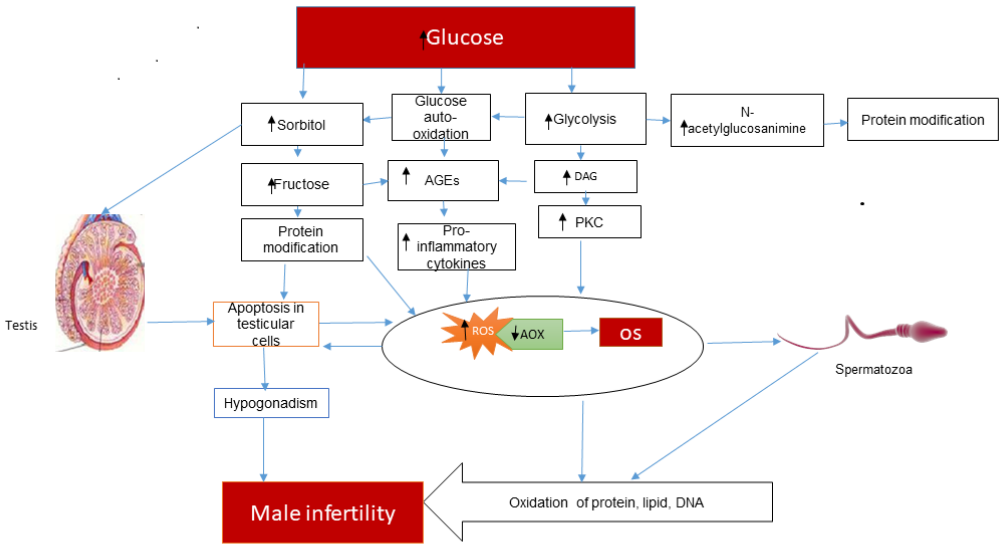

Figure 2.4: Hyperglycaemia-induced ROS generation and the effect on male fertility

ROS: reactive oxygen species, AOX: antioxidant, OS: oxidative stress, PKC: protein kinase C, DAG: diacylglycerol, AGE: advanced glycation end-products

2.5 Hypertension and male infertility

2.5.1 Background on hypertension

Hypertension (HT) is a condition characterized by persistently elevated blood pressure in arterial vessels (Mucci *et al.*, 2016). According to the American Heart Association (AHA) and Medical Guidelines (2017), HT in humans refers to a systolic pressure (SP) that is higher than 130 mmHg and a diastolic pressure (DP) higher than 80 mmHg (>130/80 mmHg). HT is a global health problem and even the younger population of reproductive age are predisposed to HT (Grad *et al.*, 2015). HT is associated with complications such as stroke, vision loss, heart failure/heart attack, kidney diseases/failure and sexual dysfunction (Guo *et al.*, 2017).

2.5.2 Causes of hypertension

There is no single known cause of HT. Excessive weight gain, especially when associated with increased visceral adiposity, is a major cause of HT, accounting for 65 to 75% of the risk for human

primary hypertension. Western food consumption causes obesity, which in turn induces HT through the alteration of renal pressure natriuresis (Hall *et al.*, 2015). Accumulation of fatty acids inside and around the kidney impairs renal pressure natriuresis, increases sodium reabsorption, decreases sodium excretion and increases water uptake (Hall *et al.*, 2014; Hall *et al.*, 2015). These conditions are the risk factors resulting in increased blood pressure (BP), consequently activating the sympathetic nervous system, renin-angiotensin-aldosterone system (RAAS) and renal compression. Moreover, overexpression of angiotensinogen, hyperleptinaemia, insulin resistance, dyslipidaemias, glucose intolerance and inflammation mechanisms link obesity to the development of HT (Yanai *et al.*, 2008).

2.5.3 RAAS

The RAAS is one mechanism that the body uses to regulate blood pressure and fluid balance (Yanai *et al.*, 2008). This mechanism starts with the renin enzyme which is secreted by the kidney and released into the blood stream. Renin converts the plasma protein angiotensinogen to angiotensin I (ATI). The lung produces converting enzyme; ACE, which converts ATI to angiotensin II (ATII). Furthermore, ATII has several effects: increased vasoconstriction, decreased glomerular filtration rate and thirst. ATII also stimulates the release of aldosterone from the adrenal gland and causes reabsorption of Na^+ and water, thereby increasing blood volume. ATII interacts with the hypothalamus and releases antidiuretic hormone (ADH), which causes reabsorption of water and as a secondary function, also vasoconstriction. Both aldosterone and ADH hormones increase blood volume. However, abnormal activation of the RAAS causes the high BP (Figure 2.5).

The presence of all the components of the RAAS has been reported in the testis and epididymis via receptors, implying a relationship between RAAS dysfunction and male infertility (Weissheimer *et al.*, 2012). Previous studies have shown that abnormal expression of ACE and ATI/II results in hypertension and male reproductive disorders. The stimulation of ATII receptors in Leydig cells inhibits the ability of LH to stimulate testosterone production. Moreover, this stimulation inhibits the cAMP pathway, thereby modifying seminiferous tubule contraction (Rossi *et al.*, 2002).

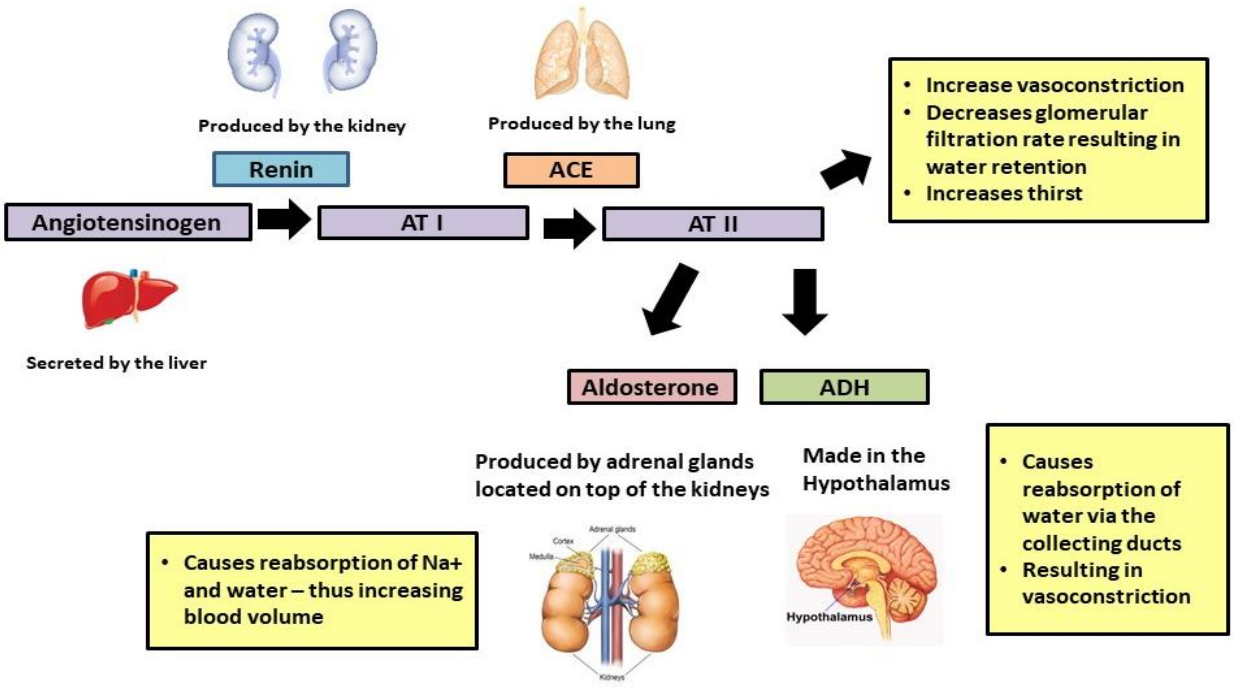

Figure 2.5: RAAS (adapted from Yanai *et al.*(2008))

ACE: angiotensin converting enzyme, ADH: antidiuretic hormone, ATI: angiotensinogen to angiotensin I, ATII: angiotensin II

2.5.4 Hypertension and male reproductive function

The direct end-organ effects of hypertension have been studied in depth on the arteries and kidneys, but little is known about the effect on the testes (Guo et al., 2017). Prior research has addressed the relationship between hypertension and the endocrine axis, which may affect reproductive ability.

Normally, blood and nerve supply for the epididymis and testis are found on the posterior side. The testes receive blood supply from the testicular arteries, the cremasteric arteries and the deferential arteries (Patel, 2017). The testicular artery arises from the abdominal aorta just below the renal artery and becomes a component of the spermatic cord above the internal inguinal ring. It is furthermore intimately associated with a network of anastomotic veins, which eventually form the pampiniform plexus. Testicular cells receive nutrients and perform multiplication, steroidogenesis and spermatogenesis. Any disconnection between blood supply and testicular cells may impact the HPG axis by altering androgen biosynthesis and sperm production.

The testis and epididymis may be susceptible to oxidative damage, as the blood vessels supplying blood to these tissues often show sclerotic changes (Azu, 2015). Such vascular anomalies have been observed in a variety of mammals, such as the spontaneously hypertensive rat. Mainly, disturbances of the seminiferous epithelium lead to testicular atrophy and the impairment of hormone and sperm production (Adedara *et al.*, 2018; Azu, 2015). A Brazilian group employed a rat model for renovascular hypertension to demonstrate impaired spermatogenesis, which they attributed to imbalances in T and E as well as in the follicle stimulating hormone (Guo *et al.*, 2017).

Importantly, HT, dyslipidaemia and inflammation are also associated with decreased endogenous testosterone production. For example, several studies have reported an inverse association between testosterone levels and indicators of hypertensive vascular change, including arterial wall thickening, vessel wall stiffness and endothelial dysfunction (Dockery *et al.*, 2003; Fogari *et al.*, 2005; Kyriazis *et al.*, 2011; Muraleedharan & Jones, 2010; Oskui *et al.*, 2013; Svartberg *et al.*, 2004; Traish *et al.*, 2009). In addition, metabolic risk factors which commonly co-occur with hypertension (e.g. obesity) have been associated with impaired sperm quality, although descriptions of the individual effects of high BP on sperm functioning remain sketchy (Schisterman *et al.*, 2014; Sermondade *et al.*, 2013). Testosterone replacement therapy has been accordingly shown to ameliorate these adverse effects on the vascular system as well as on male reproductive health (Oskui *et al.*, 2013). However, it is important to note that the use of certain anabolic steroids supplements or medications may also increase BP (Rockhold, 2002), suggesting a bi-directional relationship between metabolic risk factors and testosterone levels.

As mentioned previously, HT can result from obesity-induced insulin resistance, which may in turn induce OS via changes in intracellular signalling and macromolecules. Additionally, inflammation and apoptosis may result in this dysregulation, or vice versa, and thereby cause hypogonadism and or lead to a varicocele.

2.6 Management of hypertension and male reproductive function

Some anti-hypertensive medications are aimed at interrupting different steps in the RAAS system to lower BP. These mechanisms include (i) diuretics: by removing excess sodium and water from the body via the kidneys; ii) beta blockers (BBs): by helping the heart to beat slower and with less force, stabilizing systolic and diastolic cycles; (iii) ACE inhibitors: by blocking the conversion of ATI into ATII in most target vessels, the adrenal glands and hypothalamus; (iv) angiotensin II receptor blockers (ARBs): by blocking ATII receptors thereby protecting the cardiovascular system from the

effects of ATII; and v) calcium channel blockers (CCBs): by preventing calcium from entering the cardiomyoctes and blood vessels (Konzem *et al.*, 2002).

Patients with DM have a much higher rate of HT than would be expected in the general population (Konzem *et al.*, 2002). Regardless of the anti-hypertensive agent used, a reduction in BP helps to prevent diabetic complications. Barring contra-indications, ACE inhibitors are considered first line therapy in patients with DM and HT because of their well-established renal protective effects. The ACE inhibitor Captopril is often used to treat HT and DM, together with atenolol (a beta-adrenergic antagonist). It was found that the two agents are very similar in terms of reducing microvascular and macrovascular complications (Konzem *et al.*, 2002).

2.6.1 The effect of anti-hypertensive drugs on male reproductive function

According to a systematic literature review of the most common anti-hypertensive drugs, various positive and negative effects have been reported on male reproductive function.

The available data suggest that calcium channel antagonists, ACE inhibitor and ARBs do not have detrimental effects on sexual function. For instance, hypertensive patients treated with an ACE inhibitor or ARBs showed an increase in sexual activity compared with patients who use other therapies such as β-blockers (Baumhäkel *et al.*, 2008; Becker *et al.*, 2001; Fogari *et al.*, 1996). ARBs seem to have beneficial effects on sexual function and can be used to combat sexual side effects from other cardiovascular agents or in men with pre-existent ED. ACE inhibitors, particularly Captopril, have been associated with improved sexual function (Fogari *et al.*, 1996; Rastogi *et al.*, 2005). The fact that ACE inhibitors work independently of the sympathetic nervous system in lowering BP potentially explains their reduced impact on sexual function. Alternatively, it was demonstrated that activation of RAAS in the testicular tissue (Bader & Ganten, 2008; Franke *et al.*, 2003) is involved in the pathophysiology induced by OS (Fischer *et al.*, 2000; Liu *et al.*, 2007; Scribner *et al.*, 2003). ACE inhibitors have been reported to reverse endothelial dysfunction by preventing the effects of angiotensin II, prolonging the half-life of nitric oxide and decreasing degradation of bradykinin (Mancini *et al.*, 2012). Captopril also decreases the circulating and tissue levels of angiotensin II. Furthermore, Captopril contains a thiol or sulfhydryl group which scavenges different types of ROS and prevents lipid peroxidation (Fischer *et al.*, 2000).

In contrast, anti-hypertensive drugs such as CCBs, BBs and diuretics have been implicated in male infertility through various mechanisms. CCBs act directly on the reproductive tissues and cells

without interacting with HPG axis in male rats, resulting in a reversible anti-fertility (Morakinyo *et al.*, 2009).

BBs have shown to negatively impact sperm functional parameters in clinical studies via alteration of HPG axis combined with hormone imbalance (Aitken, 2016; Guo *et al.*, 2017). BBs resulted in lower semen volume, concentration, motility, total sperm count and total motile sperm count, compared to men receiving other anti-HT medications. Furthermore, BB can also cause anxiety and inhibit the sympathetic nervous system, which results in poor integration of erection, emission and ejaculation, dysregulation of LH secretion and poorer stimulation of T release (Barksdale & Gardner, 1999). Diuretics can also negatively affect penile blood flow, erectile dysfunction and desire, thereby diminishing quality of life and often resulting in noncompliance with the therapy (Nicolai *et al.*, 2014). Therefore, a search for alternative medications has been undertaken to minimise high cost and side effects caused by synthetic anti-hypertensive medications. Alternative treatments have been suggested, including plant-derived medications and lifestyle changes (Mahomoodally, 2013; Muller *et al.*, 2018; Wyk & Gorelik, 2017).

2.7 Management of male infertility

In the event that a woman is unable to fall pregnant after twelve months of sexual intercourse with the intent to conceive, infertility in one or both partners should be considered. It is estimated that 30–40% of couples seeking fertility treatments are diagnosed with male factor infertility (Kumar & Singh, 2015). The different approaches used in clinical diagnosis and treatment of male factor infertility depend on the original cause. Either testis or sperm abnormalities are evaluated physically and biologically.

To understand and characterise these causes, semen analysis is performed according to WHO guidelines in terms of the primary-care level for infertility diagnosis (WHO, 2010). The following criteria are adapted to evaluate the semen analysis: physical parameters (volume, liquefaction, appearance, constancy, pH and agglutination) and biological parameters (sperm viability, concentration, motility and kinematics, morphology and auto-antibodies). Furthermore, a reported case from semen analysis should be treated by using counselling, pharmacological drugs, assisted reproductive technologies (ARTs) and alternative medications.

Drugs used to treat male infertility change the male hormonal system by primarily increasing the bioavailable T and decreasing estradiol (E2) levels. Anti-oestrogen drugs/aromatase inhibitors (AI) block the conversion of T to E2 and of androsterone to estrone. These drugs are prescribed to patients

with low T and high E2 levels to help increase T levels, as well as to facilitate spermatogenesis. For instance, obese males have high levels of aromatase, which cause the transformation of T into the female hormone, E. Therefore, it is recommended in certain instances that this enzyme is blocked in obese men in order to regulate the male sex hormones (Cheshenko *et al.*, 2008; Lephart, 2015).

With modernization and the advances in technology since 1980, ARTs have been employed to help infertile couples fall pregnant (Wahlberg, 2016). ARTs include *in vitro* fertilization (IVF), intra-cytoplasmic sperm injection (ICSI) and gamete intra-fallopian transfer (GIFT) (Ombelet & Van Robays, 2015; Wahlberg, 2016).

Pharmacological anti-infertility and ART applications are costly, can have side effects and are sometimes not successful. Several researchers have suggested that micronutrients and antioxidant supplementations can be used as alternative male infertility management treatments (Agarwal *et al.*, 2004). Male reproductive organs contain naturally free radical scavengers, including vitamins C and E, uric acid, superoxide dismutase (SOD), catalyse (CAT) and glutathione. However, this natural mechanism can fail and requires supplementation of antioxidants to upgrade the system. Supplementation with synthetic antioxidants includes vitamins C, D3 and E, folic acid, zinc, selenium and L-carnitine. However, these synthetic antioxidant supplementations may or may not be effective, depending on the pathology of the infertility (Agarwal *et al.*, 2004).

Currently, researchers worldwide are investigating plant extracts to ascertain their antioxidant activities and ability to treat male infertility. Some indigenous African medicinal plants have been used to treat male reproductive pathology, most of which are rich in polyphenol/flavonoid compounds.

2.8 Rooibos (Aspalathus linearis)

Aspalathus linearis (rooibos) is a member of the *fabaceae* family, which comprises more than 270 species indigenous to the Cederberg mountain region of SA (Jaman *et al.*, 1981) (Figure 2.7A). The leaves of the rooibos plant are used to make herbal tea (Joubert & De Beer, 2011). Depending on the method of processing, rooibos is either fermented (red) (Figure 2.7B) or unfermented (green) (Figure 2.7C). The production of unfermented GRT requires special handling and processing to avoid oxidation and preserve the natural activities of important phytocompounds (Joubert & De Beer, 2011; Joubert *et al.*, 2010; Miller *et al.*, 2017). GRT retains its natural colours and has a higher polyphenol content and antioxidant properties compared to fermented rooibos tea (Miller *et al.*, 2017). Rooibos tea is consumed worldwide, and is highly regarded due to its taste, absence of caffeine and high levels

of the polyphenolic antioxidant compound aspalathin. In addition, green rooibos is used as a raw material in the pharmaceutical industry to make cosmetic products and dietary supplements (Joubert & De Beer, 2011).

A nutraceutical company, Afriplex Pty Ltd, produces Afriplex GRT^{TM} (GRT in short) from unfermented rooibos. This is a standardized spray dried GRT product containing high levels of apsalathin. Phytochemical screening of GRT with high-performance liquid chromatography (HPLC) analysis have identified different polyphenolic compounds (g/100 dry matter): phenylpyruvicacid-2-Oglucoside (0.423265), aspalathin (12.78348), nothofagin (1.974419), isoorientin (1.427281), orientin (1.255839), ferulic A (nq), vitexin (0.338513), isovitexin (0.298022), quercetin-3- robinobioside (1.040565), hyperoside (0.398773), rutin (0.496034) and isoquercitrin (0.572251852) (SAMRC laboratory, 2012).

Figure 2.6: Aspalathus linearis (A), fermeted rooibos (B) and unfermented rooibos (C) (Rooibos tea – Cape Point Press, 2015)

2.8.1 Phenolic compounds and mechanisms

GRT is rich in polyphenol compounds, which are classified in different categories, including dihydrochalcones/flavonoids (aspalathin, nothofagin), flavones (orientin, iso-orientin, vitexin, isovitexin, luteolin, luteolin-7-O-β-D-glucoside, chrysoeriol) and flavonols (quercetin, hyperoside, rutin). Importantly, the aspalathin (C-glucoside) (Figure 2.7C) content is 10-fold higher compared to the other phytochemicals in green rooibos (Joubert & De Beer, 2011). Rather than exerting direct antioxidant effects, the mechanisms by which polyphenols express these beneficial properties appear to involve their interaction with cellular signalling pathways and related machinery that mediate cell function under both normal and pathological conditions (antioxidant and redox, PKB, AMPK and

apoptotic signalling molecules) (Hong *et al.*, 2014; Vauzour *et al.*, 2010). Therefore, the diversity of biological properties of flavonoids depends on the chemical structures, as well as on the number, nature, position and substituents of hydroxyl groups and unsaturated bonds (Kumar & Pandey, 2013; Treml & Šmejkal, 2016).

2.8.2 Health benefits

In a study done by Marnewick *et al.* (2011), 40 human adults at risk of cardiovascular disease consumed six cups of fermented rooibos per day for a period of 6 weeks and were shown to have increased total blood plasma polyphenol levels, and improved redox status and lipid profiles (Marnewick *et al.*, 2011). Another study showed that antioxidant capacity in the blood was elevated after the consumption of 500 mL of both fermented and unfermented rooibos tea (Villaño *et al.*, 2010). This study also compared the two types of rooibos in an *in vitro* study and found that green rooibos tea has a higher ability to boost antioxidant system defences than red rooibos tea (Villaño *et al.*, 2010). Furthermore, in a study done on male rat reproductive function, green rooibos was also shown to enhance sperm concentration, viability and motility (Opuwari & Monsees, 2014).

GRE retains a particular biochemical structure (a dihydrochalcone C-glucoside) (Figure 2.7) and is rich in aspalathin (Joubert *et al*., 2008). These features make GRE a potential antioxidant (Dludla *et al.*, 2014; Muller *et al.*, 2018), a stimulant of glucose clearance in muscle cells (Muller *et al.*, 2012) and a regulator of energy metabolism (Son *et al.*, 2013). Aspalathin is absorbed and metabolized and its glucuronidated and sulfonated conjugated metabolites are excreted in urine (Courts & Williamson, 2009). Furthermore, these aspalathin characteristics highlight its role in the treatment of diseases associated with OS, including CVDs, T2DM and male infertility. Similar to other flavonoids, aspalathin suppresses ROS formation either by inhibition of NADPH oxidases, chelation of trace elements or upregulation and protection of antioxidant defences (Mishra *et al.*, 2013) including CAT and SOD enzymes. Furthermore, it prevents lipid peroxidation and could act as an antioxidant.

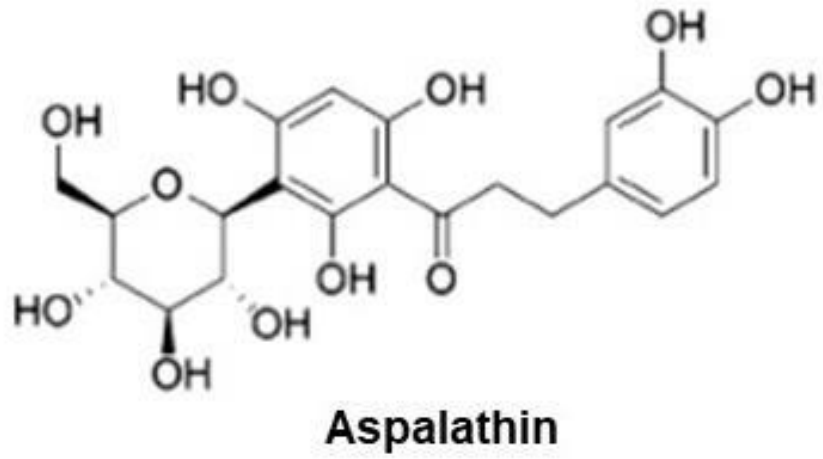

Figure 2.7: Structure of aspalathin. Image adapted from Joubert and colleagues (2008)

CHAPTER THREE

METHODOLOGY

3.1 Study design

This study used a prospective randomized control and experimental animal study design. Two different diets were used to induce obesity-related insulin resistance with or without HT in male Wistar rats. Subsequently, the possible protective properties of GRT on the male reproductive system were evaluated. Animals (120±10g weight, ~7 weeks old) were randomly assigned to seven groups, which each group had seven rats. All rats had unrestricted access to their respective diets and water for 16 weeks (Figure 3.1). At baseline (week 0–10), three groups were established: 1) lean control (LC) animals received standard rat chow, 2) obese (OB) rats received a diet able to induce obesity associated with insulin resistance, 3) obese with HT (OBHT) received a diet aimed at inducing obesity (DIO) as well as HT (Table 3.1). From weeks 11 to 16, one LC, OB and OBHT group were each treated with GRT (manufactured and supplied by Afriplex Pty (Ltd)) at 60 mg/kg/day as a dietary supplement in the form of jelly GRT blocks while an equivalent group received jelly blocks without treatment. A further group of OBHT animals were treated during the same period for 6 weeks with the Captopril, an ACE inhibitor (positive control for HT) of 50 mg/kg per day (Huisamen *et al*., 2013). After the 16-week period, animals were euthanized and blood, testis and epididymal tissue were harvested for further analysis.

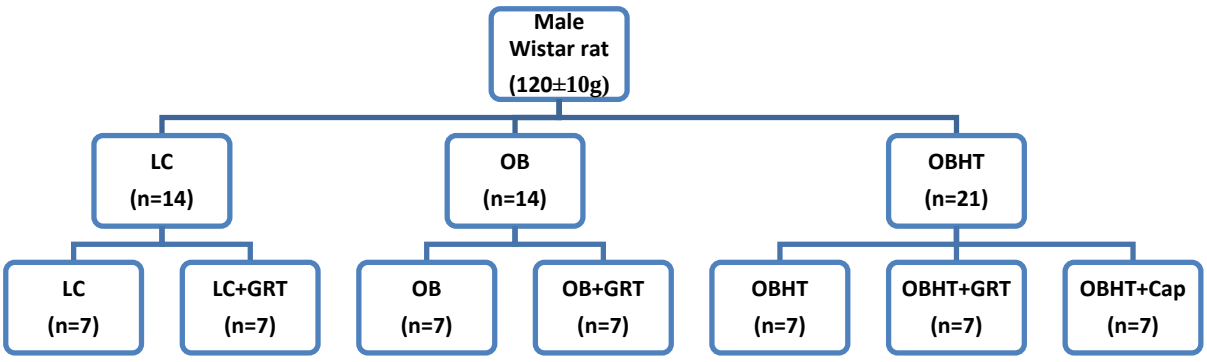

Figure 3.1: Schematic representation of the experimental groups

LC: lean control rats, OB: obese rats, OBHT: obese with hypertension, GRT: Afriplex GRT™ extract, LC+GRT: LC treated with GRT, OB+GRT: obese rats treated with GRT, OBHT+GRT: obese hypertensive rats treated with GRT, OBHT+Cap: obese hypertensive rats treated with Captopril.

3.2 Ethics

This project resorted under two larger ongoing studies with existing ethical clearance (Number SU-ACUD 15-00102 and SU-ACUD 16-000-80). Amended ethical approval was subsequently obtained for this project from the Animal Research Ethics Committee of the Faculty of Medicine and Health Sciences at Stellenbosch University.

3.3 Organizing of research activities

Animals were housed at the Central Research Facility of the Faculty of Medicine and Health Sciences on the Tygerberg Campus of Stellenbosch University. The candidate received specialized training in the handling of animals and was accredited by the veterinarian from the Central Research Facility. Training with regards to experimental techniques were provided by the supervisors and research assistants, while self-optimization of assays was performed by the candidate.

3.3.1 Feeding and animal care

The Wistar strain of rats was identified as early as 1906 as a suitable animal model for experimental purposes and for the teaching physiology. Since then, Wistar rats have been used extensively in numerous *in vivo* studies in various fields of research with great success, as data are highly reproducible and reliable. The development, growth and lifespan of rats are much shorter than that of humans. However, it is comparable to that of humans. Rats reach sexual maturity between 6 to 8 weeks of age and it is believed that a single rat month equates to approximately three human years (Yoon *et al.*, 2014). The use of these rats as an experimental model thus allows researchers to predict and control the development of diseases within a short period. Furthermore, it has been documented that male Wistar rats have morphological and physiological reproductive organ features similar to those of humans (Yoon *et al.*, 2014).

Healthy adult male Wistar rats (n=49) were used in this *in vivo* study (Figure 3.2). The animals were housed 4 to 5 to a cage in the ethically approved and accredited Animal Research Facility. This allowed for control of the environment with 12 hours light and dark cycles, humidity between 45% to 55% and an ambient temperature of 22ºC to 28ºC. The cages consisted of stainless steel wire roofs and plastic bottoms and were equipped with water bottles and feeders. The cages were also furnished with sufficient bedding material composed of sterilized ground maize cobs and were cleaned at least twice per week or as necessary. All the rats were fed with commercial pellets and tap water prior to dietary manipulation. The food, water, body weights (BWs), blood pressure (BP) and blood glucose

were regularly monitored during the 16-week feeding period. Any abnormality was reported to the veterinary staff in order to avoid injury or death of the rats.

On completion of the study, the rats were euthanized with a lethal dose of sodium pentobarbital (160 mg/kg). The aforementioned procedure minimised animal distress and was in accordance with the recommendations of the Laboratory Animal Care of the National Society of Medical Research and the National Institute of Health's Guide for the Care and Use of Laboratory Animals of the National Academy of Sciences (National Institutes of Health publication no. 80-23, revised 1978).

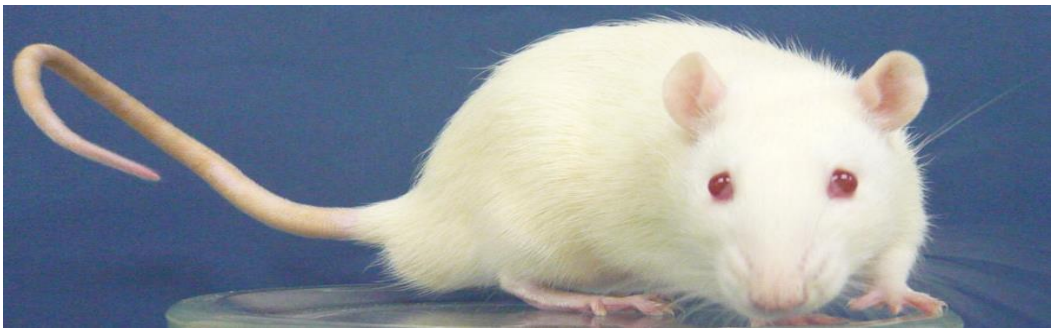

Figure 3.2: Example of a healthy male Wistar rat as was used in this experimental animal model (Rat Strains, 2012)

3.3.2 Preparation of diets

The current study adopted the modified protocol which has been previously used in our laboratories to induce obesity and insulin resistance via diet (Salie *et al.*, 2014). The source of nutrients was modified in order to induce obesity/insulin resistance with or without HT by referring to the specially formulated high caloric diet (HCD) (Table 3.1). The DIO associated with insulin resistance diet was prepared from water and pellets supplemented with sucrose, condensed milk and Holsum^{TM} cooking fat, while the DIO associated with hypertension diet was prepared from pellets supplemented with fructose, Holsum^{TM} cooking fat, casein and cholesterol. Refer to Table 3.1 for the specific composition of the three diets.

Table 3.1: Composition of standard and HCD to induce obesity/insulin resistance with or without hypertension

	Fat (g/100 g)	Cholesterol (mg/100 g)	Protein (%)	Fructose (g/100 g)	Sucrose (g/100 g)	Carbohydrate (%)
Standard rat pellets	4.8	-	17.1	-	5.3	34.6
DIO	11.5	6.4	8.3	-	20.4	42
DIO associated with HT	27.9	13	14.6	11	-	29.5

DIO: diet-induced obesity, HT: hypertension

3.3.3 Preparation of jelly blocks, GRT blocks and Captopril blocks

The GRT was made by the company Afriplex (Pty) Ltd and supplied by the South African Medical Research Council (SAMRC). Captopril was obtained from Sigma, while food grade strawberry jelly and gelatine were purchased locally. The compositions of diets were analysed by Microchem, SA.

Normal strawberry jelly blocks, GRT blocks and Captopril blocks were freshly prepared every day according to the relative weight of each rat and the daily dosage requirements. Jelly blocks were made from a mixture of jelly powder (5.6 g) and gelatine powder (5.6 g), which was dissolved in 35 mL of boiling water. After cooling, the GRT was added to the mixture in accordance with the dosage determined for each animal. A GRT dose of 60 mg/kg/day was used, which is similar to that of previously published studies (Kamakura *et al.*, 2015; Muller *et al.*, 2012). Furthermore, Captopril was prepared and administered in the same way as the GRT. The respective solutions were pipetted (1 mL) into an ice tray and left overnight in a fridge to set. This positive control anti-hypertensive medication was administered at a dose of 50 mg/kg/day, as was previously used in our laboratories in the Division of Medical Physiology (Huisamen *et al.*, 2013). Lastly, unsupplemented strawberry jelly/gelatine blocks were prepared for the untreated groups (LC, OB, OBHT) in order to normalise for the additional sugar content present in the jelly/gelatine blocks. Jelly blocks were fed to each individual animal to ensure treatment adherence.

3.3.4 Body weight, food and water intake

Animals were fed a specific amount of food every morning. The daily food and water intake were monitored over a 24-hour period by weighing leftover food and measuring the water consumption. BWs were also recorded on a weekly basis throughout the study period.

3.3.5 BP

The BPs of all animals were regularly recorded, i.e. once per week throughout the experimental period, with a CODA® non-invasive BP acquisition system (Kent Scientific). This system uses a volume pressure recording (VPR) tail-cuff to measure DP and SP. Prior to monitoring the BPs, the animals were habituated to the procedures over a period of 2 weeks. The values recorded two weeks before commencing with the treatment were regarded as baseline. During each session, 10 systolic and 10 diastolic readings were taken per animal and used to calculate the mean SP, DP and mean arterial pressures (MAP). The following formula was used to determine MAP:

MAP = Mean DP + $^{1}/_{3}$ × (Mean SP - Mean DP).

3.3.6 Oral glucose tolerance tests

Insulin sensitivity was examined by using the OGTT. This is a standard experimental procedure that monitors the responsiveness to glucose in the body after oral administration of sugar (Stern *et al.*, 2002). In this study, OGTTs were performed during the 10th week after the onset of the respective diets and during the 16th week before euthanizing the animals. The animals were fasted overnight before the procedure with free access to drinking water.

Animals were anaesthetized by an intra-peritoneal injection of 0.1 µL Euthanize (53 mg/kg sodium pentobarbital) and the baseline (0 min or fasting) glucose level was measured. Following this, a 50% sucrose solution was administered at 1 g/kg body weight by gastric gavage and the disappearance of glucose from the circulation was subsequently monitored. Blood was collected by a tail prick and analyzed on a hand-held glucometer (Accu-check, Roche, Germany). The blood glucose readings were taken at 3 min, 5 min, 10 min, 15 min, 20 min, 30 min, 45 min, 60 min, 90 min and 120 min respectively, whereafter the animals were left to recover from the anaesthezia.

3.3.7 Sample collection and preparation

After the 16-week experimental period, the rats were weighed and anaesthetized via an intra-peritoneal injection of sodium pentobarbital (160 mg/kg). Blood was collected from the tip of the tail and measured with a hand-held glucometer (Accu-check, Roche, Germany). Following complete anaesthesia, a trans-abdominal incision was performed and the heart was removed from the chest cavity by excising the pulmonary artery, pulmonary vein, vena cavae and aorta (Metallo, 2015). Therefore, exsanguination occurred and the blood was collected from the chest cavity with a pasteur pipette and placed in vacutainer tubes (yellow top serum collection tubes). Tubes remained at room temperature for 15 min before centrifugation (3 500 rpm, 15 min). The serum was transferred into cryo-tubes, frozen in liquid nitrogen and stored at -80°C. The intra-peritoneal fat deposits were then removed surgically. Both testes and epididymides were removed, freed of fat and connective tissue by blunt dissection and placed on ice. The epididymides were separated from the testes and the various organs were rinsed in phosphate buffer saline (PBS) and weighed. One testis and epididymis were snap frozen in liquid nitrogen and stored at -80°C until further use. The other testis was used for histological and histomorphometric analysis, while the remaining epididymis was used for sperm isolation.

3.3.8 Sperm isolation and evaluation of basic and functional parameters

The harvested epididymis was rinsed by placing it in a petri dish containing a 5 mL solution of Hams F-12 nutrient media (Sigma Chemicals, St Louis, MO, USA) supplemented with 3% bovine serum albumin (BSA) (Roche Diagnostics GmbH Mannheim, Germany) on a hot plate at 37°C. The mature sperm was extracted from the caudal part of the epididymis after isolating its most distal part through dissection. The distal part of the cauda was placed in 2 mL of 3 % Hams-BSA solution, allowing sperm to swim out. Subsequently, sperm motility and kinematics were performed after 30 seconds of incubation by sampling the sperm at the edge of the sperm cloud. Directly afterwards, the cauda was cut in five equal pieces and incubated in the same solution for 5 min, thereby allowing “all” spermatozoa to freely swim into the solution. The retrieved sperm solution was diluted 10x in order to perform viability and morphology analysis (SURRG laboratory protocols).

3.3.8.1 Sperm concentration, motility and kinematics

Sperm concentration, motility and kinematics parameters were measured via computer-aided sperm analysis (CASA) using the Sperm Class Analyser (SCA, Microptic, version 5, Barcelona, Span).

Sperm motility parameters of interest include percentage motile cells, progressive motility, average path velocity (VAP), curvilinear velocity (VCL) and straight line velocity (VSL). In brief, 2.5 µl of the sperm suspension was transferred to a pre-warmed (37°C) 20 µm deep Leja slide (Leja, Netherlands) and placed on the heated stage of a Nikon E-200 microscope (Tokyo, Japan). The settings for the SCA were Pseudo Negative phase, Ph2/3 condenser, 4x objective lens, no filter, brightness ±450, contrast ±100 and frame rate of 50 fps.

3.3.8.2 Sperm morphology

Fixative and Sperm Blue® (Microptic SL, Barcelona, Spain) were used to prepare sperm for morphology analysis. Firstly, 10 µL of sperm was pipetted onto a glass slide and thinly smeared. After air drying at room temperature, slides were immersed into the fixative for 16 min. Following this, the slide was moved from the fixative to the staining tray containing SpermBlue® (Microptic SL, Barcelona, Spain) for 16 min. Stained slides were then gently immersed in distilled water for 3 seconds to remove excess stain, allowed to air-dry overnight and mounted the following day with a coverslip using DPX mountant (Merk Millipore, Modderfontein, Gauteng). Sperm morphology analysis was performed by means of computer-aided sperm morphometry analysis (CASMA) using the SCA Analyser (SCA®; Microptic, Barcelona, Spain) software and a Nikon E-200 microscope (Tokyo, Japan) with bright field optics at 600x magnification under a blue filter. The SCA settings were as follows: optics ph+; contrast 166; brightness 465; scale 600x; capture 50 images per slide. The SCA software automatically analyze spermatozoa by detecting and measuring the head and midpiece, classifying them as morphologically normal or abnormal, which is then expressed as the percentage of morphologically normal spermatozoa.

3.3.8.3 Sperm viability

Sperm viability was calculated after staining with eosin-nigrosin. This dye-exclusion staining technique depends on the integrity of the spermatozoa's plasma membranes. All viable spermatozoa remain unstained as their membranes are impermeable to eosin, while dead sperm stained pink, indicating permeability and a damaged membrane. Sperm (10 µL) was mixed with eosin and nigrosin in a 1:2:3 ratio in a 2 mL Eppendorf. The mixture (10 µL) per slide was pipetted onto a glass slide and a thin smear was made, allowed to air-dry and mounted with a coverslip using DPX mounting medium. The prepared slide was examined using a Nikon Eclipse E-200 light microscope (Tokyo, Japan) at 40x magnification. A total of 200 cells (100 in duplicate) were evaluated. Pink-stained dead

sperm was differentiated from unstained live sperm, and their numbers were recorded. The number of viable sperm was expressed as a percentage of the total number of sperm counted.

3.3.9 Oxidative stress (OS) and antioxidant status

OS means that an imbalance developed between either ROS or RNS and the antioxidant defence mechanisms of the body. Testicular tissue generates ROS under both physiological and pathophysiological conditions. Furthermore, the cytoplasmic membrane of sperm cells is rich in PUFAs, which are susceptible to ROS attack. Oxidation of lipid membranes or LPO generates different products, including MDA. Furthermore, testicular tissue has different defence mechanisms, including antioxidant enzymes, which include SOD and CAT. Therefore, it was of interest to check the concentrations of MDA levels and antioxidant enzyme activities in lysates from testicular tissue. MDA is an end product of LPO and gives an indication how ROS reacted with cytoplasmic membrane PUFAs. It has been widely adopted as a measure of free radical formation.

3.3.9.1 Lysate preparation and protein concentration determination

Samples used to measure antioxidant enzymes SOD and catalase (CAT) as well as MDA were prepared using the same method, but a specific buffer was prepared for each assay, namely SOD assay (50 mM sodium phosphate, 0.5% (w/v) Triton X-100, pH 7.5), CAT assay (50 mM potassium phosphate, 0.5% Triton X-100, pH 7.0) and MDA assay (50 mM Potassium phosphate, 1.15% potassium chloride, pH 7.0).

Frozen tissue samples were thawed on ice in Eppendorf tubes before being cut to a weight ranging from 50–60 mg. An equal mass of stainless steel 1.6 mm beads and a double volume of ice-cold buffer was successively added to the sample tube. Samples were homogenised with a Bullet Blender 24 (Next Advance, NY, USA) during the three episodes of 1 minute at speed setting 9, with a 1 minute resting interval in between. The homogenates were allowed to stand on ice for 30 min before centrifuging to allow for stabilization of the tissue homogenate. Homogenates for SOD and CAT analysis were centrifuged (Sigma Laborzentrifugen, type 1-4 K, Germany) at 1 500 rpm for 20 min at 4°C. However, samples for MDA analyses were not centrifuged.

The prepared samples were equally aliquoted into four different tubes for each sample. One tube was used for protein determination on the same day of making the lysate. Other remaining tubes were kept at -80°C for a maximum period of one month. Protein concentration was determined immediately after lysate preparation using a bicinchoninic acid (BCA) kit assay (Sigma) according to the

manufacturer's instructions. Absorbance was read at 562 nm using FLUOstar Omega Microplate Reader (BMG Labtech, Offenburg, Germany).

3.3.9.2 Thiobarbituric acid reactive substance assay

The thiobarbituric acid reactive substance (TBARS) assay is used to quantify MDA in a reaction with two molecules of thiobarbituric acid (TBA) under acid conditions and a high temperature (95˚C). This product is calorimetrically quantified through spectrophotometric techniques at a wavelength of 530 nm. The modified protocol of Esterbauer and Cheeseman (1990) was applied to quantify MDA levels according to standard MDA concentrations and the protein contents in the sample. MDA standard samples of different concentrations (Table 3.2) were prepared to generate the standard curve in order to determine MDA concentrations in the various samples**.** A 10 mL solution of MDA standard solution (500 µM) was prepared by diluting 1.23 µL of the MDA stock solution with 998.77 mL of deionised water (deiH_2O). From this solution, 2 mL MDA solution (125 µM) was prepared by diluting 500 µL of MDA (500 µM) in 1.5 mL deiH_2O. Subsequently, the MDA (125 µM) was considered as initial concentration and used to make a dilution series according to values indicated in Table.3.2.

Following this, samples were loaded in different glass vials (tubes). A reaction mixture of a 4.2 mL comprising 0.1 mL sample, 0.1 mL sodium dodecyl sulfate (SDS; 2%), 2 mL trichloroacetic acid (TCA) + butylated hydroxytoluene (BHT; 10% TCA + 0.8 g/mL ethanol) was added to the tubes, vortexed and incubated for 10 min at room temperature. Finally, 2 mL of colour reagent, TBA (0.67 %), was added to the mixture and the tubes were placed in water bath and boiled at 95°C for 60 min. After heating, the tubes were removed from the water bath and cooled down by placing them in ice-cold water for 15 min. The sample tubes were subsequently centrifuged at 3 000 rpm for 15 min at 40°C. The supernatants were aliquoted into new tubes. Successively, a triplicate assay was run in 96 plate wells, with each well containing 250 µL of supernatant. The absorbance was read at a wavelength of 532 nm on a FLUOstar Omega Microplate Reader (BMG LABTECH, Offenburg, Germany). The resultant MDA levels of the samples were calculated from the MDA standard curve and expressed as µM/mg protein.

Table 3.2: MDA standard curve

Tubes	MDA (µL)	Water (mL)	[MDA] µM
A	0	1000	0
B	2.5	997.5	0.3125
C	5	995	0.625
D	10	990	1.25
E	20	980	2.5
F	40	960	5
G	80	920	10
H	200	800	25
I	400	600	50

3.3.9.3 SOD activity assay

SOD is an antioxidant enzyme, which converts the superoxide radical ($O_2^{\bullet-}$) to hydrogen peroxide (H_2O_2) and molecular oxygen (O_2). The activity of SOD in testicular homogenates was assessed according to the method modified from previous studies (Ellerby & Bredesen, 2000). This assay is dependent on the auto-oxidation of 6-hydroxydopamine (6HOD) and diethylenetriaminepentaacetic acid (DETAPAC), both of which are used as sources of superoxide anions with colorimetric variation signals in the sample. This implies that the formation of many free radicals indicates less SOD activity and vice versa.

The samples were placed in ice-cold water and diluted 10x with SOD assay buffer (50 µM sodium phosphate buffer, pH 7.4). The SOD assay was run in a clean 96-well plate with a maximum of eight samples in duplicate. Each well contained a 200 µL mixture consisting of the following components: 5 µL SOD buffer was added to 10 µL of homogenate and subsequently 170 µL of DETAPAC solution (0.4 mg in 10 mL SOD buffer and sonicate) and 15 µL of 6-HOD were respectively added. A pinkish colour with different intensities would appear, depending on the amount of SOD in the sample. This means that high activity of SOD corresponds to light colour/reduced pinkish colour and less auto-oxidation. The auto-oxidation and linear increase in absorbance were recorded at a wavelength of 490 nm by using FLUOstar Omega Microplate Reader (BMG LABTECH, Offenburg, Germany) every 1 minute for 5 min at 25°C. One unit of SOD is defined as the amount of enzyme needed to exhibit 50%

dismutation of the $O_2^{\bullet-}$. The final activity was dependent on the dilution factor and total protein content in the sample. The SOD activity was expressed in U/mg protein.

3.3.9.4 CAT activity assay

The CAT antioxidant enzyme plays a role in converting H_2O_2 into O_2 and water (H_2O). In this study, CAT activity was determined by using the protocol adapted from the method previously described by Ellerby and Bredesen (2000). Tissue homogenates were diluted to 0.1 µg/µL protein using CAT assay buffer (50 mM potassium phosphate, pH 7.0). A triplicate assay was run in a 96-well UV plate, and each well contained a mixture of 170 µL assay buffer (50 mM KH_2PO_4, pH 7.0), 5 µL of sample and 50 µL H_2O_2 (34 µL of 30% H_2O_2 in 10 mL CAT assay buffer). The kinetics assay of CAT activity was determined by measuring the change in absorbance every 30 seconds of a period of 5 min of H_20_2 conversion. The linear decline in absorbance was read at UV light with wavelength of 240 nm with microplate reader (BioTek Synergy™ HTX Multi-Mode Microplate Reader with Gen5 Software). The CAT activity was determined using the molar extinction coefficient of 43.6 M^{-1} cm^{-1} and was expressed as µmole H_2O_2 consumed/min/µg protein.

3.3.9.5 Hormonal level analysis

Serum samples were used to quantify T and estradiol (E2), which were measured using commercial Enzyme-linked Immunosorbent Assays (ELISA) (Elaboscience, USA). Assay sample manipulations were performed according to the ELISA principle and the manufacturer's instructions. Mainly, ELISA is used to detect and quantify the concentration of antibodies (enzymes) or antigens (proteins) in the sample. The absorbance was read at specific optical density with IMark™ microplate reader (Bio-RAD laboratory, SA), and the results were calculated and interpreted according to the standard curve. T and E2 levels were expressed as ng/mL and pg/mL (0.001 ng/mL) respectively.

3.3.9.6 Inflammatory cytokines

Inflammatory cytokine levels IL-1β, IL-6, IL-12, IL-18 and TNF-α, were analysed in rat serum by using Milliplex MAP rat cytokines kit (Merck, SA). Assay sample manipulations were performed according to the Luminex technology in 96-well plate. This technique detects multiple cytokines in one small amount of the sample by using magnetic beads. Bio-Rad Bio-Plex ™ 200 system instrument

and data manager 6.1 software were used to analyse these cytokines. The concentration was calculated from standard curves and expressed in ng/ mL.

3.3.10 Evaluation of protein expression and phosphorylation in testicular tissue

Western blotting techniques were used to detect and analyse total PKB (T-PKB; 60 kDa), phosphorylated PKB serine 473 (P-PKB; 60 kDa), total AMPK (T-AMPK; 62 kDa), phosphorylated AMPK threonine 172 (P- AMPK; 62 kDa), Caspase 7 (45 kDa) and PARP (89 kDa) proteins in the testicular extract. These proteins were separated by gel electrophoresis using an SDS- polyacrylamide gel (SDS-PAGE). The separated proteins were transferred to a polyvinylidene fluoride (PVDF) membrane, whereafter they were probed detected using specific antibodies procured from Cell Signalling Technology®. As part of this study, total and phosphorylated PKB and AMPK, caspase 7 and Cleaved PARP were measured. The following steps summarize the protocol that was used to determine the proteins of interest.

3.3.10.1 Sample preparation and protein extraction

Proteins were extracted from frozen testicular tissue by using lysis buffer, mechanical and enzymatic processes. The lysis buffer of 30 mL was prepared with different chemical reagents (Table 3.3). Each reagent had a specific role in the mixture. Thirty mL lysis buffer was prepared and 700 µL of the buffer was aliquoted into different Eppendorf tubes containing sample tissue. Furthermore, the entire process of protein extraction was performed on ice.

Table 3.3: Lysis buffer composition for testicular tissue

Reagent	Stock solution	Concentration of working solution	Amount for 30 mL lysis buffer
Tris-HCl EGTA (pH 7.5)	200 mM	20.0 mM	3 mL
EDTA	100 mM	1 mM	300 µL
NaCl	1 M	150 mM	4.5 mL
B-glycerolphosphate		1 mM	0.006 g
Tetra-Na-Pyrophosphate		2.5 mM	0.03 g
Na_3VO_4	0.018 mg/10 mL	1.0 mM	3 mL
Leupeptin and Aprotinin	10 µg/µL	10 µg/ µL	30 µL
Triton X-100	10 %	1%	3 mL
PMSF	50 µg/µL	10 µg/µL	90 µL
dH_2O			fill up to 30 mL

3.3.10.2 Testicular tissue pulverization and homogenization

Testicular tissue was pulverized using a liquid nitrogen-precooled mortar and pestle in order to preserve the intact protein in the sample. Approximately 70 mg of the pulverized powder was weighed off and added into an Eppendorf tube together with 700 µL lysis buffer. Seven stainless steel beads (SSB16, 1.6 mm in diameter; 1 lb.) (Next Advance, USA) were added to the sample tube which was immediately homogenized with a Bullet Blender 24 (Next Advance, NY, USA) at 4ºC for three episodes of 1 min at speed setting 9, with a 5 min resting interval in between. Thereafter, the homogenized samples were left on ice for 20 min in order to allow their optimal reaction with the lysis buffer before centrifuging for 20 min at 15 000 rpm (Sigma Laborzentrifugen, type 1-4 K, Germany). The supernatant was aliquoted and 700 µL transferred into clean Eppendorf tubes and kept on ice until the Bradford assay was performed.

3.3.10.3 Protein concentration determination in the supernatant

Both a Bradford protein assay (BPA) (Bradford, 1976) and BSA standard curve were used to determine the protein concentration in the supernatant.

Reagents: 100 mg of Coomasie Brilliant Blue G-250, 50 mL 95% Ethanol, 100 mL 85% (w/v) Phosphoric Acid, 850 mL dH_2O (Bradford Stock Reagent), BSA.

Bradford stock was prepared by dissolving 500 mg Coomassie Brilliant Blue in 250 mL 95% ethanol, whereafter 500 mL phosphoric acid was added and the final volume made up to 1L with distilled water and mixed. Subsequently, a prepared Bradford solution was diluted five times (5x) with distilled water and filtered twice using Wathman filter papers (0.4 µm pores). A 10 µL of each sample supernatant was added to 90 µL of distilled water into luckam tubes to prepare the first ten times (10x) dilution in order to dilute any detergents in the lysis buffer that may interfere with the assay. From the 10x diluted set, another 5 µL volume was drawn and added to another set of duplicate tubes with 95 µL of distilled water for the second dilution (a twenty times (20x) dilution). To prepare standards, 100 µL BSA of the known concentration (5 mg/ml) was diluted 5x by adding 400 µL of distilled water and preparing it in increasing concentrations. 900 µL of the Bradford solution was added, as shown in the table below (Table 3.4).

900 µL of Bradford solution was also added to the duplicate set of diluted samples, mixed (using a vortex) and left to stand for 15 min before absorbance at wavelength of 595 nm was measured using a spectrophotometer (Cat. 4001/4, Spectronic Instruments, USA). From the absorbance, protein concentrations were calculated against the BSA standard curve (absorbance against concentration). From the above concentrations, the volume of supernatant to load on the SDS-PAGE was calculated against a standard concentration and a total volume of 50 µg/ 9 µL loaded in each gel well. One third of the volume of lysates was composed of the Laemmli sample buffer (62.5 mM Tris-HCl (pH 6.8), 4% SDS and 10% glycerol, 0.03% bromophenol blue and 5% β-mercaptoethanol), and the volume difference was topped up with the lysis buffer. The prepared lysate samples were boiled in a water bath for 5 min to denature proteins and were preserved at -80°C.

Table 3.4: BSA standard concentrations for BPA

BSA concentration µg/ml	BSA volume (µL)	Distilled water volume (µL)	Bradford solution (µL)
0	0 (blank)	100	900
1.25	5	95	900
2.5	10	90	900
5	20	80	900
10	40	60	900
15	60	40	900
20	80	20	900

3.3.10.4 Protein separation by gel electrophoresis

Reagents and their compositions are illustrated in Table 3.5 and this is followed by preparation of the gel and sample loading.

Table 3.5: **Reagents used for protein separation and protein transfer**

Reagents	Composition
Running buffer	192 mM Glycine, 0.1% SDS, 25 mM Tris-HCl
Trans-Blot Turbo Buffer	200 mL Ethanol, 200 mL Trans-Blot® Turbo™ buffer 600 mL dH_2O
TBS-Tween Buffer Solution pH 7.6	137 mM NaCl, 20 mM Tris-HCl, 0.1% Tween-20
Ponceau Red (Sigma-Aldrich)	5 mL acetic acid, 0.5 g Ponceau Red/ 100 mL dH_2O

3.3.10.5 Stain free precast gels preparation and sample loading

A 4–20% Criterion™ TGX™ Precast Midi Protein Gel with 26 wells were procured from Bio-Rad, USA, and were used to separate the proteins. Gels were removed from their containers according to the manufacturer's instructions. Thereafter, the gels were placed in a Midi-protean® dual system

(Bio-Rad Laboratories Inc., USA) and the tanks were filled with running buffer up to the demarcations.

The samples were loaded into the wells by starting with 5 µL pre-stained protein ladder (molecular weight marker) (Thermo Scientific, Lithuania, European Union) in the first well. Subsequently, 9 µL of each sample containing 50 µg of protein were loaded; control samples were 3 per group (LC, OB, OBHT), treatments samples were 4 per group (LC+GRT, OB+GRT, OBHT+GRT, OBHT+Captopril). On completion of sample loading, the outer compartment of the electrophoresis system was filled with running buffer and the system was connected to electrodes (matching the anode to anode and cathode to cathode) and set to run at 200 V, 200 mA for 40 min. After separation, gels were activated in the ChemiDoc™ MP system (Bio-Rad Laboratories Inc., USA) and the image stored. Separated proteins were transferred to a membrane.

3.3.10.6 Transfer of gel proteins to a polyvinylidene fluoride membrane

The Millipore Immobilon-P Transfer membrane is a polyvinylidene fluoride (PVDF) microporous membrane (Immobilon®-PMerck KGaA, Darmstadt, Germany) that was used to bind proteins from the gel through an electro-transfer system. An appropriate membrane size was cut and placed in a dish of fresh methanol for 5 min. Subsequently, the membrane, sponges, blotting paper (chromatography paper) and plastic sandwiches were soaked in cold transfer buffer for at least 15 min to equilibrate before starting the transfer. Thereafter, one sponge was placed on the black side of the open plastic sandwiches, followed by three blotting papers and then the gel. The gel was continuously soaked with transfer buffer. The membrane was placed on top of the gel and followed by three blotting papers and one sponge. The bubbles were removed by using a glass roller before the sandwich was closed. The closed sandwich was placed in the transfer cassette. The cassette was inserted in the filled transfer tank, and an ice pack placed behind the cassette to maintain the temperature at < 10°C. The system was connected to the electrophoresis power supply (Amersham Pharmacia Biotech, Cape Town, SA) and transfer was set at 200 V and 200 mA for an hour. The membrane was removed from the transfer system and visualized using the Chemidoc™ (Bio-Rad) imaging system to check whether the transfer was successful. Automatic software Image Lab™ 5.2.1 captured and saved the image for analysis and normalization purposes. The membrane was soaked in methanol for 30 sec in order to fix the proteins on the membrane. Membranes were left to air-dry at room temperature for 2 min. The membranes were stored at -20°C until later use.

3.3.10.7 Primary and secondary antibody incubation

The membrane was removed from the freezer and left at room temperature for 5 min. The membrane was soaked in Ponceau Red for 2 min to visualize all protein bands. After rinsing out Ponceau Red with dH_20, the bands were visible and subsequent cutting was performed according to the size of the proteins of interest. The membrane pieces were washed three times with TBS-Tween buffer for 5 min on a shaker (lab rotor V1.00). Following this, 5% fat free milk TBS-Tween solution was used to block non-specific binding sites on the membrane. The membrane was left in the milk solution for 60 min on a shaker (lab rotor V1.00) and subsequently washed for 15 min (3 x 5 min replacing TBS-Tween buffer in between each wash). Thereafter, the membranes were probed overnight (4^oC) with the respective primary antibody (1:1 000 dilution).

The following day, the membrane was washed with TBS-Tween buffer for 15 min (3 x 5 min, replacing with fresh TBS-Tween buffer in between each wash) on a shaker (lab rotor V1.00). The membrane was then probed with secondary antibody/anti-rabbit secondary (1:4 000 dilution) for 1 hour on shaker at room temperature. The principle of using these two antibodies respectively is that the anti-rabbit secondary antibody is linked to horseradish peroxidase. It recognizes and binds to the primary antibody. When exposed to a chemiluminescent agent, the reaction produces luminescence in proportion to the amount of protein. The emitted light can then be captured by a camera for qualitative and quantitative analysis. After the incubation with 2 mL ECL, the membranes were transferred to the Chemidoc™ (Bio-Rad) imaging system and images were captured using the Image Lab™ 5.2.1 image acquisition and analysis software. The images were saved and the corresponding images with total proteins were used for normalization.

3.3.10.8 Normalization method for quantitative analysis of blots

Normalization consists of checking equal amounts of loading of samples, transferring protein to the membrane and recording values after probing protein with the Ab and exposing to ChemiDoc™ MP system (Bio-Rad Laboratories Inc., USA). By using Image Lab Software 6.0.0 Analyser, lanes and bands were selected from Chemi-Hi blot and automatically quantified. Next, lanes were only selected from original membrane/total stain free membranes (blot before probing) and quantified. Both detected lanes on Chemi-Hi blot image and total stain free membranes were subsequently compared (Figure 3.3). The software calculates a normalization factor from the amount of protein transferred per lane to the PVDF membrane. Using the total amount of transferred protein in each lane to normalize negates the use of an additional loading control. The data were exported to Excel and

analysis was performed. Firstly, the control samples were averaged. This value was set as one, and all other values were calculated and expressed as a ratio. Following this, the ratio between the relative amount of phosphorylated proteins and total protein was determined by dividing the phosphorylated protein with total protein expression (for example P-PKB/T-PKB).

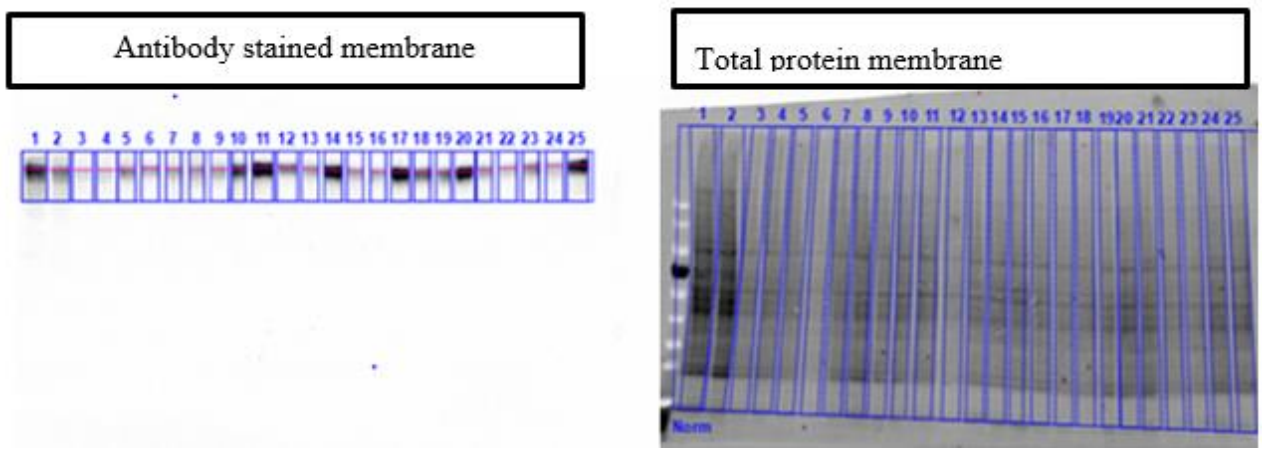

Figure 3.3: Normalization of total protein per lane (right side) versus total intensity of antibody stained sample (left side)

3.3.11 Histology and morphometric analysis

Haematoxylin and Eosin (H & E) staining techniques were used to analyze the histological and morphological characteristics of testicular tissue. Furthermore, this technique facilitated the identification of spermatozoa where haematoxylin stained the cell nucleus blue and eosin stained the cytoplasm pink. To perform this technique, the following steps were applied: fixation of the tissue, processing, embedding, sectioning and staining.

3.3.11.1 Fixation of the tissue

The right testis was harvested and placed immediately in specimen jars containing a 10% formalin solution and left at room temperature for 48 hours. This fixing step prevents tissue degradation, deterioration and preserves tissue structure.

3.3.11.2 Tissue processing

The fixed tissues were sectioned into smaller pieces and placed in labelled embedding cassettes. An automated processing system (Duplex processor, Shandon Elliot; Optolabor (Pty) Ltd, Johannesburg, SA) was used to process the tissue. This tissue processing was performed in different solutions,

including alcohol, xylene and paraffin, which were used successively. Alcohol dehydrated the tissue, while xylene removed alcohol from the tissue and paraffin wax infiltrated the “empty” spaces in the tissue. Full details and the protocol of tissue processing are listed in the Table 3.6.

Table 3.6: Standard tissue processing protocol for H & E staining

Step	Solution	Time (min)	Temperature (°C)
1	10% Formalin	30	Room temperature
2	70% Ethanol	30	Room temperature
3	96% Ethanol	30	Room temperature
4	96% Ethanol	30	Room temperature
5	99.9% Ethanol	30	Room temperature
6	99.9% Ethanol	30	Room temperature
7	99.9% Ethanol	30	Room temperature
8	Xylene	30	Room temperature
9	Xylene	30	Room temperature
10	Paraffin	60	60
11	Paraffin	60	60
12	Paraffin	60	60

3.3.11.3 Embedding

The processed tissues were embedded in paraffin wax at 60°C using the Leica EG1160 Embedder (Leica Biosystems, Germany; supplied by SIMM Instruments (Pty) Ltd, Cape Town, SA). The wax mold was placed on an iced surface for it to set and subsequently stored at temperatures ranging from 20–25°C before sectioning.

3.3.11.4 Tissue block sectioning

The tissue blocks were placed in a freezer (-20°C) for at least two hours before trimming and sectioning. A Leica RM 2125 RT Microtome (Leica Biosystems, Germany; supplied by SIMM Instruments (Pty) Ltd, Cape Town, SA) was used to cut uniform 5 µm sections. These cut sections were placed in a water bath (40–45°C) to allow the section to stretch, and thereafter they were transferred onto a slide.

3.3.11.5 Staining

The slides were incubated at 60°C for 2 min in order for the wax to melt before staining. Filtered H&E solutions were placed into the automated stainer, the Leica Auto-Stainer XL (Leica Biosystems, Germany; supplied by SIMM Instruments (Pty) Ltd, Cape Town, SA). The staining protocol consists of three steps: deparaffinization, rehydration and clearing of the tissue. The H&E protocol is shown in the Table 3.7.

Table 3.7: H&E staining protocol

Step	Solution	Time (min)	Repetitions
1	Oven (60 ºC)	2	x1
2	Xylene	5	x2
3	Ethanol (99%)	2	x2
4	Ethanol (96%)	2	x1
5	Ethanol (70%)	2	x1
6	Tap water	2	x1
7	Haemotoxylin	8	x1
8	Running water	5	x1
9	Eosin	4	x1
10	Running water	1	x1
11	Ethanol (70%)	0.5	x1
12	Ethanol (96%)	0.5	x2
13	Ethanol (99%)	0.5	x1
14	Xylene	1	x1

3.3.11.6 Mounting

A cover slip was mounted with DPX (Sigma-Aldrich, USA) onto the slide to protect the tissue and left for two days to air-dry. The slides were used to identify the testicular histology and histomorphometry under the microscope at 20x and 10x magnification respectively.

3.3.11.7 Histological and morphometrical parameters

Histological evaluation according to the modified Johnsen score was based on 50 cross-sections of seminiferous tubules per testis. The degree of spermatogenesis was graded between 1 and 10 according to the most advanced germ cell in the tubule, where 10 is the normal healthy status and 1 is the most damaged, i.e. with germ and somatic cell loss. The total score is then determined by dividing the total score by the number of evaluated tubules.

Morphometric parameters, including tubular diameter, tubular height, epithelial height and lumen diameter, were evaluated under 10x magnification. Different images were captured and 50 tubules and 50 lumens per animal were analyzed by using ZENLite 2.3SP1 software (Figure 3.4).

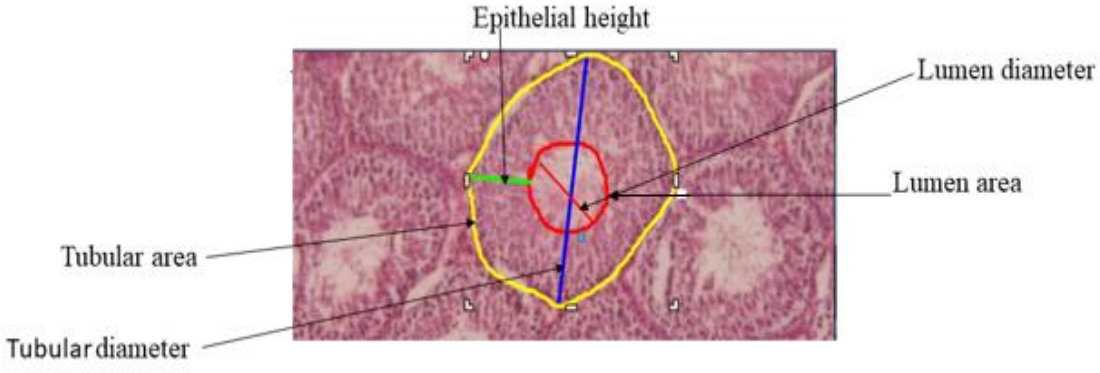

Figure 3.4: Morphometric analysis of a seminiferous tubule in the testis

3.4 Statistical analysis

Data were analyzed and expressed as means ± standard error of the mean (mean + SEM). Significant difference between mean values of two groups was calculated with Student's t- test, while mean values of different groups were calculated using one-way or two-way analysis of variance (ANOVA). Furthermore, the Bonferroni Multiple Comparison analysis was used to compare differences between groups with GraphPad ™ Prism 5.0 (GraphPad Software, San Diego, CA, USA).

CHAPTER FOUR

RESULTS AND INTERPRETATION

4.1 Introduction

This chapter is divided into two parts according to the diet used to induce obesity associated with insulin resistance (OB) and obesity associated with hypertension (OBHT). The effects of GRT on both animal groups were investigated. The first part included four groups, namely LC, LC+GRT, OB and OB+GRT, while the second part comprised five groups, namely LC, LC+GRT, OBHT, OBHT+GRT and OBHT+Captopril. Moreover, both parts ran concurrently in order to adhere to ethics and limit the number of animals used. Animals were handled similarly, and therefore LC and LC+GRT were shared. The difference lies in the diet-induced OB or OBHT (refer to Figure 3.1 and Section 3.3.1).

4.2 The effects of a green rooibos extract on the reproductive function of obesity-induced insulin resistant Wistar rats

In this section, the effect of a HCD on the development of obesity associated with insulin resistance is described. Obesity-related insulin resistance was hypothesized to have side effects on male reproductive function through pathophysiological mechanisms. Subsequently, the 6-week treatment period with GRT was evaluated by monitoring different parameters as set out below.

4.2.1 Biometric data before and after initiation of GRT treatment

Water and food intake as well as the change in body weight and glucose levels were monitored during the 16-week treatment period before onset of GRT treatment (from 0 to 10 weeks) and during the treatment phase (from week 11–16). Additionally, visceral fat weight in relation to the total body weight (adiposity index) were determined in four groups (LC, LC+GRT, OB and OB+GRT).

4.2.1.1 Food intake

Figure 4.1 illustrates the mean food intake in both lean (LC) and obese (OB) animal groups at 10 weeks before the start of GRT treatment. The average food intake was significantly higher in the OB

compared to the LC group (18.72 ± 0.19 g/rat/day vs. 13.90 ± 0.08 g/rat/day, p<0.001). Treatment with GRT was started at 11 weeks of the diet period. Both groups (LC and OB) were further divided in two subgroups: LC+GRT and OB+GTR. Food intake was further monitored daily until 16 weeks.

According to a two-way ANOVA, diet significantly increased food intake between untreated OB and LC (16.49 ± 0.59 g/rat/day vs 13.52 ± 0.14 g/rat/day, p<0.001) as well as treated OB+GRT and LC group (17.88 ± 0.76 g/rat/day vs 13.52 ± 0.14 g/rat/day, p<0.001). The OB+GRT group showed a significant higher food intake when compared to LC+GRT group (17.88 ± 0.76 g/rat/day vs 13.99 ± 0.77 g/rat/day, p<0.001) (Figure 4.2). However, GRT treatment did not show any effect on food intake in the LC+GRT or OB+GRT animals when compared either to the LC or OB animals.

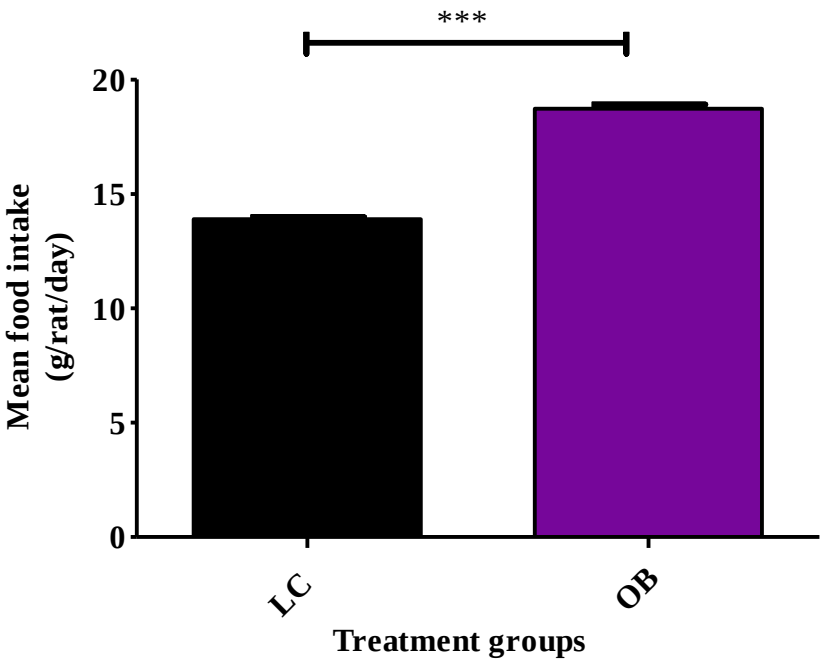

Figure 4.1: Mean food intake of the OB and LC animals over 10 weeks

*Data are presented as mean ± SEM. ***p<0.001 according to Student's t-test, LC: lean control, OB: obese group. N=14 per group.*

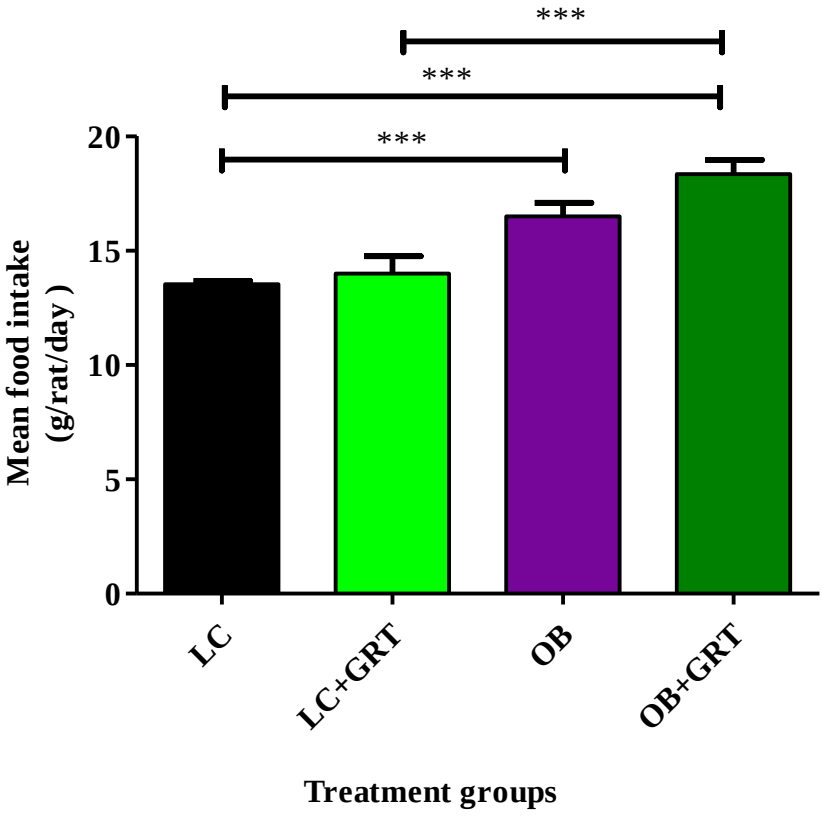

Figure 4.2: Mean food intake of the treatment groups from 11 to 16 weeks

*Data are presented as mean ± SEM. ***p<0.001 according to 2-way ANOVA, LC: lean control, LC+GRT: lean group treated with GRT, OB: obese group, OB+GRT: obese animals treated with GRT. N=7 per group.*

4.2.1.2 Water intake

Before onset of treatment, the OB group consumed less water than the LC group (16.07 ± 0.44 mL/rat/day vs 22.02 ± 0.42 mL/rat/day, p<0.001) (Figure 4.3). Similarly, after GRT treatment, the average water intake in the OB group was less compared to that of the LC group (16.20 ± 1.59 mL/rat/day vs 20.73 ± 0.50 mL/rat/day, p<0.001) (Figure 4.4). There was no significant difference between LC+GRT and the LC group and between OB+GRT and the OB group. The OB+GRT group showed a significant decrease in water intake when compared to the LC+GRT group (15.68 ± 1.00 mL/rat/day vs 20.47 ± 1.04 mL/rat/day, p<0.001) as well as compared to the LC group (15.68 ± 1.00 mL/rat/day vs 20.73 ± 0.50 mL/rat/day, p<0.001) (Figure 4.4). According to the two-way ANOVA, diet, and not GRT treatment, influence water consumption.

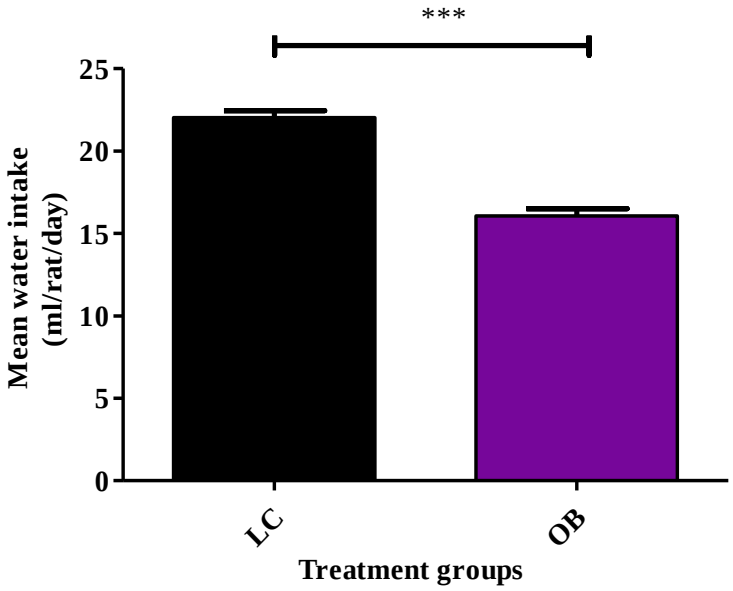

Figure 4.3: Mean water intake of lean and obese animals over 10 weeks

*Data are presented as mean ± SEM. ***p<0.0001 according to Student's t-test, LC: lean control, OB: obese group. N=14 per group.*

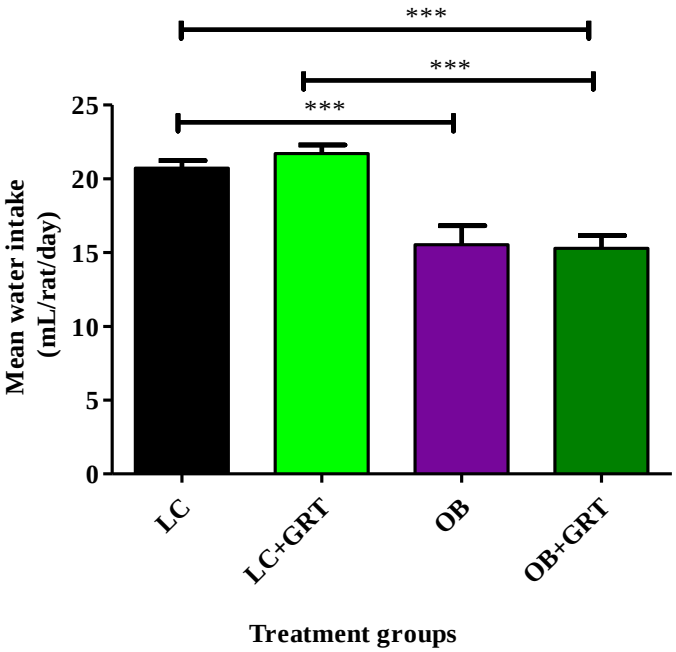

Figure 4.4: Mean water intake from week 11 to week 16 in treatment groups

*Data are presented as mean ± SEM. ***p<0.001 according to a two-way ANOVA, LC: lean control, LC+GRT: lean group treated with GRT, OB: obese group, OB+GRT: obese animals treated with GRT. N=7 per group.*

4.2.1.3 Body weights

Initially, animal body weights (BWs) were measured (120.00 ± 10.00g) and grouped into different treatment groups. The changes in BW were monitored before and after GRT treatment. In week 10, the OB group showed a trend of increase in the mean BW at baseline (before the onset of GRT treatment) when compared to the LC group (299.00 ± 5.51 g vs 285.40 ± 4.44 g, $p>0.05$) (Figure 4.5). In week 16, the OB animals presented a significant higher BW when compared to the LC animals (378.12 ± 11.69 g vs 346.30 ± 7.05 g, $p<0.05$) (Figure 4.6). The OB+GRT group had a significant lower BW compared to the OB group (340.00 ± 9.01 g vs 378.12 ± 11.69 g). Additionally, the LC+GRT group did not present with changes in BW compared to the LC group as well as compared to OB+GRT groups (Figure 4.6).

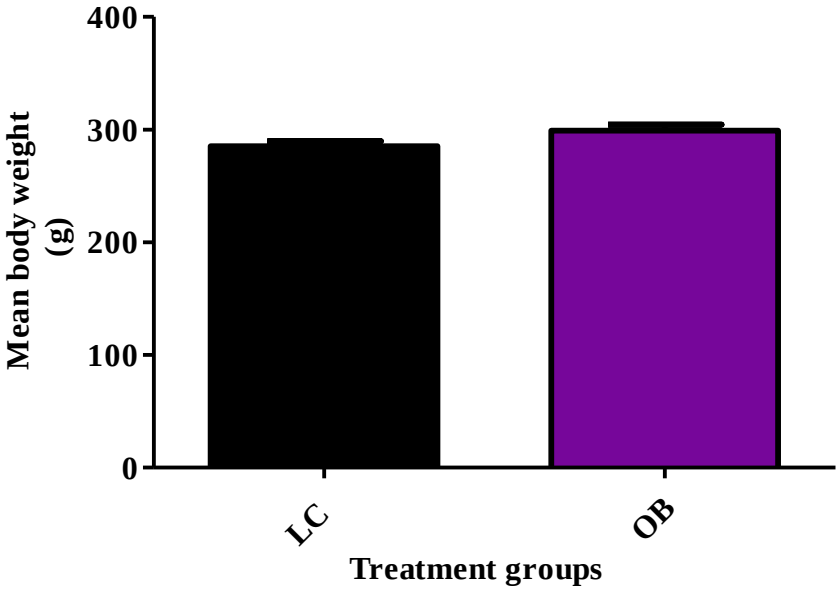

Figure 4.5: Mean body weight of lean and obese group in week 10

Data are presented as mean ± SEM. $p>0.05$ according to Student's t-test, LC: lean control group, OB: obese group. N=14 per group.

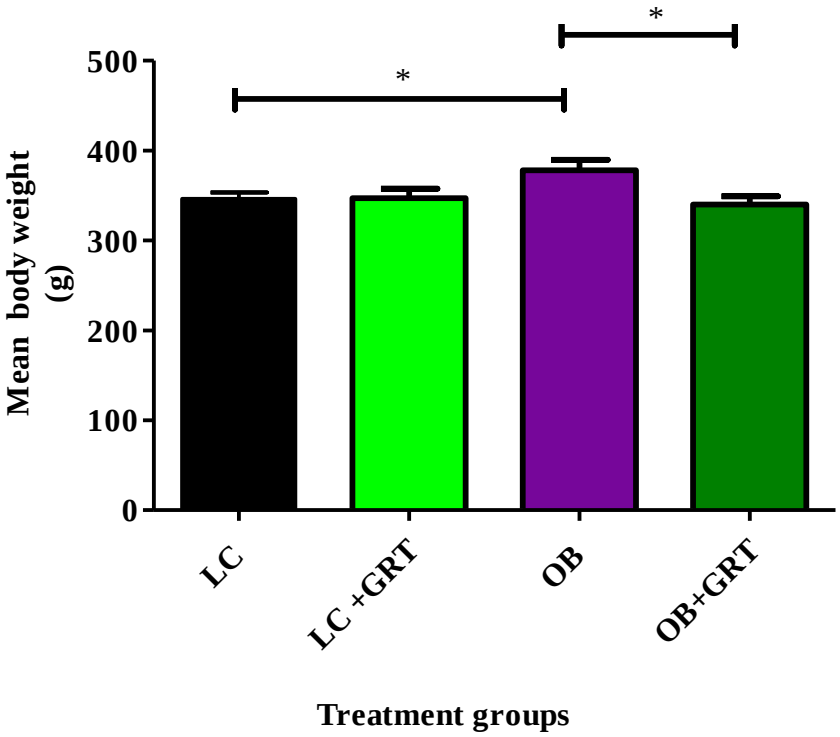

Figure 4.6: Mean body weight per experimental group at the time of sacrifice

*Data are presented as mean ± SEM. * p<0.05 according to a one-way ANOVA, LC: lean control, LC+GRT: lean group treated with GRT, OB: obese group, OB+GRT: obese animals treated with GRT. N=7 per group.*

4.2.1.4 Intra-peritoneal fat weight

Intra-peritoneal (IP) fat weight was expressed as a ratio of the BW and presented as an adiposity index (IP/BW*100) expressed in %. The adiposity index was significantly higher in the OB group compared to the LC group (3.60 ± 0.10% vs 1.96± 0.32%, p<0.001). The OB+GRT group showed a significantly lower adiposity index compared to the OB group (2.06 ± 0.07% vs 3.60 ± 0.10%, p<0.001) and there was no difference between OB+GRT and LC groups. The ingestion of GRT in the LC+GRT group did not show any significant difference in the adiposity index compared to the LC as well as compared to OB+GRT groups (Figure 4.7).

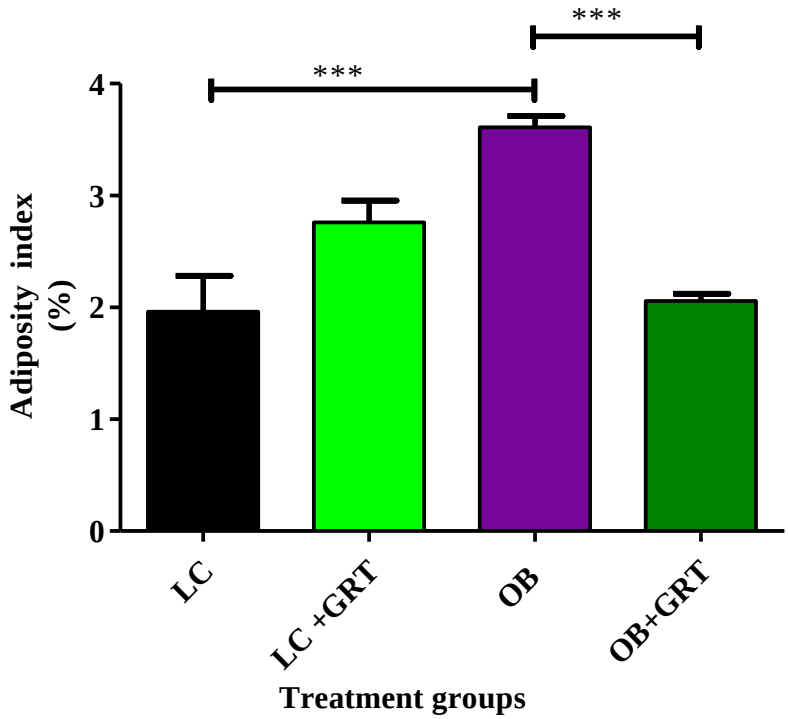

Figure 4.7: Adiposity index in the experimental groups at the time of sacrifice

*Data are presented as mean ± SEM. ***p<0.001 according to a one-way ANOVA, LC: lean control, LC+GRT: lean group treated with GRT, OB: obese group, OB+GRT: obese animals treated with GRT. N=7 per group.*

4.2.1.5 Insulin sensitivity and glucose levels

4.2.1.5.1 OGTT results at baseline level in week 10

After oral administration of the 50% sucrose solution, the monitoring of glucose levels for 2 hours OB animals showed higher glucose levels compared to the LC animals at different time points respectively: 0 min (5.99 ± 0.24 mmol/L vs 4.87 ± 0.21 mmol/L, $p<0.05$), 10 min (7.24 ± 0.12 mmol/L vs 6.23 ± 0.21 mmol/L, $p<0.05$), 15 min (7.95 ± 0.16 mmol/L vs 6.31 ± 0.40 mmol/L, $p<0.01$) and 30 min 7.64 ± 0.11 mmol/L vs 6.73 ± 0.27 mmol/L, $p<0.001$) (Figure 4.8). Furthermore, according to the area under the curve (AUC), the OB group showed significantly increased blood glucose levels compared to the LC group (768.00 ± 17.45 arbitrary units vs 690.80 ± 13.45 arbitrary units, $p<0.05$) (Figure 4.9).

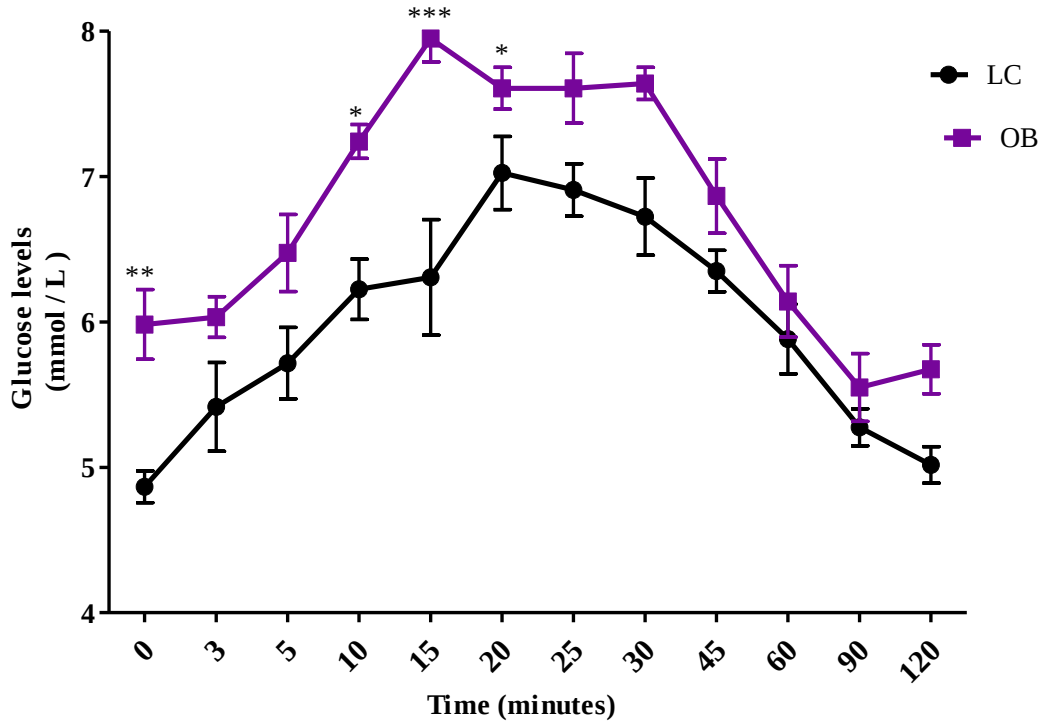

Figure 4.8: Glucose levels in two experimental animal groups (LC and OB) at 10th week on diet

*Data are presented as mean ± SEM. *p<0.05 vs OB according to a two-way ANOVA, LC: lean control group, OB: obese group. N=7 per group.*

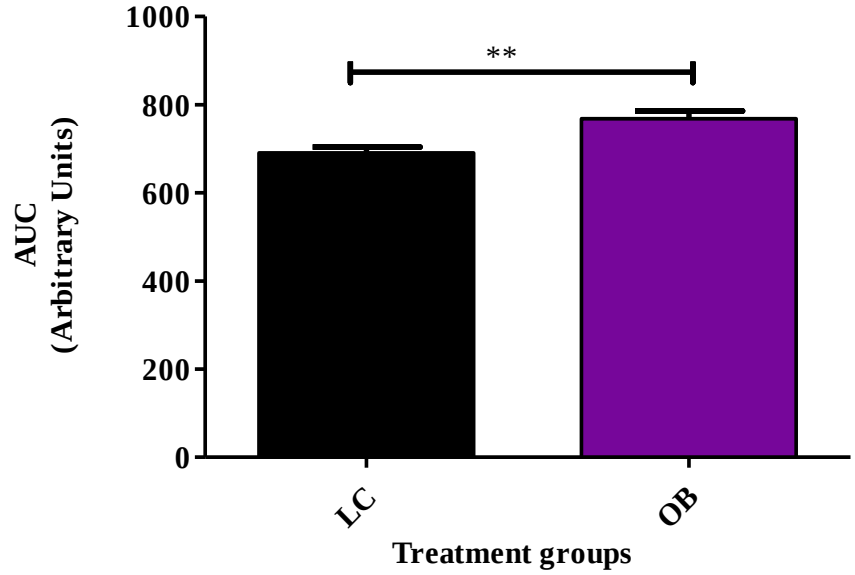

Figure 4.9: AUC representing the effect of diet on glucose tolerance of LC and OB at week 10

*Data are presented as mean ± SEM. *p<0.05 according to Student's t-test, LC: lean control group, OB: obese group. N=14 per group.*

4.2.1.5.2 OGTT results after GRT treatment

In week 15 (i.e. after 5 weeks of GRT treatment), the blood glucose levels in the different treatment groups were changed at different time checking points after gavaging animals with 50% sucrose solution. The OB group presented with significantly higher glucose levels in the plasma when compared to the LC group at 10 min, 15 min, 20 min, 25 min, 30 min and 60 min time points respectively (7.77 ± 0.27 mmol/L vs 6.37 ± 0.12 mmol/L, $p<0.001$), (8.17 ± 0.21 mmol/L vs 6.91 ± 0.25 mmol/L, $p<0.01$), (8.17 ± 0.24 mmol/L vs 6.87 ± 0.18 mmol/L, $p<0.001$),8.00 + 0.30 mmol/L vs 6.67+ 0.17 mmol/L, $p<0.001$), (7.74 ± 0.21 mmol/L vs 6.48 ± 0.25, $p<0.01$) and (6.97 + 0.33 mmol/L vs 5.89 ± 0.14 mmol/L, $p<0.01$), (Figure 10). According to the calculation of AUC, the OB presented higher blood glucose levels compared to the LC group (820.70 ± 21.49 arbitrary units vs 714.00 ± 12.14 arbitrary units, $p<0.05$) (Figure 4.11).

GRT treatment in the LC group (LC+GRT) and in the OB group (OB+GRT) did not show any significant effect on glucose levels when compared to the untreated group (LC and OB). However, it was demonstrated that the two treated groups (OB+GRT and LC+GRT) were significantly different at 0 min (6.19 ± 0.20 mmol/L, vs 5.06 ± 0.06 mmol/L, $p<0.01$), 5 min (7.13 ± 0.25 mmol/L vs 5.83 ± 0.19 mmol/L, $p<0.001$), 10 min (7.77 ± 0.25 mmol/L vs 6.40 ± 0.21 mmol/L, $p<0.001$), 15 min (8.20 ± 0.27 mmol/L vs 6.36 ± 0.12 mmol/L, $p<0.001$), 20 min (8.10 ± 0.30 mmol/L vs 6.39 ± 0.13 mmol/L, $p<0.001$), 25 min (8.04 ± 0.28 mmol/L vs 6.23 ± 0.18 mmol/L, $p<0.001$), 30 min (7.81 ± 0.33 mmol/L vs 6.24 ± 0.19 mmol/L, $p<0.001$), 45 min (7.29 ± 0.27 mmol/L vs 5.54 ± 0.21, $p<0.001$), 60 min (7.09 ± 0.35 mmol/L vs 5.44 ± 0.01 mmol/L, $p<0.001$) and 90 min (6.34 ± 0.39 mmol/L vs 5.09 ± 0.16 mmol/L, $p<0.01$) (Figure 4.10). These significant differences were also observed when calculating the AUC where the OB+GRT group showed a significant increase of AUC compared to the LC+GRT (839.60 ± 32.64 arbitrary units vs 667.70 ± 14.21 arbitrary units, $p<0.001$) as well compared to the LC group (839.60 ± 32.64 arbitrary units vs 714.00 ± 12.14 arbitrary units, $p<0.01$) (Figure 4.11).

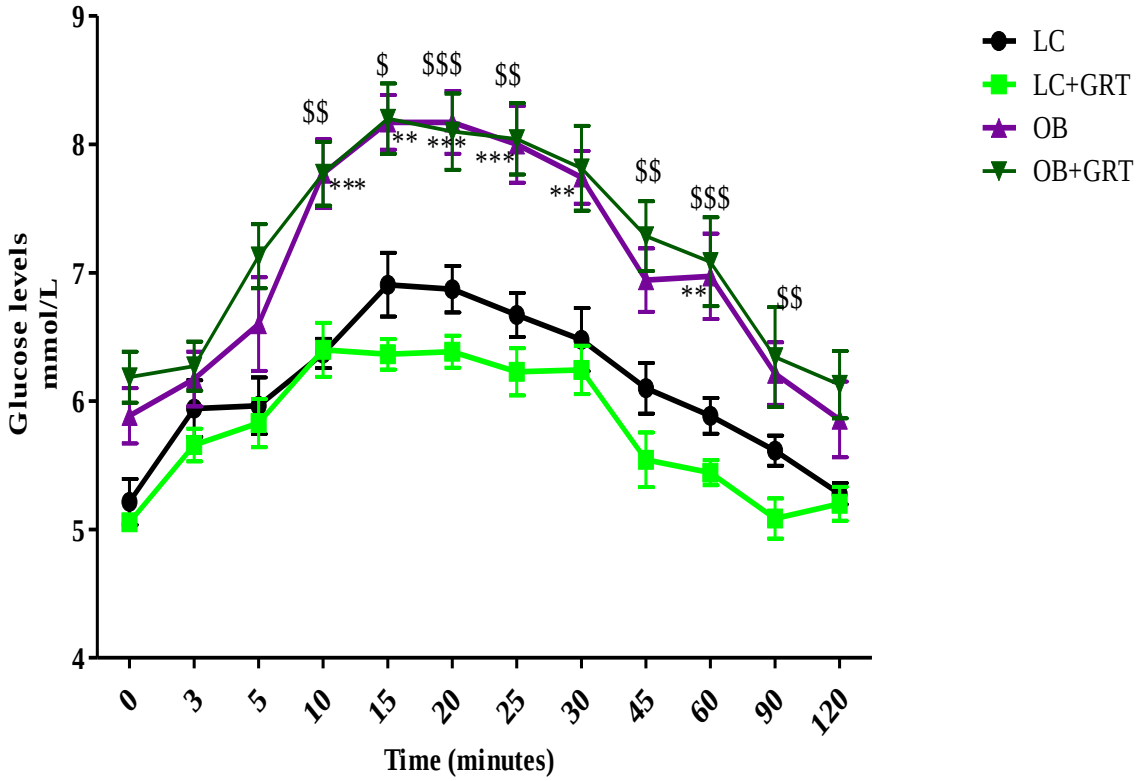

Figure 4.10: Glucose levels after treating animals with GRT

*Data are presented as mean ± SEM. *p<0.05, **p<0.01 OB vs LC group, $p<0.05, $$p<0.01, $$$p<0.005 OB+GRT vs LC+GRT according to a two-way ANOVA. LC: lean control, LC+GRT: lean group treated with GRT, OB: obese group, OB+GRT: obese group treated with GRT. N=7 per group.*

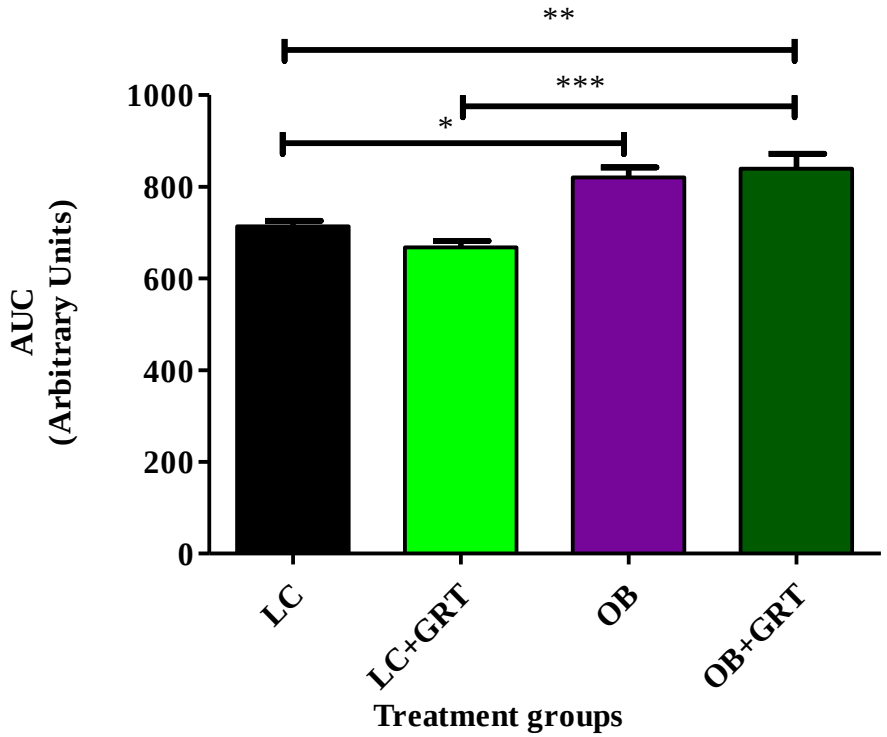

Figure 4.11: AUC representation of the effect of diet in glucose tolerance of LC and OB

**p<0.05, **p<0.01 according to ANOVA, LC: lean control, LC+GRT: lean group treated with GRT, OB: obese group, OB+GRT: obese animals treated with GRT. N=7 per group.*

4.2.1.5.3 Non-fasting blood glucose levels

On the day of sacrifice, an increase in the non-fasting blood glucose levels was observed in the OB group compared to the LC group (7.5 ± 0.2 mmol/ L vs 6.7 ± 0.1 mmol/L, $p<0.05$). GRT treatment in OB (OB+GRT) resulted in a significant decrease in glucose levels when compared to the untreated OB group (6.8 ± 0.1 mmol/L vs 7.5 ± 0.2 mmol/ L, $p<0.05$). There was no difference between LC and OB+GRT groups. No significant difference in glucose levels was also observed between LC and LC+GRT as well as between LC+ GRT and OB+GRT groups (Figure 4.12).

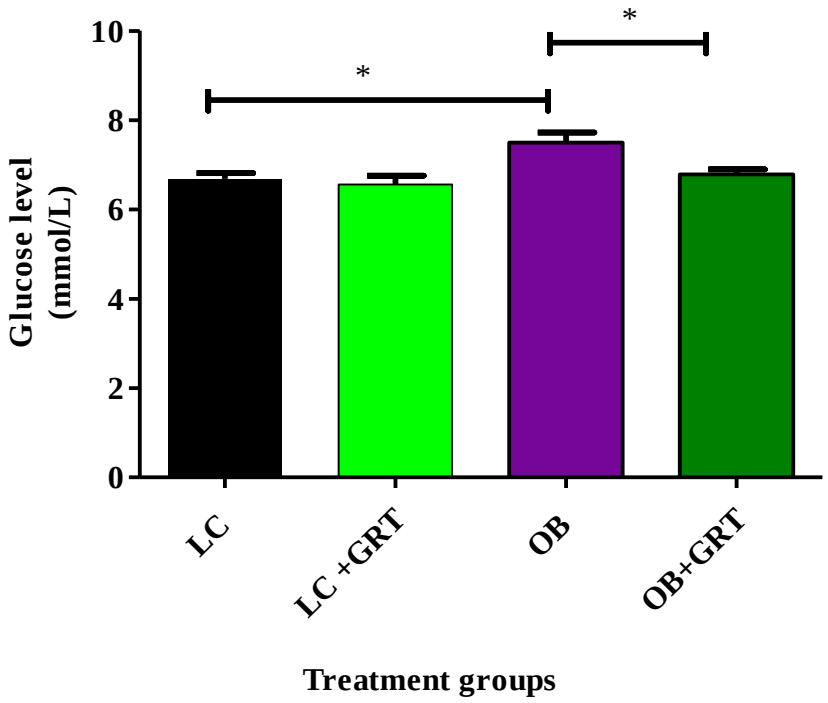

Figure 4.12: Non-fasting blood glucose levels in treatment groups

*Data are presented as mean ± SEM. *p<0.05 according to one-way ANOVA, LC: lean control, LC+GRT: lean group treated with GRT, OB: obese group, OB+GRT: obese animals treated with GRT. N=7 per group.*

4.2.2 Inflammatory cytokines

4.2.2.1 IL-1β

IL-1β was significantly increased in the OB compared to the LC group (73.19 ± 3.12 pg/mL vs 56.10 ± 3.93 pg/mL, $p<0.05$). GRT treated LC+GRT animals presented with significantly higher IL-1β levels when compared to the LC group (70.10 ± 1.85 pg/mL vs 56.10 ± 3.94 pg/mL, $p<0.05$). Furthermore, there was a significantly lower IL-1β level in the OB+GRT group compared to the OB group (60.00 ± 3.81 pg/mL vs 73.19 ± 3.12 pg/mL, $p<0.05$). There was no difference between the LC and OB+GRT groups (Figure 4.13).

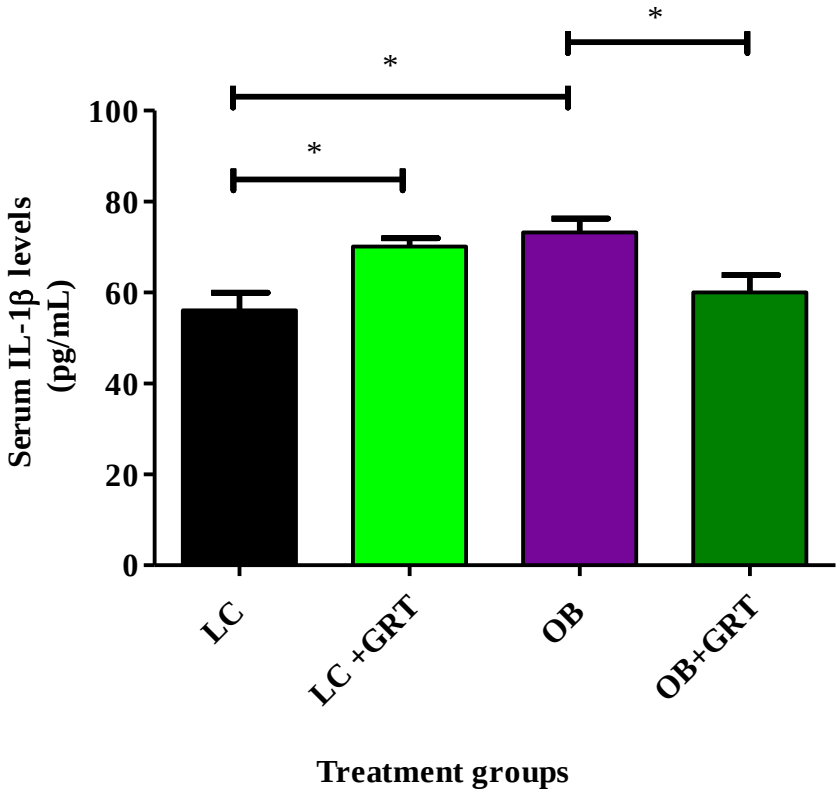

Figure 4.13: IL-1 β levels in treatment groups

*Data are presented as mean ± SEM. *p<0.05 according to ANOVA, LC: lean control, LC+GRT: lean group treated with GRT, OB: obese group, OB+GRT: obese animals treated with GRT. N=6 per group.*

4.2.2.2 IL-6

A statistical analysis of IL-6 using a one-way ANOVA did not show any significant difference between the treatment groups (Figure 4.14).

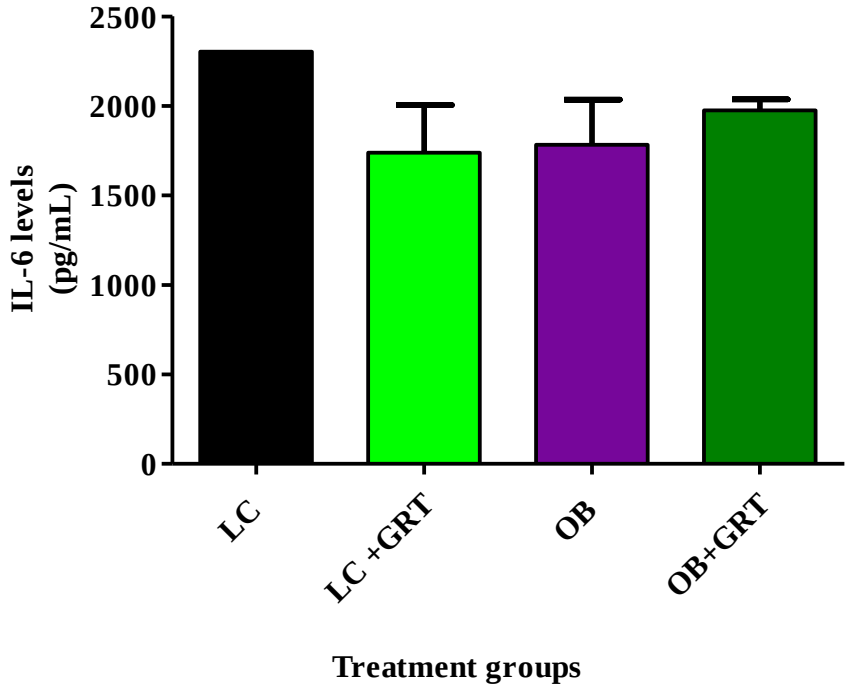

Figure 4.14: Serum IL-6 levels in treatment group

Data are presented as mean ± SEM. p>0.05 according to one-way ANOVA, LC: lean control, LC+GRT: lean group treated with GRT. OB: obese group, OB+GRT: obese animals treated with GRT. N=6 per group.

4.2.2.3 IL-12

A statistical analysis of IL-12 using a one-way ANOVA did not show any significant difference between treatment groups (Figure 4.15).

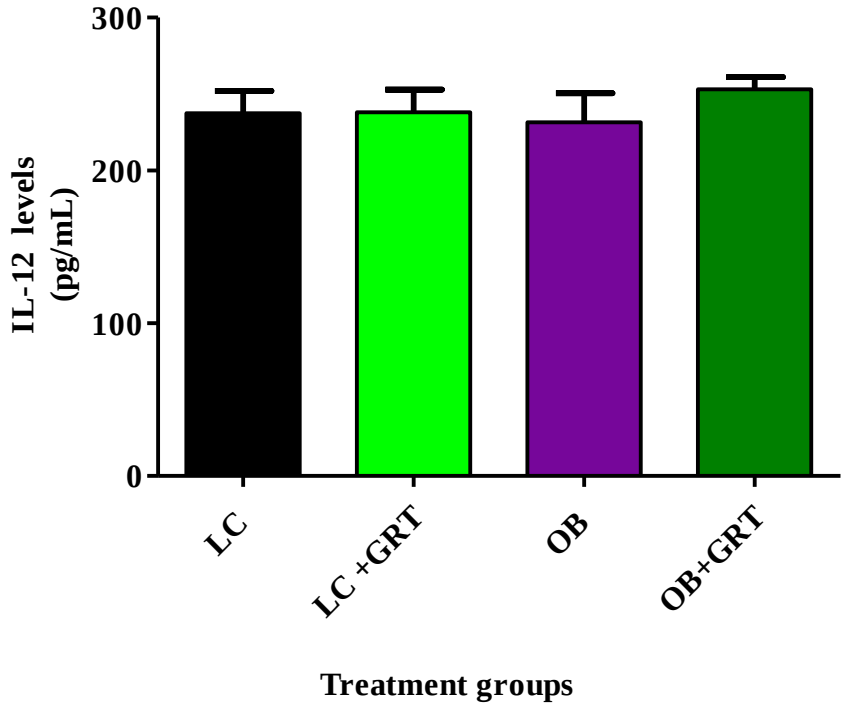

Figure 4.15: Serum IL-12 levels in treatment groups

Data are presented as mean ± SEM. p>0.05 according to one-way ANOVA, LC: lean control, LC+GRT: lean group treated with GRT, OB: obese group, OB+GRT: obese animals treated with GRT. N=6 per group.

4.2.2.4 IL-18

The IL-18 levels were significantly increased in the OB group compared to the LC group (280.20 ± 14.90 pg/mL vs 224.80 ± 2.20 pg/mL). The GRT treated OB+GRT group presented with significantly lower IL-18 levels when compared to the OB group (192.10 ± 9.92 pg/mL vs 280.20 ± 14.90 pg/mL, $p<0.05$). There was also a significantly lower IL-18 level in the OB+GRT group compared to the LC+GRT group (192.10 ± 9.92 pg/mL vs 230.60 ± 3.80 pg/mL, $p<0.05$) and the LC group (192.10 ± 9.92 pg/mL vs 224.80 ± 2.20 pg/mL, $p<0.05$). Furthermore, there were no significant difference between the LC+GRT and LC group (Figure 4.16).

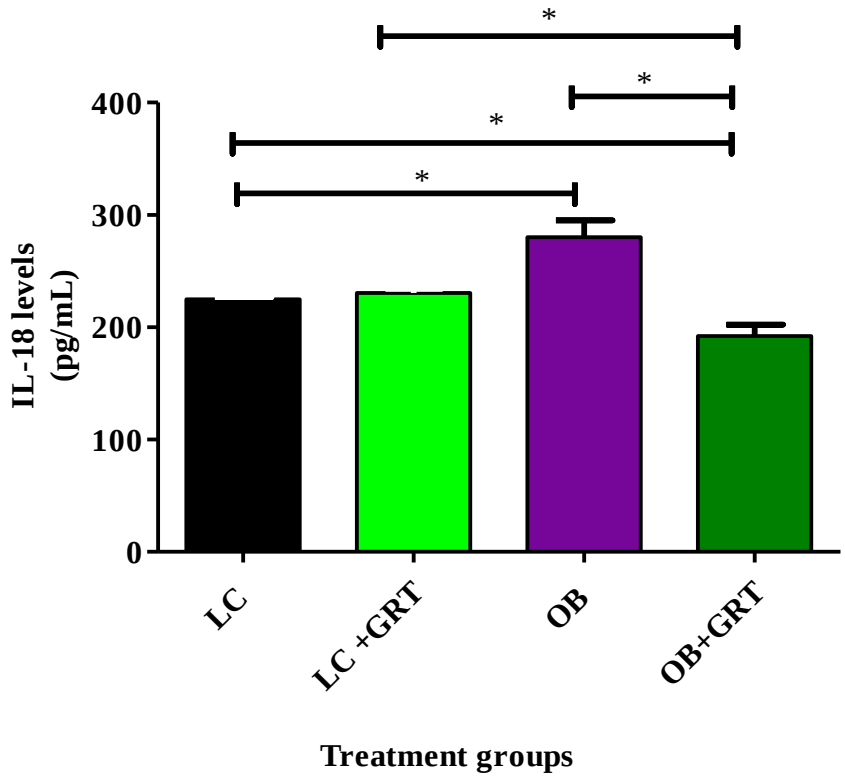

Figure 4.16: Serum IL-18 levels in treatment groups

*Data are presented as mean ± SEM. *p<0.05 according to one-way ANOVA, LC: lean control, LC+GRT: lean group treated with GRT, OB: obese group, OB+GRT: obese animals treated with GRT. N=6 per group.*

4.2.2.5 TNF-α

A significantly lower TNF-α level was observed in the OB animals compared to the LC group (3.43 ± 0.33 pg/mL vs 5.33 ± 0.69 pg/mL, p<0. 05). The GRT treated obese rats (OB+GRT) showed significantly higher TNF-α levels when compared to the OB group (5.20 ± 0.54 pg/mL vs 3.43 ± 0.33 pg/mL, p<0.05), and there was no difference between the OB+GRT and LC groups. There was no significant difference in TNF-α levels between LC+GRT vs LC group, and OB+GRT vs LC+GRT respectively (Figure 4.17).

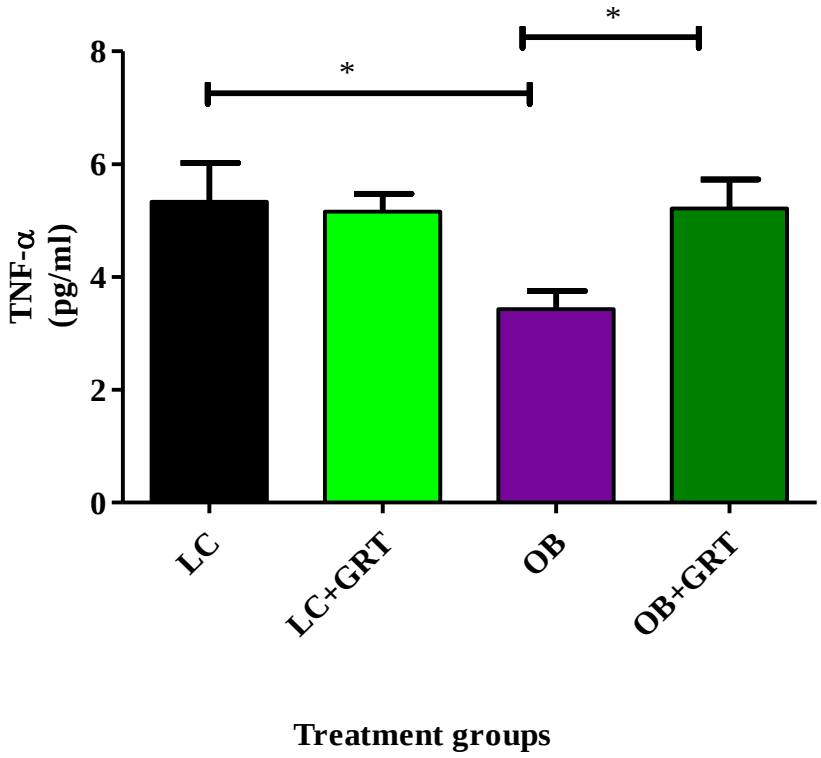

Figure 4.17: Serum TNF-α in treatment groups

*Data are presented as mean ± SEM. *p<0.05 according to one-way ANOVA, LC: lean control, LC+GRT: lean group treated with GRT. OB: obese group, OB+GRT: obese animals treated with GRT. N=6 per group.*

4.2.3 Testicular weight and body weight ratio

There was no significant difference in testicular weight (TW) between treatment groups (Figure 4.18). However, TW:BW was significantly lower in the OB group when compared to the LC group (0.0070 ± 0.0008 vs 0.0086 ± 0.0008, $p<0.05$). An ingestion of GRT in the OB+GRT group resulted in an increase in TW:BW, with no such increase in the untreated OB group (0.0085 ± 0.0005 vs 0.0070 ± 0.0008, $p<0.05$). However, the GRT supplementation in LC+GRT group did not change the TW:BW significantly when compared to untreated LC group (Figure 4.19).

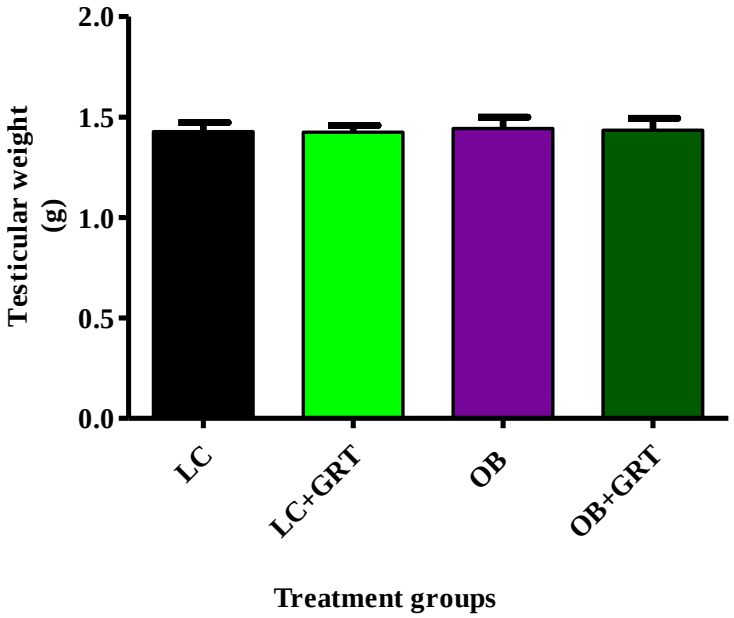

Figure 4.18: TWs in experimental groups

Data are presented as mean ± SEM. p>0.05 according to ANOVA, LC: lean control, LC+GRT: lean group treated with GRT, OB: obese group, OB+GRT: obese animals treated with GRT. N=7 per group.

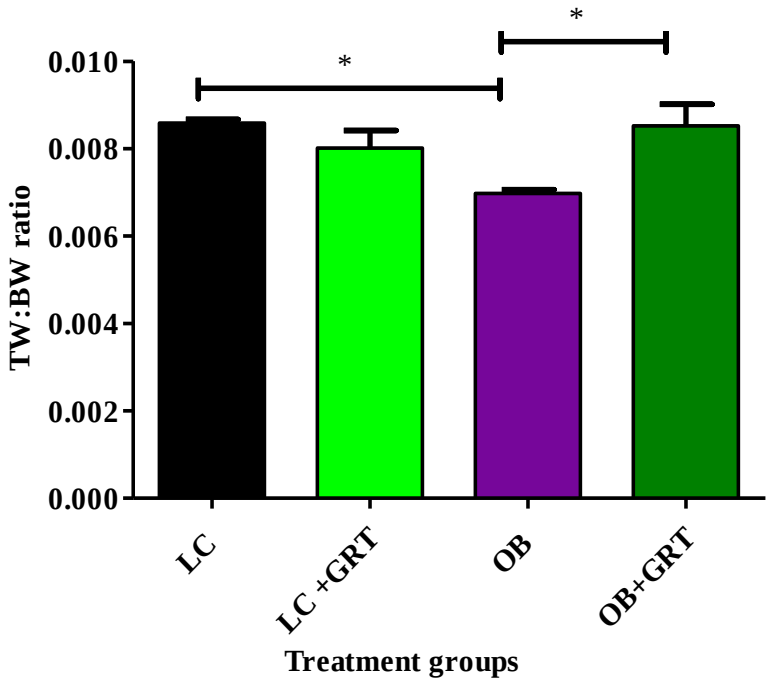

Figure 4.19: TW and body weight ratio

*Data are presented as mean ± SEM. *p<0.05 according to one-way ANOVA, LC: lean control, LC+GRT: lean group treated with GRT, OB: obese group, OB+GRT: obese animals treated with GRT. N=7 per group.*

4.2.4 Testicular histology and morphometry

The Johnsen scoring system for 50 cross-sections of seminiferous tubules per testis did not show any statistically significant difference between treatment groups (Table 4.1). Significant differences were only observed in seminiferous tubule parameters. There was a significant increase in seminiferous tubule area in the OB group when compared to the LC group (296587 ± 82452 µm² vs 118347 ± 6073 µm², $p<0.05$) (Table 4.2). Similarly, seminiferous tubule diameter was significantly increased in the OB group compared to the LC group (631.9 ± 95.6 µm vs 386.2 ± 9.5 µm, $p<0.05$). The treatment with GRT in the OB+GRT showed a significantly lower area and diameter of seminiferous tubules respectively when compared to OB animals [(98770 ± 2934 µm² vs 296587 ± 82452 µm², $p<0.05$), 354.2 ± 5.3 vs 631.9 ± 95.6 µm, $p<0.05$)]. Moreover, OB+GRT group had a smaller area and diameter than the LC group (98770 ± 2934 µm² vs 118347 ± 6073 µm², 354.2± 5.34 µm vs 386.2 ± 9.451 µm, $p<0.05$).

Table 4.1: Histomorphometric analysis of seminiferous tubules and lumen

	LC	LC +GRT	OB	OB+GRT
Johnsen scores Mean of 50 seminiferous tubule/testis	9.20 ± 0.01	9.10 ± 0.02	9.20 ± 0.04	9.10 ± 0.04
Seminiferous tubule area (µm²)	118347 ± 6073	111270 ± 1591	296587 ± 82452*	98770 ± 2934$^{\#*}$
Seminiferous tubule diameter (µm)	386.2 ± 9.5	375.9 ± 2.7	631.9 ± 95.6*	354.2± 5.3$^{\#*}$
Lumen areas (µm²)	30058 ± 3639	23084 ± 3561	43869 ± 14950	16491 ± 1016
Lumen diameter (µm)	191.2 ± 12.2	178 ± 13.5	254.2 ± 45.7	144.2 ± 4.4
Epithelial height (µm)	115.4 ± 9.0	112.3 ± 6.5	157.7 ± 28.4	113.2 ± 6.2

*All data is expressed as mean ± SEM. * $p<0.05$ vs LC, $^{\#}p<0.05$ vs OB according to one-way ANOVA. LC: lean control, LC+GRT: lean group treated with GRT, OB: obese group, OB+GRT: obese animals treated with GRT. N=5 per group.*

4.2.5 Testosterone and estradiol

There was a significantly lower T hormone level in the OB group compared to the LC group (16.25 ± 0.23 ng/mL vs 17.37 ± 0.11 ng/mL, $p<0.01$). The T hormone level of the OB+GRT group was significantly higher when compared to the OB group (17.36 ± 0.15 ng/mL, vs 16.25 ± 0.23 ng/mL, $p<0.01$). There was no difference between the LC and the LC+GRT, OB+GRT and LC+GRT groups (Figure 4.20).

The E2 hormone level was significantly increased in the OB group compared to the LC group (0.74 ± 0.01 ng/mL vs 0.67 ± 0.02 ng/mL, $p<0.05$). GRT treatment did not show any significant effect on the treated OB+GRT group when compared to the untreated OB group. Furthermore, there was no difference in E2 level of OB+GRT compared to that of the LC groups. However, GRT supplementation in LC+GRT animals showed a significantly higher E2 hormone level when compared to the LC animals (0.07 ± 0.01 ng/mL vs 0.74 ± 0.01 ng/mL, $p<0.05$) (Figure 4.21).

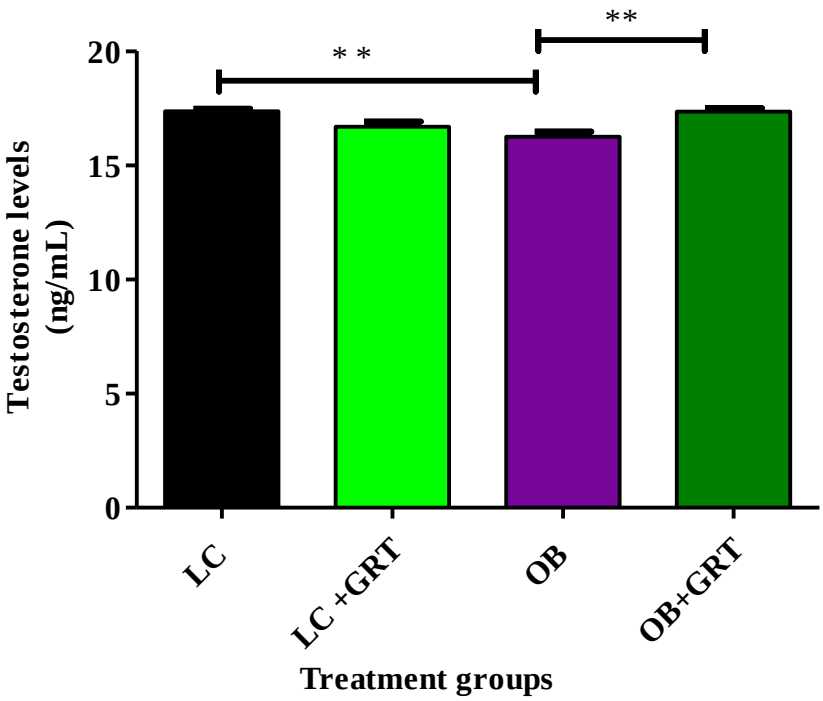

Figure 4.20: Serum testosterone levels in treatment groups

*Data are presented as mean ± SEM. **p<0.01 according to one-way ANOVA, LC: lean control, LC+GRT: lean group treated with GRT. OB: obese group, OB+GRT: obese animals treated with GRT. N=6 per group.*

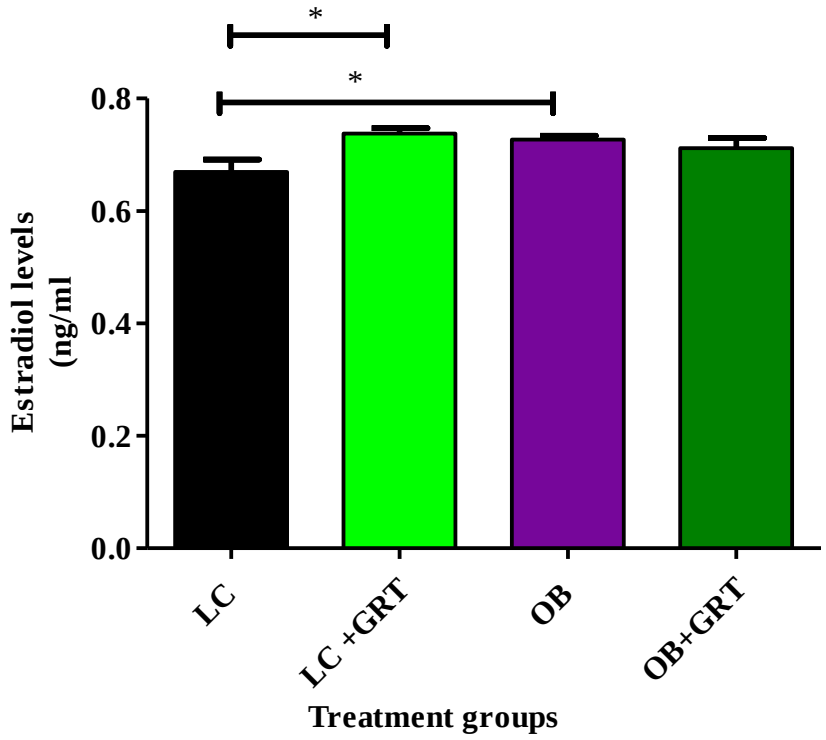

Figure 4.21: Serum estradiol levels in treatment groups

*Data are presented as mean ± SEM. *p<0.05 according to one-way ANOVA, LC: lean control, LC+GRT: lean group treated with GRT, OB: obese group, OB+GRT: obese animals treated with GRT. N=6 per group.*

4.2.6 Testosterone and estradiol ratio

The testosterone and estradiol (T:E2) ratio was significantly lower in the OB group compared to the LC group (21.69 ± 0.37 vs 24.40 ± 0.18, $p<0.001$). Treatment with GRT resulted in a significantly higher T:E2 ratio when compared to untreated OB group (23.99 ± 0.99 vs 21.69 ± 0.37, $p<0.05$), and there was also no difference between OB+GRT and LC. Additionally, a significantly lower T:E2 ratio in the LC+GRT group compared to the LC group was observed (22.60 ± 0.28 vs 24.40 ± 0.18, $p<0.01$) (Figure 4.22).

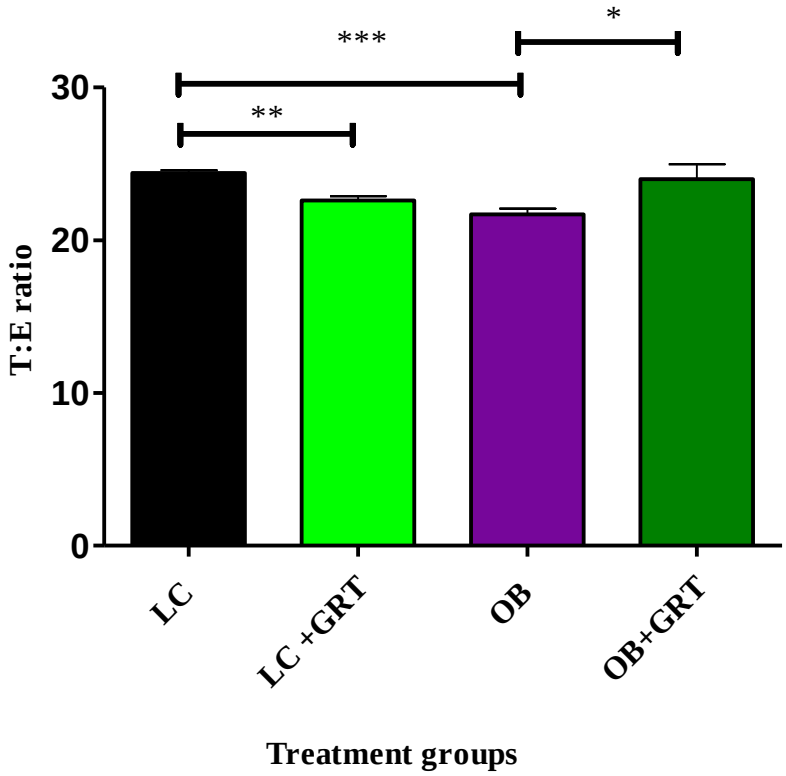

Figure 4.22: Testosterone and estrogen ratio in treatment groups

*Data are presented as mean ± SEM. *p<0.05; **p<0.01; ***p<0.001 according to one-way ANOVA, LC: lean control, LC+GRT: lean group treated with GRT, OB: obese group, OB+GRT: obese animals treated with GRT. N=6 per group.*

4.2.7 Testicular protein expression and phosphorylation

4.2.7.1 Total PKB expression, PKB phosphorylation and P-PKB/T-PKB ratio

The expression of testicular total PKB (T-PKB) in treatment groups are presented in Figure 4.23. The statistical results showed that there was no significant difference in T-PKB in the OB when compared to the LC group. The LC+GRT showed a significantly lower T-PKB expression compared to the LC group (0.22 ± 0.05 Densitometry units vs 1.22 ± 0.27 Densitometry units, $p<0.01$). The OB+GRT group did not show a significant difference compared to the OB group. However, a significantly higher T-PKB expression in OB+GRT was observed when compared to the LC+GRT (0.56 ± 0.06 vs 0.22 ± 0.05 Densitometry units, $p<0.05$).

Figure 4.24 and Figure 4.25 represent the respective PKB phosphorylation (P-PKB) and P-PKB/ T-PKB ratio in testicular tissue of rats subjected to different treatments. No significant differences were observed in the P-PKB and in P-PKB/T-PKB ratio.

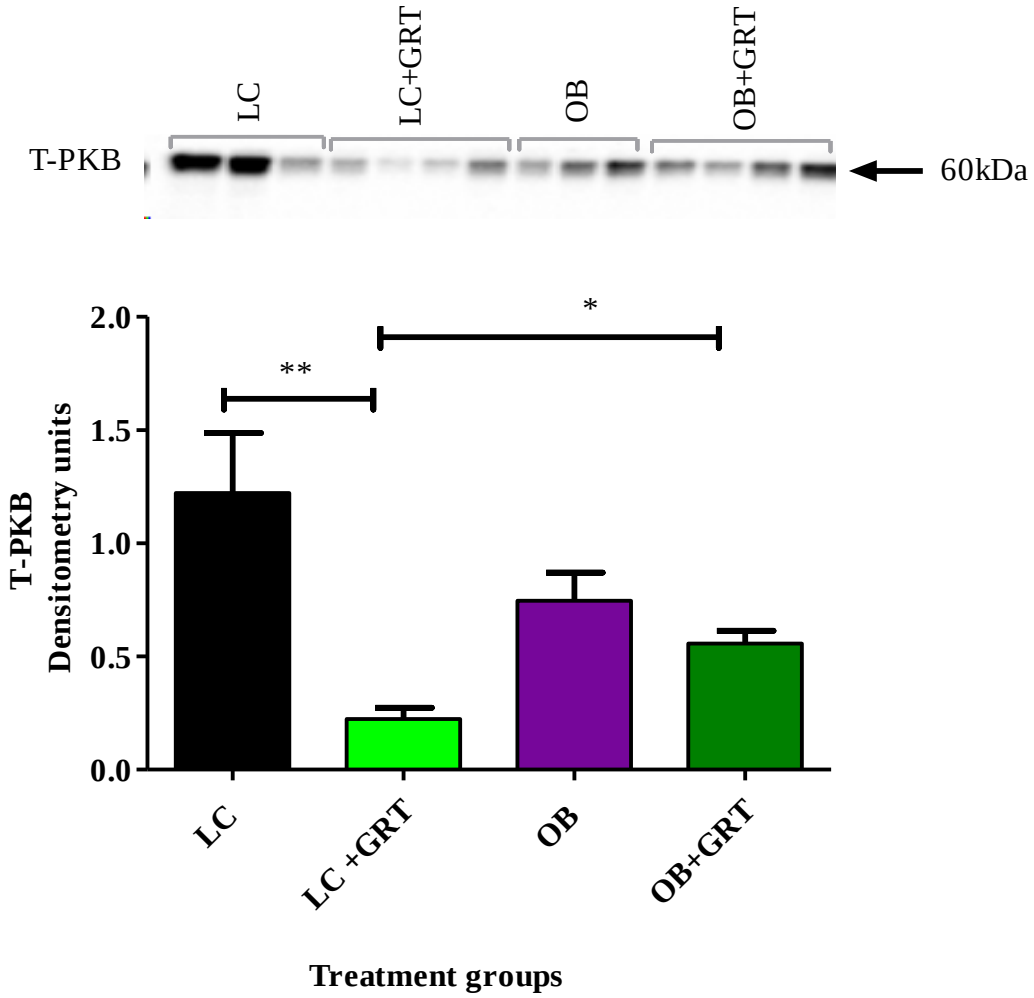

Figure 4.23: Testicular T-PKB expression in the treatment groups

*Data are presented as mean ± SEM. *p<0.05; **p<0.01 according to one-way ANOVA, LC: lean control, LC+GRT: lean group treated with GRT, OB: obese group, OB+GRT: obese animals treated with GRT. N=3–4 per group.*

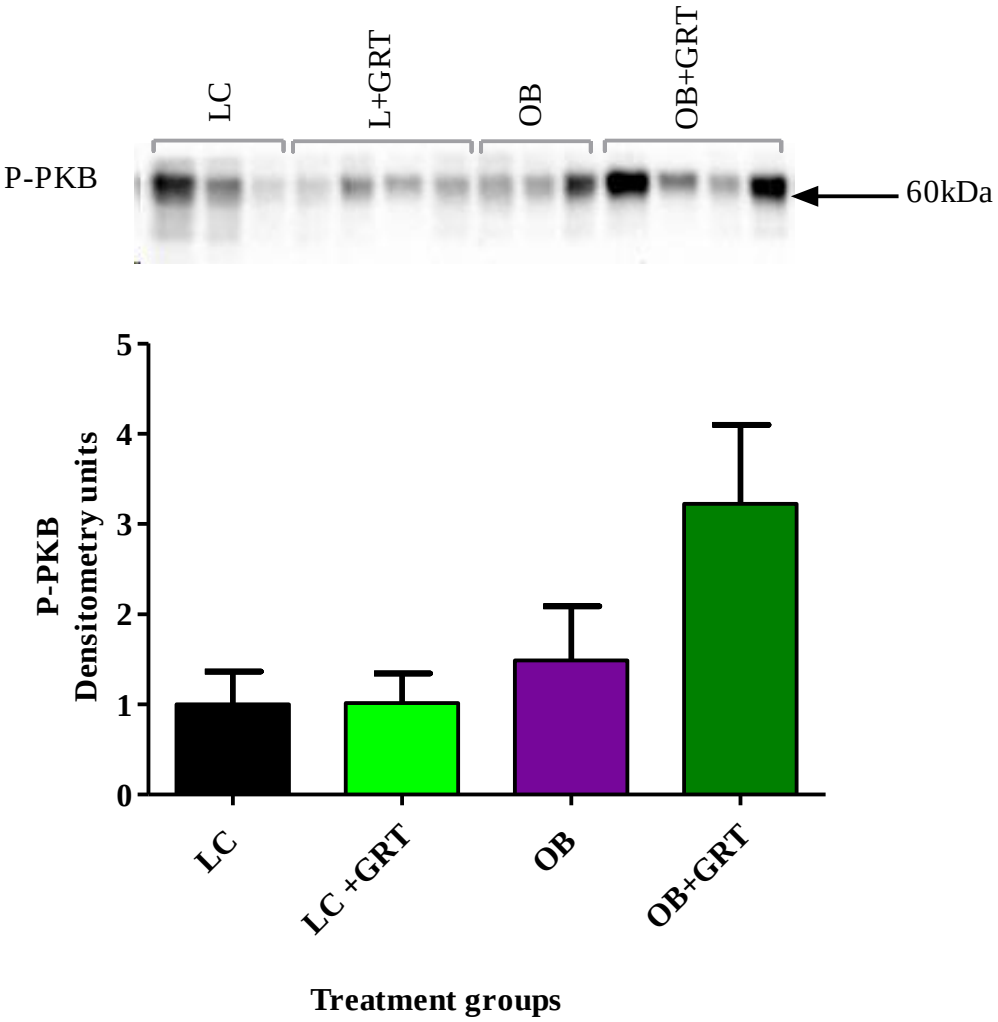

Figure 4.24: Testicular P-PKB in the treatment groups

Data are presented as mean ± SEM. p>0.05 according to one-way ANOVA, L+GRT: lean group treated with GRT, OB: obese control group, OB+GRT: obese group treated with GRT. N=3–4 per group.

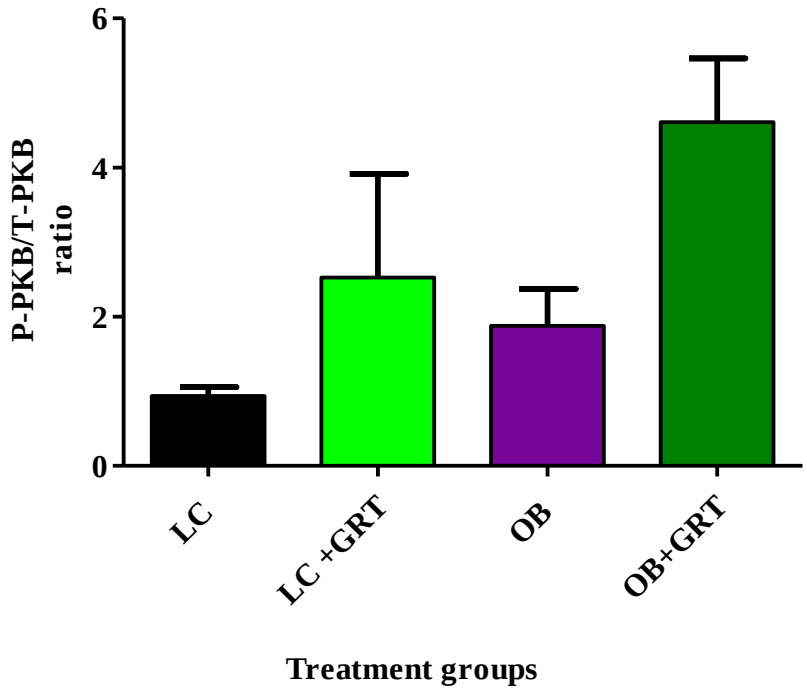

Figure 4.25: Testicular P-PKB and T-PKB ratio in the treatment groups

Data are presented as mean ± SEM. p>0.05 according to one-way ANOVA, LC: lean control, LC+GRT: lean group treated with GRT, OB: obese group, OB+GRT: obese animals treated with GRT. N=3–4 per group.

4.2.7.2 Total AMPK and phosphorylated AMPK

A significantly lower T-AMPK expression was observed in the OB group when compared to the LC group (0.04 ± 0.01 densitometry units vs 1.00 ± 0.19 densitometry units, $p<0.001$). The GRT decreased T-AMPK levels in the LC+GRT (0.28 ± 0.06 vs 1.00 ± 0.19, $p< 0.01$). GRT did not have any effect on the OB+GRT group when compared to the OB group. However, a significantly lower T-AMPK was observed in OB+GRT when compared to the LC+ GRT group (0.06 ± 0.01 ensitometry units vs 0.28 ± 0.06 densitometry units, $p<0.05$) (Figure 4.26). No phosphorylated AMPK could be detected in the samples.

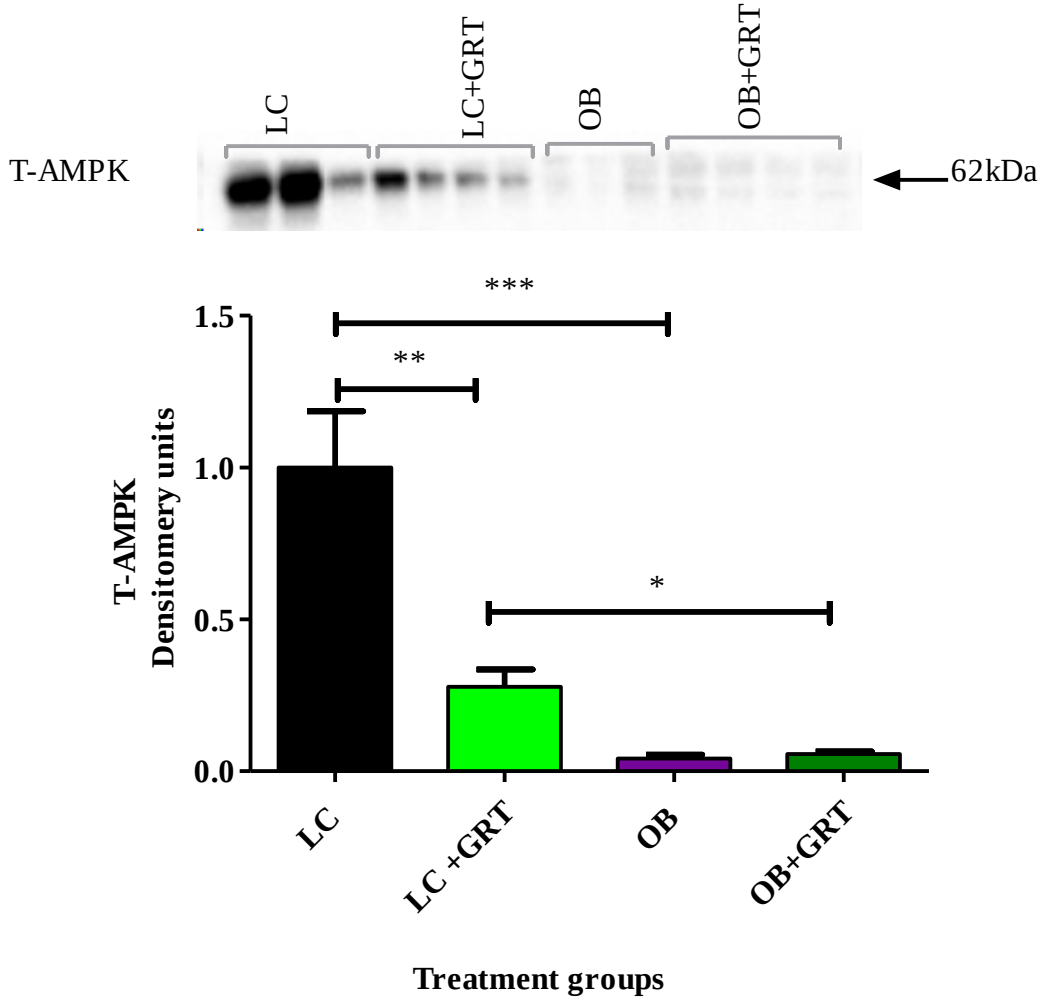

Figure 4.26: Testicular total expression of T-AMPK in treatment groups

*Data are presented as mean ± SEM. *p<0.05, **p<0.01, ***p<0.001 according to one-way ANOVA, LC: lean control, LC+GRT: lean group treated with GRT, OB: obese group, OB+GRT: obese animals treated with GRT. N=3–4 per group.*

4.2.7.3 Cleaved PARP expression in testicular tissue

The western blot and statistical results of testicular Cleaved PARP are presented in Figure 4.27. Cleaved PARP was significantly reduced in the OB group when compared to the LC (0.47 ± 0.15 vs 1.88 ± 0.06, p<0.001). Treatment of LC rats with GRT (LC+GRT) showed a significant difference in Cleaved PARP when compared to the LC (0.45 ± 0.05 densitometry units vs 1.88 ± 0.06 densitometry units, p<0.001), while no differences were observed in the levels of Cleaved PARP in OB rats treated with GRT (OB+GRT) vs untreated OB animals. There was a significantly higher Cleaved PARP

expression in animals from the OB+GRT group compared to the LC+GRT group (0.72 ± 0.08 densitometry units vs 0.45 ± 0.05 densitometry units, $p<0.05$).

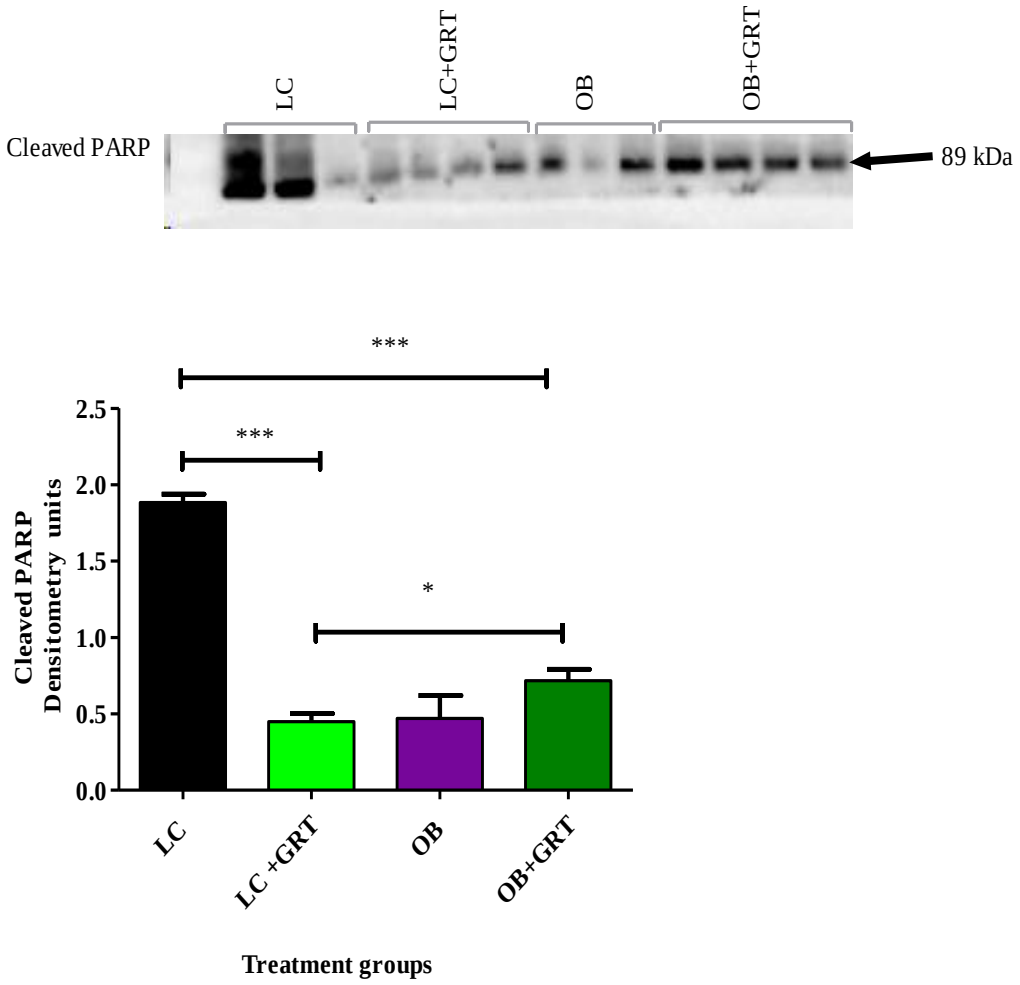

Figure 4.27: Cleaved PARP expression in testicular tissue

*Data are presented as mean ± SEM. *p<0.05, ***p<0.001 according to one-way ANOVA, LC: lean control, LC+GRT: lean group treated with GRT, OB: obese group, OB+GRT: obese animals treated with GRT. N=3–4 per group.*

4.2.7.4 Caspase 7 expression in testicular tissue

The untreated OB group showed a significant decrease in caspase 7 expression when compared to the untreated LC group (0.43 ± 0.08 densitometry units vs 1.35 ± 0.29 densitometry units, $p<0.01$). Administration of GRT to LC animals (L+GRT) lowered caspase 7 expression significantly compared to the untreated LC (0.10 ± 0.03 densitometry units vs 1.35 ± 0.30 densitometry units, $p<0.001$).

However, no significant differences were observed in caspase 7 expression between treated OB with GRT (OB+GRT) when compared to untreated OB group (Figure 4.28)

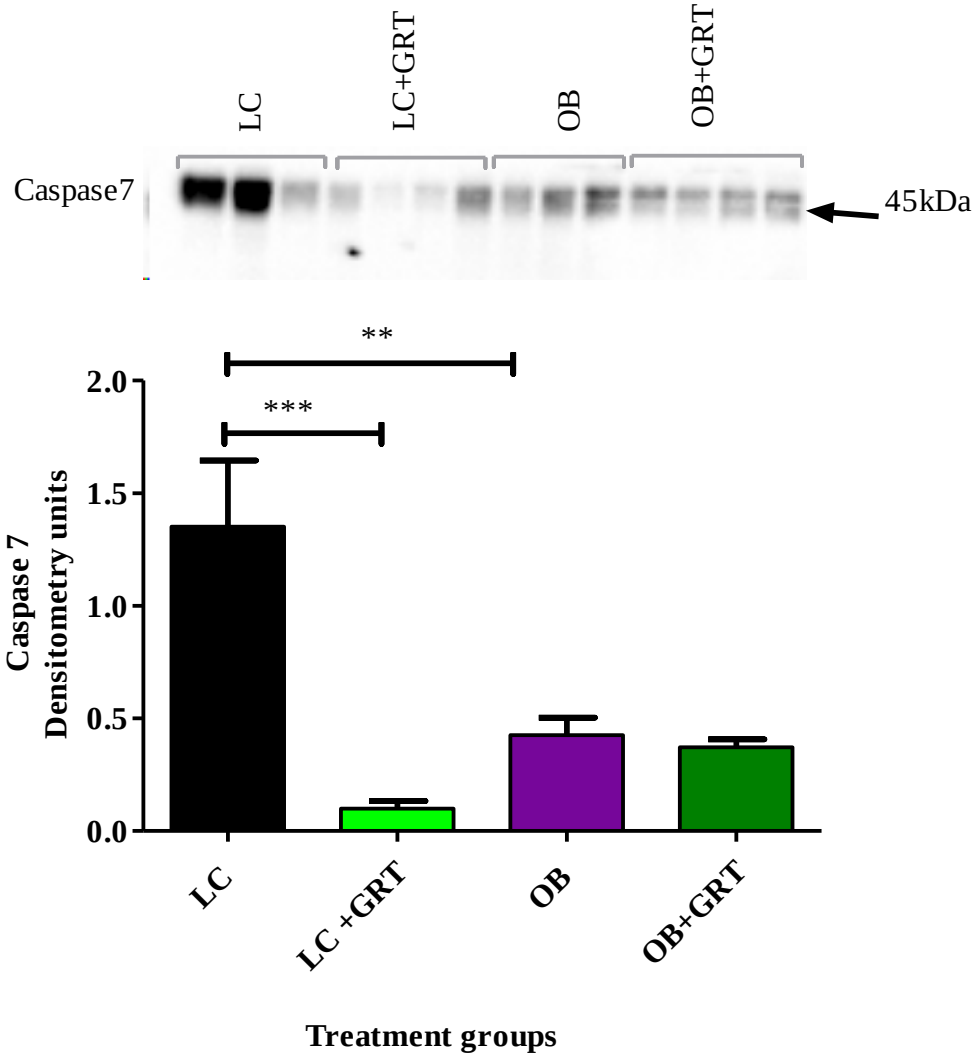

Figure 4.28: Testicular caspase 7 expression in treatment groups

*Data are presented as mean ± SEM. **p<0.01; *** p<0.001 according to one-way ANOVA, LC: lean control, LC+GRT: lean group treated with GRT, OB: obese group, OB+GRT: obese animals treated with GRT. N=3–4 per group.*

4.2.8 Testicular oxidative stress (OS)

4.2.8.1 Testicular SOD activity

Testicular SOD activity in treatment groups is presented in Figure 4.29. The SOD activity was significantly lower in the OB group than in the LC group (52.25 ± 1.69 U/mg protein vs 91.65 ± 5.22

U/mg protein, p<0.001). GRT supplementation resulted in a significantly lower SOD activity in the LC+GRT group compared to that of the LC group (63.48 ± 4.08 U/mg protein vs 91.65 ± 5.22 U/mg protein, p<0.001). Moreover, a significantly higher SOD activity was observed in the OB+GRT group when compared to the OB group (70.13 ± 3.19 U/mg protein vs 52.25 ± 1.69 U/mg protein, p<0.05). The OB+GRT group presented lower SOD activity compared to the LC group (70.13 ± 3.19 U/mg protein vs 91.65 ± 5.22 U/mg protein, p<0.05). No significant difference in SOD activity was observed between OB+GRT vs LC+GRT groups.

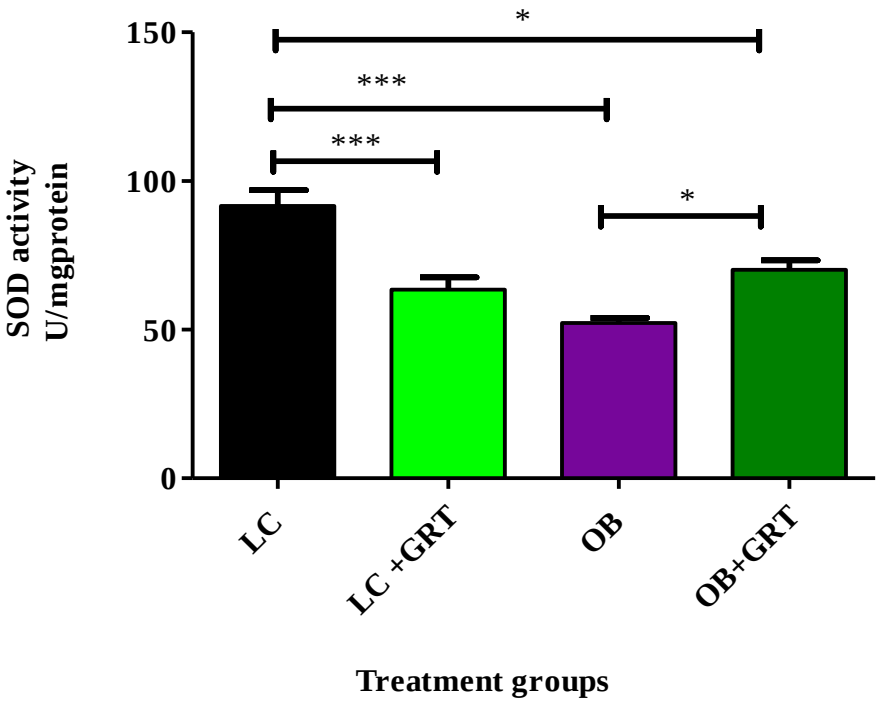

Figure 4.29: Testicular SOD activity in treatment groups

*Data are presented as mean ± SEM. *p<0.05, ***p<0.001 according to one-way ANOVA, LC: lean control, LC+GRT: lean group treated with GRT, OB: obese group, OB+GRT: obese animals treated with GRT. N=7 per group.*

4.2.8.2 Testicular CAT activity

Figure 4.30 represents testicular CAT activity of the treatment groups. The OB animals showed significantly lower CAT activity in testicular tissue compared to the LC group (10.51 ± 1.34 µmole H_2O_2 consumed/min/µg protein vs 53.08 ± 4.10 µmole H_2O_2 consumed/min/µg protein, p<0.001). CAT activity in the LC+GRT group was not significantly changed when compared to either LC group or OB+GRT group. Furthermore, OB+GRT group showed significantly higher CAT activity when

compared to the OB group (54.80 ± 4.84 µmole H_2O_2 consumed/min/µg protein vs 10.51 ± 1.34 µmole H_2O_2 consumed/min/µg protein, $p<0.001$), while the OB+GRT group did not differ significantly from the LC group.

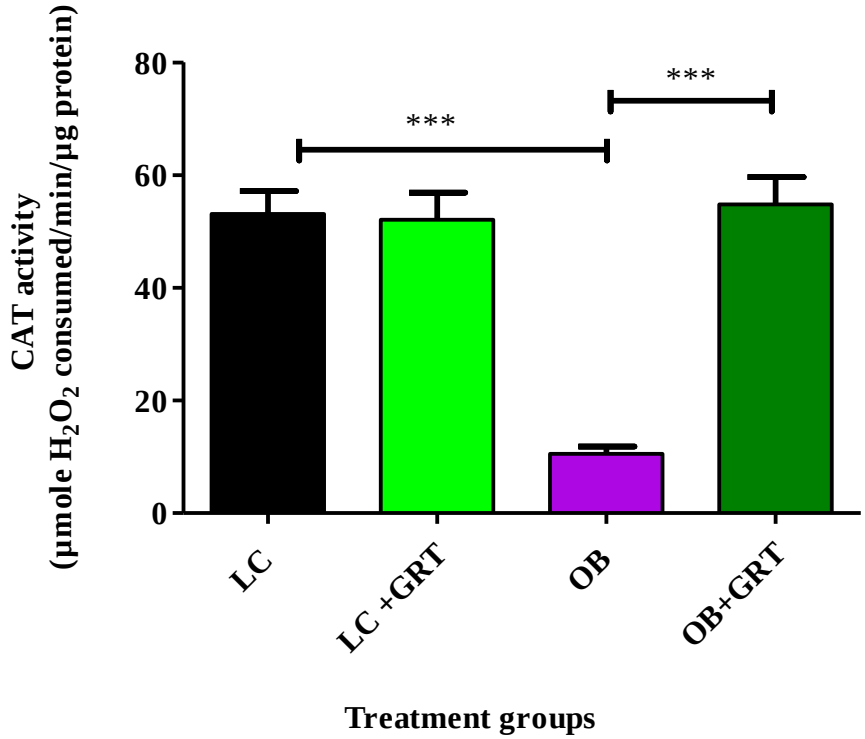

Figure 4.30: Testicular CAT activity in the treatment groups

*Data are presented as mean ± SEM.***p<0.001 according to one-way ANOVA, LC: lean control, LC+GRT: lean group treated with GRT, OB: obese group, OB+GRT: obese animals treated with GRT. N=7 per group.*

4.2.8.3 Testicular MDA levels

The statistical results of MDA levels in the testis are presented in Figure 4.31 for all treatment groups. The testicular MDA level was significantly higher in the OB group compared to the LC group (4.94 ± 0.45 µmol/mg protein vs 3.06 ± 0.31 µmol/mg protein, $p<0.01$). The MDA level in the testes of LC supplemented with GRT was not significantly different compared to that of the LC group. There were significantly lower testicular MDA levels in the OB+GRT group of rats compared to that of the OB group (3.49 ± 0.11 µmol/mg protein vs 4.94 ± 0.45 µmol/mg protein, $p<0.05$), while the OB+GRT group did not differ from either the LC or the LC+GRT groups.

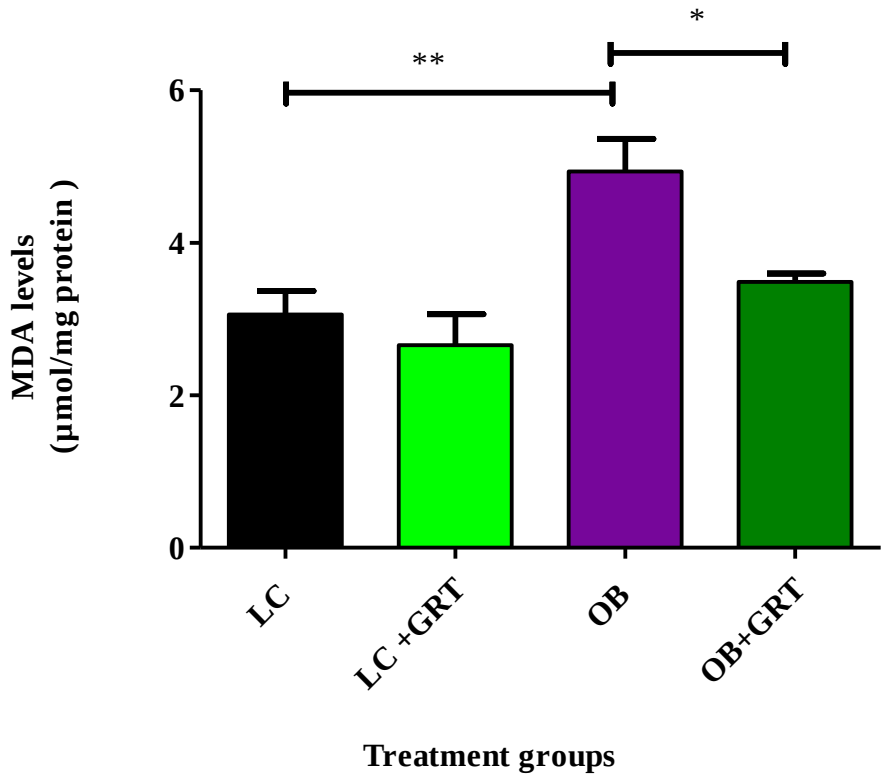

Figure 4.31: Testicular MDA levels in the treatment groups

*Data are presented as mean ± SEM. *p<0.05, **p<0.01 according to one-way ANOVA, LC: lean control, LC+GRT: lean group treated with GRT, OB: obese group, OB+GRT: obese animals treated with GRT. N=7 per group.*

4.2.9 Epididymal weight

Epididymal weight of the OB animals was significantly higher when compared to that of the LC animals (1.29 ± 0.04 g vs 1.14 ± 0.03 g, p<0.05). OB+GRT animals had significantly higher epididymal weights when compared to the OB animals (1.39 ± 0.02 g vs 1.29 ± 0.04, p<0.05), and also, the OB+GRT animals presented with a higher epididymal weight compared to the LC animals (1.39 ± 0.02 g vs 1.14 ± 0.03, p<0.001). Interestingly, the epididimides of LC animals supplemented with GRT were significantly heavier than those of their counterparts (1.24 ± 0.02 g vs 1.14 ± 0.03 g, p<0.05). However, the weight of LC+GRT was lower than OB+GRT (1.23 ± 0.02 g vs 1.39 ± 0.02 g, p<0.001) (Figure 4.32).

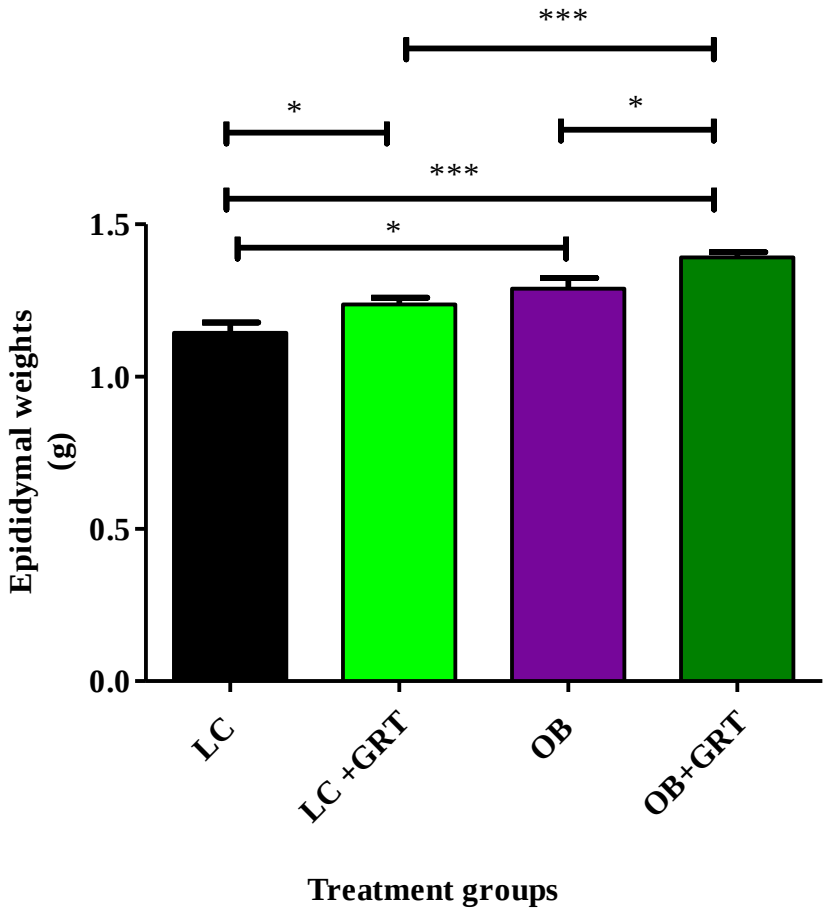

Figure 4.32: Total epididymal weights in the treatment groups

*Data are presented as mean ± SEM. *p<0.05, ***p<0.001 according to one-way ANOVA, LC: lean control, LC+GRT: lean group treated with GRT, OB: obese group, OB+GRT: obese animals treated with GRT. N=7 per group.*

4.2.10 Epididymal sperm parameters

The results in Table 4.2 represent sperm parameters: sperm concentration, viability, normal morphology, head defects, midpiece defects, and teratozoospermy index, total motility, progressive motility, curvilinear velocity (VC), straight line velocity (VSL) and average path velocity (VAP).

Table 4.2: Summary of basic and functional sperm parameters

	LC	LC+GRT	OB	0B+GRT
Sperm concentration (10^6 sperm /mL)	1.79 ± 0.15	1.72 ± 0.13	1.22 ± 0.14*	2.15 ± 0.16$^{\#}$
Viability (%)	57.14 ± 2.75	61.00 ± 3.61	42.71 ± 2.28**	55.14 ± 2.08$^{\#}$
Normal morphology (%)	52.55 ± 3.45	56.33 ± 3.24	45.45 ± 3.24*	64.75 ± 2.73$^{\#\#*}$
Head defects (%)	47.12 ± 3.26	41.71 ± 3.36	56.84 ± 1.91*	33.93 ± 2.46$^{\#\#\# **}$
Midpiece defects (%)	1.33 ± 0.84	1.67± 0.33	3.30 ± 0.87	3.88 ± 0.97$^{\$}$
Teratozoospermy index (%)	1.02 ± 0.02	1.06 ± 0.01	1.05 ± 0.02	1.03 ± 0.01
Total motility (%)	81.16 ± 4.91	89.85 ± 2.18	76.95 ± 3.71	81.94 ± 3.03
Progressive motility (%)	59.21 ± 2.82	72.0 ± 5.0*	48.19 ± 2.57*	65.86± 4.36$^{\#\# \$}$
VCL (µm/s)	183.80 ± 13.20	169.20 ± 9.31	144.50 ± 8.39*	180.30 ± 5.32$^{\#}$
VSL (µm/s)	46.97 ± 2.44	55.59 ± 2.55*	38.26 ± 3.52*	51.98 ± 2.14$^{\#\#}$
VAP (µm/s)	76.07 ± 2.52	88.29 ± 3.48*	71.42 ± 2.25*	83.60 ± 5.02$^{\#}$

*All data is expressed as mean ± SEM. * p < 0.05, ** p < 0.01 vs LC, $^{\$}p<0.05$, $^{\$\$}p<0.01$, $^{\$\$\$}p<0.001$ vs LC + GRT, $^{\#}p<0.05$, $^{\#\#}p<0.01$ vs OB according to one-way ANOVA. LC: lean control, LC+GRT: lean group treated with GRT, OB: obese group, OB+GRT: obese animals treated with GRT. N=7 per group.*

4.2.10.1 Sperm concentration

OB animals showed a significant decrease in sperm concentration when compared to the LC animals ($1.22 \pm 0.14 \times 10^6$ sperm/mL vs $1.98 \pm 0.14 \times 10^6$ sperm/mL, $p<0.05$). OB+GRT group showed significantly higher sperm concentration compared to the untreated OB ($2.15 \pm 0.16 \times 10^6$ sperm/mL vs $1.22 \pm 0.14 \times 10^6$ sperm/mL, $p<0.05$). Furthermore, there was no significant difference between the OB+GRT and LC+GRT groups, and the LC+GRT and LC groups (Table 4.2).

4.2.10.2 Sperm viability

The animals from the OB group showed significantly lower sperm viability compared to that of the LC group (42.71 ± 2.28% vs 57.14 ± 2.75%, $p<0.01$). The sperm viability of LC+GRT animals was not significantly different than that of the LC group. Furthermore, there was a significantly higher sperm viability in the OB group treated with GRT (OB+GRT) when compared to the untreated OB (55.14 ± 2.08% vs 42.71 ± 2.28%). The OB+GRT did not differ from L+GRT and LC groups (Table 4.2).

4.2.10.3 Sperm morphology

Normal sperm morphology in the OB group was decreased compared to that of the LC group (45.45 ± 3.24% vs 52.55 ± 3.45%, $p<0.05$). The normal sperm morphology of LC animals subjected to GRT (LC+GRT) did not show any significant difference compared to the untreated LC animals. The OB+GRT group showed a significantly higher normal sperm morphology when compared to the untreated OB animals (64.75 ± 2.73% vs 45.45 ± 3.24%, $p<0.01$), and the OB+GRT group had a higher % of normal morphology than the LC group (64.75 ± 2.73% vs 52.55 ± 3.45%, $p<0.05$) (Table 4.2).

4.2.10.3.1 Sperm head defects

OB animals presented with significantly higher sperm head defects when compared to the LC animals (56.84 ± 1.91% vs 47.12 ± 3.26%, $p<0.05$). No significant differences were observed between the LC+GRT and LC groups. Interestingly, the OB+GRT group presented with significantly decreased sperm head defects when compared to the OB group (33.93 ± 2.46% vs 56.84 ± 1.91%, $p<0.001$), while the OB+GRT group presented with low head defects compared to LC group (33.93 ± 2.46% vs

47.12 ± 3.26%, p<0.01). There were no statistically significant differences between the OB+GRT and LC+GRT groups (Table 4.2).

4.2.10.3.2 Sperm midpiece defects

The statistical results showed that the only significant difference in sperm midpiece defects was observed between OB+GRT and LC+GRT groups (3.88 ± 0.97% vs 1.67 ± 0.33%, p<0.05) (Table 4.2).

4.2.10.3.3 Teratozoospermy index

No statistically significant difference in teratozoospermy index was observed between the four treatment groups (Table 4.2).

4.2.10.4 Sperm motility

From the statistical analysis in Table 4.2, it can be ascertained that the total motility across four treatment groups did not differ significantly, despite an increasing trend after GRT treatment.

4.2.10.4.1 Progressive motility

The statistical results of progressive motility are shown in (Table 4.2). The progressive motility was significantly lower in the OB than in the LC group (48.19 ± 2.57% vs 58.12 ± 3.03%, p<0.05). A significantly higher percentage in progressive motility was observed in the LC+GRT when compared to the LC group (72.0 ± 5.0 ± 2.21% vs 58.12 ± 3.03%, p<0.05). The OB+GRT group showed a significantly higher percentage of progressive motility when compared to the OB group (65.86 ± 4.36% vs 48.19 ± 2.57%, p<0.01). Furthermore, OB+GRT animals presented a significantly lower percentage of progressive motility when compared to the LC+GRT group (65.86 ± 4.36% vs 72.0 ± 5.0± 2.20%, p<0.05).

4.2.10.4.2 Sperm kinematics/velocity parameters

VCL: The VCL of the OB group was significantly reduced compared to that of the LC group (144.5 ± 8.4 µm/s vs 183.8 ± 13.2 µm/s, p<0.05). The VCL of animals from LC+GRT was not significantly

different to that of the LC group and OB+GRT. A significantly higher VCL was observed in OB+GRT when compared to the OB group (180.3 ± 5.3 µm/s ± 144.5 ± 8.4 µm/s, $p<0.05$) (Table 4.2).

VSL: The OB group showed a significantly reduced VSL when compared to the LC group (38.26 ± 3.52 µm/s vs 46.97 ± 2.44 µm/s, $p<0.05$). A significantly higher VSL was observed in the LC+GRT group when compared to the LC group (55.59 ± 2.55 µm/s vs 38.26 ± 3.52 µm/s, $p<0.05$). Also, the OB+GRT group showed a significantly higher VSL than that of the OB group (51.98 ± 2.14 µm/s vs 38.26 ± 3.52 µm/s, $p<0.01$) (Table 4.2). There was no significant difference between the OB+GRT group and the L+GRT or between the OB+GRT and the LC groups.

VAP: Table 4.2 indicates that the VAP of the spermatozoa of the OB group was significantly lower when compared to that of the LC group (71.42 ± 2.25 µm/s vs 76.07 ± 2.52 µm/s, $p< 0.05$). A significantly higher VAP was observed in the LC+GRT when compared to the LC group (76.07 ± 2.52 µm/s vs 88.29 ± 3.48 µm/s, $p<0.05$). The VAP of OB+GRT was significantly higher compared to that of the OB group (83.60 ± 5.02 µm/s vs 71.42 ± 2.25 µm/s, $p<0.05$).

4.3 The effects of a green rooibos Extract on the reproductive function of obesity-induced hypertensive Wistar rats

4.3.1 Biometric data before and after initiation of GRT treatment

The biometric parameters that were monitored during the 16-week experimental period were water and food intake, the change of BWs, IP fat weights and glucose levels.

4.3.1.1 Food intake

Figure 4.33 shows the mean food intake in both LC and OBHT groups before the start of GRT treatment. The average food intake was significantly higher in the OBHT compared to the LC group (16.84 ± 0.26 g/rat/day vs 13.90 ± 0.08 g/rat/day, $p<0.001$). At 11 weeks, the animals started to receive the GRT treatment and therefore the food intake was subsequently monitored over the next 6 weeks in the four treatment groups (LC, LC+ GTR, OBHT, OBH+GRT). The OBHT animals showed a significant increase in food intake when compared to the LC animals (16.49 ± 0.59 g/rat/day vs 13.52 ± 0.14 g/rat/day, $p<0.001$). GRT treatment did not show any effect on food intake when compared either to the LC or OBHT animals. However, there was a significant difference between OBHT+GTR and LC+GRT (16.32 ± 0.69 g/rat/day vs 13.99 ± 0.77 g/rat/day, $p<0.05$) (Figure 4.34).

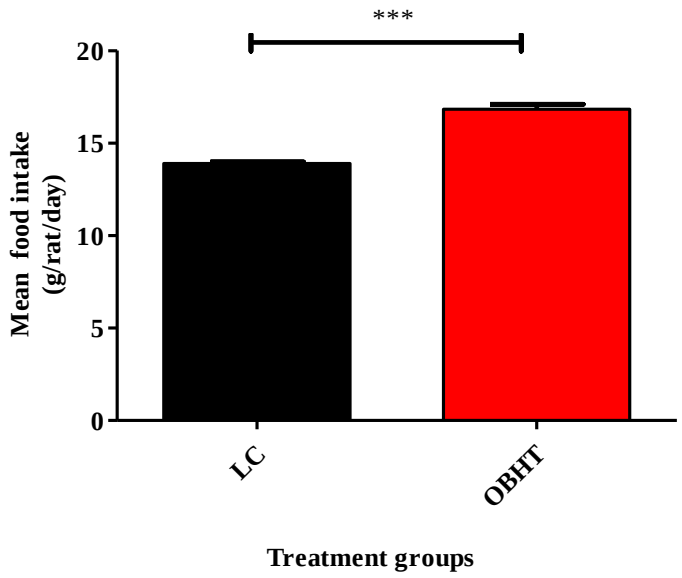

Figure 4.33: Mean food intake of the obese hypertensive and lean animals over 10 weeks

*Data are presented as mean ± SEM. *** p<0.001 according to a Student's t-test, LC= lean control group OBHT: obesity associated with hypertension group. N=14–21 per group.*

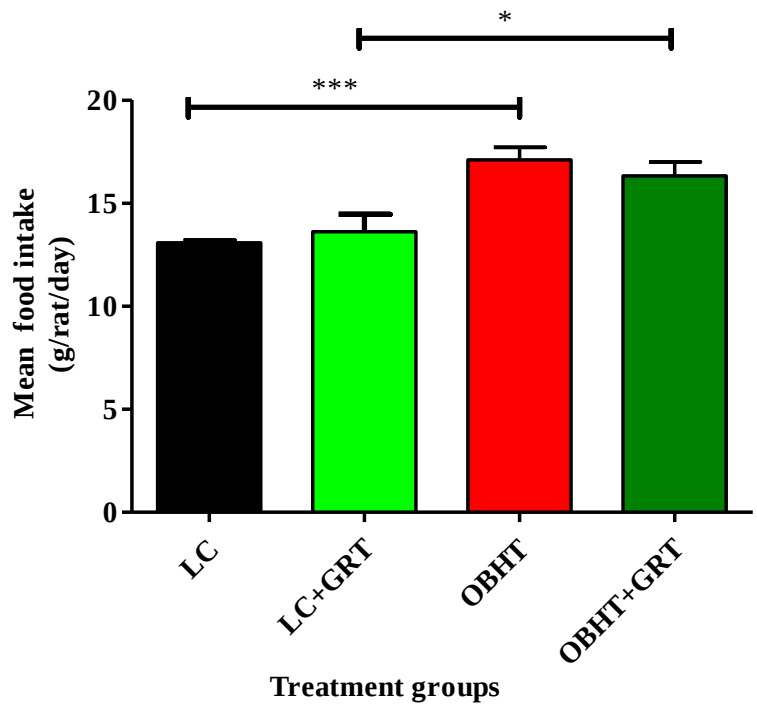

Figure 4.34: Mean food intake of the treatment groups from week 11 to week 16

*Data are presented as mean ± SEM. *p<0.05, ***p<0.001 according to one-way ANOVA test, LC: lean control, LC+GRT: lean group treated with GRT, OBHT: Obesity-induced hypertensive animal group, OBHT+GRT: obesity-induced hypertensive animals treated with GRT. N=7 per group.*

4.3.1.2 Water intake

Water intake of all the experimental animals was monitored once per week. Before the onset of treatment, the OBHT group consumed less water than the LC group (12.86 ± 0.31 mL/rat/day vs 22.02 ± 0.42 mL/rat/day, p<0.001) (Figure 4.35). Similarly, after GRT treatment, the average water intake of the OBHT group was less compared to that of the LC group (10.83 ± 0.54 mL/rat/day vs 20.73 ± 0.50 mL/rat/day, p<0.001) (Figure 4.36). The LC+GRT animals consumed more water than OBHT+GRT (20.47 ± 1.04 mL/rat/day vs 11.00 ± 0.55 mL/rat/day, p<0.001). A significantly lower water intake was observed in the OBHT+GRT group when compared to LC group (11.00 ± 0.55 mL/rat/day vs 20.73 ± 0.50 mL/rat/day, p<0.001). However, no significant difference in water intake was observed between the OBHT+GRT and OBHT groups (Figure 4.36).

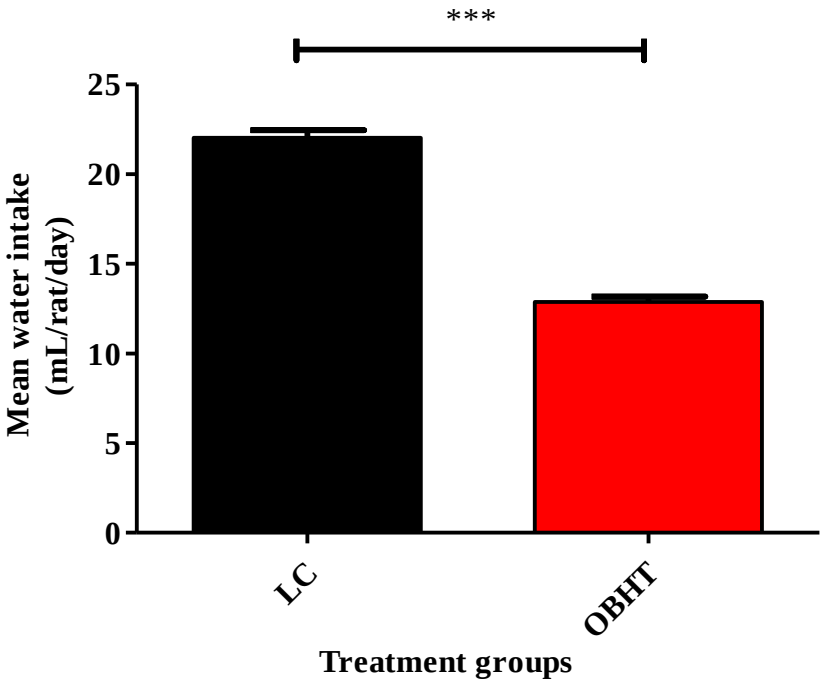

Figure 4.35: Mean water intake of LC animals and OBHT animals over 10 weeks

*Data are presented as mean ± SEM. ***p<0.001 according to a Student's t-test, LC: lean control animals, OBHT: Obesity-induced hypertensive animal group. N=14–21 per group.*

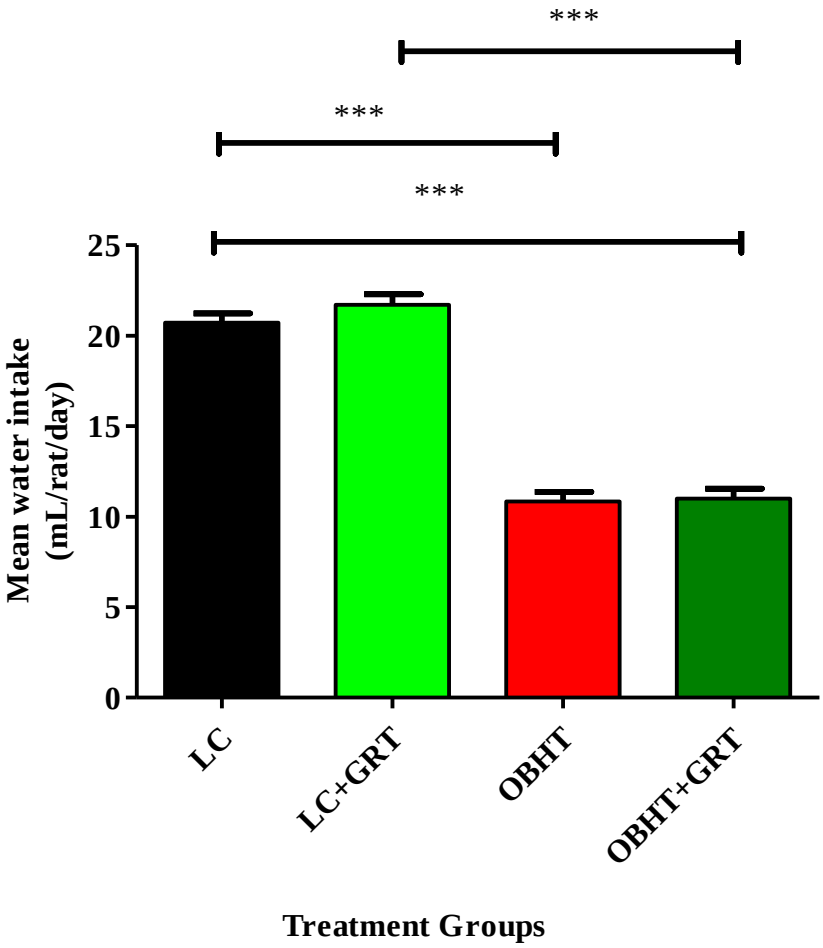

Figure 4.36: Mean water intake from week11 to week 16 in treatment groups

*Data are presented as mean ± SEM. ***p < 0.001 according to one-way ANOVA, LC: lean control, LC+GRT: lean group treated with GRT, OBHT: obesity-induced hypertensive animal group, OBHT+GRT: obesity-induced hypertensive animals treated with GRT. N=7 per group.*

4.3.1.3 Body weights

The change of BW was monitored before and after GRT treatment. In week 10 (before the onset of GRT treatment), the OBHT group showed a significantly higher mean BW compared to that of the LC group (322.9 ± 8.5 g vs 285.4 ± 4.4 g, p< 0.001) (Figure 4.37).

Figure 4.38 shows a statistical analysis of mean total BW after 6 weeks of GRT treatment (week 11–16) in week 16 (when the animals were euthanized). The mean BW of OBHT animals was significantly higher than that of the LC group (402.5 ± 11.7 g vs 346.3 ± 7.05 g, p<0.01). Treatment of OBHT+GRT with GRT resulted in a significantly lower BW than that of the untreated OBHT group (337.4 ± 12.21 g vs 402.5 ± 11.7 g, p<0.01). It was also observed that Captopril treatment

reduced mean BW in OBHT+Captopril group when compared to both the untreated OBHT group (254.6 ± 7.7 g vs 402.5 ± 11.7 g, p<0.001) and the OBHT+GRT group respectively (254.6 ± 7.7 g vs 337.4 ± 12.2 g, p< 0.001). However, there was no significant difference between the LC+GRT and LC groups; the LC+GRT and OBHT+GRT groups; or the LC and OBHT+GRT groups.

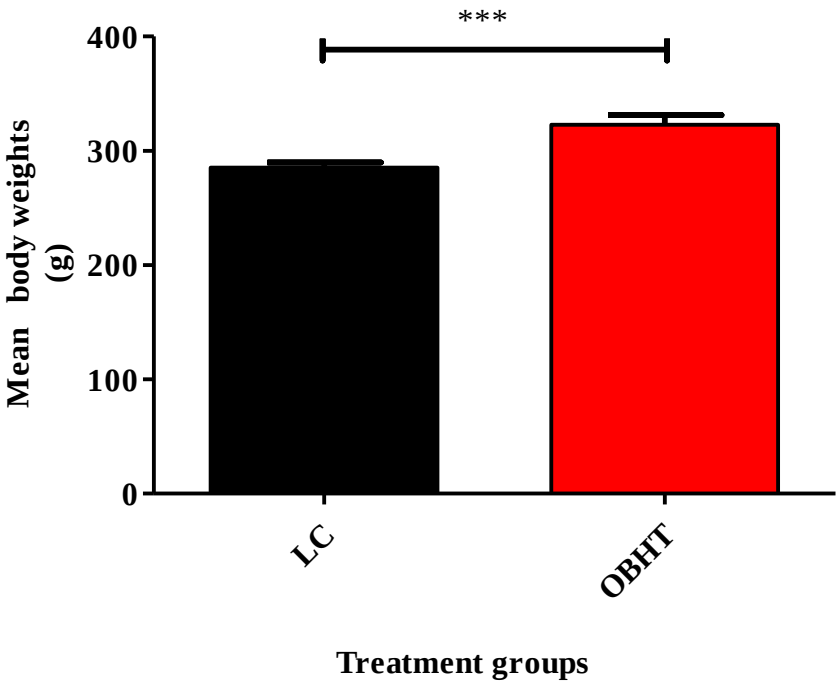

Figure 4.37: Mean total body weight of LC and OB group in week 10

*Data are presented as mean ± SEM. *** p<0.001 according to Student's t-test, LC: lean control, OBHT: obesity-induced hypertensive animal group. N=14–21 per group.*

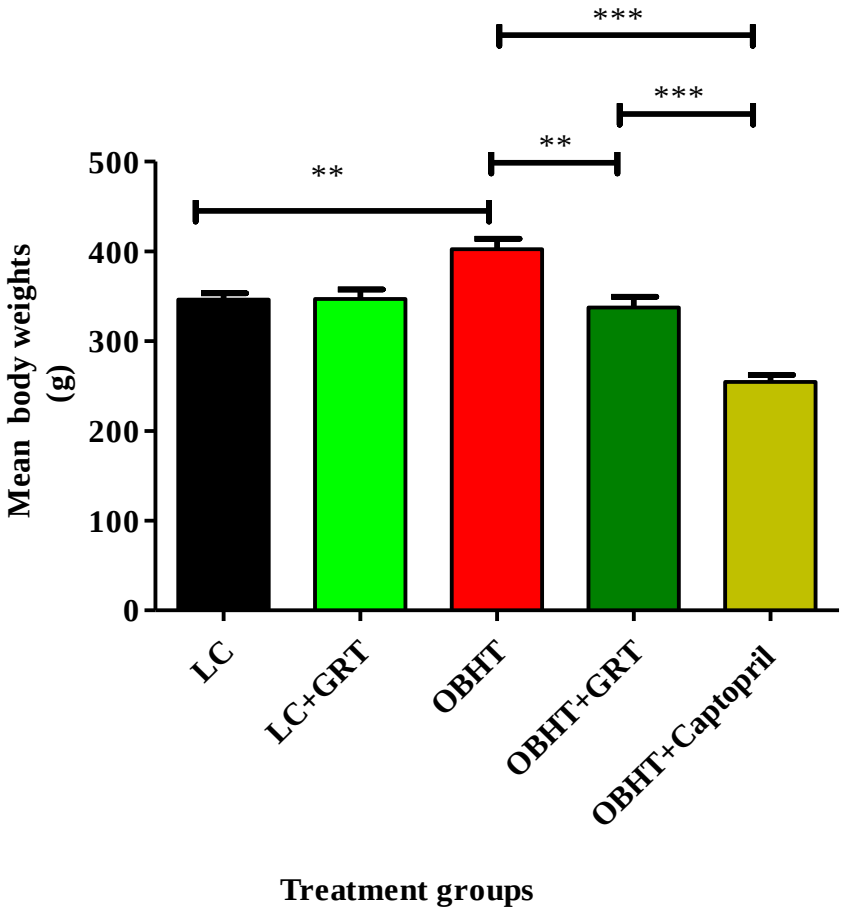

Figure 4.38: Mean total BW of treatment in week 16

*Data are presented as mean ± SEM. **p<0.01, ***p<0.001 according to one-way ANOVA test, LC: lean control, LC+GRT: lean group treated with GRT, OBHT: obesity-induced hypertension group, OBHT+GRT: obesity-induced hypertension animals treated with GRT, OBHT+Captopril: obesity-induced hypertension animals treated with Captopril. N=7 per group.*

4.3.1.4 Intra-peritoneal fat weight

The mean IP fat in relation to the BW per group was measured and expressed in percentage (%) as an adiposity index. IP fat % was higher in OBHT experimental groups than in the LC groups (5.34 ± 0.39% vs 1.96 ± 0.32%, p<0.001). It was observed that the adiposity index of OBHT+GRT was significantly lower compared to that of the OBHT group (3.73 ± 0.14% vs 5.34 ± 0.39%, p<0.01). Furthermore, adiposity index in OBHT+Captopril was significantly lower than both the OBHT group (2.36 ± 0.09% vs 5.34 ± 0.39% p<0.001) and the OBHT+GRT group respectively (2.36 ± 0.09% vs 3.73 ± 0.14%, p<0.05). There was no difference between the LC+GRT and LC groups, and between OBHT+GRT and LC (Figure 4.39).

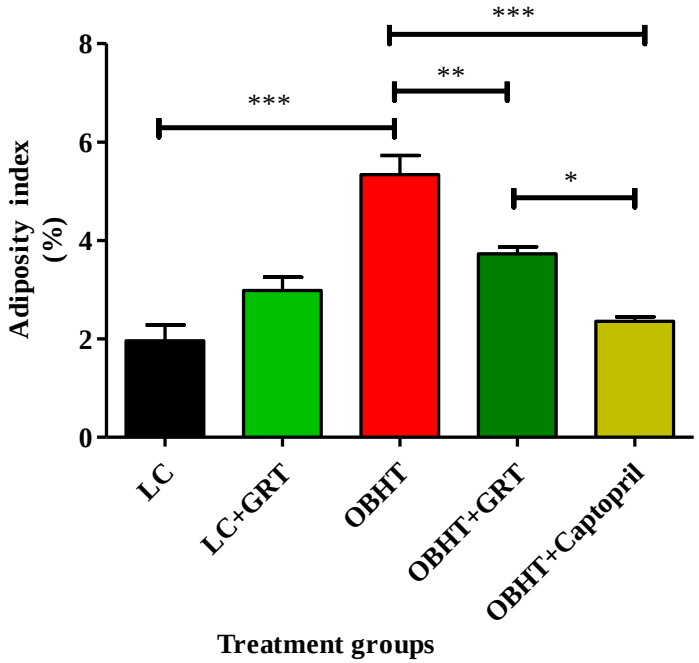

Figure 4.39: Adiposity index in different treatment groups

*Data are presented as mean ± SEM. *p<0.05, **p<0.01, ***p<0.001 according to one-way ANOVA. LC: lean control, LC+GRT: lean group treated with GRT, OBHT: obesity-induced hypertension group, OBHT+GRT: obesity-induced hypertension animals treated with GRT, OBHT+Captopril: obesity-induced hypertension animals treated with Captopril. N=7 per group.*

4.3.1.5 Insulin sensitivity and glucose levels

4.3.1.5.1 OGTT results at baseline level in week 10

From Figure 4.40, it is clear that the blood glucose levels of the OBHT animals were significantly increased from 10 min and 15 min after oral administration of sucrose solution when compared to the LC group (7.7±0.5 mmol/L vs 6.2 ± 0.2 mmol/L, $p<0.001$) and 8.3 ± 0.3 mmol/L vs 6.3 ± 0.4 mmol/L. Moreover, AUC in the OBHT group was higher than in the LC (728.8 ± 10.3 arbitrary units vs 690.8 ± 13.5 arbitrary units, $p<0.05$) (Figure 4.41).

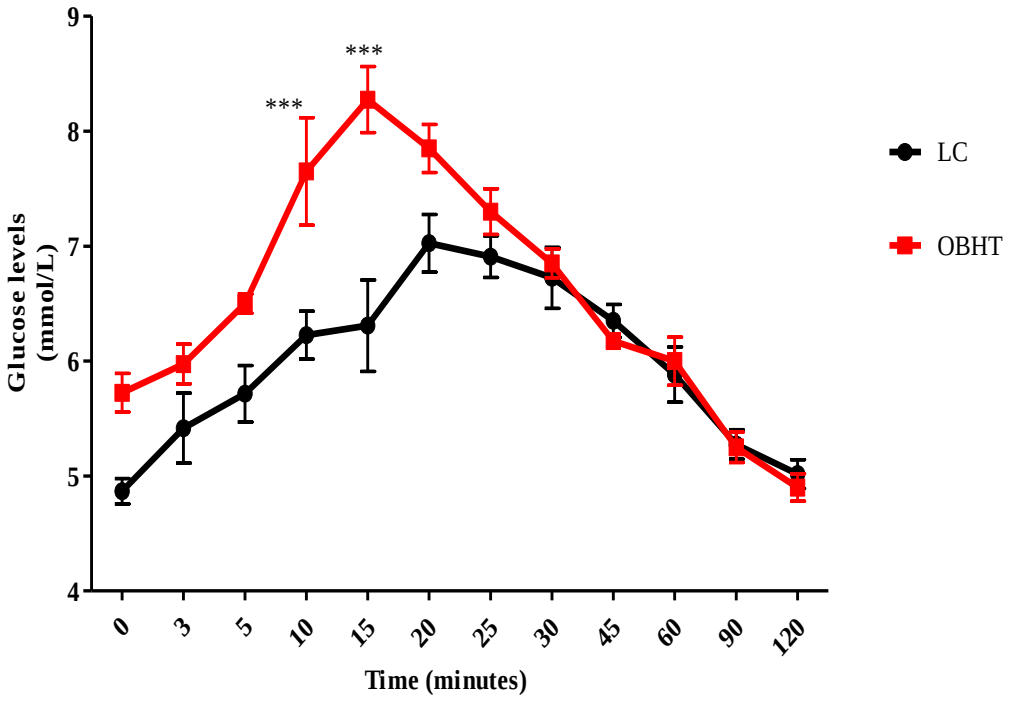

Figure 4.40: Oral glucose tolerance test results at baseline level in week 10 in the two experimental groups

*Data are presented as mean ± SEM. ***p<0.001 vs LC according to a two-way ANOVA, LC: lean control group, OBHT: obesity-induced hypertensive animal group. N=14–21 per group.*

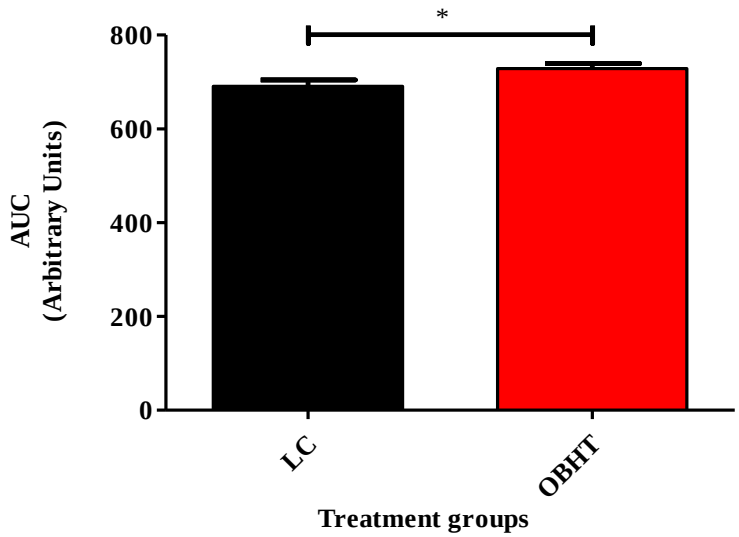

Figure 4.41: AUC representation of the effect of diet in glucose tolerance of LC and OBHT animals

*Data are presented as mean ± SEM. *p<0.05 according to a Student's t-test, LC: lean control group, OBHT: obesity-induced hypertensive animal group. N=14–21 per group.*

4.3.1.5.2 OGTT results after GRT treatment

In week 15, the curves of the groups, generated after gavaging animals with 50% sucrose solution, differed. The plasma glucose levels of the OBHT group was significantly higher than that of the LC group at 10 min (7.9 ± 0.4 mmol/L vs 6.4 ± 0.1 mmol/L, $p<0.01$) (Figure 4.42). The OBHT group presented significantly higher AUCs than the LC group (754.5 ± 12.8 arbitrary units vs 714.0 ± 12.1 arbitrary units $p<0.05$) (Figure 4.43). GRT treatment in the LC group did not show any significant change in glucose levels when compared to the untreated LC group. On the other hand, after only 20 min of the OGTT test, GRT treatment reduced glucose levels in OBHT+GRT group significantly when compared to that of the untreated OBHT group (6.0 ± 1.0 mmol/L vs 7.5 ± 0.4 mmol/L, $p<0.01$) (Figure 4.42). However, its AUC did not change significantly (Figure 4.43). According to AUC and ANOVA test, only diet (and not the GRT) had an effect on blood glucose levels.

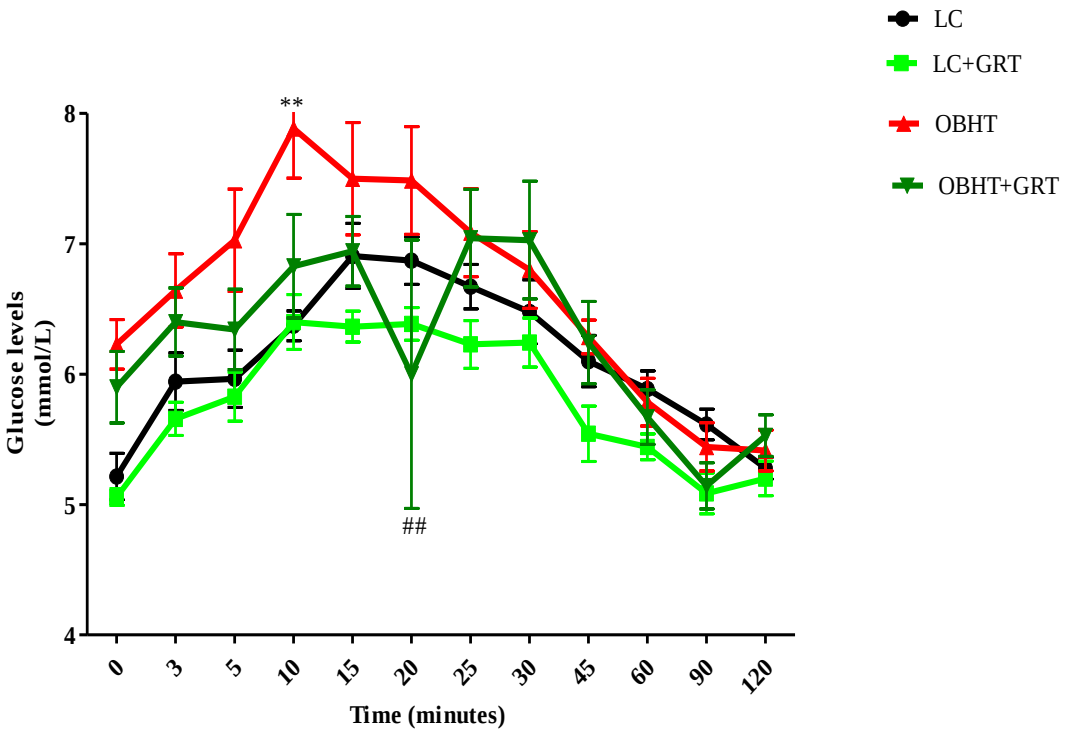

Figure 4.42: Glucose levels in treatment groups at 15th week in experimental group

*Data are presented as mean ± SEM. **$p < 0.01$ vs LC animals, $^{\#\#}p<0.01$ vs OBHT animals, $^{\$}p < 0.05$ vs LC+GRT animals according to a two-way ANOVA, LC: lean control, LC+GRT: lean group treated with GRT, OBHT: obesity-induced hypertension group, OBHT+GRT: obesity-induced hypertension animals treated with GRT, N=7 per group.*

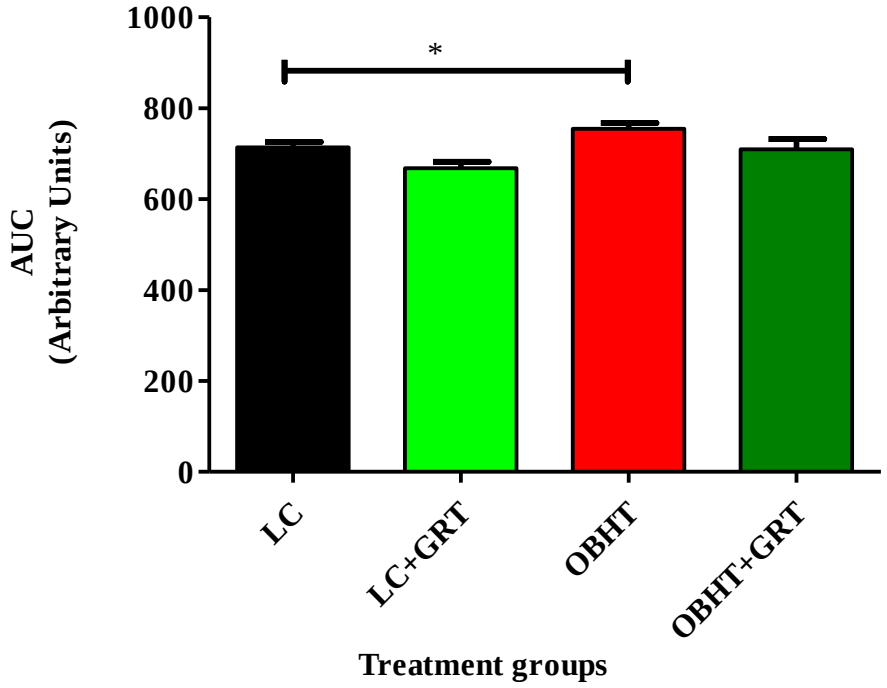

Figure 4.43: AUC representation of the effect of diet and GRT on glucose tolerance.

*Data are presented as mean ± SEM. **p<0.05 according to one-way ANOVA test, LC: lean control, LC+GRT: lean group treated with GRT, OBHT: obesity-induced hypertension group, OBHT+GRT: obesity-induced hypertension animals treated with GRT, N= 7 per group.*

4.3.1.5.3 Non-fasting blood glucose levels

An increase in non-fasting blood glucose levels were observed in OBHT animals compared to the LC group (8.2 ± 0.4 mmol/mL vs 6.7 ± 0.1 mmol/mL, $p<0.05$). Treatment with either the GRT or Captopril did not affect the blood glucose levels of the treated LC or OBHT animals. However, a significant difference was observed between the OBHT+GRT and LC+GRT groups (8.4 ± 0.2 mmol/mL vs 6.6 ± 0.2 mmol/mL, $p<0.001$) (Figure 4.44).

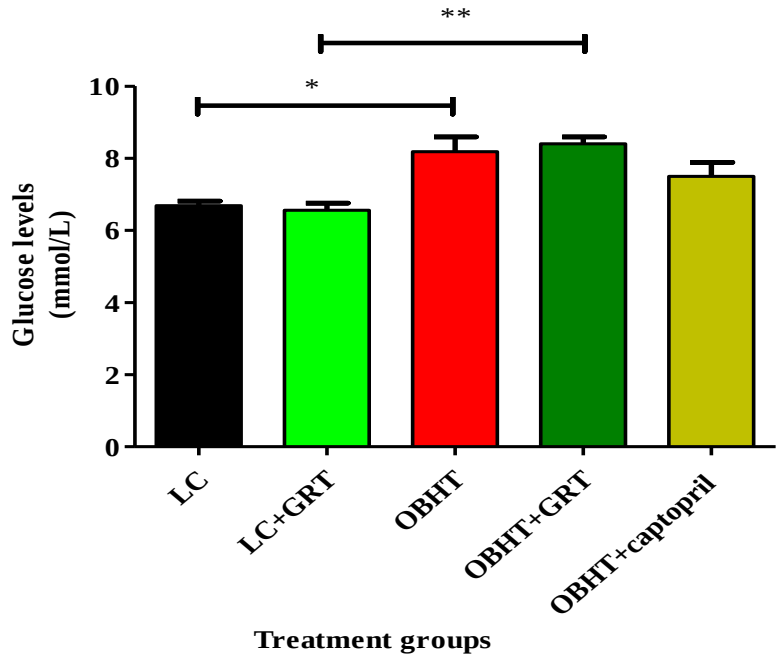

Figure 4.44: Non-fasting blood glucose levels

*Data are presented as mean ± SEM. *p<0.05, **p<0.01 according to one-way ANOVA, LC: lean control, LC+GRT: lean group treated with GRT, OBHT: obesity-induced hypertension group, OBHT+GRT: obesity-induced hypertension animals treated with GRT, OBHT+Captopril: obesity-induced hypertension animals treated with Captopril. N=7 per group.*

4.3.1.6 Inflammatory cytokines

The statistical analysis of inflammatory cytokine levels in rat serum, which includes 1 IL-1β, IL-6, IL-12, IL-18 and TNF-α, are presented in Table 4.3. IL-1β and IL-18 were significantly increased in OBHT group compared to the LC group ($p<0.05$). The LC+GRT group showed significantly higher IL-1β and IL-18 levels in comparison to the LC group ($p<0.05$). However, treatment of OBHT with either GRT or Captopril did not change IL-1β and IL-18 levels (no difference to that of the untreated OBHT group).

There was no significant difference in IL-6 levels between OBHT and LC animals. The GRT supplementation in LC+GRT animals did not significantly change IL-6 levels when compared to the LC group; however, GRT significantly reduced IL-6 levels in OBHT+GRT animals when compared to the untreated OBHT group (1897 ± 68 pg/mL vs 2310 ± 114). Consecutively, Captopril-treated OBHT animals showed a significantly lower IL-6 level compared to that of the untreated OBHT group (1617 ± 153 pg/mL vs 2310 ± 114 pg/mL, $p< 0.05$).

There was not a significant difference between the IL-12 and TNF-α levels of the treatment groups.

Table 4.3: Cytokines levels in different treatment groups

Cytokines	LC	LC+GRT	OBHT	OBHT+GRT	OBHT+ Captopril
IL-1β (ng/mL)	56.10 ± 3.93	68.82 ± 1.81*	79.99 ± 5.04*	65.99 ± 4.15	60.68 ± 18.66
IL-6 (ng/mL)	2303 ± 142	1740 ± 265	2310 ± 114	1897 ± 68$^{\#}$	1617 ± 153$^{\#}$
IL-12 (ng/mL)	257.0 ± 10.5	238.2 ± 14.8	253.2 ± 7.1	234.1 ± 11.8	196.7 ± 12.7
IL-18 (ng/mL)	224.0 ± 2.2	285.3 ± 54.9*	243.3 ± 31.0*	232.4 ± 19.4	201.3 ± 16.0
TNF-α (ng/mL)	4.65 ± 0.19	5.16 ± 0.31	4.37 ± 0.19	4.36 ± 0.23	3.37 ± 0.15

*All data are expressed as mean ± SEM. * $p < 0.05$ vs LC, $^{\#}p < 0.05$ vs OBHT according to one-way-ANOVA. LC: lean control, LC+GRT: lean group treated with GRT, OBHT: obesity-induced hypertension group, OBHT+GRT: obesity-induced hypertension animals treated with GRT, OBHT+Captopril: obesity-induced hypertension animals treated with Captopril. N=7 per group.*

4.3.2 Monitoring of blood pressure (BP) during treatment period

4.3.2.1 Systolic BP, diastolic BP and mean arterial pressure before GRT treatment

The statistical results of BP measurements before GRT treatment are summarized in Table 4.4. A significant high systolic (Figure 4.45), diastolic (Figure 4.46) and mean arterial pressure (Figure 4.47) were respectively observed in OBHT animals when compared to LC animals.

Table 4.4: Mean systolic, diastolic and arterial pressure of the OBHT and lean group

Groups	Mean **s**ystolic **p**ressure (mmHg)	Mean **d**iastolic pressure (mmHg)	Mean **a**rterial **p**ressure (mmHg)
LC	127.5 ± 2.6	79.4 ± 2.1	98.6 ± 2.3
OBHT	135.2 ± 1.8**	91.9 ± 2.9**	107.7 ± 1.6**

*All data are expressed as mean ± SEM. **p < 0.01 vs LC according to a Student's t-test. LC: lean control, OBHT: obesity-induced hypertension. N=14–21 per group.*

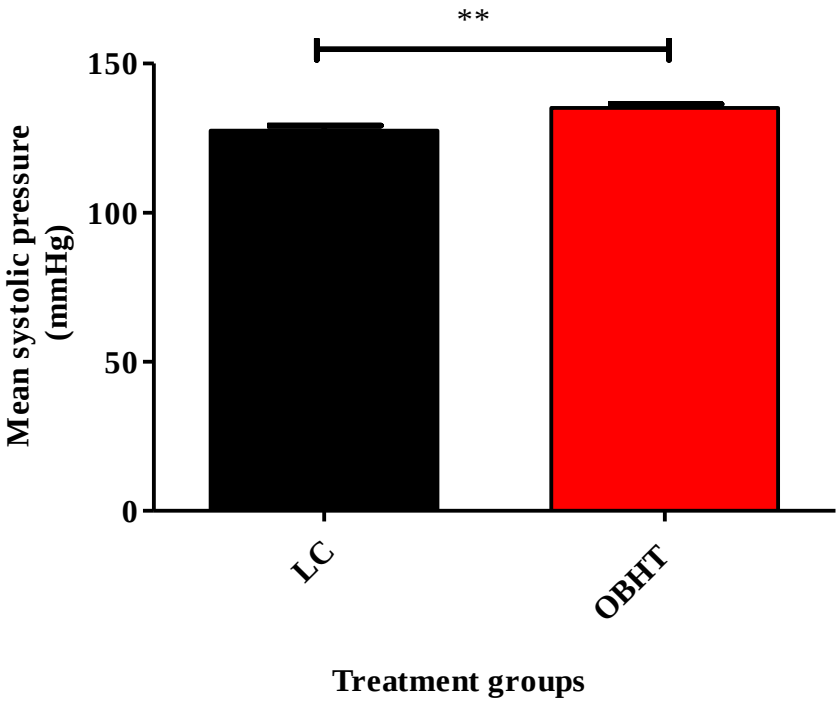

Figure 4.45: Mean systolic BP of the OB and LC animals

*Data are presented as mean ± SEM. **p<0.01 according to a Student's t-test, LC: lean control, OBHT: obesity-induced hypertensive animal group. N=14–21 per group.*

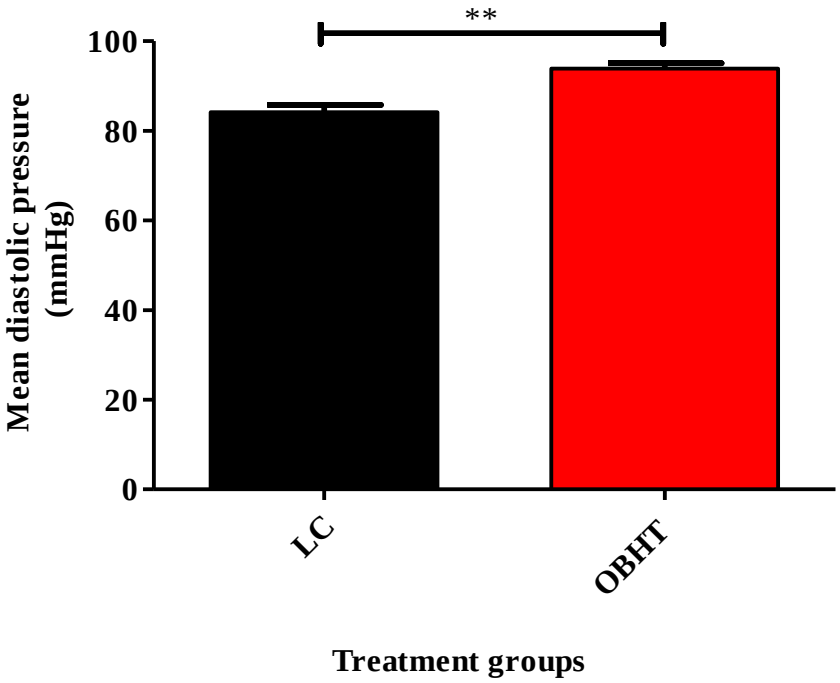

Figure 4.46: Mean diastolic BP of the OBHT and LC animals

*Data are presented as mean ± SEM. **p<0.01 according to a Student's t-test, LC: lean control, OBHT: obesity-induced hypertensive animal group. N=14–21 per group.*

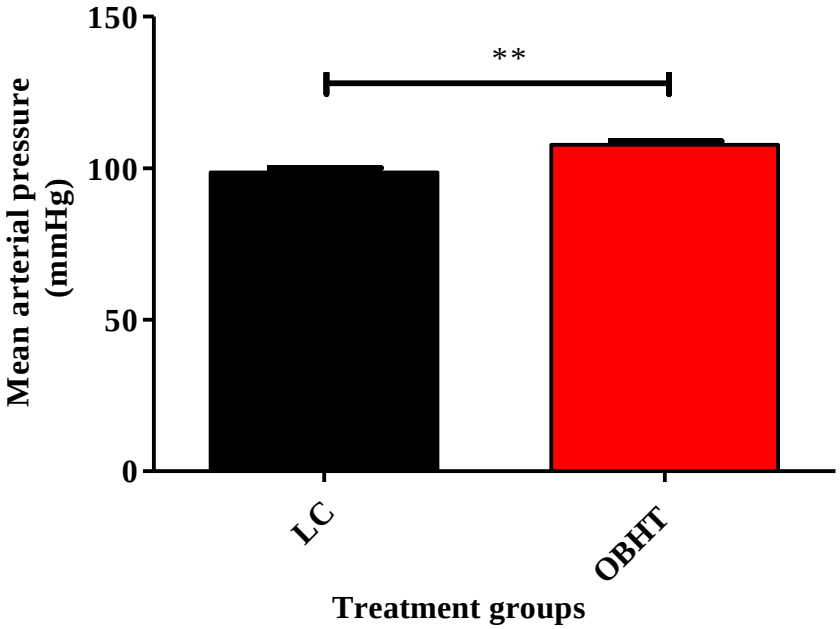

Figure 4.47: Mean arterial pressure of the OBHT and lean animals

*Data are presented as mean ± SEM. **p<0.01 according to a Student's t-test, LC: lean control, OBHT: obesity-induced hypertensive animal group. N=14–21 per group.*

4.3.2.2 Systolic BP, diastolic BP and mean arterial pressure after 6 weeks of GRT treatment

Table 4.5 represents the BP measurements of all experimental groups after 6 weeks of GRT treatment. Mean systolic BP (Figure 4.48), diastolic BP (Figure 4.49) and arterial pressure (Figure 4.50) were significantly increased in the OBHT group when compared to that of the LC group. GRT treatment significantly reduced the mean systolic (Figure 4.48), diastolic (Figure 4.49) and arterial pressure (Figure 4.50) in the OBH+GRT group when compared to that of the untreated OBHT group (Table 4.5). Furthermore, OBHT treated with Captopril showed a significantly lower mean systolic, diastolic and arterial pressure when compared to the untreated OBHT group. There was only a significant difference in mean systolic pressure between OBHT+Captopril and OBHT+GRT (Figure 4.48). The systolic, diastolic and arterial pressure of the LC animals supplemented with GRT (LC+GRT) were not significantly different to that of the lean animals (Table 4.5).

Table 4.5: Systolic BP, diastolic BP and mean arterial pressure after 6 weeks of GRT treatment

Groups	Mean systolic pressure (mmHg)	Mean diastolic pressure (mmHg)	Mean arterial pressure (mmHg)
LC	122.1 ± 1.0	83.2 ± 1.1	96.4 ± 1.6
LC+GRT	119.6 ± 1.5	83.2 ± 2.7	95.5 ± 2.2
OBHT	130.6 ± 3.1*	91.8 ± 1.8*	104.2 ± 2.3*
OBHT+GRT	122.5 ± 0.6$^{\#}$	85.6 ± 1.5$^{\#}$	98.0 ± 1.2$^{\#}$
OBHT+ Captopril	111.6 ± 2.3$^{\#\#\#\&\&}$	80.9 ± 1.6$^{\#\#}$	90.9 ± 1.4$^{\#\#\#}$

*All data is expressed in mean ± SEM. * $p<0.05$ vs LC, $^{\#}p<0.05$ vs OBHT, $^{\#\#}p<0.01$ vs OBHT, $^{\#\#\#}p<0.001$ vs OBHT, $^{\&\&}p< 0.01$ vs OBHT+GRT according to one-way ANOVA. LC: lean control, LC+GRT: lean group treated with GRT, OBHT: obesity-induced hypertension group, OBHT+GRT: obesity-induced hypertension animals treated with GRT, OBHT+Captopril: obesity-induced hypertension animals treated with Captopril. N=7 per group.*

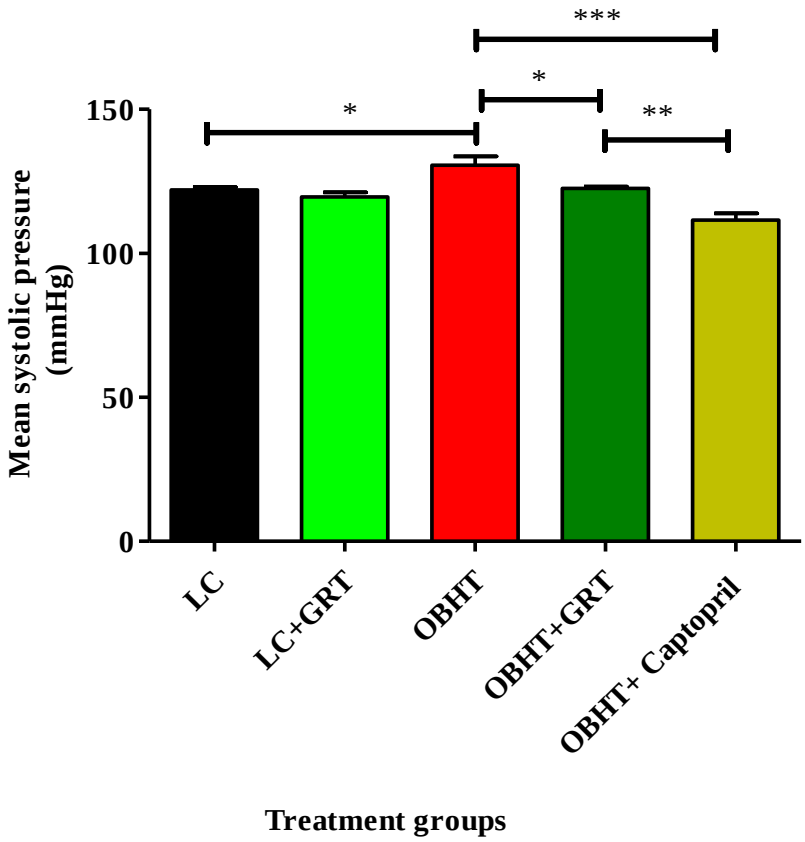

Figure 4.48: Mean systolic of experimental groups after GRT treatment

*Data are presented as mean ± SEM. *p < 0.05, **p<0.01, ***p<0.001 according to one-way-ANOVA, LC: lean control, LC+GRT: lean group treated with GRT, OBHT: obesity-induced hypertension group, OBHT+GRT: obesity-induced hypertension animals treated with GRT, OBHT+Captopril: obesity-induced hypertension animals treated with Captopril. N=7 per group.*

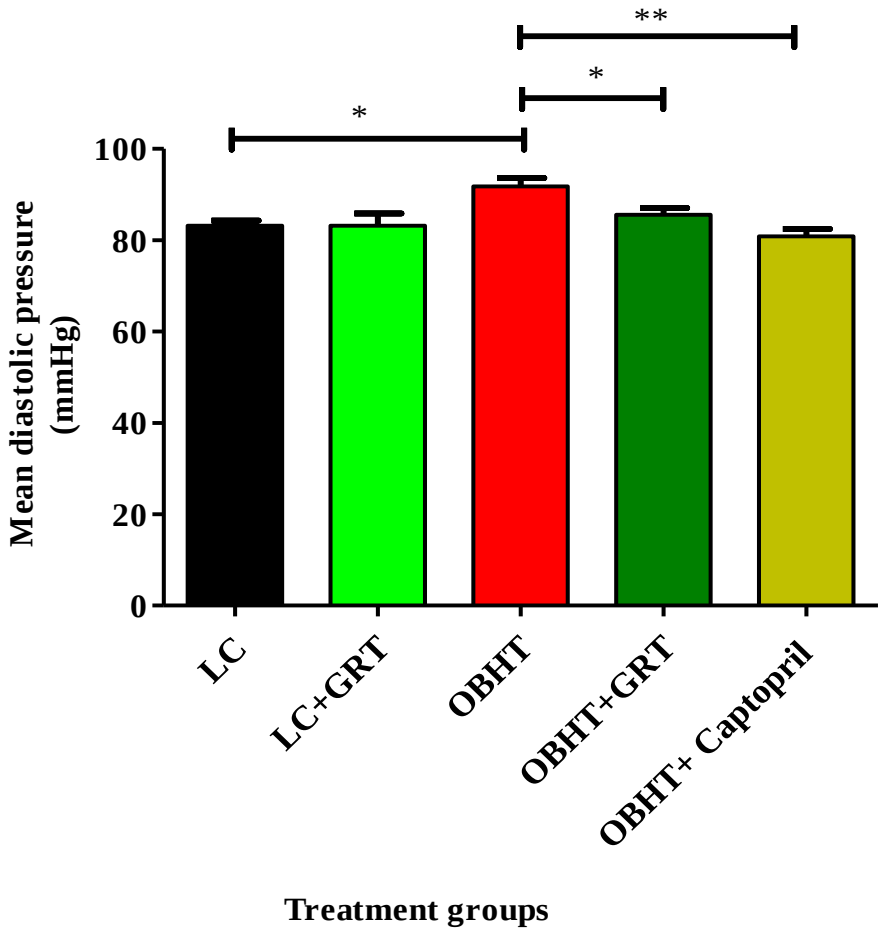

Figure 4.49: Mean diastolic pressure of experimental groups after GRT treatment

*Data are presented as mean ± SEM. *p < 0.05, **p<0.01 according to one-way-ANOVA, LC: lean control, LC+GRT: lean group treated with GRT, OBHT: Obesity-induced hypertension group, OBHT+GRT: obesity-induced hypertension animals treated with GRT, OBHT+Captopril: obesity-induced hypertension animals treated with Captopril. N=7 per group.*

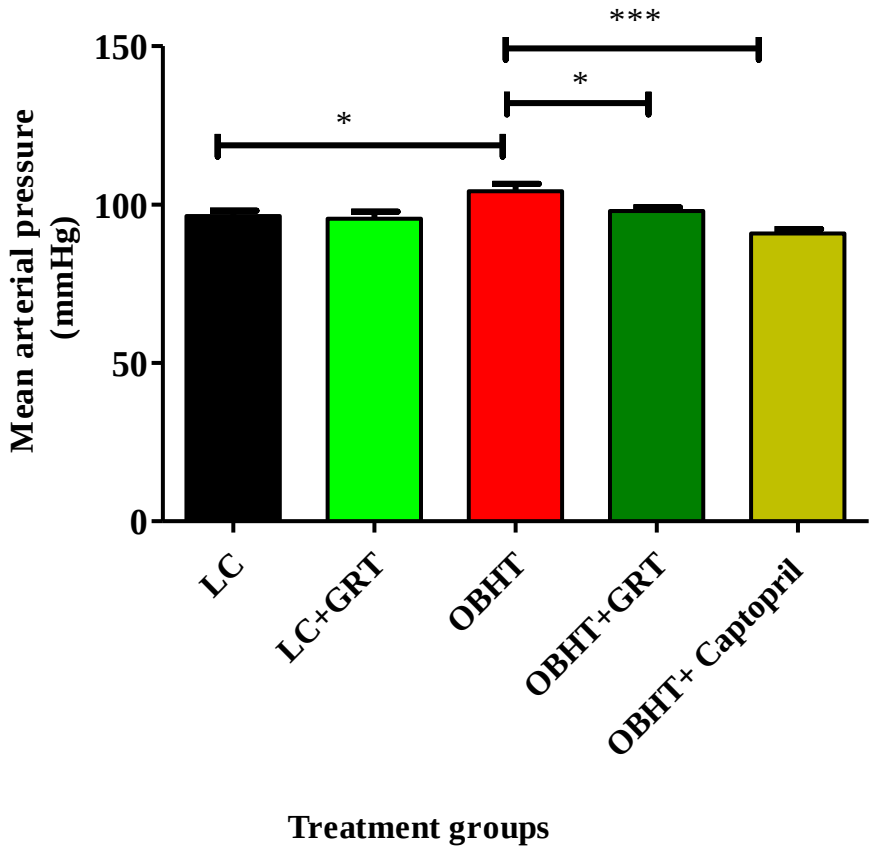

Figure 4.50: Mean arterial pressure of experimental groups after GRT treatment

*Data are presented as mean ± SEM. *p<0.05, ***p<0.001 according to one-way-ANOVA, LC: lean control, LC+GRT: lean group treated with GRT, OBHT: Obesity-induced hypertension group. OBHT+GRT: obesity-induced hypertension animals treated with GRT, OBHT+Captopril: obesity-induced hypertension animals treated with Captopril. N=7 per group.*

4.3.3 TW and body weight ratio

There was no significant difference in the TWs of the treatment groups (Figure 4.51). However, when TW is expressed in relation to total BW (shown in Figure 4.52), the OBHT group showed a significant decrease in the TW to BW ratio when compared to the LC group (0.0070 ± 0.0002 vs 0.0087± 0.0002, $p<0.01$). Ingestion of GRT by the OBHT group did not show any significant change in TW:BW ratio compared to the untreated OBHT group. However, in a similar group treated with Captopril, the TW:BW ratio increased significantly (0.0101 ± 0.0003 vs 0.0068 ± 0.0002, $p<0.001$). The OBHT+Captopril group also had a higher TW:BW ratio than the OBHT+GRT group (0.0101 ± 0.0003 vs 0.0074 ± 0.0003, $p<0.001$).

On the other hand, the GRT supplementation in the LC+GRT group did not change the TW: BW ratio when compared to the untreated LC group.

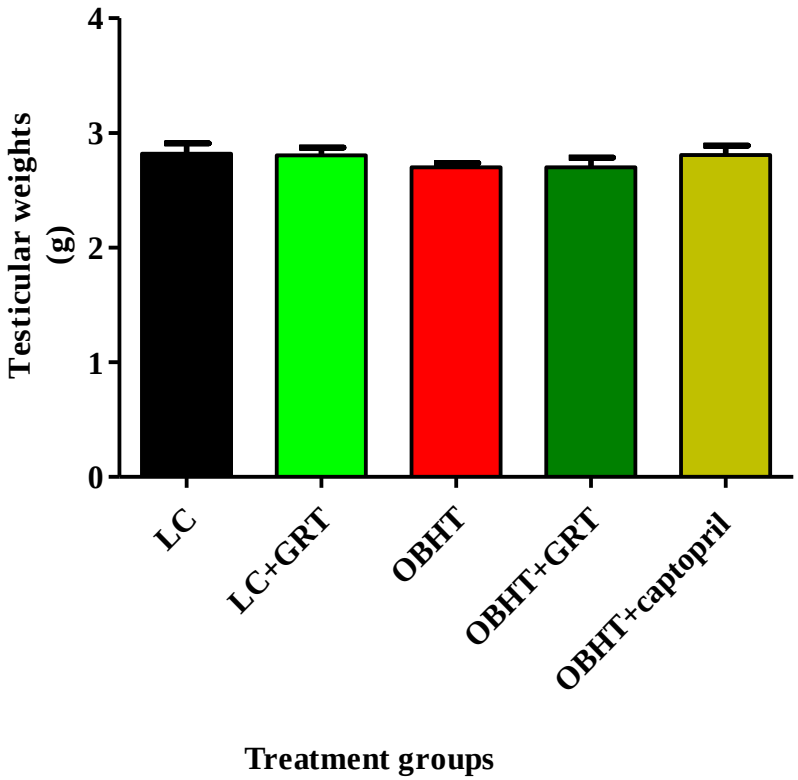

Figure 4.51: TWs in treatment groups

Data are presented as mean ± SEM. p>0.05 according to one-way-ANOVA, LC: lean control, LC+GRT: lean group treated with GRT, OBHT: obesity-induced hypertension group. OBHT+GRT: obesity-induced hypertension animals treated with GRT, OBHT+Captopril: obesity-induced hypertension animals treated with Captopril. N=7 per group.

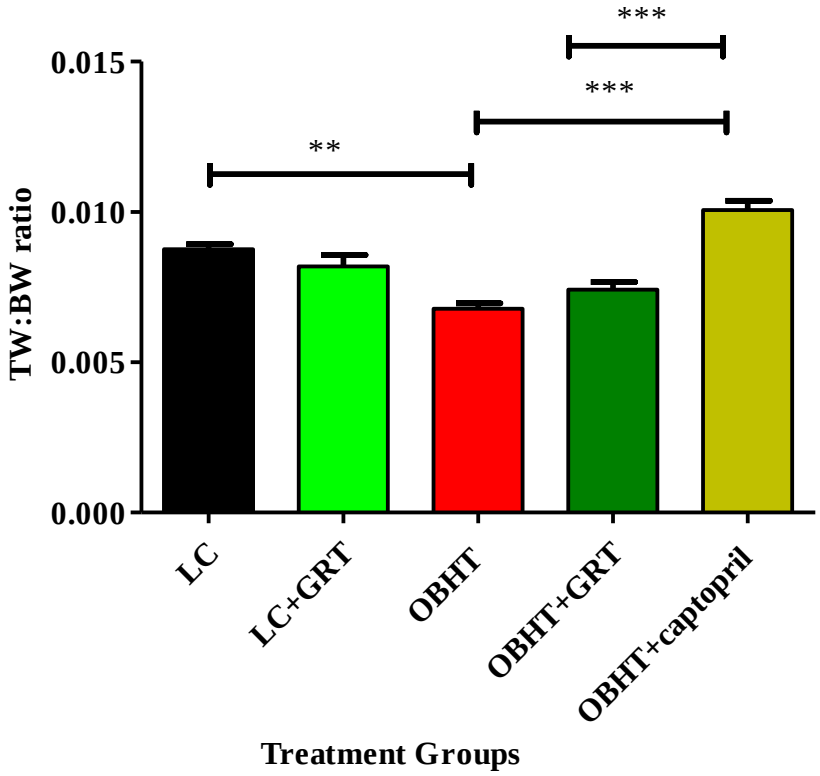

Figure 4.52: TW and body weight ratio

*Data are presented as mean ± SEM. **p<0.01, ***p<0.001 according to one-way-ANOVA, LC: lean control, LC+GRT: lean group treated with GRT, OBHT: obesity-induced hypertension group, OBHT+GRT: obesity-induced hypertension animals treated with GRT, OBHT+Captopril: obesity-induced hypertension animals treated with Captopril. N=7 per group.*

4.3.4 Testicular histomorphometric analysis

The means of 50 cross-sections of seminiferous tubules per testis did not show any significant differences between treatment groups as analyzed according to the Johnsen scoring method (Table 4.6). Furthermore, morphometric parameters, including seminiferous tubule area, seminiferous diameter, lumen areas, lumen diameter and epithelial height were statistically calculated (Table 4.6). There was a significant decrease in the seminiferous tubule area in the OBHT group when compared to the LC group (97807 ± 1488 µm² vs 118347 ± 6073 µm², $p<0.05$) (Table 4.6). Similarly, the seminiferous tubule diameter was significantly decreased in the OBHT group compared to that of the LC group (354.0 ± 3.0 µm vs 386.2 ± 9.5 µm, $p<0.05$). The lumen area was significantly decreased in the OBHT (19891±1717 µm² vs 30058 ± 3639 µm², $p<0.01$), with a significant decrease in lumen diameter (157.8 ± 7.3 µm vs 191.2 ± 12.2 µm, $p<0.05$) compared to the LC group. Furthermore, the

epithelium height was significantly decreased in the OBHT group (99.0 ± 4.8 µm vs 115.4 ± 9.0 µm, $p<0.05$) compared to the LC group.

The treatment with GRT in the OBHT+GRT group showed a significantly high area and higher diameter of seminiferous tubules respectively when compared to OBHT animals [(793501 ± 58820 µm² vs 97807 ± 1488 µm², $p<0.05$), (413.1 ± 9.2 µm vs 354.0 ± 3.0 µm, $p<0.05$)]. Both the lumen area and lumen diameter were significantly reduced in the OBHT+GRT group [(15605 ± 1958 µm² vs 19891±1717 µm², $p<0.05$), (133.0 ± 7.2 µm vs 157.8 ± 7.3 µm, $p<0.05$)] compared to the untreated OBHT group.

Table 4.6: Histomorphometric analysis of seminiferous tubules and lumen

	LC	LC+GRT	OBHT	OBHT+GRT	OBHT+Captopril
Johnsen scoring (Mean for 50 tubules/testis)	9.2 ± 0.1	9.1 ± 0.1	9.3 ± 0.1	9.2 ± 0.1	9.1 ± 0.1$^{\#}$
Seminiferous tubule area (µm²)	118347 ± 6073	111270 ± 1591	97807 ± 1488*	7930501 ± 580820$^{\# \$}$	93084 ± 3936
Seminiferous tubular diameter (µm)	386.2 ± 9.5	375.9 ± 2.7	354.0 ± 3.0*	413.1 ± 9.2$^{\# \$\$}$	354.3 ± 2.2
Lumen area (µm²)	30058 ± 3639	23084 ± 3561	19891±1717**	15605 ± 1958$^{\#}$	12986 ± 1194
Lumen diameter (µm)	191.2 ± 12.2	178.0 ± 13.5	157.8 ± 7.3*	133.0 ± 7.2$^{\#}$	127.6 ± 6.1$^{\#}$
Epithelial height (µm)	115.4 ± 9.0	112.3 ± 6.5	99.0 ± 4.8*	104.2 ± 5.9	136.7 ± 5.8$^{\#}$

*All data are expressed in mean ± SEM. *$p<0.05$ vs LC ** $p<0.01$ vs LC, $^{\#}p<0.05$ vs OBHT, $^{\$\$}p<0.01$ vs LC+GRT according to one-way-ANOVA. LC: lean control, LC+GRT: lean group treated with GRT, OBHT: obesity-induced hypertension group, OBHT+GRT: obesity-induced hypertension animals treated with GRT, OBHT+Captopril: obesity-induced hypertension animals treated with Captopril. N=5 per group.*

4.3.5 Testosterone and estradiol levels

A significantly higher T level was observed in OBHT animals compared to that of the LC group (18.25 ± 0.12ng/mL vs 17.37 ± 0.11 ng/mL, $p<0.01$). GRT treatment presented a significantly lower T in OBHT+GRT group when compared to the OBHT group (16.52 ± 0.15 ng/mL vs 18.25 ± 0.12 ng/mL, $p<0.001$). However, there was no significant difference in T between the OBHT+GRT and LC, OBHT+GRT and LC+GRT, and L+GRT and LC groups. Captopril reduced T levels in the OBHT+Captopril compared to untreated OBHT group (16.93 ± 0.48 ng/mL vs 18.25 ± 0.12 ng/mL, $p<0.05$). There was no difference between GRT treatment and Captopril treatment groups (Figure 4.53).

E2 levels were significantly increased in the OBHT group compared to the LC group (0.92 ± 0.06 ng/mL vs 0.67 ± 0.03 ng/mL, $p<0.05$). Both GRT- and Captopril-treated OBHT animals respectively showed a significant lower E2 level when compared to the untreated OBHT group ($p<0.001$). Additionally, the E2 levels of LC animals treated with GRT did not significantly differ from those of the untreated LC group (Figure 4.54).

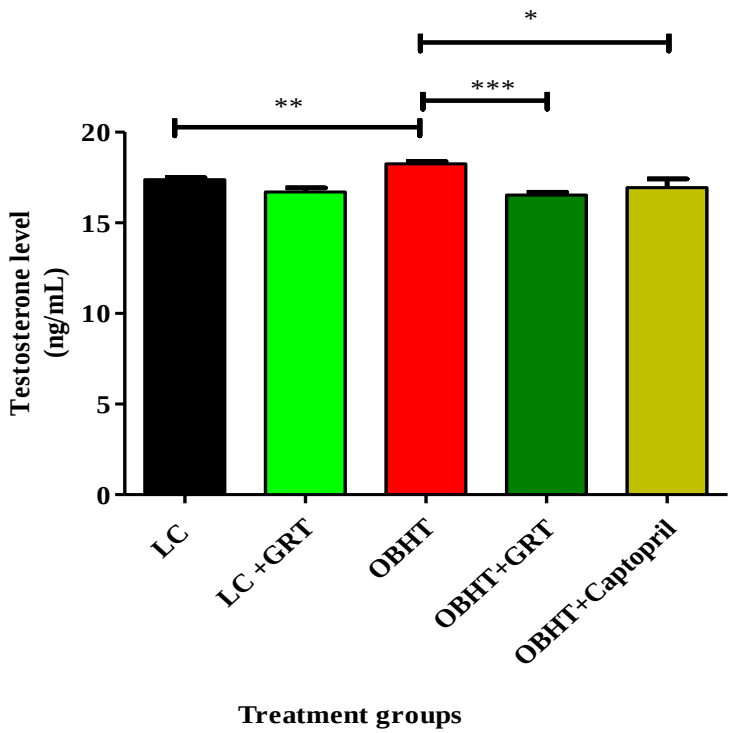

Figure 4.53: Serum testosterone levels

Data are presented as mean ± SEM. $^{*}p<0.05$ according to one-way-ANOVA, LC: lean control, LC+GRT: lean group treated with GRT, OBHT: obesity-induced hypertension group, OBHT+GRT: obesity-induced hypertensive animals treated with GRT, OBHT+Captopril: obesity-induced hypertensive animals treated with Captopril. N=6 per group.

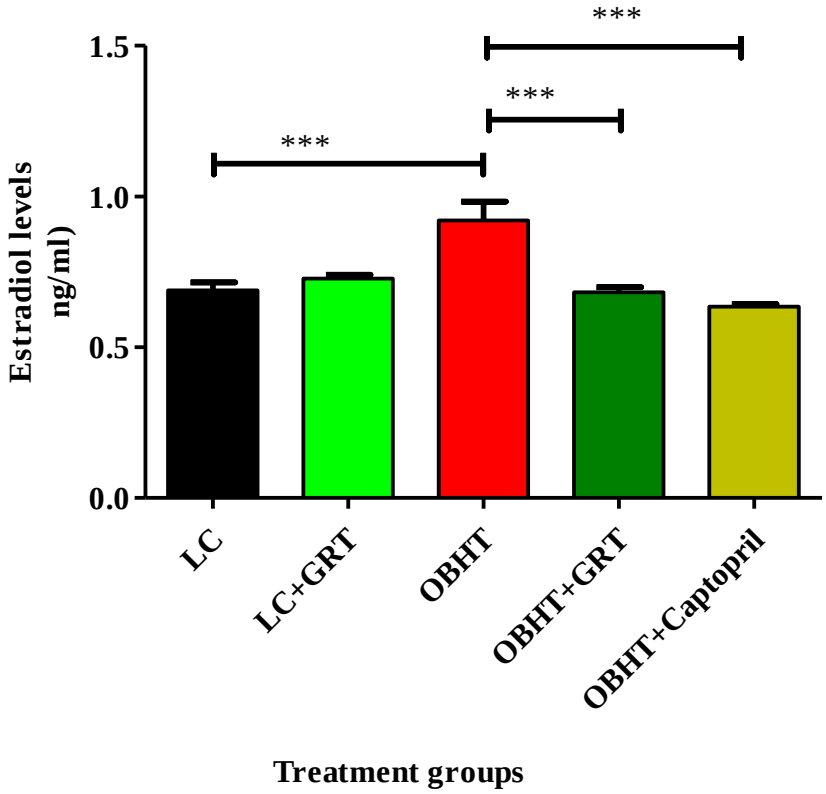

Figure 4.54: Serum estradiol levels

*Data are presented as mean ± SEM. ***p<0.001 according to one-way-ANOVA, LC: lean control, LC+GRT: lean control group treated with GRT, OBHT: Obesity-induced hypertension group, OBHT+GRT: obesity-induced hypertension animals treated with GRT, OBHT+Captopril: obesity-induced hypertension animals treated with Captopril. N=6 per group.*

4.3.6 Testosterone and estradiol ratio

The T:E2 ratio was significantly reduced in OBHT animals when compared to the LC group (18.29 ± 1.30 vs 23.91 ± 0.58, p< 0.05). Treatment with GRT did not present with a significant difference between LC+GRT and LC. However, the T:E2 ratio of OBHT+GRT treated with GRT significantly increased in comparison to that of the untreated OBHT group (24.95 ± 0.55 vs 18.29 ± 1.30, p<0.01). Treatment with Captopril also resulted in a significantly higher T:E2 when compared to the untreated OBHT group (24.39 ± 1.50 vs 18.29 ± 1.30, p<0.01) (Figure 4.55).

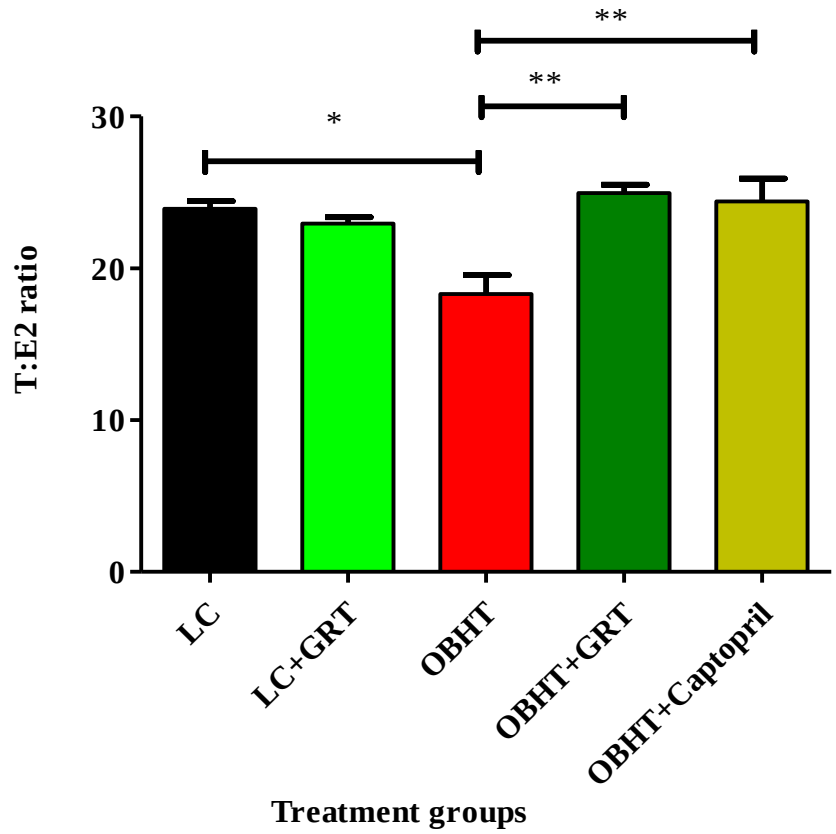

Figure 4.55: Testosterone and estradiol ratio

*Data are presented as mean ± SEM. *p<0.05, **p<0.01 according to one-way-ANOVA, LC: lean control, LC+GRT: lean group treated with GRT, OBHT: obesity-induced hypertension group, OBHT+GRT: obesity-induced hypertension animals treated with GRT, OBHT+Captopril: obesity-induced hypertension animals treated with Captopril. N=6 per group.*

4.3.7 Testicular protein expression and phosphorylation

4.3.7.1 Total PKB expression, PKB phosphorylation and P-PKB:T-PKB ratio

T-PKB expression was significantly lower in the OBHT group when compared to the LC group (0.64 ± 0.10 densitometry units vs 1.20 ± 0.30 densitometry units, $p<0.05$). Treatment with either GRT or Captopril did not show a significant effect compared to the untreated OBHT group. Additionally, LC+GRT animals presented with a significantly lower T-PKB expression than the untreated LC group (0.22 ± 0.05 densitometry units vs 1.20 ± 0.30 densitometry units, $p<0.001$) and OBHT+GRT group (0.22 ± 0.05 densitometry units vs 0.75 ± 0.06 densitometry units, $p=0.05$). There was no significant difference between OBHT+GRT and OBHT+Captopril groups (Figure 4.56).

Activation of PKB (P-PKB) and P-PKB:T-PKB ratio is presented in Figure 4.57 and Figure 4.58 respectively. No significant differences were observed in the P-PKB as well as in P-PKB:T-PKB ratio.

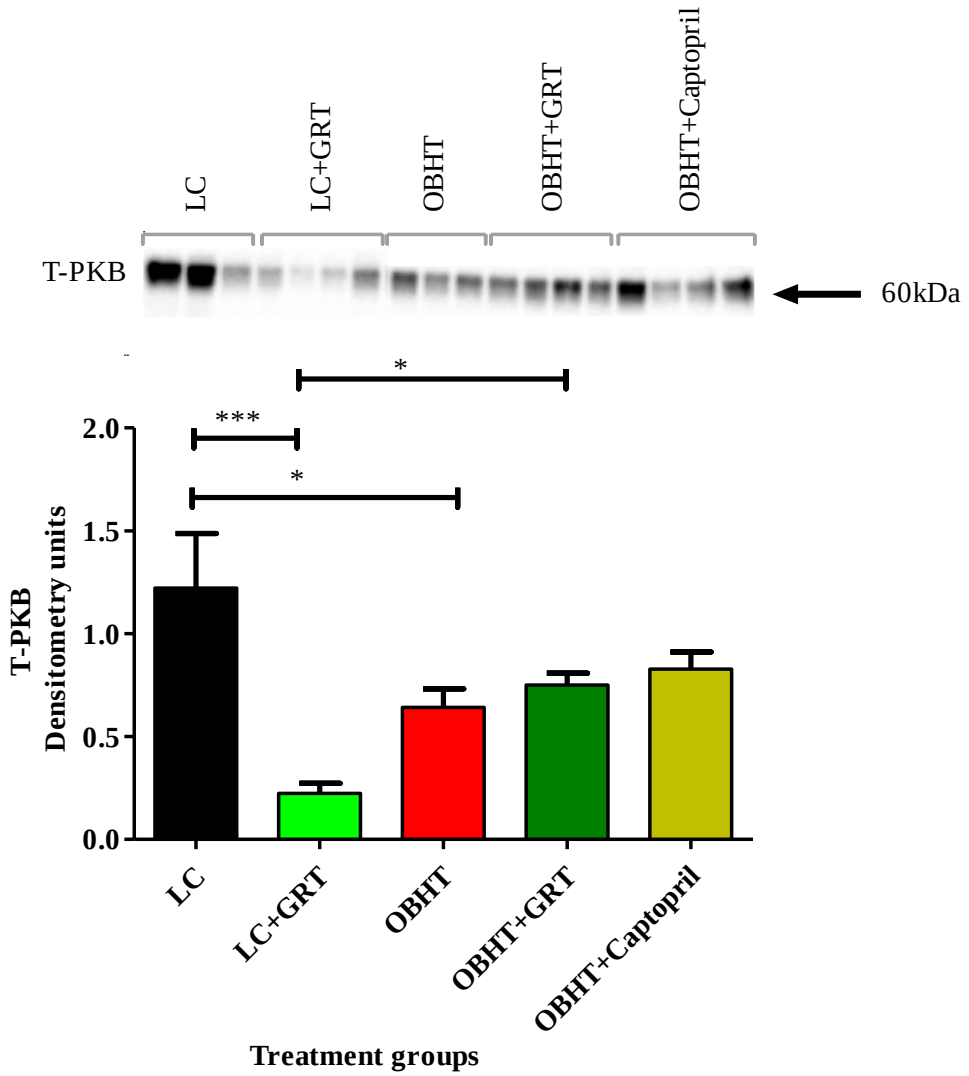

Figure 4.56: Testicular total PKB expression

*Data are presented as mean ± SEM.*p<0.05, ***p<0.001, LC: lean control, LC+GRT: lean group treated with GRT, OBHT: Obesity-induced hypertension group, OBHT+GRT: obesity-induced hypertension animals treated with GRT, OBHT+Captopril: obesity-induced hypertension animals treated with Captopril. N=3–4 per group.*

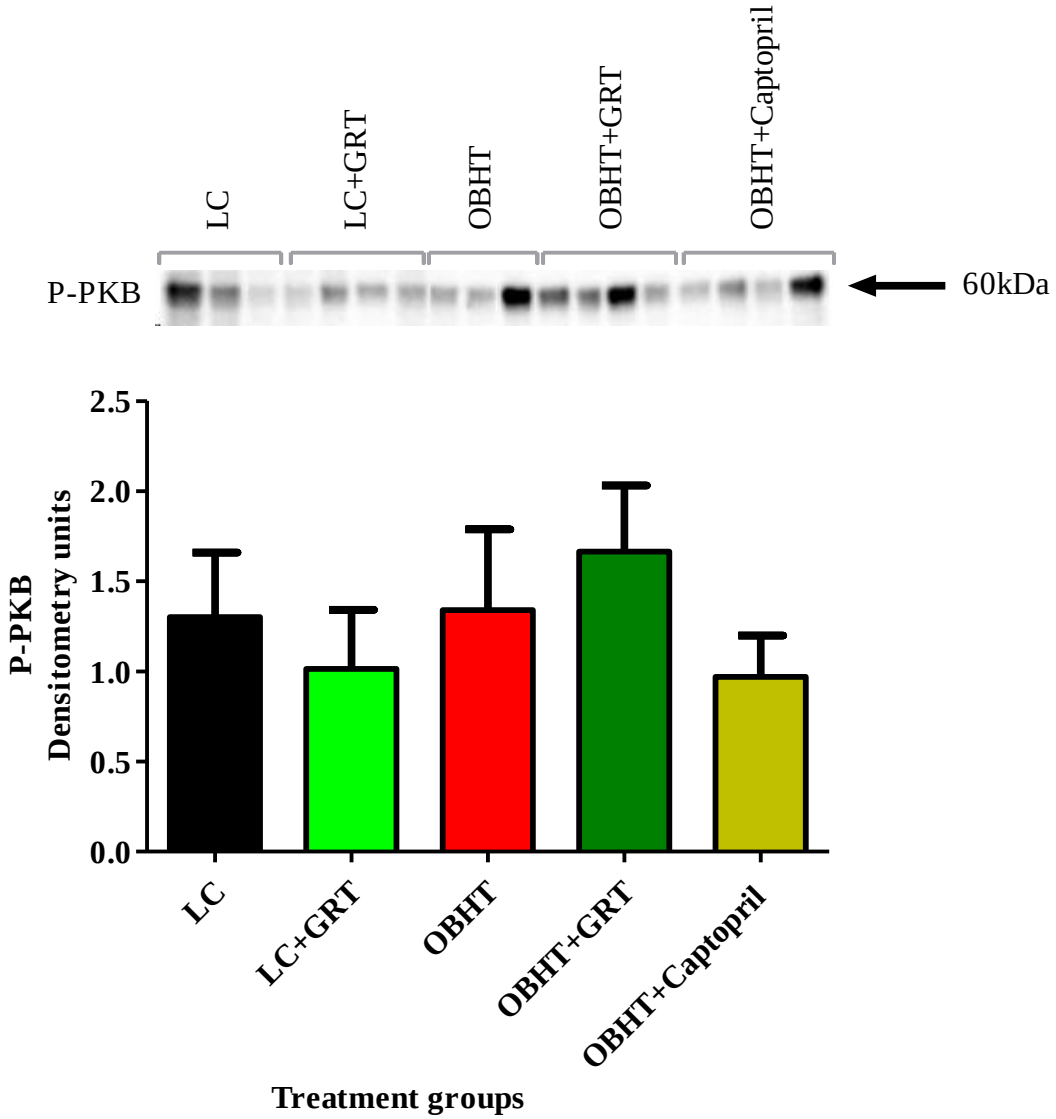

Figure 4.57: Testicular PKB phosphorylation

Data are presented as mean ± SEM. p>0.05 according to one-way-ANOVA, LC: lean control, LC+GRT: lean group treated with GRT, OBHT: obesity associated with hypertension group, OBHT+GRT: obesity associated hypertensive group treated with GRT, OBHT+Captopril: obesity associated with hypertensive group treated with Captopril. N=3–4 per group.

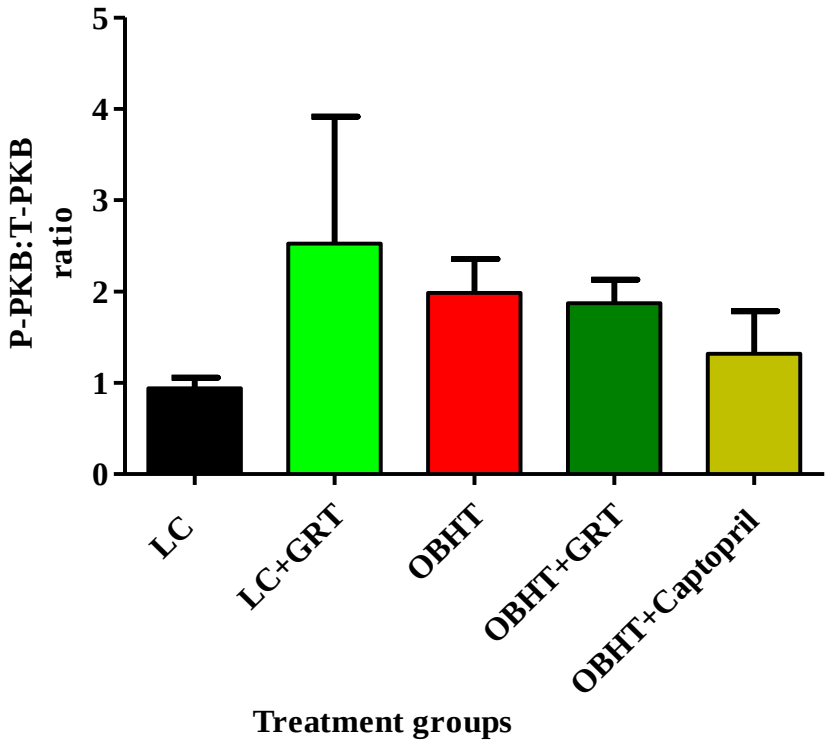

Figure 4.58: Testicular P-PKB:T-PKB ratio

Data are presented as mean ± SEM. p>0.05 according to one-way-ANOVA, LC: lean control LC+GRT: lean group treated with GRT. OBHT: obesity associated with hypertension group, OBHT+GRT: obesity associated hypertensive group treated with GRT, OBHT+Captopril: obesity associated with hypertensive group treated with Captopril. N=3–4 per group.

4.3.7.2 T-AMPK and P-AMPK

A significantly lower T-AMPK expression was observed in the OBHT group when compared to the LC group (0.04 ± 0.20 densitometry units vs 1.20 ± 0.20 densitometry units, $p<0.001$). Treatment with either GRT or Captopril did not show any significant change in T-AMPK when compared to the untreated OBHT group. However, a significantly lower T-AMPK was observed in LC+GRT animals, in OBHT+GRT and in OBHT+Captopril respectively when compared to the LC group (0.05 ± 0.20 densitometry units vs 1.20 ± 0.20 densitometry units, $p<0.01$), (0.064 ± 0.013 densitometry units vs 1.20 ± 0.20 densitometry units, $p<0.001$) and (0.092 ±0.013 densitometry units vs 1.20 ± 0.20 densitometry units, $p< 0.001$) (Figure 4.59).

P-AMPK was not found in the testicular samples.

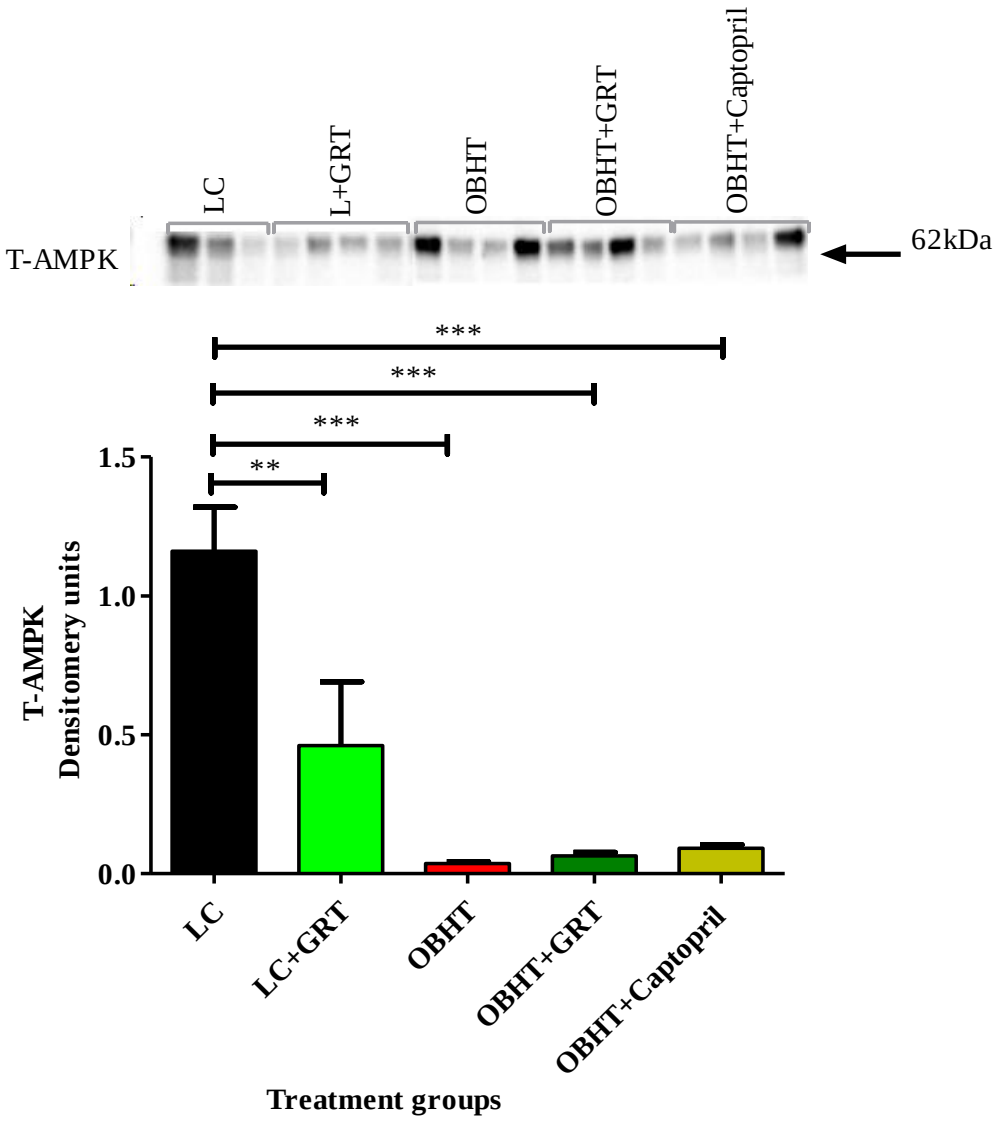

Figure 4.59: Testicular total AMPK expression

*Data are presented as mean ± SEM. ***p<0.001 according to one-way ANOVA, LC: lean control, LC+GRT: lean group treated with GRT, OBHT: obesity-induced hypertensive group, OBHT+GRT: obesity-induced hypertensive animals treated with GRT, OBHT+Captopril: obesity-induced hypertension animals treated with Captopril. N=3–4 per group.*

4.3.7.3 Cleaved PARP expression in testicular tissue

The presence of Cleaved PARP was significantly reduced in the OBHT group when compared to the LC group (0.41 ± 0.02 densitometry units vs 1.90 ± 0.05 densitometry units, p<0.001). Treatment with either GRT or Captopril did not show any significant difference when compared to the untreated OBHT group. However, treatment with GRT in the LC+GRT group and OBHT+GRT group showed

respectively a significant lower Cleaved PARP when compared to the LC group (0.40 ± 0.05 densitometry units vs 1.90 ± 0.06 densitometry units, p<0.001) and (0.23 ±0.04 densitometry units vs 1.90 ± 0.06 densitometry units, p<0.001). Treatment with Captopril in the OBHT + Captopril group presented a significantly lower Cleaved PARP when compared to the LC group (0.26 ± 0.05 densitometry units vs 1.90 ± 0.06 densitometry units, p<0.001). There was a significant difference between LC+GRT and OBHT+GRT (0.40 ± 0.05 densitometry units vs 0.20 ± 0.04 densitometry units, p<0.05) (Figure 4.60).

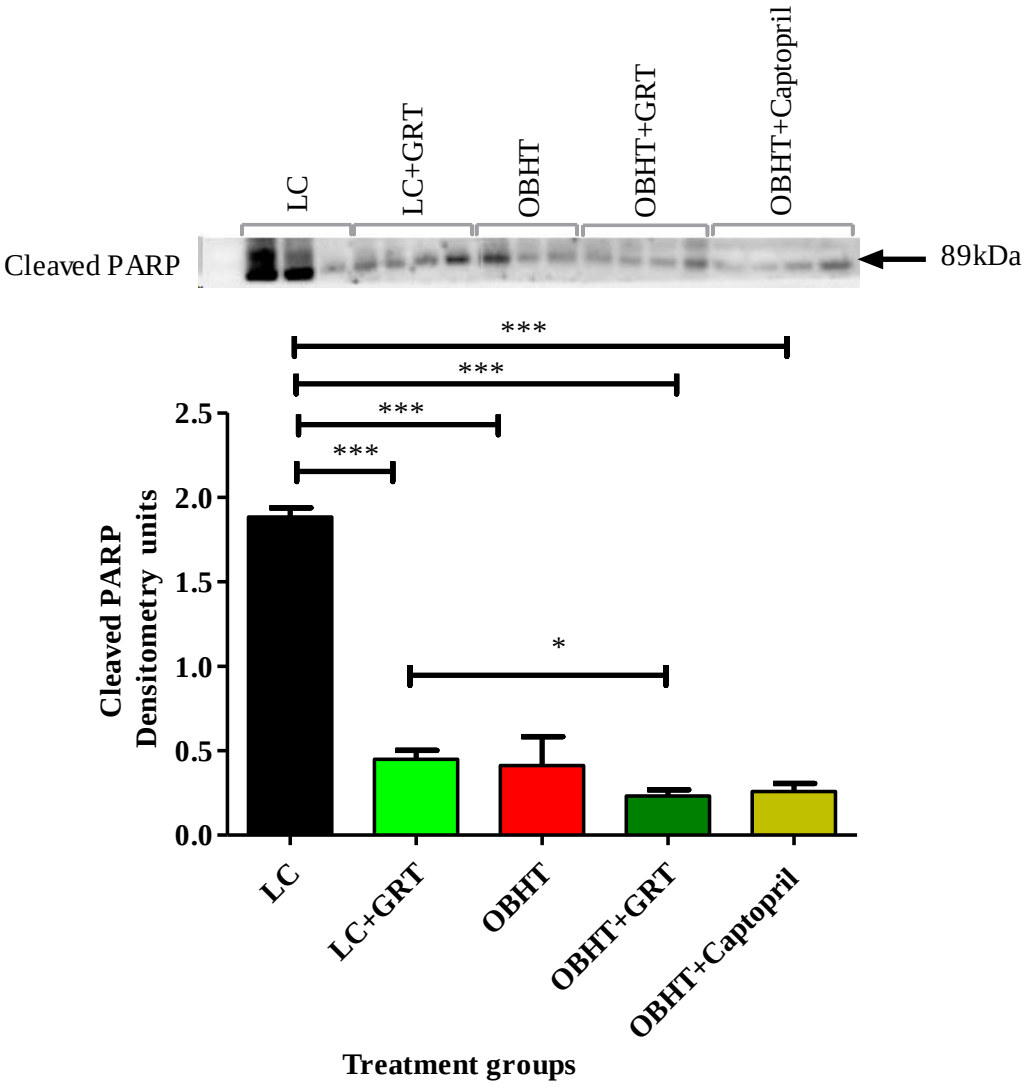

Figure 4.60: Testicular Cleaved PARP expression

*Data are presented as mean ± SEM.*p<0.05, ***p<0.001 according to one-way ANOVA, LC: lean control, LC+GRT: lean group treated with GRT, OBHT: obesity-induced hypertensive group, OBHT+GRT: obesity-induced hypertensive animals treated with GRT, OBHT+Captopril: obesity-induced hypertension animals treated with Captopril. N=3–4 per group.*

4.3.9.4 Caspase 7 expression in testicular tissue

OBHT animals presented with a significantly lower caspase 7 expression when compared to the untreated LC group (0.05 ± 0.30 densitometry units vs 1.20 ± 0.30 densitometry units, $p<0.05$). The treatment of OBHT animals with either GRT or Captopril did not change caspase 7 levels in comparison to the untreated OBHT group. However, LC+GRT showed a significantly reduced caspase 7 level when compared to the LC group (0.10 ± 0.30 densitometry units vs 1.20 ± 0.30, $p< 0.01$). There was also a significantly lower caspase 7 expression in LC+GRT when compared to OBHT+GRT ($p<0.05$) (Figure 4.61).

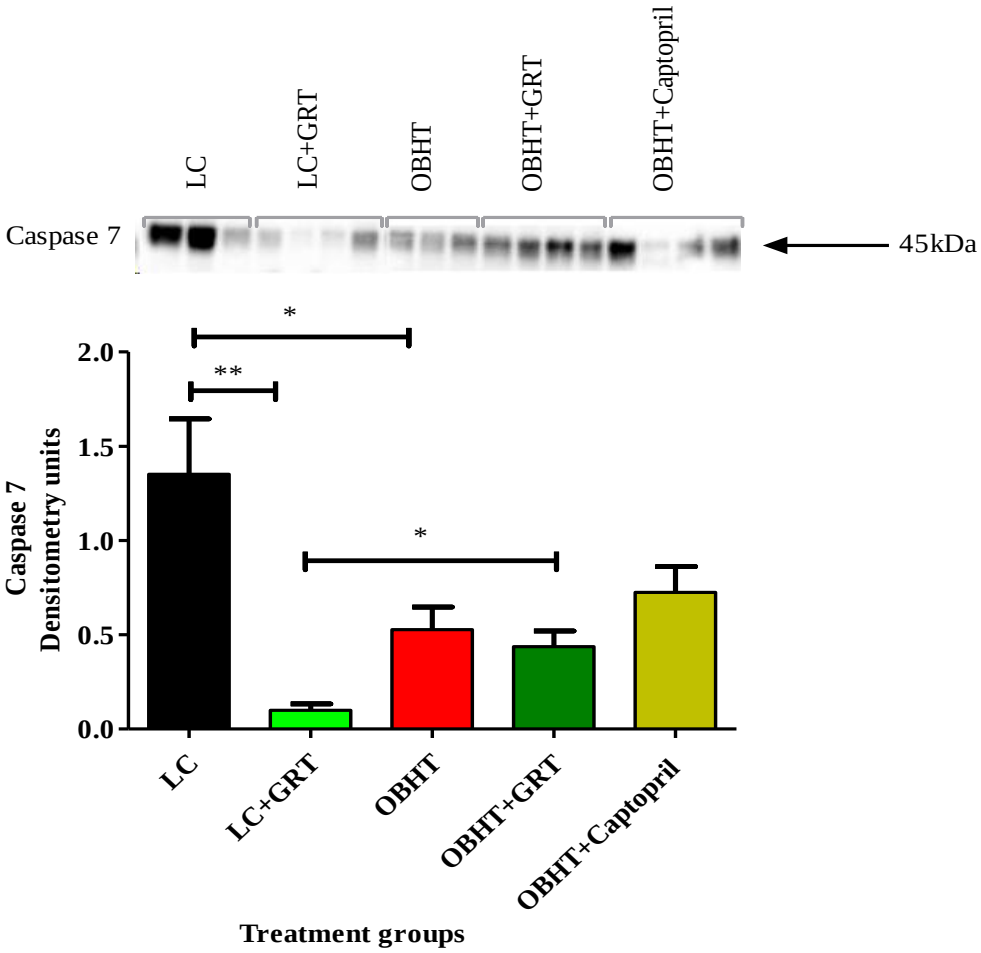

Figure 4.61: Testicular caspase 7 expression

*Data are presented as mean ± SEM. *p<0.05, **p<0.01 according to one-way ANOVA, LC: lean control, LC+GRT: lean group treated with GRT, OBHT: obesity-induced hypertension group, OBHT+GRT: obesity-induced hypertensive animals treated with GRT, OBHT+Captopril: obesity-induced hypertensive animals treated with Captopril. N=3–4.*

4.3.8 Testicular OS

4.3.8.1 Testicular SOD activity

SOD activity was significantly lower in the OBHT group when compared to the LC group (40.8 ± 2.2 U/mg protein vs 98.2 ± 4.2 U/mg protein, $p<0.001$). Treatment with GRT or Captopril did not show any significant effect on SOD activity in treated OBHT+GTR as well as OBHT+Captopril group when compared to the OBHT group. On the other hand, GRT treatment resulted in a significantly lower SOD activity in the LC+GRT group when compared to that of the LC group (63.5 ± 4.1 U/mg protein vs 98.2 ± 4.2 U/mg protein, $p<0.001$). A significant difference in SOD activity was observed between the LC+GRT and OBHT+GRT groups (63.5 ± 4.1 U/mg protein vs 49.2 ± 1.7 U/mg protein, $p<0.05$) (Figure 4.62).

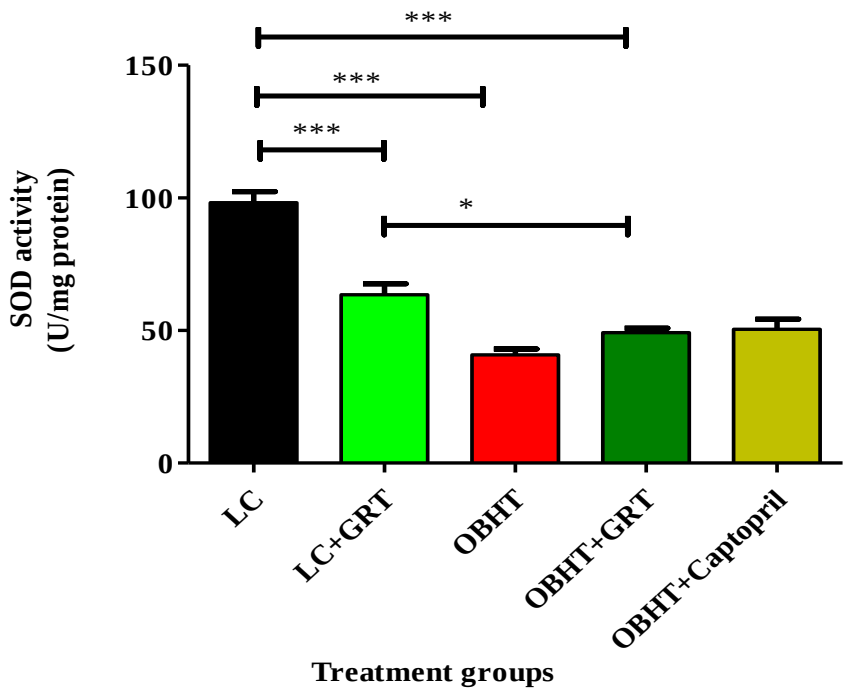

Figure 4.62: Testicular total SOD activity

*Data are presented as mean ± SEM. *p<0.05, ***p<0.001 according to one-way ANOVA, LC: lean control, LC+GRT: lean group treated with GRT, OBHT: obesity-induced hypertension group, OBHT+GRT: obesity-induced hypertensive animals treated with GRT, OBHT+Captopril: obesity-induced hypertensive animals treated with Captopril. N=7 per group.*

4.3.8.2 Testicular CAT activity

The OBHT animals showed significantly lower CAT activity in testicular tissue compared to the LC group (36.6 ± 1.8 µmole H_2O_2 consumed/min/µg protein vs 58.5 ± 2.3 µmole H_2O_2 consumed/min/µg protein., $p<0.001$). Animals from the OBHT group treated with GRT presented with significantly increased CAT activity compared to the untreated OBHT group (66.8 ± 2.0 µmole H_2O_2 consumed/min/µg protein vs 36.6 ± 1.8 µmole H_2O_2 consumed/min/µg protein, $p<0.001$). Similarly, treatment with Captopril significantly elevated CAT activity in the OBHT+Captopril group when compared to that of the untreated OBHT group (69.5 ± 2.1 µmole H_2O_2 consumed/min/µg protein vs 36.6 ± 1.8 µmole H_2O_2 consumed/min/µg protein, $p<0.001$). No significant difference was observed between the LC+GRT and LC groups (Figure 4.63).

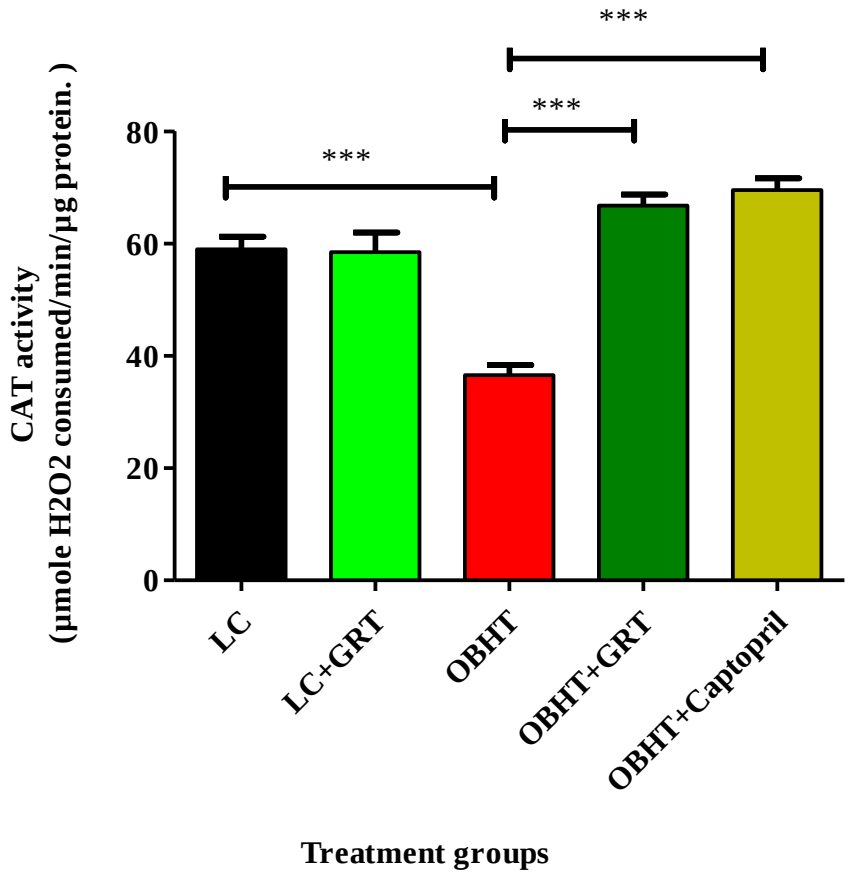

Figure 4.63: Testicular CAT activity

*Data are presented as mean ± SEM. ***p<0.001 according to one-way ANOVA, LC: lean control, LC+GRT: lean group treated with GRT, OBHT: obesity-induced hypertensive group, OBHT+GRT: obesity-induced hypertensive animals treated with GRT, OBHT+Captopril: obesity-induced hypertensive animals treated with Captopril. N=7 per group.*

4.3.8.3 Testicular MDA levels

The testicular MDA level was significantly higher in the OBHT group compared to the LC group (6.3 ± 0.5 µmol/mg protein vs 3.1 ± 0.3 µmol/mg protein, $p<0.01$). There were significantly lower testicular MDA levels in the OBHT+GRT group compared to that of the OBHT group (3.2 ± 0.3 µmol/mg protein vs 6.3 ± 0.5 µmol/mg protein, $p<0.001$). Treatment with Captopril significantly lowered MDA levels compared to that of the untreated OBHT (4.5 ± 0.3 µmol/mg protein vs 6.3 ± 0.5 µmol/mg protein, $p<0.05$). The MDA levels in the testes of LC animals supplemented with GRT were not significantly different to that of the LC group. It was also noted that there was no significant difference in MDA levels between the OBHT+GRT and LC+GRT groups (Figure 4.64).

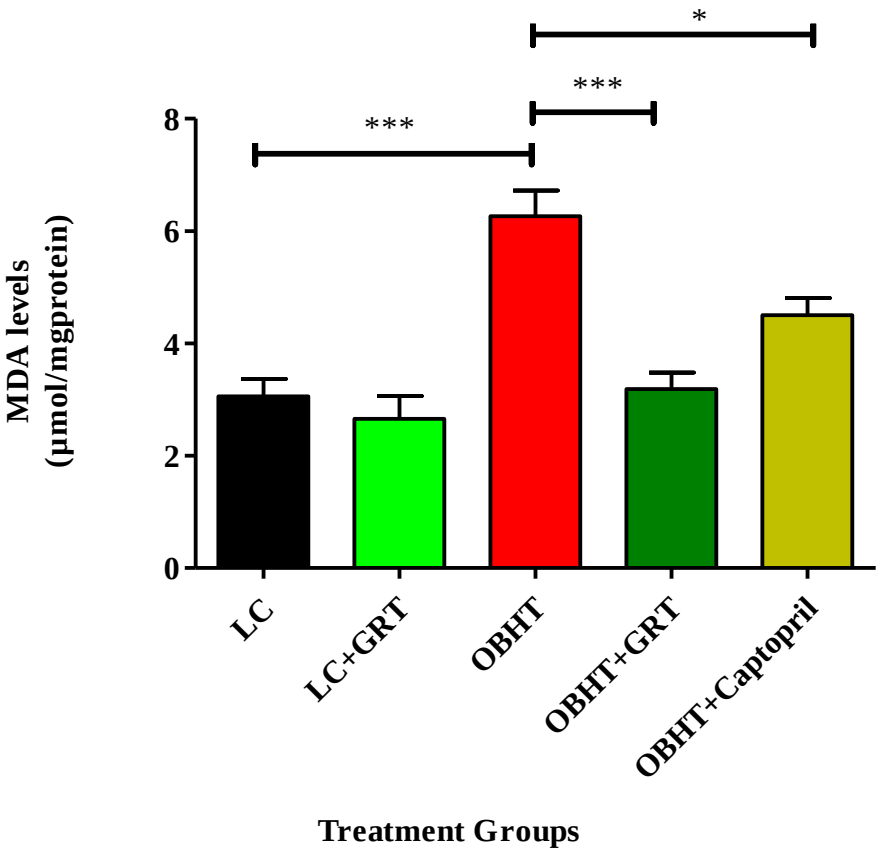

Figure 4.64: Testicular MDA levels

*Data are presented as mean ± SEM.*p<0.05, ***p<0.001 according to one-way ANOVA, LC: lean control, LC+GRT: lean group treated with GRT, OBHT: obesity-induced hypertensive group, OBHT+GRT: obesity-induced hypertensive animals treated with GRT, OBHT+Captopril: obesity-induced hypertension animals treated with Captopril. N=7 per group.*

4.3.9 Epididymal weight

A significantly higher total epididymal weight was observed in the OBHT compared to the LC group (1.28 ± 0.03 g vs 1.14 ± 0.03 g, $p<0.05$). The OBHT+GRT and OBHT+Captopril groups had lower total epididymal weights compared to that of the OBHT group (1.16 ± 0.03 g vs 1.28 ± 0.03 g, $p<0.05$), (0.94 ± 0.03 g vs 1.28 ± 0.03 g, $p<0.001$). A significant difference was observed between the OBHT+GRT and OBHT+Captopril groups (1.16 ± 0.03 g vs 0.94 ± 0.03 g, $p<0.001$) (Figure 4.65). Futhermore, GRT supplementation resulted in a significant higher total epididymal weight in the LC+GRT group when compared to that of the LC group (1.25 ± 0.025g vs 1.14 ± 0.03 g, $p<0.05$).

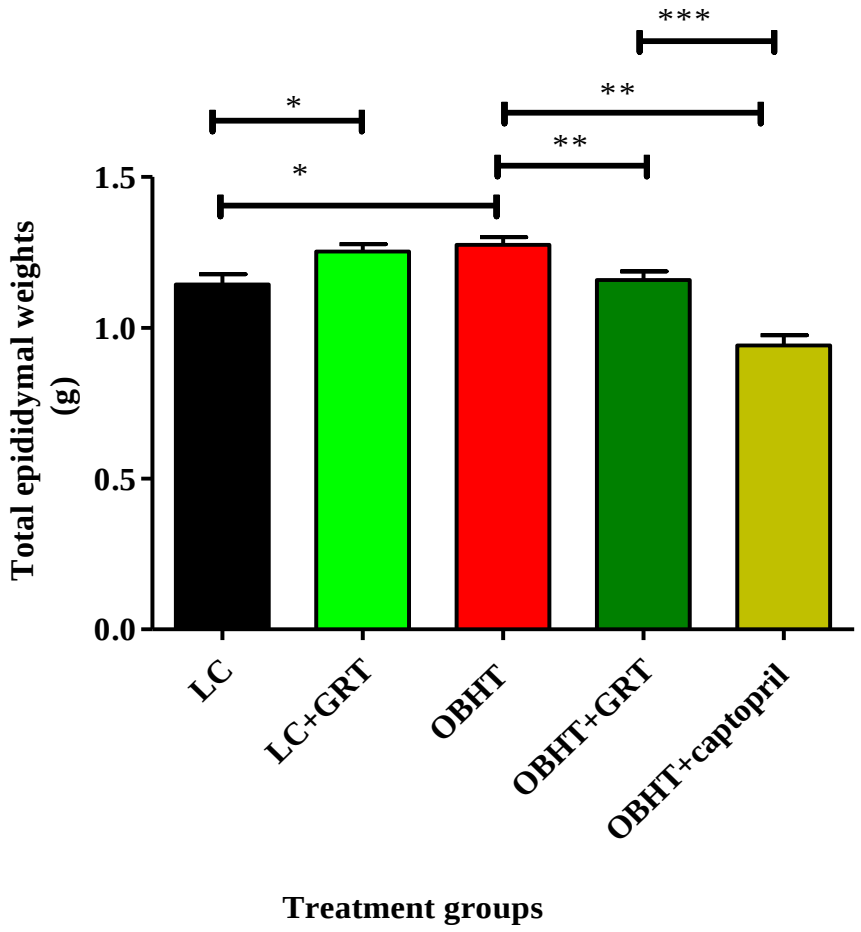

Figure 4.65: Total epididymal weights in experimental groups

*Data are presented as mean ± SEM. *p<0.05, ***p<0.001 according to one-way ANOVA, LC: lean control, LC+GRT: lean group treated with GRT, OBHT: Obesity-induced hypertensive group, OBHT+GRT: obesity-induced hypertensive animals treated with GRT, OBHT+Captopril: obesity-induced hypertensive animals treated with Captopril. N=7 per group.*

4.3.10 Epididymal sperm function parameters

Sperm concentration, viability, total motility, progressive motility, VCL, VSL, VAP, normal morphology, head defects, midpiece defects, and teratozoospermy index of caudal epidymal part were investigated in the experimental groups (Table 4.8).

Table 4.7: Summary of basic and functional sperm parameters

	LC	LC +GRT	OBHT	OBHT +GRT	OBHT +Captopril
Sperm concentration (10^6sperm /mL)	1.79 ± 0.15	1.72 ± 0.13	1.40 ± 0.08*	1.80 ± 0.03$^{\#}$	1.49 ± 0.10$^{\&}$
Viable sperm (%)	57.10 ± 2.70	61.0 ± 3.60	23.40 ±1.70***	57.60 ± 2.60***	55.70 ± 2.70***
Normal morphology (%)	52.60 ± 3.50	56.30 ± 3.20	27.60 ± 3.60**	53.50 ± 4.40**	36.10 ± 6.80
Head defects (%)	47.10 ± 3.30	41.70 ± 3.40	73.90 ± 3.70***	53.20 ± 3.50$^{\#\#\#}$	56.80 ± 5.80$^{\#}$
Midpiece defects (%)	1.30 ± 0.80	1.70 ± 0.30	6.20 ± 0.90*	2.40 ± 1.00$^{\#}$	5.10 ± 1.40
Teratozoospermy index	1.02 ± 0.02	1.06 ± 0.01*	1.05 ± 0.02	1.04 ± 0.01	1.07 ± 0.01
Total motility (%)	81.16 ± 4.91	89.90 ± 2.20	72.60 ± 1.20*	86.70 ± 2.00$^{\#}$	94.40 ± 1.10
Progressive motility (%)	59.21 ± 2.82	72.00 ± 5.00	47.60 ± 3.00*	68.40 ± 2.60$^{\#\#\#}$	76.00 ± 5.40$^{\#\#}$
VCL (µm/s)	165.20 ± 6.20	162.40 ± 7.60	208.20 ± 10.00**	174.30 ± 11.00	62.00 ± 2.60$^{\#\#\#\&\&\&}$
VSL (µm/s)	47.00 ± 2.40	55.60 ± 2.60*	50.80 ± 2.00	50.70 ± 3.00	105.10 ± 4.50$^{\#\#\#}$ $^{\&\&\&}$
VAP (µm/s)	76.10 ± 2.50	88.30 ± 3.50*	84.70 ± 4.20	87.50 ± 3.40	26.30 ± 1.40$^{\#\#\#}$

*All data is expressed in mean ± SEM. *p<0.05 vs LC, **p<0.01 vs LC, ***p<0.001 LC, $^{\#}$p<0.05 vs OBHT, $^{\#\#}$p<0.01 vs OBHT, $^{\#\#\#}$p<0.001 vs OBHT, $^{\&\&}$p<0.01 vs OBHT+GRT. $^{\&\&\&}$p<0.001vs OBHT+GRT according to one-way ANOVA. LC: lean control, LC+GRT: lean group treated with GRT, OBHT: obesity-induced hypertensive group, OBHT+GRT: obesity-induced hypertensive animals treated with GRT, OBHT+Captopril: obesity-induced hypertensive animals treated with Captopril. N=7 per group.*

4.3.9.1 Sperm concentration

A significantly lower sperm concentration was observed in the OBHT compared to the LC group (1.40 ± 0.08 x 10^6 sperm/mL vs 1.79 ± 0.15 x 10^6 sperm/mL, $p<0.05$). The OBHT+GRT group showed a significant higher sperm concentration compared to the untreated OBHT (1.80 ± 0.03 x 10^6 sperm/mL vs 1.40 ± 0.08 x 10^6 sperm/mL, $p<0.05$). A significant difference in sperm concentration was also observed between the OBHT+Captopril and OBHT+GRT groups (1.49 ± 0.11 sperm/mL vs 1.80 ± 0.03 x 10^6 sperm/mL, $p<0.05$). Furthermore, there was no significant difference between the OBHT+GRT and LC+GRT groups or between the LC+GRT and LC groups (Table 4.7).

4.3.9.2 Sperm viability

The animals from the OBHT group showed significantly lower sperm viability compared to that of the LC group (23.40 ± 1.70% vs 57.10 ± 2.70%, $p<0.001$). The sperm viability of the LC+GRT animals was not significantly different from that of the LC group. Furthermore, there was a significantly higher in sperm viability of the OBHT+GRT group as well as OBHT+Captopril group when compared to untreated OBHT group ($p<0.001$) (Table 4.7).

4.3.9.3 Normal morphology

Normal sperm morphology was decreased in the OBHT group compared to the lean group (27.60 ± 3.60% vs 52.60 ± 3.50%, $p<0.01$). OBHT animals treated with GRT (OBHT+GRT) presented with a significantly higher in normal sperm morphology when compared to the untreated OBHT animals (53.50 ± 4.40% vs 27.60 ± 3.60%, $p< 0.001$). Treatment with Captopril did not show any significant differences of normal sperm morphology in OBHT+Captopril group when compared to the untreated OBHT group. Furthermore, the normal sperm morphology of LC animals subjected to GRT was not significantly different to that of the untreated LC animals (Table 4.7).

4.3.9.3.1 Head defects

OBHT animals had significantly higher sperm head defects than LC animals (73.90 ± 3.70% vs 47.10 ± 3.30%, $p<0.001$). The same group was treated with GRT (OBHT+GRT), and subsequently the percentage of sperm head defects were reduced compared to the untreated OBHT group (43.20 ± 3.50% vs 73.90 ± 3.70%, $p<0.001$). Similar to this, treatment with Captopril demonstrated a significantly lower the percentage of sperm head defects compared to the untreated OBHT group

(56.80 ± 5.80% vs 73.90 ± 3.70%, p<0.05). There were no statistically significant differences between the LC+GRT group and the untreated LC group (Table 4.7).

4.3.9.3.2 Midpiece defects

The percentage of midpiece defects was significantly higher in OBHT animals than in LC animals (6.20 ± 0.90% vs 1.30 ± 0.80%, p<0.01). Treatment with GRT reduced the percentage of midpiece defects when compared to untreated OBHT (2.40 ± 1.00% vs 6.20 ± 0.90%, p<0.05). No effect of Captopril was observed. Additionally, the supplementation of GRT in the LC group did not have any significant effect when compared to the untreated LC group (Table 4.7).

4.3.9.3.3 Teratozoospermy index

The only significant difference in teratozoospermy index was observed between the LC+GRT and LC groups (1.06 ± 0.006 vs 1.02 ± 0.015, p<0.05) (Table 4.7).

4.3.9.4 Sperm total motility

A significantly lower total motility was observed in OBHT animals when compared to LC animals (72.6 ± 1.2% vs 81.2± 4.9%, p<0.05). OBHT+GRT presented with a significant higher total motility when compared to untreated OBHT group (86.7 ± 2.0% vs 75.9 ± 2.8%, p<0.05). Treatment with Captopril also demonstrated a significantly higher total motility when compared to the untreated OBHT group (94.4 ± 1.1% vs 75.9 ± 2.8%, p<0.05). No significant difference was observed between the LC+GRT and LC animals (Table 4.7).

4.3.9.4.1 Progressive motility

The progressive motility was significantly lower in OBHT than in the LC group (47.60 ± 3.00% vs 59.21 ± 2.82%, p<0.05). Treatment with either GRT or Captopril revealed a significantly higher progressive motility in treated OBHT animals when compared to the untreated OBHT group (68.4 ± 2.60% vs 47.60 ± 3.00%, p<0.001 and 76.00 ± 5.40 vs 47.60 ± 3.00 %, p<0.001). There was no significant difference in percentage progressive motility between the LC group treated with GRT and the untreated LC group (Table 4.7).

4.3.9.4.2 Sperm kinematics

VCL: There was significantly higher VCL in the OBHT group compared to that of the LC group (208.20 ± 10.00 µm/s vs 165.20 ± 6.20 µm/s, $p<0.01$). Treatment with GRT did not affect VCL when compared to the untreated OBHT group. However, the same group treated with Captopril (OBHT+Captopril) presented with a significantly lower VCL when compared to untreated OBHT (62.00 ± 2.60 µm/s vs 208.20 ± 10.0 µm/s, $p<0.05$, $p<0.001$). The OBHT+Captopril group also had a significantly lower VCL compared to the OBHT+GRT group (62.00 ± 2.60 µm/s vs 174.30 ± 11.00, $p<0.001$). Lastly, VCL of animals from the LC+GRT group was not significantly different when compared to the LC group or the OBHT+GRT group (Table 4.7).

VSL: No significant difference in VSL was observed between the OBHT and LC groups or between the OBHT+GRT groups. A significantly higher in VSL was observed between OBHT+Captopril and OBHT group ($p<0.001$), and OBHT+Captopril and OBHT+GRT ($p<0.001$). Additionally, VSL was significantly higher in the LC+GRT group when compared to the LC group ($p<0.05$) (Table 4.7).

VAP: No significant difference in VAP was observed between OBHT and the LC group. A significant difference was only observed in treated groups (LC+GRT, OBHT+Captopril) when compared to the untreated LC and OBHT groups (Table 4.7).

CHAPTER FIVE

DISCUSSION

It is known that food is a source of energy, used by the organ systems to perform specific functions. However, changes in eating behaviour may cause either calorie restriction or excess. Masek and Fabry (1959) were the first persons to discover and confirm that the intake of high calorie food influences the development of obesity and its metabolic disorders in animal models, while Buettner *et al.* (2006) claim that these metabolic disorders tend to disturb the body's entire system. Researchers around the world have used diets to create experimental obesity, because it is a simple, inexpensive and available method (Salie *et al.*, 2014).

This chapter is divided into two sections corresponding to two conditions of diet-induced obesity (DIO) (Table 3.1). The first DIO group was exposed to a high caloric diet (HCD), containing mostly carbohydrates, especially sucrose, which is known to influence the development of obesity and T2DM (Barbosa-da-Silva *et al.*, 2014; Walker *et al.*, 2006). The other HCD was rich in fructose and cholesterol. A high-fructose diet results in the development of an overlapping of MetS features, with obesity playing a central role (Zhang *et al.*, 2017). Additionally, an excess of cholesterol intake is transferred to the blood and binds to protein, thereby causing fatty deposits in the arterial walls (Simon, 2014). The arteries become hard and narrow, resulting in HT (Matsuura, 2001; Simon, 2014). Both diets and the complications of induced metabolic disorders on male reproductive health will be discussed in detail in the following sections. Furthermore, the results will be discussed according to the objectives cited earlier (Section 1.4).

The first part of this chapter focusses on the results obtained in DIO associated with insulin resistance, followed by a discussion of the results obtained in DIO associated with HT. The last section of this chapter will compare all the results generated from induced insulin resistance and/or HT. Finally, general conclusions and recommendations will be made at the end of the discussion.

5.1 DIO associated with insulin resistance and a 6-week treatment with GRT

5.1.1 Food and water intake, body weights (BWs), glucose levels and cytokine levels

The induction of obesity through a HCD is time-dependent and influenced by the calorie composition of the specific carbohydrates included in the prepared diet. The inclusion of sucrose, which is highly palatable, further increases food intake and leads to hyperphagia, which impairs body metabolism (Du Toit *et al.*, 2008; Huisamen *et al.*, 2013; Nduhirabandi *et al.*, 2014; Salie *et al.*, 2014). In the

current study, OB animals demonstrated hyperphagia due to the sweetness of sucrose (Figure 4.1), hyperglycaemia (Figure 4.8) and glucose intolerance (Figure 4.9) after ten weeks. Subsequently, these animals (Figure 4.1) drank less water (Figure 4.3), more than likely because their food contained more moisture. High sucrose food affects the liver and insulin function, thereby affecting glucose metabolism and enlarging the entire body (Barbosa-da-Silva *et al.*, 2014; Walker *et al.*, 2006). However, BW did not change (Figure 4.5). We therefore suggest that the low protein content in DIO (Table 3.1) may affect muscle tissue or the development of subcutaneous fat. The muscle could also degenerate because of the low protein.

In summary, the OB animals were classified as prediabetic because of the elevated glucose levels which were slightly increased above the normal levels but remained less than diabetic levels (11mmol/L) (Figure 4.8 and Figure 4.9). These values correlated with the values proposed by the American Diabetes Association for humans, 2010. Therefore, the OB animals fed with a HCD for 16 weeks consumed more food than their age-matched controls (Figure 4.2) and became hyperphagic and obese, similar to findings reported in previous studies (Du Toit *et al.*, 2008; Nduhirabandi *et al.*, 2014). The BW (Figure 4.6) and adiposity index (Figure 4.7) increased with the concomitant increase in blood glucose levels (Figure 4.10, Figure 11 and Figure 4.12), as previously reported by Huisamen *et al.* (2013). This metabolic dysregulation may be due to the imbalance of calorie intake and expenditure.

It has been reported that an increase in IP fat was accompanied by upregulation of pro-inflammatory cytokines, which interfere with insulin signalling (Appari *et al.*, 2017; Jung & Choi, 2014; Koenen *et al.*, 2011). In the current study, OB animals presented with elevated IL-1β (Figure 4.13) and IL-18 (Figure 4.16). These inflammatory cytokines have previously been shown to be associated with the development of insulin resistance (Membrez *et al.*, 2009; Osborn *et al.*, 2011). An increase in cytokine levels can be ascribed to the hyperplasia and hypertrophy of adipocytes, correlating with the increased adiposity index (Figure 4.7). These cytokines and fat interfere with insulin signalling pathways in testicular tissue by deactivating intermediates in the pathway, resulting in insulin not being able to stimulate glucose uptake into the cells. The glucose therefore remains in circulation, leading to hyperglycaemic conditions (Figure 4.10, Figure 11 and Figure 4.12). Insulin levels have previously been shown to be higher in OB rat model (Huisamen *et al.*, 2011; Nduhirabandi *et al.*, 2017), but it is a shortcoming of the current study in the sense that it was not determined. The other investigated pro-inflammatory cytokines, including TNF-α levels, were lower in OB animals compared to LC animals (Figure 4.17), while the IL-6 (Figure 4.14) and IL-12 (Figure 4.15) levels of treatment groups did not differ significantly. These results were different from known literature

(Appari *et al.*, in press; Jung & Choi, 2014; Koenen *et al.*, 2011). Unexpected results might be due to various critical factors, including the age of animals, exposure time and quantity of given HCD or the adaptation mechanisms of the immunity systems of these animals to resist metabolic changes.

In summary, OB animals presented with dysregulated metabolic parameters, including hyperphagia, increased body weight and IP fat, hyperglycaemia and inflammation. These metabolic disorders could interact and cause insulin resistance. Therefore, the HCD was successful in inducing insulin resistance in the OB group. This insulin resistance influenced the risks of developing diabetes but in fasted and unfasted blood samples, glucose levels were less than 11 mmol/L. Therefore, according to the American Diabetes Association (2010), the rats in the OB group were not diabetic.

GRT, administered for six weeks, reduced body weight gain (Figure 4.6) and visceral adiposity (Figure 4.7) without influencing food (Figure 4.2) and water intake (Figure 4.4). It also did not affect blood glucose levels (Figures 4.10, 4.11 and 4.12). The reduction in visceral adiposity could account for the lower body weight as well as IL-1β and IL-18 levels evident for OB animals treated with GRT (OB+GRT) (Figure 4.13 and 4.16). In a study conducted on hyperlipidaemic mice, it was shown that rooibos has significant anti-obesity potential (Beltrán-Debón *et al.*, 2011). Furthermore, another *in vitro* study showed that rooibos inhibited adipogenesis (Sanderson *et al.*, 2014), which may have been associated with the reduced body weight gain and decreased inflammation observed in the current study. GRT treatment in LC+GRT animals did not influence metabolic parameters compared to untreated LC animals.

5.1.2 Effect of obesity-induced insulin resistance on testicular function parameters

Prediabetes has shown to impair male reproductive function at different levels (Alves, *et al.*, 2013; Rato *et al.*, 2014, 2012). Furthermore, the anatomy and physiology of the testis depend on different factors, including nutritional status and energy metabolism (Dupont *et al.*, 2014). In the present study, testicular weight (Figure 4.18) and histological features (Table 4.1) in OB animals fed a HCD remained unchanged compared to LC animals. These results were consistent with previously reported studies (Alves, *et al.*, 2013; Campos-Silva *et al.*, 2015). We suggest that the testicular tissue might have undergone mechanistic metabolic adaptations that allow them to minimize the negative effects promoted by the disease. OB animals had a low TW:BW ratio (Figure 4.19), which implies that these animals had much higher BW (due to fat) compared to the TW. Even if TW did not change, the excess BW can impair the feedback regulation of the HPG axis, which may affect testicular function. This can also affect sperm quality and quantity, and therefore result in male infertility. Furthermore, the

morphometric analysis showed that the area and diameter of the seminiferous tubules of OB animals were larger compared to that of the LC group (Table 4.1). These findings are in contrast with evidence that DIO is associated with atrophic seminiferous tubules with smaller diameters (Campos-Silva *et al.*, 2015; Yan *et al.*, 2015). The changes observed in the current study may be explained by reduced expression of apoptotic proteins, including Cleaved PARP and caspase 7 (Figure 4.27 and 4.28). Inappropriate or inadequate apoptosis may have led to a greater number of divided cells, which accumulated within tubules and caused the increase in size. It is therefore suggested that the changes in seminiferous tubules could affect hormone production and spermatogenesis.

Testicular Leydig cells produce T, which regulates spermatogenesis within Sertoli cells. T is either converted to E by the P450 aromatase or to dihydrotestosterone by 5α-reductase (Dong & Hardy, 2003). Hence, the metabolic changes observed in this study could have caused an imbalance in hormonal secretion. The T levels of OB animals were decreased (Figure 4.20) and their E2 levels elevated (Figure 4.21) compared to that of LC animals, thus leading to a reduced T:E2 ratio (Figure 4.22). These findings are in agreement with the literature (Kasum, 2016; Katib, 2015; Du Plessis *et al.*, 2010), which showed increased aromatization occurring in adipocytes in response to obesity. This hypersecretion of oestrogens results in the inhibition of the HPG axis via kisspeptin neurons and subsequently affects testosterone levels negatively, which can impair spermatogenesis.

Rooibos extract has been used in various studies and is known to possess biological effects or curative properties (Awoniyi *et al.*, 2012; Joubert & De Beer, 2011; Muller *et al.*, 2018; Opuwari & Monsees, 2014). The current study showed that GRT treatment in control animals did not influence TW or testicular histomorphometry. This might be due to non-effect of GRT on metabolic parameters (Section 5.1.1). Interestingly, treatment with the GRT significantly increased the TW:BW ratio in the OB+GRT group when compared to the untreated OB group (Figure 4.19). From these results it is evident that the difference between OB and OB+GRT was dependent on BW and not on testicular tissue because it was shown that GRT reduced BW gain (Section 5.1.1), which could normalize the ratio between TW and BW. Therefore, testicular function was probably also restored. Furthermore, the OB animals treated with GRT displayed a reduction in tubule area and a decrease in tubule diameter (Table 4.1); subsequently, these changes could affect Leydig cells as well as hormone production. These effects of GRT could result from its polyphenol composition, which might interact with body metabolism and homeostasis.

Aspalathus linearis contain flavonoids as major compounds (Joubert, 1996; Opuwari & Monsees, 2014), many of which are classified as endocrine disruptors. However, rooibos affects the steroidogenesis process, depending on experimental conditions where it can activate or inhibit

different steps of this process. In the current study, GRT treatment in LC+GRT animals was associated with a lower T:E2 ratio, which was expressed in lower T levels and higher E2 levels (Figure 4.22) and supports the role of rooibos as anti-androgenic agent in lean animals. This was similar to previous findings that showed that green rooibos extract possesses anti-androgenic properties in TM3 Leydig cells (Opuwari & Monsees, 2015). We speculate that the GRT could also interfere with different steps or reactions occurring in steroidogenesis in normal physiological conditions. GRT could affect the cholesterol level, which is a precursor to steroid hormones and might also inhibit the conversion of cholesterol to pregnenolone. GRT treatment in the OB group was associated with upregulation of T:E ratio towards normal levels (Figure 4.22), which supports the role of rooibos as a potential anti-estrogenic agent in obese animals. Anti-estrogenic properties of GRT might be due to its beneficial antioxidant activity, which could activate 17α-hydrogenase and 5α-reductase and inhibit P450 aromatase.

5.1.3 Expression and activation of intermediate molecule of the insulin signalling pathway in the insulin resistant testicular tissue

Insulin-independent AMPK and insulin-dependent PKB pathways control energy metabolism, homeostasis and insulin signalling (Berridge, 2014; Dupont *et al.*, 2014; Yu & Cui, 2016).

The OB group did not differ from the LC group in testicular expression of T-PKB (Figure 4.23) or baseline P-PKB (Figure 4.24). The PKB pathway depends on insulin receptor (IR) and insulin receptor substrate (IRS) phosphorylation; however, IR and IRS were not investigated, therefore this association could not be confirmed. The results suggest that high production of inflammatory cytokines (IL-1β and Il-18) could damage IR expression, thereby affecting PKB. In this study, OB animals had lower testicular expression of T-AMPK compared to LC (Figure 4.26), and subsequently AMPK was not activated in any of the treatment groups. This finding was expected, since dysregulation of glucose levels, high adipocyte index and an increase in inflammatory cytokines (IL-1 and IL-18) could contribute to the inhibition of AMPK phosphorylation, which is consistent with previous reports (Nandipati *et al.*, 2017). The AMPK pathway controls the steroidogenesis process, and its inhibition was associated with an imbalance of T and E2, as indicated in this study. This perturbation can affect sperm production and maturation, which could develop into male infertility. Interestingly, hyperoestrogen and AMPK inhibition in testicular tissue, due to adipocyte aromatization, is similar to that described for Peutz-Jeghers Syndrome, an autosomal-dominant disorder (Ham *et al.*, 2013).

GRT administration was associated with significantly lower testicular T-AMPK (Figure 4.26) and T-PKB (Figure 4.23) expression in LC+GRT, while the GRT did not have a significant effect on T-AMPK and T-PKB expression in OB+GRT animals. From the data, GRT (used as a supplement) could interfere with T-AMPK and T-PKB expression, which were also linked to lower T: E2 ratio in normal physiological conditions. This implies that testicular cells could not get energy to perform steroidogeneses and spermatogenesis. In prediabetic conditions, GRT treatment did not influence expression and activation of the intermediate molecules (PKB and AMPK) of insulin signalling in the testis. This might be due to various critical factors, including exposure duration (6 weeks of GRT treatment) and GRT dose.

5.1.4 Effect of obesity-induced insulin resistance on testicular apoptosis

Caspase 7 and its substrate PARP are both activated by internal or external stimuli and can lead to apoptosis (Chaitanya *et al.*, 2010; Elmore, 2007). Altered regulation of apoptosis contributes to many diseases due to cell accumulation (e.g. cancer, restenosis, inflammation) or cell loss (neurodegeneration). Programmed germ cell death plays a key role during fetal, neonatal, postnatal and adult spermatogenesis (Bejarano *et al.*, 2018).

In the present study, cleaved caspase 7 and PARP were significantly lower in the testicular tissue of the OB group compared to that of the LC group (Figure 4.27 and 4.28). These findings are in conflict with those previously reported for apoptotic protein expression in prediabetic conditions (Banerjee *et al.*, 2016; Celik-Ozenci & Tasatargil, 2013; Chaitanya *et al.*, 2010; Sishi *et al.*, 2011). However, our study suggests that inappropriate or deficient testicular apoptosis resulted from a disturbance in energy homeostasis due to hyperglycaemia (inactivation or dephosphorylating PKB and AMPK) as well as OS. Additionally, the study found that the seminiferous tubules were large, which could be due to more or bigger germinal or Sertoli cells. Abnormal distribution of these cells could also affect Leydig cells as well as the T: E2 ratio and sperm quality.

In this study, GRT administration was also associated with differences in caspase 7 (Figure 4.28) and PARP expression (Figure 4.27) between LC+GRT and LC, and LC+GRT and OB+GRT animals, while no differences were observed in the expression between OB+GRT and OB animals (Figure 4.25 and 26). The effect of GRT observed in treated LC animals may be related to the GRT supplementation, which inhibited T-AMPK and T-PKB under normal physiological conditions. The GRT dose used in this study might be responsible for downregulating or inhibiting the insulin signalling and apoptosis process by suppressing or interfering their intermediate receptors in treated

LC animals. Furthermore, as far as we are aware, this is the first time the effect of GRT on testicular tissue was investigated and these findings lay the foundation for future investigations.

5.1.5 Effect of obesity-induced insulin resistance on antioxidant activity and lipid peroxidation

Hyperglycaemia may interfere with natural antioxidant defences by changing intracellular signalling in addition to increasing the production of free radicals (Berdja *et al.*, 2016; Rolo & Palmeira, 2006; Taheri *et al.*, 2012). Since SOD and CAT enzymes are part of the first line of defence against free radicals, it is expected that the activity of these enzymes may be affected by OS before the other antioxidant enzymes are (Hamden *et al.*, 2009). The data from this study indicate that SOD (Figure 4.29) and CAT activity (Figure 4.30) are very significantly lower, with high MDA levels (Figure 4.31) in OB animals compared to non-obese animals, which define an OS state. The observed reduction in antioxidant enzyme activities could be due to the oxidative inactivation of the enzyme by ROS or by the glycation of the enzymes (Berdja *et al.*, 2016). Thus, different testicular cells are susceptible to the accumulation of $O_2^{\bullet-}$ and H_2O_2, which leads to an oxidative environment and cellular damage such as LPO (high level of MDA), DNA fragmentation as well as consequent sperm abnormalities and germinal cell apoptosis (Agarwal *et al.*, 2014). Furthermore, the high MDA levels might be linked to the increase of IL-1β and IL-18, which was also observed in the OB animals.

Rooibos has been shown to alleviate OS in diabetic conditions (Ayeleso *et al.*, 2014). Interestingly, treatment of OB rats with GRT attenuated testicular oxidative damage by upgrading SOD and CAT activity (Figure 4.29 and Figure 4.30), thereby leading to a reduction in LPO and MDA (Figure 4.31), similar to findings of a previous study (Awoniyi *et al.*, 2012). The ameliorating effects of GRT on testicular OS is probably due its flavonoids, aspalathin, and other potent antioxidant components which affect natural antioxidant enzymes by upregulating them and thereby reducing LPO. Polyphenols have been reported to suppress ROS formation either by inhibition of NADPH oxidases, chelation of trace elements, or upregulation and protection of antioxidant defences (Mishra *et al.*, 2013), including SOD and CAT enzymes. Furthermore, polyphenols prevent LPO, and could therefore act as an anti-oxidant, which was also indicated in the current study.

5.1.6 Effect of obesity-induced insulin resistance on the basic sperm parameters

Prediabetic conditions impair several male reproductive parameters due to altered testicular metabolism and mitochondrial bioenergetics (Rato *et al.*, 2013; 2014). OS, inflammation and apoptosis are closely interlinked with hyperglycaemic conditions and consequently may cause

testicular cell damage and have a negative impact on hormone and sperm production (Berdja *et al.*, 2016; Rolo & Palmeira, 2006). Additionally, thermoregulation defects and scrotal lipomatosis may result from high accumulation of fat, affecting spermatogenesis and sperm function (Du Plessis *et al.*, 2010; Oyeyipo *et al.*, 2015).

In the current study, testicular OS, testicular apoptosis inhibition and histomorphometric changes were accompanied by a decrease in the T:E2 ratio. Together, this could contribute to a higher epididymal weight (Figure 4.32) and impairment of sperm functional parameters (Table 4.2) in OB animals. The current study showed that spermatogenesis and sperm maturation were impaired based on the low sperm concentration, and reduction in viability, progressive motility, VSL, VCL and VAP. These findings are similar to previous findings (Oyeyipo *et al.*, 2015). Furthermore, morphological abnormalities increased with elevated head and midpiece defects in OB animals. Therefore, altered basic sperm function parameters may contribute to male infertility in obesity. Co-treatment with GRT ameliorated epididymal weight (Figure 4.32) as well as the above-mentioned sperm functional parameters in treated OB+GRT animals (Table 4.2). This effect could have resulted from bioflavonoids and other potent antioxidants, found in GRT, as well as improved accumulation of fat and inflammatory cytokines.

5.1.7 Summary of DIO-associated insulin resistance effect on male fertility

A diagrammatic summary of the relationship between obesity and insulin resistance and their effects on male fertility is depicted in Figure 5.1 (A). From the discussed results, the current findings show that HCD with sucrose led to hyperphagia and caused hyperplasia and hypertrophy of WAT. This abnormal accumulation of adipose tissue results in elevated FFAs, which cause upregulation of pro-inflammatory cytokines (IL-1β, IL-18). Altogether, high sucrose intake, fat accumulation and inflammation interfere with insulin signalling pathways by deactivating IRs, resulting in insufficient glucose uptake by target cells and a build-up of glucose in the bloodstream (hyperglycaemia). Hyperglycaemia may interfere with intracellular signalling pathways of testicular tissue by affecting energy metabolism (reduced T-PKB, T-AMPK), apoptosis (reduced caspase and PARP), antioxidant activities (decreased SOD and CAT) and lipid peroxidation (increased MDA levels). Subsequently, seminiferous tubules possibly increased in size due to decreased apoptosis and dysregulated energy metabolism. We therefore suggest that the changes observed in the seminiferous tubules could impair steroidogenesis (reduced T:E2) by affecting Leydig cells and spermatogenesis (reduced sperm function parameters), thereby reducing male fertility. Furthermore, an imbalance of antioxidant

activities and MDA levels could also affect sperm functional parameters and consequently reduce male fertility.

Lastly, increased adiposity increases aromatization, which affect steroidogenesis and reduce T:E2. The consequent hypersecretion of E2 impairs spermatogenesis and further lead to reduced male fertility.

5.1.8 Summary of GRT's effects on DIO-associated insulin resistance and male fertility

A diagrammatic summary of the possible ameliorative effect of GRT treatment on the pathophysiological mechanisms linked to obesity/insulin resistance and subsequent improvement in male reproductive parameters is displayed in Figure 5.1 (B). In this study, adipose tissue was reduced (potentially via inhibition of lipidaemia), resulting in lower cytokine levels (IL-1β, IL-18) and therefore implicating GRT's anti-inflammatory effects. Furthermore, SOD and CAT activities were improved, while MDA levels were reduced, thus also implicating GRT to have anti-oxidative properties. Lastly, the decrease in adipose tissue implies lessened aromatization, thereby reducing E2 production and normalizing the ratio of T to E2. Therefore, GRT was also anti-oestrogenic. Taken together, these factors resulted in subsequent improvements in sperm quantity and quality, which associate GRT treatment with the ability to restore male fertility.

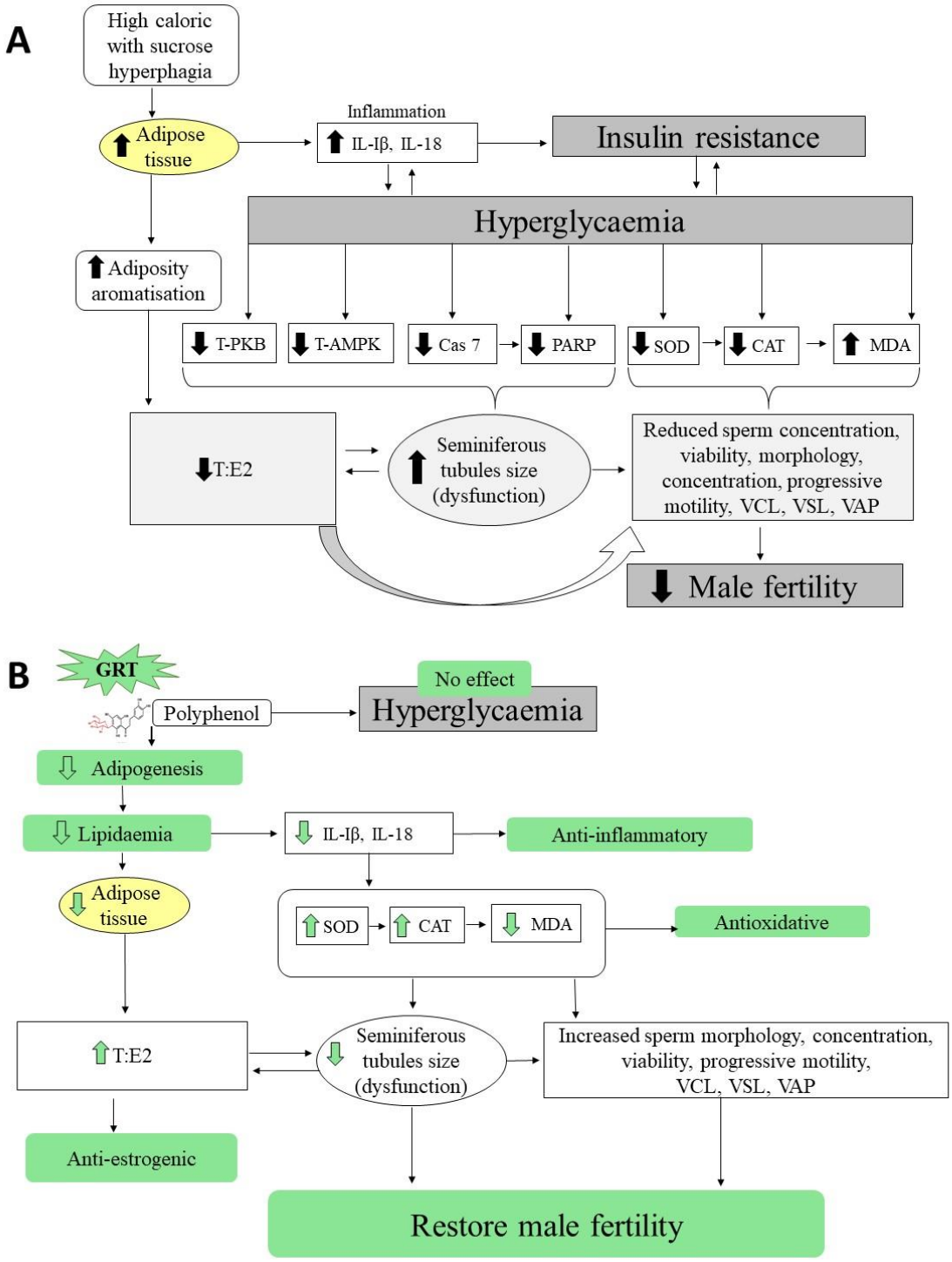

Figure 5.1: The mechanisms through which obesity associated with insulin resistance affect male reproduction (A) and the possible ameliorating mechanisms of GRT treatment (B)

CAT: Catalase, Cas 7: Caspase 7, IL-18: Interleukin-18, IL-1β: Interleukin-1 beta, MDA: Malondialdehyde, PARP: Poly ADP ribose polymerase, SOD: Superoxide dismutase, T-AMPK: Total adenosine 5' monophosphate-activated protein kinase, T:E2: Ratio of testosterone to estradiol, VAP: Average path velocity, VCL: Curvilinear velocity, VSL: Straight line velocity.

5.2 DIO associated with hypertension and 6-week treatment with GRT

5.2.1 Metabolic parameters

Food intake, water intake, BW, IPF weights, glucose levels, cytokines and blood pressure (BP) were used to describe and validate or define an experimental animal model of OBHT. In the present study, male Wistar rats were fed a special HCD over a period of 16 weeks to induce obesity and its associated metabolic complications, including HT. Similar findings were reported in a previous study (Kant *et al.*, 2009). Specifically, OBHT animals consumed more food and drank less water compared to LC animals (Figure 4.33, 4.34, 4.35 and 4.36) because the food contained fructose (sweetener) and was moist. BW (Figure 4.37 and 4.38) and adiposity index (Figure 4.38) increased significantly in the OBHT group compared to the LC group. This was to be expected, since the high-fructose content in the diet is associated with hyperphagia and obesity (Codella *et al.*, 2017; Lenoir *et al.*, 2007), which was also evident in the current study. We were therefore able to successfully induce obesity in male Wistar rats over a period of 16 weeks by using the same dietary protocol as previously used in our laboratory (Huisamen *et al.*, 2013; Salie *et al.*, 2014).

Obesity, especially visceral obesity, is strongly associated with impaired glucose metabolism (D'Alessandro *et al.*, 2015), which results in hyperglycaemia. From the present study, OBHT animals were hyperglycaemic or glucose intolerant compared to LC animals (Figure 4.40, 4.41, 4.42,4.43 and 4.44), the result of which is supported by a previous finding (Huisamen *et al.*, 2013). In addition to developing hyperglycaemia, the pro-inflammatory cytokines IL-β and IL-18 increased in OBHT (Table 4.3). This may be due to the high adiposity index. Both hyperglycaemia and inflammation are known to impair insulin sensitivity by interfering with the insulin signalling pathways or inhibiting insulin signal transduction (Luca *et al.*, 2009).

Hypertension results from the pathogenesis of obesity due to activation of the sympathetic nervous system and the RAAS, resulting in arterial vasoconstriction and sodium retention and excessive intra-vascular and intra-abdominal fat, which triggers inflammation (and consequently endothelial dysfunction) and physical compression of the kidneys due to the excessive fat accumulation around the kidneys (Hall *et al.*, 2015). In the present study, OBHT rats had higher systolic and diastolic BP as well as mean arterial pressure compared to LC (Table 4.4 and 4.5). This implies that OBH animals developed HT, which could potentially be a result of a greater BW and higher adiposity index, hyperglycaemia, glucose intolerance and inflammation, as indicated in this study. These findings are consistent with the known association between obesity induced with fructose and HT (Chandra *et al.*, 2014; Hall *et al.*, 2015). We therefore conclude that we successfully established a model displaying both obesity and hypertension, which is in accordance with a previous study that used the same DIO

(Huisamen *et al.*, 2013) . It is important to note that the rats in the current study specifically had stage 1 HT according to the classification of HT development (Giles *et al.*, 2009).

In summary, OBHT animals presented with dysregulated metabolic parameters (including hyperphagia), increased BW and IP fat, hyperglycaemia, inflammation and HT. Additionally, this animal model presented with a MetS, which occurs when an animal model has more than three of the associated medical conditions (Cheung & Li, 2012). Furthermore, both GRT and Captopril, administered for six weeks on MetS features, were evaluated respectively.

GRT treatment lowered BW and adiposity index in treated OBHT animals (Figure 4.38), which is consistent with the anti-obesity potential or adipogenesis inhibition of GRE and is attributable to its high polyphenol content (Sanderson *et al.*, 2014). However, GRT treatment did not influence glucose uptake in the OBHT+GRT group (Figure 4.42, 4.43 and 4.44). These results were unexpected because it had been previously shown that GRE and aspalathin improved glucose uptake and lipid metabolism *in vivo* (Mazibuko *et al.*, 2015). The current results could more than likely be ascribed to several reasons, such as GRT dose, time of administration and other environmental conditions of animal handling. These factors should be taken into consideration during future studies.

The OBHT animals treated with GRT had lower BP compared to the untreated OBHT group (Table 4.5). This GRT effect was expected because previous *in vitro* and *in vivo* studies had proved the anti-hypertensive effects of unfermented rooibos (Persson *et al.*, 2006; Persson, 2012). In the current study, the decrease in BP could have been ascribed to the reduction in BW and subsequent less IP fat accumulation in these animals. On the other hand, anti-hypertensive properties of GRT are associated with its high aspalathin content (Joubert & De Beer, 2011). Furthermore, the inhibition of the RAAS system might also be a potential reason for decreased BP; however, this mechanism was not investigated in the current study.

GRT treatment in LC animals did not significantly alter BW (Figure 4.38), adiposity index (Figure 4.39), glucose levels (Figure 4.42, 4.43 and 4.44) and BP (Table 4.5). We therefore speculate that the polyphenols present in GRT did not interfere with body metabolism or altered adipocyte differentiation.

Treatment with Captopril also led to a lower BW and adiposity index (Figure 4.38 and 4.39). This reduction could be due to a decrease in food intake and high consumption of water. It has been reported that Captopril intake decreases BW via angiotensin-(1–7) (Oh *et al.*, 2012) and could also influence lipolysis, which can reduce IP fat and also reflect the reduction of BW. Importantly, it was observed that treatment with GRT maintained the BW and adiposity index to close to normal weight,

while Captopril reduced body weight and adiposity index to below the normal weight (Figure 4.38 and 4.38). It therefore appears as if treatment with Captopril could have an outspoken effect on body weight. This might be due to the pharmacological RAAS effect, which interferes with energy balance and glucose homeostasis.

Captopril treatment lowered BP in the OBHT+Captopril group compared to the untreated OBHT group (Table 4.5), which is consistent with the literature and clinical diagnosis of HT (Foëx & Sear, 2004). Captopril inhibits the conversion of ATI to ATII, thereby decreasing vasoconstriction and BP. In addition, BP was also associated with decreased BW and adipocyte index in OBHT+Captopril animals.

5.2.2 Hypertension and testicular histomorphometry

The OBHT animals had a lower TW:BW ratio (Figure 4.52). However, TW (Figure 4.51) and histological features remained unchanged compared to that of LC animals (Table 4.6). The differences between LC and OBHT groups in terms of TW:BW was therefore merely dependent on BW and not the TW, as these animals were bigger. These findings differed from that of a previous study where a higher TW was observed in spontaneously hypertensive rats (Bechara *et al.* 2015). The current study used DIO associated with a hypertensive rat model, while others used spontaneously hypertensive rats, which is a genetically selected animal model with naturally high arterial BP and with end-organ and vascular alterations. To our best knowledge, this is the first time TW and testicular structure were evaluated in obesity associated with HT. The results might be due to the development of HT, where the current HT animal model was in stage 1. This means that OBHT animals were not chronically HT and therefore the testes could resist and adapt to these metabolic changes.

Treatment with the GRT did not influence TW:BW in the treated OBHT group when compared to the untreated OBHT group (Figure 4.52). This implies that the reduction in BW with GRT treatment (Fig 4.38) did not influence TW. This might be due to the GRT dose used in this study, which could be too low or high to influence TW. However, treatment with Captopril significantly improved the TW:BW ratio in treated OBHT compared to untreated OBHT and OBHT+GRT groups (Figure 4.52). As previously discussed, treatment with Captopril reduced BW to below of LC, thus this could have a detrimental effect on BW as well as on testicular tissue. This might be due to the pharmacological RAAS effect, which interferes with energy balance and glucose homeostasis.

The testicular histological features of the OBHT animals were unchanged compared to all treated groups (Table 4.6), which was consistent with previous findings regarding spontaneously

hypertensive rats (Bechara *et al.* 2015). This unchanged testicular structure might be due to the ability of the testicular mechanism to adapt to metabolic disorders. Additionally, the obesity-induced HT was in stage 1, which could not be chronically causing changes to the testicular structure. However, this HT altered testicular morphometric parameters (Table 4.6). Atrophic seminiferous tubules (decreased area and diameter) could be linked to a narrow lumen (decreased lumen area and diameter), which is lined with a thinner layer of epithelium in OBHT animals compared to LC animals. Similarly, this was the case in the previously reported studies on hypertensive animal models (Akagashi *et al.*, 1996; Azu, 2015). The changes that occurred in OBHT animals could possibly be attributed to testicular artery damage due to the HT, resulting in hypoperfusion of testicular tissue, causing a reduced supply of oxygen and nutrients. It is possible that these testicular morphometric changes could impair spermatogenesis and steroidogenesis, and consequently lead to infertility.

Treatment with GRT reduced the diameter and area measurements of the lumen, which enhanced the size of the seminiferous tubules and the epithelium height in treated OBHT+GRT animals compared to the untreated OBHT group (Table 4.6), suggesting the favourable effects of treatment on spermatogenesis and steroidogenesis due to its high bioflavonoid content. Furthermore, OBHT+Captopril animals had a smaller lumen diameter, which might be linked to hypertrophic seminiferous tubule diameter and a higher epithelial height (Table 4.6). This side effect could be linked to Captopril's effect of reducing BW. We therefore suggest that the GRT treatment could be used as an alternative treatment to Captopril treatment, as the latter could have side effects on testicular structure as well as on the overall male reproductive function. Further studies should be considered to help elucidate the side effects of anti-hypertensive substances and associated mechanisms linked to male reproductive disorders.

5.2.3 Hypertension and male steroid hormone production

Leydig cells are found in the interstitial spaces between the seminiferous tubules of the testis in the male reproductive system and produce T, thereby influencing spermatogenesis (Ye *et al.*, 2017). In this study, the high levels of T in the OBHT animals were unexpected (Figure 4.53), since an inverse relationship between T production and hypotensive conditions was previously shown (Liu *et al.*, 2004). However, the difference between the current and previous studies could be the result of the methods used to induce HT or the stage of HT development. Liu *et al.* (2004) used high-salt food to induce HT, while the current study used a HCD. We speculated that the overproduction of T in OBHT animals could have resulted from the diet that contained additional cholesterol, which acts as the universal precursor for steroid hormones. This increase in cholesterol consumption could have

affected T production; however, cholesterol was not measured. A higher T level could have also resulted from the inhibition of caspase 7 (reduction in apoptosis) and Cleaved PARP (Fig 4.60, 4.61) as well as testicular OS (Fig 6.3, 6.4), resulting in impaired or increased proliferation of Leydig cells that produce T. It is well-known that in pathophysiology, any biological molecule which has a low or high expression or production may have an impact on body metabolism as well as personal behaviour (Metallo & Vander Heiden, 2013; Silverman & Deuster, 2014). The abnormal production of T could suppress gonadotropin secretion via negative feedback on the hypothalamus and pituitary, leading to the alteration of Sertoli cells and spermatogenesis. Moreover, these high levels of T production could induce frustration or stress in animals.

Circulating T in the body is the substrate for E2, which is produced by aromatization in the liver, muscles, brain and the fat cells. Furthermore, E2 is proportional to adipocyte aromatization (Li *et al.*, 2016). The current study shows an increased E2 in OBHT animals because these animals presented with a high adiposity index/high adipocyte aromatization, which is consistent with previous reports (Hilborn *et al.*, 2015; Vihma *et al.*, 2017). This could have resulted in hypogonadism and induce male reproductive disorders. Furthermore, T levels were measured and compared to E2 by determining T:E2 ratio (Figure 4.55). It was found that in the OBHT group, T (Figure 4.53) and E2 (Figure 4.54) levels were both increased but the E levels remained higher than T, consequently causing a reduction in the T:E2 when compared to the LC group (Figure 4.55). The OBHT animals developed HT with obesity as a central mechanism, which caused imbalanced hormone secretion, shown by the low T:E ratio. This is in accordance with the literature (Hilborn *et al.*, 2015; Katib, 2015; Vihma *et al.*, 2017).

Importantly, treatment with GRT and Captopril lowered both T (Figure 4.53) and E (Figure 4.54) levels, but since T was higher than E, the ratio is higher (Figure 4.55) in OBHT animals. The hormone levels of OB+GRT or OB+Captopril were not different from untreated LC animals. This implies that the T levels of treated OBHT animals could be improved to normal levels. No other studies reported these effects, and the current study suggests that GRT and Captopril could enhance fertility properties in male rats – a possible result of their potent antioxidant properties and androgenic activities. GRT is rich in polyphenolic compounds, which are known to be an ROS scavenger. Captopril also contains a sulfhydryl or thiol group that is able to scavenger ROS. From previous studies, it is evident that androgen activity depends on the experimental conditions where polyphenol may activate or inhibit testosterone production. In the current study, GRT, rich in polyphenol compounds, improved T levels in hypertensive conditions. The mechanism of action by which GRT has increased both T and the T:E2 ratio and decreased E2 could have resulted from reduced adipocyte index, antioxidant, anti-obesogenic and anti-hypertensive properties of GRT which were found in this study. Moreover, the

results of the present study indicate that both Captopril and GRT provided significant and comparable protective effects against HT-induced hormone aberrations. Therefore, we suggest the use of GRT treatment as an alternative therapy.

5.2.4 Hypertension and energy homeostasis

PKB regulates a variety of cellular responses ranging from metabolism, growth, cell survival and intracellular signal transduction (Mansuri *et al*., 2014). In the present study there were lower levels of T-PKB expression in the OBHT group than in the LC group (Figure 4.56), and furthermore, this protein did not undergo activation (Figure 4. 57) compared to the LC group. This affected the ratio of P-PKB and T-PKB (Figure 4.58). The metabolic changes observed in the OBHT animals could interfere with testicular insulin signalling transduction components (IRs and IRS), which initiate PKB pathways. This implied that GLUTs were not translocated, which was unfortunately not measured in this study. It is therefore speculated that the abnormal functioning of the insulin-dependent PKB pathway may be due to the impairment of IRs and IRS, which results in testicular pathologies and ultimately male infertility.

The testicular T-PKB expression of the OBHT+GRT animals was restored to the normal expression levels compared to LC (Figure 4.56). This positive effect of GRT reflects some potent health properties that could resist or reverse metabolic changes. The supplementary GRT in LC animals reduced T-PKB expression compared to that of LC animals. This implies that the GRT dose (60 mg/kg) used in this experimental study could be harmful to testicular function in lean animals. We suggest that this dose could be used to treat testicular pathologies in obesity but that effects on lean animals need further elaboration. Furthermore, the T-PKB expression was not influenced by Captopril exposure in OBHT+Captopril animals, which linked to T-AMPK results, suggesting that Captopril does not have any effect on the insulin-dependent or insulin-independent pathways.

AMPK, a highly conserved sensor of cellular energy, is activated in response to deficiency in caloric energy intake, ischemic conditions or hypoxia (Hardie *et al.*, 2012), some metabolic hormones (leptin), and therapeutic substances (plant extract, antidiabetics) (Hardie, 2017; Rice *et al.*, 2013). When activated for preserving cellular energy homeostasis, it switches off energy-consuming processes and switch on energy-generating pathways (Galardo *et al.*, 2007; Hardie, 2017). In the current study, T-AMPK was also less expressed in OBHT rats (Figure 4.59), which is in accordance with the shared inter-relationship between hypertension and energy metabolism via underlying pathways. Unfortunately, activated (phosphorylated) AMPK was not detected in the testicular

sample. Several factors may be responsible for this, including insufficient signals to activate the AMPK pathways, the western blot technique or ineffective antibodies. According to our knowledge, this is the first time that the AMPK antibody was used to evaluate metabolic disorders in testicular tissue. It is recommended that the AMPK pathway should be explored further in future studies of HT and testicular pathologies.

Testicular T-AMPK expression in OBHT animals treated with either GRT or Captopril did not change compared to LC animals (Figure 4.59). This may be due to the glucose levels that were not affected by GRT treatment. However, LC+GRT animals had a significantly lower T-AMPK expression, which might be linked to the lower T-PKB expression and reduced SOD activity. This non-effect and limited effect of GRT treatment could be the result of multiple factors, which includes GRT dose administration. Therefore, the treated animals could have had dysregulated energy homeostasis, thereby contributing to the disturbance of male reproductive health.

5.2.5 Hypertension and testicular apoptosis

Cleaved PARP and caspase 7 are apoptotic markers involved in spermatogenesis and contribute to sperm maturation by eliminating excess germinal cells or abnormal spermatozoa (Agarwal *et al.*, 2009). With internal or external stimuli, these markers could be slightly or highly activated in testicular tissue, thereby generating male infertility indicators. In the current study, Cleaved PARP and caspase 7 were also lower in OBHT testicular tissue compared to the LC group (Figure 4.60 and 4.61). These results are linked to MetS features associated with testicular energy depletion (low T-PKB and T-AMPK as well their inactivation) and OS. We suggest that the altered testicular intracellular signalling can affect its structure as well as sperm production and maturation.

Treatment with GRT or Captopril did not influence Cleaved PARP or caspase 7 in OBHT animals compared to untreated OBHT animals (Figure 4.60 and 4.61). GRT treatment's inability to affect these apoptotic markers may be due to the significantly raised glucose levels. AMPK also did not change with GRT treatment. However, GRT reduced Cleaved PARP and caspase 7 levels in treated LC controls (Figure 4.60 and 4.61). This finding is linked to the lower expression of T-PKB and T-AMPK under the same physiological condition, which shows an alteration of energy homeostasis in treated LC animals. This implies that GRT supplementation with 60 mg/kg could interfere with normal physiological mechanisms. The reduced testicular apoptosis will cause huge proliferation of testicular cells or excess of germinal cells and subsequently some abnormalities could develop (testicular cancer, etc.).

5.2.6 Hypertension and testicular oxidative stress (OS)

The testis is susceptible to oxidative damage, as the blood vessels supplying these tissues often show sclerotic changes when BP increases in the arteries (Azu, 2015). Moreover, all the components of the RAAS have been reported to be present in the testis (Bader & Ganten, 2008; Franke *et al.*, 2003), and their overexpression or deficiency could be involved in the pathophysiology of testicular tissue. In the current study, obesity and insulin resistance, also associated with OS, could stimulate the RAAS system and cause HT, which in turn, could exacerbate OS. The ATII, the most active component in this system, is a well-known OS inducer that increases the generation of $O_2^{\bullet -}$, H_2O_2 and hydroxyl radicals ($HO^{\bullet}$) by activating the NADPH oxidase enzyme (Cai *et al.*, 2003). In the current study, the MDA levels (Figure 4.64) and CAT activity (Figure 4.63) were higher and the SOD activity was lower (Figure 4.62) in OBHT rats than in LC rats. These findings are consistent with other findings that found a link between HT and OS (Adedara *et al.*, 2018; Azu, 2015; Berdja *et al.*, 2016; Redón *et al.*, 2003; Rolo & Palmeira, 2006). Since SOD and CAT enzymes are part of the first line of defence against free radicals, it is expected that the activity of these enzymes may be affected by OS before the other antioxidant enzymes are affected (Hamden *et al.*, 2009). The abnormal function or activity of SOD and CAT in testis may result in several deleterious effects due to the accumulation of $O_2^{\bullet -}$ and H_2O_2 respectively. The H_2O_2 reacts with lipids, leading to LPO, which in turn results in the formation of several products including MDA (Agarwal *et al.*, 2014). This process also occurred in the current study. The associated LPO may point to the impairment of the sperm membrane, which is more than likely responsible for the morphological alterations found in this study (Table 4.8). Moreover, spermatozoa become more permeable to external substances or ROS, which could impair intracellular biological components, DNA and protein (Agarwal *et al.*, 2014).

Previous studies have reported that polyphenol-rich plant extracts might be used to protect the male reproductive function against induced OS (Awoniyi *et al.*, 2012; Manirafasha, 2014). The dietary antioxidant intake helps to maintain an adequate antioxidant status in the body, thereby protecting against OS. In the current study, the protective mechanism of GRT has been examined in the onset of OS related to obesity-induced HT, and its effect was compared to that of Captopril. The findings from the study showed that both GRT and Captopril treatments attenuated OS, as demonstrated by reduced MDA levels and increased CAT activity in treated OBHT rats (Figure 4.64 and 4.63). This effect of GRT treatment was expected as polyphenol-rich aspalathin is a known natural antioxidant and could offer protective effects against OS (Dludla *et al.*, 2014; Marnewick *et al.*, 2011). These findings are in agreement with a previous study, which has shown that both fermented and green rooibos extracts could offer a measure of protection against induced oxidative damage by increasing

the antioxidant defence (Awoniyi *et al.*, 2012). The ability of polyphenol compounds to act as antioxidant results from its ability to donate a hydrogen ion to the peroxyl radical produced as a result of LPO (Kumar & Pandey, 2013; Treml & Šmejkal, 2016).

Captopril's ability to lower BP, as observed in this study, could reflect male reproductive organ function. Captopril, an ACE inhibitor, decreases the circulating and tissue levels of angiotensin II. Captopril also possesses antioxidant activity due to its thiol or sulfhydryl group, which acts as a free radical scavenger of various ROS and prevents LPO, thereby serving as a protection against OS (Fischer *et al.*, 2000; Liu *et al.*, 2007; Scribner *et al.*, 2003). The differences between the results obtained with Captopril and GRT were insignificant, suggesting that both treatments equally protected the testicular tissue from the detrimental effects of HT of reducing CAT activity and inducing LPO.

Nevertheless, treatment with GRT or Captopril did not affect SOD activity in OBHT+GRT animals, while GRT supplementation showed a significantly lower SOD activity in the treated LC+GRT group when compared to the matched control animals (Figure 4.62). These findings are linked to the discussed findings on T-AMPK, T-PKB, Cleaved PARP and caspase 7 in the same treatment conditions. Both rooibos and Captopril are known to have beneficial health properties, therefore we speculate that a GRT dose (60mg/kg) and Captopril 50mg/kg were the cause of unexpected findings.

5.2.7 Hypertension and epididymal sperm function

The epididymis is critical for post-testicular maturation and storage of sperm, and epididymal weight is a marker of not only epididymal structure, but also epididymal sperm reserves (De Grava Kempinas & Klinefelter, 2014). The current study showed that OBHT animals had heavier epididymides compared to the age-matched LC animals (Figure 4.65). This finding differs from that of previous studies which found that the epididymal weight did not change due to induced HT with N(G)-Nitro-L-arginine-methyl ester (Akinyemi *et al.*, 2015). This difference might be due to the diet or method used to induce HT. The heavier epididymides in the current study might be due to elevated arterial pressure, high E2, testicular OS and reduced Cleaved PARP and caspase 7. Furthermore, these disorders could affect sperm quantity and quality.

The OBHT animals presented with a lower sperm concentration, lower sperm viability and normal sperm morphology with an increased percentage of head and midpiece defects as well as impaired sperm motility (specifically VCL) when compared to LC animals (Table 4.7). These findings were in agreement with literature on the pathophysiology of spermatozoa and MteS features (Schisterman *et*

al., 2014; Sermondade *et al.*, 2013). This implies that spermatozoa of OBHT animals will be unable to fertilize an ovum. Abnormal function of sperm could result from hormonal aberrations and OS. Furthermore, during hypertensive conditions, increased intracellular calcium, activation of growth and inflammatory signalling pathways could impair the sperm membrane; however, these pathways were not investigated. Additionally, other velocity parameters, namely VSL and VAP, were not significantly changed in OBHT animals, possible due to the stage of induced HT not being strong enough to alter these parameters. We suggest that future studies should explore the mechanisms that link sperm kinematics and MetS features.

Treatment with either GRT or Captopril reversed changes in epididymal weight (Figure 4.65), which could also influence sperm quality and function (Table 4.7) in OBHT+GRT animals. GRT treatment effects are consistent with that of previous studies (Awoniyi *et al.*, 2012; Opuwari & Monsees, 2014). GRT could offer protective effects due to its high polyphenolic composition, which could play multiple functions, including being antioxidant and anti-oestrogenic. It is well-known that the diversity of biological properties of polyphenols depend on the chemical structures and the number, nature, position and substituents of hydroxyl groups and unsaturated bonds (Kumar & Pandey, 2013; Treml & Šmejkal, 2016). Furthermore, the effect of Captopril on epididymal sperm function might be due to its antioxidant activity (Fischer *et al.*, 2000; Liu *et al.*, 2007; Scribner *et al.*, 2003). Captopril could stimulate spermatogenesis via inhibition of the kallikrein kinin system and activation of bradykinin (Monsees *et al.*, 1996; Okeahialam *et al.*, 2006; Siems *et al.*, 2003). However, the differences between the results obtained with Captopril and GRT were insignificant, suggesting that both treatments equally protected the epididymal sperm function from the detrimental effects of HT due to OS.

5.2.8 Summary of DIO-associated hypertension on male fertility

A diagrammatic summary of the relationship between obesity and HT and their effects on male fertility is depicted in Figure 5.2 (A). The findings show that HCD with fructose and cholesterol leads to hyperphagia, which can cause MteS features, including HT. This affects testicular and sperm function parameters through different pathophysiological mechanisms. HCD with fructose and cholesterol hyperphagia caused hyperplasia and hypertrophy of WAT and hyperglycaemia, which both cause upregulation of pro-inflammatory cytokines (IL-1β, IL-18). Due to elevated FFAs, fat accumulation and inflammation therefore interfere with insulin signalling pathways by deactivating intermediates in these pathways. This is followed by insufficient glucose uptake, which leads to a build-up of glucose in the bloodstream (hyperglycaemia). Inflammation-induced insulin resistance

also contributes to HT due to the activation of the sympathetic nervous system. Furthermore, a high cholesterol intake changes lipid profiles, elevates FFAs and causes inflammation. This contributes to endothelial dysfunction and atherosclerosis, ultimately resulting in HT. Additionally, the increased adiposity, together with high cholesterol intake, also affects steroidogenesis (reduced T:E2) and consequently impairs spermatogenesis and male fertility. HT results in reduced oxygen and nutrient supply, which changes testicular signalling pathways and impacts on spermatozoa. Subsequently, testicular homeostasis were disturbed through altered energy metabolism (reduced T-PKB and T-AMPK), apoptosis (reduced caspase and PARP), antioxidant activities (decreased SOD and CAT) and lipid peroxidation (increased MDA levels). These factors affect sperm functional parameters, thereby reducing male fertility. Furthermore, seminiferous tubules possibly decreased in size due to dysregulated energy metabolism. We therefore suggest that the changes in seminiferous tubules could impair steroidogenesis (reduced T:E2) by affecting Leydig cells and spermatogenesis and consequently reducing male fertility.

5.2.9 Summary of GRT's effects on DIO-associated hypertension and male fertility

The possible ameliorative effect of GRT treatment on the pathophysiological mechanisms linked to obesity-induced HT and subsequent improvement in male reproductive parameters are displayed in Figure 5.2 (B). In this study, the adipose tissue was reduced (potentially via lipidaemia inhibition), resulting in low cytokine levels, which lowered BP. This associates GRT with possible anti-hypertensive properties. Subsequently, CAT activity was improved, while MDA levels were reduced, which serves to show that GRT possess anti-oxidative properties. Lastly, the reduction in adipose tissue also led to less E2 production, thereby normalizing the T:E2 ratio. Therefore, GRT is to a certain extent also anti-oestrogenic. Taking all of this into consideration, it is clear that GRT treatment has the ability to restore male fertility as treatment resulted in improved sperm quantity and quality.

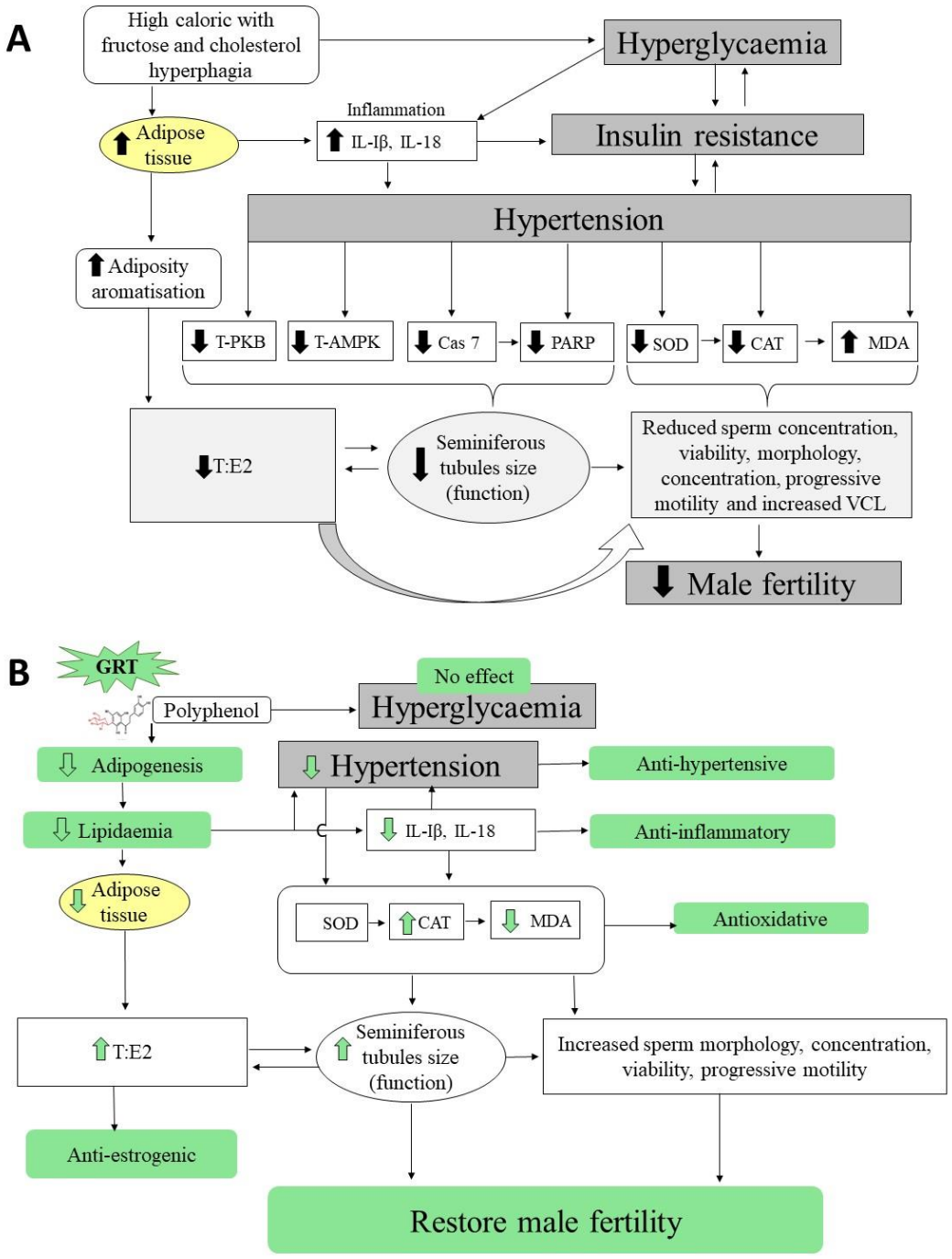

Figure 5.2: The mechanisms through which obesity associated with hypertension affect male reproduction (A) and the possible ameliorating mechanisms of GRT treatment (B)

CAT: Catalase, Cas 7: Caspase7, IL-18: Interleukin-18, IL-1β: Interleukin-1 beta, MDA: Malondialdehyde, PARP: Poly ADP ribose polymerase, SOD: Superoxide dismutase, T-AMPK: Total adenosine 5' monophosphate-activated protein kinase, T:E2: Ratio of testosterone to estradiol, VCL: Curvilinear velocity.

CHAPTER 6

CONCLUSION AND RECOMMENDATIONS

In the present study, two different diets were used to induce obesity-related insulin resistance and/or hypertension in male Wistar rats. The effects of the treatment of these two conditions with GRTon the male reproductive system were subsequently investigated. In particular, we explored the potential ameliorating effect of GRT on inflammation, OS and apoptosis under physiological and pathophysiological conditions. From converging lines of evidence, our findings suggest that GRT may have beneficial effects on metabolic risks and male reproductive functioning. GRT could attenuate OS by increasing SOD and CAT activity and reducing MDA levels, thereby acting as an antioxidant. This results in the amelioration of hormone levels and sperm function. The positive effects of GRT on male reproductive health could be due to its anti-lipidemic, anti-obesogenic, anti-hypertensive, anti-oestrogenic, anti-apoptotic and anti-oxidative effects. To the best of our knowledge, this is the very first study that investigated the implicit effects of Afriplex GRT^{TM} on male reproductive complications due to obesity-related insulin resistance and/or hypertension. The current findings show some of the specific properties of Afriplex GRT^{TM} on male reproductive function to be anti-oestrogenic and anti-oxidative.

In this study, in addition to elevated arterial BP, DIO with HCD is associated with changes in metabolic parameters, such as weight gain, increased adiposity index, high IL-1β secretion and a reduction in glucose tolerance. Therefore, we were successful at inducing obesity-related insulin resistance and/or hypertension by exposing male Wistar rats to different diets. These animals presented with typical MetS features, which result in the development of OS and inflammation, and the inhibition of apoptosis. These mechanisms were mainly linked to testicular and sperm dysfunction. Furthermore, it was important to identify therapeutic compounds capable of modulating these metabolic disorders in order to reduce or reverse these associated pathophysiological mechanisms and restore male reproductive health. The main findings of this study were that co-treatment with GRT counteracted the detrimental effects of both DIO-associated insulin resistance and hypertension on OS, apoptosis, hormonal levels and sperm functional parameters. The dietary GRT treatment could serve as protection against the damage caused by LPO due to OS through its influence on antioxidant enzyme activities. The improvement of antioxidant enzyme activities in DIO insulin resistant and hypertensive rats was intended to overcome the effect of ROS on intracellular pathways including apoptosis, PKB and AMPK. Treatment with GRT was able to stimulate caspase 7 and PARP; subsequently, sperm function parameters were restored. However, the effects of GRT

on blood glucose levels, AMPK and PKB were limited to both insulin resistant and hypertensive rats. In addition, we found that the impact of GRT treatment was dependent on the physiological status of the animals. Interestingly, in some instances, GRT treatment negatively affected certain parameters of physiological normal animals, while it had a positive effect on the same parameters in obese animals showing signs of insulin resistance and/or hypertension. Thus, GRT treatment can be therapeutic when used by obese patients to prevent insulin resistance, HT and the associated complications on male reproductive health.

6.1 Strengths and limitations

We acknowledge several limitations inherent to our study, including the lack of follow-up assessments over time, a small sample size and a resource-constrained research setting. Lastly, our findings are not necessarily generalizable to other animal models or humans. However, the strength of our study lies in the novelty of our findings (anti-oxidative and anti-oestrogenic potential of GRT), the inclusion of a control group, the assessment of multiple outcomes in one group, and use of standardized green rooibos extract. Future studies would do well to elucidate the mechanisms behind our findings by respecting the directions below.

6.2 Recommendations for future studies

In keeping with our study limitations, there are a number of recommendations for future studies based on our findings. It is advised that future studies should use larger sample sizes and make use of advanced techniques to a) further investigate DIO associated with insulin resistance and HT; b) clarify pathophysiological mechanisms that link MetS features and male reproductive dysfunction and properties of GRT treatment directly to male reproductive function. These suggestions could be used to advance the current knowledge, which could also be extended to clinical research. Furthermore, some of the following points should be included in future studies:

- Extend the period of DIO, thereby allowing animals to develop a more chronic form of insulin resistance and hypertension
- Extend the GRT administration period and use different doses of GRT (lower and higher than what was used in current study)
- Evaluate a wide range of intracellular signalling molecules including IRS, GLUT8 and GLUT3

- Measure leptin levels in serum and tissue in order to monitor food intake
- Determine insulin levels in order to calculate a homeostatic model assessment index
- Evaluate serum and testicular lipid profiles, namely high-density lipoprotein, low-density lipoprotein, total cholesterol and triglycerides, as well as aromatase enzymes, for evaluating androgen biosynthesis in order to provide insight into male reproductive function
- Measure pro-inflammatory cytokine and anti-inflammatory cytokines in the serum and testicular tissue
- Measure ROS production, glutathione peroxidase and redox potential in the testis and spermatozoa to elucidate the antioxidant effect of GRT
- Investigate DNA fragmentation for extending knowledge on sperm function during *in vitro* fertilization
- Perform both *in vivo* and *in vitro* studies in order to translate the finding into clinical settings
- Use a data analysis with correlation for understanding the relationship between variables

6.3 Conclusions

DIO due to the HCD predisposes an animal or human to the development of insulin resistance and or hypertension. These metabolic disorders affect male reproductive function and cause testicular oxidative stress, hormone dysregulation and impaired epididymal sperm quality and function in particular. GRT may have a beneficial effect on male reproductive function, attributable in part to its potential antioxidant activity, which has anti-oestrogenic effects. Our findings support the use of GRT as an alternative therapeutic treatment under pathological conditions. This study sheds more light on the disease-causing mechanisms of the chosen non-communicable disease models on the male reproductive system and on a possible treatment or supplementation that may target any of the observed phenotypic changes. It furthermore provides insight into the pharmacological effects of GRT in the treatment of pathophysiological changes that occur in DIO associated with insulin resistance and/or hypertension. These findings will hopefully ignite further research in the clinical setting related to the GRT and could possibly lead to the development of new drugs from this compound.

Research outputs

Conference presentation

Manirafasha C, Smit SE, Huisamen B, Aboua YP, Du Plessis SS. 2018. Protective effects of Afriplex GRT extract on male reproductive parameters in an obesity-induced pre-diabetic rat model. Conference of Biomedical and Natural Sciences and Therapeutics, 7–10 OCTOBER, Stellenbosch, SA.

REFERENCES

Adedara, I.A., Alake, S.E., Adeyemo, M.O., Olajide, L.O., Ajibade, T.O. & Farombi, E.O. 2018. Taurine enhances spermatogenic function and antioxidant defense mechanisms in testes and epididymis of L-NAME-induced hypertensive rats. *Biomedicine and Pharmacotherapy*. 97:181–189.

Agarwal, A., Nallella, K.P., Allamaneni, S.S.R. & Said, T.M. 2004. Role of antioxidants in treatment of male infertility: An overview of the literature. *Reproductive BioMedicine Online*. 8(6):616–627.

Agarwal, A., Mahfouz, R.Z., Sharma, R.K., Sarkar, O., Mangrola, D. & Mathur, P.P. 2009. Potential biological role of poly (ADP-ribose) polymerase (PARP) in male gametes. *Reproductive Biology and Endocrinology*. 7:1–20.

Agarwal, A., Virk, G., Ong, C. & du Plessis, S.S. 2014. Effect of Oxidative Stress on Male Reproduction. *The World Journal of Men's Health*. 32(1):1.

Agarwal, A., Mulgund, A., Hamada, A. & Chyatte, M.R. 2015. A unique view on male infertility around the globe. *Reproductive Biology and Endocrinology*. 13(1):1–9.

Aitken, M. 2016. *Medicines Use and Spending in the U.S.* [Online], Available: www.theimsinstitute.org.

Akagashi, K., Itoh, N., Kumamoto, Y., Tsukamoto, T., Suzuki, T. & Ohta, Y. 1996. Hypertensive changes in intratesticular arteries impair spermatogenesis of the stroke-prone spontaneously hypertensive rat. *Journal of andrology*. 17(4):367–74.

Akinyemi, A.J., Adedara, I.A., Thome, G.R., Morsch, V.M., Rovani, M.T., Mujica, L.K.S. & Duarte, T. 2015. Dietary supplementation of ginger and turmeric improves reproductive function in hypertensive male rats. *Toxicology Reports*. 2:1357–1366.

Alves, M.G., Martins, A.D., Rato, L., Moreira, P.I., Socorro, S. & Oliveira, P.F. 2013. Molecular mechanisms beyond glucose transport in diabetes-related male infertility. *Biochimica et Biophysica Acta - Molecular Basis of Disease*. 1832(5):626–635.

Alves, M.G., Dias, T.R., Cavaco, J.E., Rato, L., Oliveira, P.F., Lopes, G. & Socorro, S. 2013. High-energy diets may induce a pre-diabetic state altering testicular glycolytic metabolic profile and male reproductive parameters. *Andrology*. 1(3):495–504.

American Diabetes Association, A.D. 2010. Diagnosis and classification of diabetes mellitus.

Diabetes care. 33(1):S62-S69.

Anheim, M., Echaniz-Laguna, A., Rey, D. & Tranchant, C. 2006. Neuropathie trigéminale motrice pure révélée par un syndrome algo-dysfonctionnel de l'appareil manducateur chez une patiente co-infectée par le VIH et le VHC. *Revue Neurologique*. 162(1):92–94.

Appari, M., Channon, K.M. & McNeill, E. 2017. Metabolic regulation of adipose tissue macrophage (ATM) function in obesity and diabetes. *Antioxidants & Redox Signaling*. 29(3):297-312.

Aprioku, J.S. 2013. Pharmacology of free radicals and the impact of reactive oxygen species on the testis. *Journal of Reproduction and Infertility*. 14(4):158–172.

Awoniyi, D.O., Aboua, Y.G., Marnewick, J. & Brooks, N. 2012. The Effects of Rooibos (*Aspalathus linearis)*, Green Tea (*Camellia sinensis*) and Commercial Rooibos and Green Tea Supplements on Epididymal Sperm in Oxidative Stress-induced Rats. *Phytotherpy Research.* 26(8):1231-239.

Ayeleso, A., Brooks, N. & Oguntibeju, O. 2014. Modulation of antioxidant status in streptozotocin-induced diabetic male wistar rats following intake of red palm oil and/or rooibos. *Asian Pacific Journal of Tropical Medicine*. 7(7):536–544.

Azu, O.O. 2015. Testicular morphology in spontaneously hypertensive rat model: Oxidant status and stereological implications. *Andrologia*. 47(2):123–137.

Bader, M. & Ganten, D. 2008. Update on tissue renin-angiotensin systems. *Journal Molecular Medicine*. 86(6):615-621.

Banerjee, S., Tsutsui, K. & Chaturvedi, C.M. 2016. Apoptosis-mediated testicular alteration in Japanese quail (Coturnix coturnix japonica) in response to temporal phase relation of serotonergic and dopaminergic oscillations. *The Journal of Experimental Biology*. 219(10):1476–1487.

Barbosa-da-Silva, S., Sarmento, I.B., Bargut, T.C.L., Souza-Mello, V., Aguila, M.B. & Mandarim-de-Lacerda, C.A. 2014. Animal Models of Nutritional Induction of Type 2 Diabetes Mellitus. *International Journal of Morphology*.32(1): 1-72

Barksdale, J.D. & Gardner, S.E. 1999. The impact of first-line antihypertensive drugs on erectile dysfunction. *Pharmacotherapy*.19(5):573–5781.

Baumhäkel, M., Schlimmer, N. & Böhm, M. 2008. Effect of irbesartan on erectile function in patients with hypertension and metabolic syndrome. *International Journal of Impotence Research*. 20(5):493–500.

Bechara, G.R., De Souza, D.B., Simoes, M., Felix-Patrício, B., Medeiros, J.L., Costa, W.S., Sampaio, F.J.B. 2015. Testicular Morphology and Spermatozoid Parameters in Spontaneously Hypertensive Rats Treated with Enalapril. *Journal of Urology*. 194(5):1498–1503.

Becker, A.J., Ückert, S., Stief, C.G., Truss, M.C., Machtens, S., Scheller, F.,…Hartmann, U. 2001. Possible role of bradykinin and angiotensin II in the regulation of penile erection and detumescence. *Urology*. 57(1):193–198.

Bejarano, I., Rodríguez, A.B. & Pariente, J.A. 2018. Apoptosis Is a Demanding Selective Tool During the Development of Fetal Male Germ Cells. *Frontiers in Cell and Developmental Biology*. 6:1–7.

Beltrán-Debón, R., Rull, A., Rodríguez-Sanabria, F., Iswaldi, I., Herranz-López, M., Aragonès, G., …Alonso-Villaverde, C. 2011. Continuous administration of polyphenols from aqueous rooibos (Aspalathus linearis) extract ameliorates dietary-induced metabolic disturbances in hyperlipidemic mice. *Phytomedicine*. 18(5):414–424.

Berdja, S., Smail, L., Saka, B., Neggazi, S., Haffaf, E.M., Benazzoug, Y.,..Boudarene. 2016. Glucotoxicity induced oxidative stress and inflammation in vivo and in vitro in psammomys obesus: Involvement of aqueous extract of brassica rapa rapifera. *Evidence-based Complementary and Alternative Medicine*. 1-14.

Berridge, M.J. 2014. Module 2: Cell Signalling Pathways. *Cell Signalling Biology*. 6:1–138.

Bertoldo, M.J., Faure, M., Dupont, J. & Froment, P. 2015. AMPK: A master energy regulator for gonadal function. *Frontiers in Neuroscience*. 9:1–11.

Boura-Halfon, S. & Zick, Y. 2009. Phosphorylation of IRS proteins, insulin action, and insulin resistance. *AJP: Endocrinology and Metabolism*. 296(4):E581–E591.

Buettner, R., Parhofer, K.G., Woenckhaus, M., Wrede, C.E., Kunz-Schughart, L.A., Schölmerich, J. & Bollheimer, L.C. 2006. Defining high-fat-diet rat models: Metabolic and molecular effects of different fat types. *Journal of Molecular Endocrinology*. 36(3):485–501.

Cai, H., Griendling, K.K. & Harrison, D.G. 2003. The vascular NAD(P)H oxidases as therapeutic targets in cardiovascular diseases. *Trends Pharmacological Sciences*. 24 471–478.

Campos-Silva, P., Furriel, A., Costa, W.S., Sampaio, F.J.B. & Gregório, B.M. 2015. Metabolic and testicular effects of the long-term administration of different high-fat diets in adult rats. *International Brazilian Journal Urology*. 41(3):569–575.

Celik-Ozenci, C. & Tasatargil, A. 2013. Role of poly(ADP-ribose) polymerases in male reproduction.

Spermatogenesis. 3(2):e24194-e24198.

Chaitanya, G.V., Alexander, J.S. & Babu, P.P. 2010. PARP-1 cleavage fragments: Signatures of cell-death proteases in neurodegeneration. *Cell Communication and Signaling*. 8(1):31.

Chandra, A., Neeland, I.J., Berry, J.D., Ayers, C.R., Rohatgi, A., Das, S.R., Khera, A., McGuire, D.K., et al. 2014. The relationship of body mass and fat distribution with incident hypertension: Observations from the dallas heart study. *Journal of the American College of Cardiology*. 64(10):997–1002.

Cheshenko, K., Pakdel, F., Segner, H., Kah, O. & Eggen, R.I.L. 2008. Interference of endocrine disrupting chemicals with aromatase CYP19 expression or activity, and consequences for reproduction of teleost fish. *General and Comparative Endocrinology*.155(1):31-62.

Cheung, B.M.Y. & Li, C. 2012. Diabetes and hypertension: Is there a common metabolic pathway? *Current Atherosclerosis Reports*. 14(2):160–166.

Codella, R., Terruzzi, I. & Luzi, L. 2017. Sugars, exercise and health. *Journal of Affective Disorders*. 224:76–86.

Cooper, T.G., Noonan, E., von Eckardstein, S., Auger, J., Baker, H.W.G., Behre, H.M., Haugen, T.B., Kruger, T., et al. 2009. World Health Organization reference values for human semen characteristics. *Human Reproduction Update*. 16(3):231–245.

Courts, F.L. & Williamson, G. 2009. The C-glycosyl flavonoid, aspalathin, is absorbed, methylated and glucuronidated intact in humans. *Molecular Nutrition and Food Research*. 53(9):1104–1111.

Craig, J.R., Jenkins, T.G., Carrell, D.T. & Hotaling, J.M. 2017. Obesity, male infertility, and the sperm epigenome. *Fertility and Sterility*. 107(4):848–859.

D'Alessandro, M.E., Selenscig, D., Illesca, P., Chicco, A. & Lombardo, Y.B. 2015. Time course of adipose tissue dysfunction associated with antioxidant defense, inflammatory cytokines and oxidative stress in dyslipemic insulin resistant rats. *Food and Function*. 6(4):1299–1309.

De Grava Kempinas, W. & Klinefelter, G.R. 2014. Interpreting histopathology in the epididymis. *Spermatogenesis*. 4(2):e979114.

De Luca, C., Olefsky, J.M., Weiss, L., Zeira, M., Reich, S., Slavin, S., Raz, I. & Gallily, R. 2009. Inflammation and Insulin Resistance. *Federation of European Biochemical Societies,letters.* 582(1):97–105.

Di Meo, S., Reed, T.T., Venditti, P. & Victor, V.M. 2016. Role of ROS and RNS Sources in Physiological and Pathological Conditions. *Oxidative Medicine and Cellular Longevity*. 2016:1245049.

Dias, T.R., Alves, M.G., Silva, B.M. & Oliveira, P.F. 2014. Sperm glucose transport and metabolism in diabetic individuals. *Molecular and Cellular Endocrinology*. 396(1–2):37–45.

Dludla, P. V., Muller, C.J.F., Louw, J., Joubert, E., Salie, R., Opoku, A.R. & Johnson, R. 2014. The cardioprotective effect of an aqueous extract of fermented rooibos (Aspalathus linearis) on cultured cardiomyocytes derived from diabetic rats. *Phytomedicine*. 21(5):595–601.

Dockery, F., Bulpitt, C.J., Donaldson, M., Fernandez, S. & Rajkumar, C. 2003. The Relationship between Androgens and Arterial Stiffness in Older Men. *Journal of the American Geriatrics Society*. 51(11):1627–1632.

Dong, Q. & Hardy, M.P. 2003. Leydig Cell Function in Man: Male Hypogonadism. *Basic Clinical and Therapeutic Principles*. 396:23-43.

Dupont, J., Reverchon, M., Bertoldo, M.J. & Froment, P. 2014. Nutritional signals and reproduction. *Molecular and Cellular Endocrinology*. 382(1):527–537.

Durairajanayagam, D. 2018. Lifestyle causes of male infertility. *Arab Journal of Urology*. 16(1):10–20.

Du Plessis, S.S., Cabler, S., McAlister, D.A., Sabanegh, E. & Agarwal, A. 2010. The effect of obesity on sperm disorders and male infertility. *Nature Reviews Urology*. 7(3):153–161.

Du Toit, E.F., Smith, W., Muller, C., Strijdom, H., Woodiwiss, A.J., Norton, G.R. & Lochner, A. 2008. Myocardial susceptibility to ischemic-reperfusion injury in a prediabetic model of dietary-induced obesity. *American journal of physiology. Heart and circulatory physiology*. 294(5):H2336-H2343.

Eisenberg, M.L., Kim, S., Chen, Z., Sundaram, R., Schisterman, E.F. & Buck Louis, G.M. 2014. The relationship between male BMI and waist circumference on semen quality: Data from the LIFE study. *Human Reproduction*. 29(2):193–200.

Eladak, S., Moison, D., Guerquin, M.J., Matilionyte, G., Kilcoyne, K., N'Tumba-Byn, T., Messiaen, S., Deceuninck, Y. 2018. Effects of environmental Bisphenol A exposures on germ cell development and Leydig cell function in the human fetal testis. *Plos One*. 13(1):e0191934.

Ellerby, L.M. & Bredesen, D.E. 2000. Measurement of Cellular Oxidation, Reactive Oxygen Species, and Antioxidant Enzymes during Apoptosis. *Methods Enzymology*. 322(1996):413–421.

Elmore, S. 2007. Apoptosis: A Review of Programmed Cell Death. *Technology patology*. 35(4):495–516.

Filipponi, D. & Feil, R. 2009. Perturbation of genomic imprinting in oligozoospermia. *Epigenetics*. 4(1):27–30.

Fischer, S., MacLean, A.A., Liu, M., Kalirai, B. & Keshavjee, S. 2000. Inhibition of angiotensin-converting enzyme by captopril: A novel approach to reduce ischemia-reperfusion injury after lung transplantation. *Journal of Thoracic and Cardiovascular Surgery*. 120(3):573–580.

Foëx, P. & Sear, J.W. 2004. Hypertension: Pathophysiology and treatment. *Continuing Education in Anaesthesia, Critical Care and Pain*. 4(3):71–75.

Fogari, R., Corradi, L., Poletti, L., Zoppi, A., Lusardi, P. & Malamani, G.D. 1996. *Sexual activity in hypertensive males treated with lisinopril or atenolol:* A cross-over study. *American Journal of Hypertension*. 6:151-204.

Fogari, R., Preti, P., Zoppi, A., Fogari, E., Rinaldi, A., Corradi, L. & Mugellini, A. 2005. Serum Testosterone Levels and Arterial Blood Pressure in the Elderly. *Hypertension Research*. 28(8):625–630.

Franke, F.E., Pauls, K., Metzger, R., Danilov, S.M., Sharpe, R. & Rajpert-De Meyts, E. 2003. Angiotensin I-converting enzyme and potential substrates in human testis and testicular tumours. *Acta pathologica, microbiologica, et immunologica Scandinavic*a. 111(1):234-244.

Galardo, M.N., Riera, M.F., Pellizzari, E.H., Cigorraga, S.B. & Meroni, S.B. 2007. The AMP-activated protein kinase activator, 5-aminoimidazole-4-carboxamide-1-b-D-ribonucleoside, regulates lactate production in rat Sertoli cells. *Journal of Molecular Endocrinology*. 39(3–4):279–288.

Giles, T. D. *et al.* (2009) 'Definition and Classification of Hypertension: An Update. *Clinical Hypertension*. 11(11):611–614.

Grad, I., Mastalerz-Migas, A. & Kiliš-Pstrusińska, K. 2015. Factors associated with knowledge of hypertension among adolescents: Implications for preventive education programs in primary care. BMC Public Health. 15(1):1–8.

Grossmann, M., Tang Fui, M. & Dupuis, P. 2014. Lowered testosterone in male obesity: Mechanisms, morbidity and management. *Asian Journal of Andrology*. 16(2):223.

Guo, D., Li, S., Behr, B. & Eisenberg, M.L. 2017. Hypertension and Male Fertility. *The world journal of men's health*. 35(2):59–64.

Hall, J., Juncos, L., Wang, Z., Hall, M., do Carmo, J. & Da Silva, A. 2014. Obesity, hypertension, and chronic kidney disease. *International Journal of Nephrology and Renovascular Disease*. 7:75-88.

Hall, J.E., Do Carmo, J.M., Da Silva, A.A., Wang, Z. & Hall, M.E. 2015. Obesity-Induced Hypertension: Interaction of Neurohumoral and Renal Mechanisms. *Circulation Research*. 116(6):991–1006.

Ham, S., Meachem, S.J., Choong, C.S., Charles, A.K., Baynam, G.S., Jones, T.W., Samarajeewa, N.U., Simpson, E.R.. 2013. Overexpression of aromatase associated with loss of heterozygosity of the STK11 gene accounts for prepubertal gynecomastia in boys with peutz-Jeghers syndrome. *Journal of Clinical Endocrinology and Metabolism*. 98(12): E1979-E1987.

Hamada, A., Esteves, S.C. & Agarwal, A. 2011. Unexplained male infertility. *Human Andrology*. 1(1):2–16.

Hamden, K., Carreau, S., Jamoussi, K., Miladi, S., Lajmi, S., Aloulou, D., Ayadi, F. & Elfeki, A. 2009. 1Alpha,25 dihydroxyvitamin D3: therapeutic and preventive effects against oxidative stress, hepatic, pancreatic and renal injury in alloxan-induced diabetes in rats. *Journal of nutritional science and vitaminology*. 55(3):215–22.

Hammiche, F., Laven, J.S.E., Twigt, J.M., Boellaard, W.P.A., Steegers, E.A.P. & Steegers-Theunissen, R.P. 2012. Body mass index and central adiposity are associated with sperm quality in men of subfertile couples. *Human Reproduction*. 27(8):2365–2372.

Hardie, D.G. 2017. AMP-activated protein kinase : maintaining energy homeostasis at the cellular and whole body levels. M*olecular Cell Biology*. 66:31–55.

Hardie, D.G., Ross, F.A. & Hawley, S.A. 2012. AMPK: a nutrient and energy sensor that maintains energy homeostasis', *Nature Reviews Molecular Cell Biology*. 13(4):251–262.

Hermida, R.C., Ayala, D.E., Fernández, J.R., Mojón, A. & Smolensky, M.H. 2018. Hypertension: New perspective on its definition and clinical management by bedtime therapy substantially reduces cardiovascular disease risk. *European Journal of Clinical Investigation*. 48(5):1–12.

Hilborn, E., Stål, O. & Jansson, A. 2015. Estrogen and androgen-converting enzymes 17β-hydroxysteroid dehydrogenase and their involvement in cancer: with a special focus on 17β-hydroxysteroid dehydrogenase type 1, 2, and breast cancer. *Oncotarget*. 8(18):30552–30562.

Hong, I.S., Lee, H.Y. & Kim, H.P. 2014. Anti-oxidative effects of Rooibos tea (Aspalathus linearis) on immobilization-induced oxidative stress in rat brain. *PLoS ONE*. 9(1):1–9.

Hruby, A. & Hu, F.B. 2016. The Epidemiology of Obesity: A Big Picture. *Pharmacoeconomics*. 33(7):673-689.

Huisamen, B., Genis, A., Marais, E. & Lochner, A. 2011. Pre-treatment with a DPP-4 Inhibitor is Infarct Sparing in Hearts from Obese, Pre-diabetic Rats. *Cardiovascular Drugs and Therapy*. 25(1):13–20.

Huisamen, B., George, C., Dietrich, D. & Genade, S. 2013. Cardioprotective and anti-hypertensive effects of Prosopis glandulosa in rat models of pre-diabetes : cardiovascular topics. *Cardiovascular Journal Of Africa*. 24(2):10–16.

Inhorn, M.C. & Patrizio, P. 2015. Infertility around the globe: New thinking on gender, reproductive technologies and global movements in the 21st century. *Human Reproduction Update*. 21(4):411–426.

Jaman, M., Cowling, R., Haynes, R., Kruger, F. & Pierce, S. 1981. *South African national scientific programmes report no 53: A bibliography of fynbos ecology*. [Online], Available: https://researchspace.csir.co.za/dspace/handle/10204/2309.

Joubert, E. 1996. HPLC quantification of the dihydrochalcones, aspalathin and nothofagin in rooibos tea (Aspalathus linearis) as affected by processing. *Food Chemistry*. *Elsevier*. 55(4):403–411.

Joubert, E. & De Beer, D. 2011. Rooibos (Aspalathus linearis) beyond the farm gate : From herbal tea to potential phytopharmaceutical. *South African Journal of Botany*. 77(4):869–886.

Joubert, E., Viljoen, M., De Beer, D., Malherbe, C.J., Brand, D.J. & Manley, M. 2010. Use of green rooibos (Aspalathus linearis) extract and water-soluble nanomicelles of green rooibos extract encapsulated with ascorbic acid for enhanced aspalathin content in ready-to-drink iced teas. *Journal of Agricultural and Food Chemistry*. 58(20):10965–10971.

Jung, U. & Choi, M.-S. 2014. Obesity and Its Metabolic Complications: The Role of Adipokines and the Relationship between Obesity, Inflammation, Insulin Resistance, Dyslipidemia and Nonalcoholic Fatty Liver Disease. *International Journal of Molecular Sciences*. 15(4):6184–6223.

Jungwirth, A., Diemer, T., Dohle, G.R., Giwercman, A., Kopa, Z., Krausz, C. & Turnaye, H. 2012. Male Infertility. *European Urology*. 62(2):324–332.

Kamakura, R., Son, M.J., De Beer, D., Joubert, E., Miura, Y. & Yagasaki, K. 2015. Antidiabetic effect of green rooibos (Aspalathus linearis) extract in cultured cells and type 2 diabetic model KK-Ay mice. *Cytotechnology*. 67(4):699–710.

Kant, K., Graubard, I. & ATchison, A. 2009. Intakes of plain water, moisture in foods and beverages, and total water in the adult US population—nutritional, meal pattern, and body weight correlates: National Health and Nutrition Examination Surveys. *American journal clinical nutrition*. 90(2):655–663.

Kanu, S., Okonkwo, O.J. & Dakora, F.D. 2014. Aspalathus linearis (Rooibos tea) as potential phytoremediation agent: A review on tolerance mechanisms for aluminum uptake. *Environmental Reviews*. 21(2):85-92.

Kasturi, S.S., Tannir, J. & Brannigan, R.E. 2008. The metabolic syndrome and male infertility. *Journal of Andrology*. 29(3):251–259.

Kasum, M. 2016. Influence of Male Obesity on Fertility. *Acta Clinica Croatica*. 301–308.

Katib, A. 2015. Mechanisms linking obesity to male infertility. *Central European Journal of Urology*. 68:79–85.

Kelly, T., Yang, W., Chen, C., Reynolds, K. & He, J. 2008. Global burden of obesity in 2005 and projections to 2030. 1431–1437.

Khan, S.A., Damanhouri, G., Ali, A., Khan, S.A., Khan, A., Bakillah,…Al Harbi, G. 2016. Precipitating factors and targeted therapies in combating the perils of sickle cell disease - - A special nutritional consideration. *Nutrition and Metabolism*. 13(1):1–12.

Koenen, T.B., Stienstra, R., Van Tits, L.J., Joosten, L.A.B., Van Velzen, J.F., Hijmans, A., ...Van Der Vliet, J.A. 2011. The inflammasome and caspase-1 activation: A new mechanism underlying increased inflammatory activity in human visceral adipose tissue. *Endocrinology*. 152(10):3769–3778.

Konzem, S.L., Devore, V.S. & Bauer, D.W. 2002. Controlling hypertension in patients with diabetes. *American Family Physician*. 66(7):1209–1214.

Krausz, C. 2011. Male infertility: Pathogenesis and clinical diagnosis. *Best Practice and Research: Clinical Endocrinology and Metabolism*. 25(2):271–285.

Kristanc, L. & Kreft, S. 2016. European medicinal and edible plants associated with subacute and chronic toxicity part I: Plants with carcinogenic, teratogenic and endocrine-disrupting effects. *Food and Chemical Toxicology*. 92:150–164.

Kumar, S. & Pandey, A.K. 2013. Chemistry and Biological Activities of Flavonoids : An Overview. *Scientific World Journa*l.1-16.

Kumar, N. & Singh, A.K. 2015. Trends of male factor infertility, an important cause of infertility: A review of literature. *Journal of Human Reproductive Sciences*. 8(4):191–196.

Kwok, K.H.M., Lam, K.S.L. & Xu, A. 2016. Heterogeneity of white adipose tissue: molecular basis and clinical implications. Experimental & Molecular Medicine. 48(3):e215.

Kyriazis, J., Tzanakis, I., Stylianou, K., Katsipi, I., Moisiadis, D., Papadaki, A., Mavroeidi, V., Kagia, S., et al. 2011. Low serum testosterone, arterial stiffness and mortality in male haemodialysis patients. *Nephrology Dialysis Transplantation*. 26(9):2971–2977.

Lee, Y., Mottillo, E.P. & Granneman, J.G. 2015. Adipose tissue plasticity from WAT to BAT and in between *Biochimestry Biophysic Acta*. 1842(3):358–369.

Leisegang, K., Udodong, A., Bouic, P.J.D. & Henkel, R.R. 2014. Effect of the metabolic syndrome on male reproductive function: A case-controlled pilot study. *Andrologia*. 46(2):167–176.

Lenoir, M., Serre, F., Cantin, L. & Ahmed, S.H. 2007. Intense sweetness surpasses cocaine reward. *PLoS ONE*. 2(8):e698.

Lephart, E.D. 2015. Modulation of Aromatase by Phytoestrogens. *Enzyme Research*.1 (1):2-11.

Li, H., Pham, T., Mcwhinney, B.C., Ungerer, J.P., Pretorius, C.J., Richard, D.J., Mortimer, R.H… D'emden, M.C. 2016. Sex Hormone Binding Globulin Modifies Testosterone Action and Metabolism in Prostate Cancer Cells. *International Journal of Endocrinology*. 2016:6437585.

Lidell, M.E., Betz, M.J. & Enerbäck, S. 2014. Brown adipose tissue and its therapeutic potential. *Journal of Internal Medicine*. 276(4):364–377.

Lin, T.Y., Lim, P.S. & Hung, S.C. 2018. Impact of Misclassification of Obesity by Body Mass Index on Mortality in Patients With CKD. *Kidney International Reports*. 3(2):447–455.

Liu, J., Li, R., Zhao, H. & Yin, X. 2004. Location and Ouantification of iNOS in Testis of Dahl Hypertensive Rats. *Journal of Reproduction*. 15(2):81–86.

Liu, Y.H., You, Y., Song, T., Wu, S.J. & Liu, L.Y. 2007. Impairment of endothelium-dependent relaxation of rat aortas by homocysteine thiolactone and attenuation by captopril. *Journal of Cardiovascular Pharmacology*. 50(2):155–161.

Mahajan, R. & Gajare, S. 2012. Manifestation of erectile dysfunction with adaptogenic antioxidant aphrodisiac plants. *International Journal of Pharmaceutical and Biomedical Research*. 3(1):52–68.

Mahomoodally, M.F. 2013. Traditional Medicines in Africa : An Appraisal of Ten Potent African

Medicinal Plants. *Evidence-Based Complementary and Alternative Medicine.* 1-14.

Mancini, G.B.J., Henry, G.C., Macaya, C., O'Neill, B.J., Pucillo, A.L.& Carere, R.G. 2012. Angiotensin-Converting Enzyme Inhibition With Quinapril Improves Endothelial Vasomotor Dysfunction in Patients With Coronary Artery Disease. *Circulation*. 94(3):258–265.

Maneesh, M. & Jayalekshmi, H. 2006. Role of reactive oxygen species and antioxidants on pathophysiology of male reproduction. *Indian Journal of Clinical Biochemistry*. 21(2):80–89.

Manirafasha, C. 2014. The effects of kolaviron on epididymal and testicular function in streptozotocin induced diabetic wistar rats. Masters Thesis retrieved from etd.cput.ac.za/bitstream/.../212265547_manirafasha_c_mtech_biomed_2014.pdf.

Mansour, R., El-Faissal, Y., Kamel, A., Kamal, O., Aboulserour, G., Aboulghar, M. & Fahmy, I. 2017. Increased insulin resistance in men with unexplained infertility. *Reproductive BioMedicine Online*. 35(5):571–575.

Marnewick, J.L., Rautenbach, F., Venter, I., Neethling, H., Blackhurst, D.M., Wolmarans, P. & MacHaria, M. 2011. Effects of rooibos (Aspalathus linearis) on oxidative stress and biochemical parameters in adults at risk for cardiovascular disease. *Journal of Ethnopharmacology*. 133(1):46–52.

Masek, J & Fabry, P.1959. High-fat diet and development of obesity in albino rats. *Experientia.* 15:444-445.

Matsuura, H. 2001. Recent Advances on the Nutritional Effects Associated with the Use of Garlic as a Supplement Saponins in Garlic as Modifiers of the Risk of Cardiovascular Disease 1. *The Journal of nutrition*. 131(3):1000–1005.

Mazibuko, S.E., Joubert, E., Johnson, R., Louw, J., Opoku, A.R. & Muller, C.J.F. 2015. Aspalathin improves glucose and lipid metabolism in 3T3-L1 adipocytes exposed to palmitate. *Molecular Nutrition and Food Research*. 59(11):2199–2208.

Medley, T. & Wilson, J. 2016. *Guideline for the diagnosis and management of hypertension in adults*. [Online], Available: https://www.heartfoundation.org.au/images/uploads/publications/PRO-167_Hypertension-guideline-2016_WEB.pdf.

Membrez, M., Ammon-zufferey, C., Philippe, D., Aprikian, O., Monnard, I., Macé, K. & Darimont, C. 2009. Interleukin-18 Protein Level Is Upregulated in Adipose Tissue of Obese Mice. *Obesity (Silver Spring).* 17(2):393-395.

Metallo, C.M. & Vander Heiden, M.G. 2013. Understanding metabolic regulation and its influence on cell physiology. *Molecular and Cellular Biology*. 49(3):388-98.

Metallo, C., 2015. Metabolic analysis using stable isotopes. Academic Press. *Methods in Enzymology*. 561(1): 2-386.

Miller, N., De Beer, D. & Joubert, E. 2017. Minimising variation in aspalathin content of aqueous green rooibos extract : optimising extraction and identifying critical material attributes. *Journal of the Science of Food and Agriculture*. 97(14):4937-4942.

Mishra, A., Kumar, S. & Pandey, A.K. 2013. Scientific validation of the medicinal efficacy of tinospora cordifolia. *The Scientific World Journal*. 1-8.

Mittal, P.K., Little, B., Harri, P.A., Miller, F.H., Alexander, L.F., Kalb, B. & Master, V. 2017. Role of Imaging in the Evaluation of Male Infertility. *RadioGraphics*. 37(3):837–854.

Monsees, T.K., Miska, W. & Schill, W.B. 1996. Characterization of kininases in testicular cells. *Immunopharmacology*. 32:169–171.

Morakinyo, A.O., Iranloye, B.O. & Adegoke, O.A. 2009. Antireproductive effect of calcium channel blockers on male rats. *Reproductive Medicine and Biology*. 8(3):97–102.

Mucci, N., Giorgi, G., Ceratti, S.D.P., Mucci, F. & Arcangeli, G. 2016. Anxiety, stress-related factors, and blood pressure in young adults. *Frontiers in Psychology*. 7:1–10.

Muller, C.J.F., Joubert, E., De Beer, D., Sanderson, M., Malherbe, C.J., Fey, S.J. & Louw, J. 2012. Acute assessment of an aspalathin-enriched green rooibos (Aspalathus linearis) extract with hypoglycemic potential. *Phytomedicine*. 20(1):32–39.

Muller, C.J.F., Malherbe, C.J., Chellan, N., Yagasaki, K., Miura, Y. & Joubert, E. 2018. Potential of rooibos, its major C-glucosyl flavonoids, and Z-2-(β-D-glucopyranosyloxy)-3-phenylpropenoic acid in prevention of metabolic syndrome. *Critical Reviews in Food Science and Nutrition*. 58(2):227–246.

Muraleedharan, V. & Jones, T.H. 2010. Testosterone and the metabolic syndrome. *Therapeutic Advances in Endocrinology and Metabolism*. 1(5):207–223.

Nandipati, K.C., Subramanian, S. & Agrawal, D.K. 2017. Protein kinases: mechanisms and downstream targets in inflammation-mediated obesity and insulin resistance. *Molecular and Cellular Biochemistry*. 426(1–2):27–45.

Nduhirabandi, F., Huisamen, B., Strijdom, H., Blackhurst, D. & Lochner, A. 2014. Short-term

melatonin consumption protects the heart of obese rats independent of body weight change and visceral adiposity. *Journal of Pineal Research*. 57(3):317–332.

Nduhirabandi, F., Huisamen, B., Strijdom, H., Lochner, A. & Barbara, H. 2017. Role of melatonin in glucose uptake by cardiomyocytes from insulin-resistant Wistar rats. *Cardiovascular journal of Africa*. 28(6):362–369.

Nguyen, T.M.D. 2017. Impact of 5'-amp-activated Protein Kinase on Male Gonad and Spermatozoa Functions. *Frontiers in Cell and Developmental Biology*. 5:1–9.

Nicolai, M.P.J., Liem, S.S., Both, S., Pelger, R.C.M., Putter, H., Schalij, M.J. & Elzevier, H.W. 2014. A review of the positive and negative effects of cardiovascular drugs on sexual function: A proposed table for use in clinical practice. *Netherlands Heart Journal*. 22(1):11–19.

Oh, Y. Bin, Kim, J.H., Park, B.M., Park, B.H. & Kim, S.H. 2012. Captopril intake decreases body weight gain via angiotensin-(1-7). *Peptides*. 37(1):79–85.

Okeahialam, B.N., Amadi, K. & Ameh, A.S. 2006. Effect of Lisnopril, an angiotensin converting enzyme (ACE) inhibitor on spermatogenesis in rats. *Systems Biology in Reproductive Medicine*. 52(3):209–213.

Ombelet, W. & Van Robays, J. 2015. Artificial insemination history: hurdles and milestones. *Facts, views & vision in ObGyn*. 7(2):137–43. [Online], Available: http://www.pubmedcentral.nih.gov/articlerender.fcgi?artid=4498171&tool=pmcentrez&rendertype=abstract.

Omolaoye, T.& Du Plessis, S.2018. Diabetes mellitus and male infertility. *Asian Pacific Journal of Reproduction*. 7(1):6-14.

Opuwari, C.S. & Monsees, T.K. 2014. In vivo effects of Aspalathus linearis (rooibos) on male rat reproductive functions. *Andrologia*. 46(8):867–877.

Opuwari, C.S. & Monsees, T.K. 2015. Reduced testosterone production in TM3 Leydig cells treated with Aspalathus linearis (Rooibos) or Camellia sinensis (tea). *Andrologia*.47(1):52–58.

Osborn, O., Brownell, S.E., Sanschez-Aavez, M., Salomon, D. & Gram, H. 2011. Treatment with an Interleukin 1 beta antibody improves glycemic control in diet induced obesit. 44(1):1–22.

Oskui, P.M., French, W.J., Herring, M.J., Mayeda, G.S., Burstein, S. & Kloner, R.A. 2013. Testosterone and the cardiovascular system: a comprehensive review of the clinical literature. *Journal of the American Heart Association*. 2(6):1–22.

Oyeyipo, I.P., Maartens, P.J. & du Plessis, S.S. 2015. Diet-induced obesity alters kinematics of rat spermatozoa. *Asian Pacific Journal of Reproduction*. 4(3):235–239.

Palmer, N.O., Bakos, H.W., Fullston, T. & Lane, M. 2012. Impact of obesity on male fertility, sperm function and molecular composition. *Spermatogenesis*. 2(4):253–263.

Paniagua, J.A. 2016. Nutrition, insulin resistance and dysfunctional adipose tissue determine the different components of metabolic syndrome. *World Journal of Diabetes*. 7(19):483.

Patel, A.P. 2017. Anatomy and physiology of chronic scrotal pain. *Translational Andrology and Urology*. 6(1):S51–S56.

Persson, I.A.L. 2012. The pharmacological mechanism of angiotensin-converting enzyme inhibition by green tea, Rooibos and enalaprilat - A study on enzyme kinetics. *Phytotherapy Research*. 26(4):517–521.

Persson, I.A.-L., Josefsson, M., Persson, K. & Andersson, R.G.G. 2006. Tea flavanols inhibit angiotensin-converting enzyme activity and increase nitric oxide production in human endothelial cells. *Journal of Pharmacy and Pharmacology*. 58(8):1139–1144.

Phaniendra, A., Jestadi, D.B. & Periyasamy, L. 2015. Free Radicals: Properties, Sources, Targets, and Their Implication in Various Diseases. *Indian Journal of Clinical Biochemistry*. 30(1):11–26.

Rani G, P., Sellappan, S. & Janivara Parameswaraiah, R. 2016. *Impact of arsenic(V) on testicular oxidative stress and sperm functional attributes in Swiss albino mice*. *Environmental Science and Pollution Research.* 23(18):18200-18210.

Rastogi, S., Rodriguez, J.J., Kapur, V. & Schwarz, E.R. 2005. Why do patients with heart failure suffer from erectile dysfunction? A critical review and suggestions on how to approach this problem. *International Journal of Impotence Research*. 17:S25–S36.

Rat Strains, 2012. [Online], Available: http://www.anim.med.kyoto-u.ac.jp/nbr/strains/Strains_d.aspx?StrainID=525 [2019, May 09].

Rato, L., Alves, M.G., Socorro, S., Carvalho, R.A., Cavaco, J.E. & Oliveira, P.F. 2012. Metabolic modulation induced by oestradiol and DHT in immature rat Sertoli cells cultured *in vitro*. *Bioscience Reports*. 32(1):61–69.

Rato, L., Alves, M.G., Cavaco, J.E. & Oliveira, P.F. 2014. High-energy diets: A threat for male fertility? *Obesity Reviews*. 15(12):996–1007.

Redón, J., Oliva, M.R., Tormos, C., Giner, V., Chaves, J., Iradi, A. & Sáez, G.T. 2003. Antioxidant activities and oxidative stress byproducts in human hypertension. *Hypertension*. 41(5):1096–1101.

Rice, S., Elia, A., Jawad, Z., Pellatt, L. & Mason, H.D. 2013. Metformin Inhibits Follicle-Stimulating Hormone (FSH) Action in Human Granulosa Cells: Relevance to Polycystic Ovary Syndrome. *The Journal of Clinical Endocrinology & Metabolism*. 98(9):E1491–E1500.

Rockhold, R. 2002. Cardiovascular Toxicity of Anabolic Steroids. *Annual Review of Pharmacology and Toxicology*. 33(1):497–520.

Rolo, A.P. & Palmeira, C.M. 2006. Diabetes and mitochondrial function: Role of hyperglycemia and oxidative stress. *Toxicology and Applied Pharmacology*. 212(2):167–178.

Rooibos tea - Cape Point Press, Available: https://capepointpress.com/iced-rooibos-tea/ [2019, May 09].

Ross, F.A., MacKintosh, C. & Hardie, D.G. 2016. AMP-activated protein kinase: a cellular energy sensor that comes in 12 flavours. *Federation of European Biochemical Societies Journal*. 283:2987–3001.

Rossi, F., Ferraresi, A., Romagni, P., Silvestroni, L. & Santiemma, V. 2002. Angiotensin II stimulates contraction and growth of testicular peritubular myoid cells in vitro. *Endocrinology*. 143(8):3096–3104.

Salie, R., Huisamen, B. & Lochner, A. 2014. High carbohydrate and high fat diets protect the heart against ischaemia / reperfusion injury. *Cardiovascular Diabetology*. 13(109):1–12.

Sanderson, M., Mazibuko, S.E., Joubert, E., De Beer, D., Johnson, R., Pheiffer, C., Louw, J. & Muller, C.J.F. 2014. Effects of fermented rooibos (*Aspalathus linearis*) on adipocyte differentiation. *Phytomedicine*. 21(2):109–117.

Schisterman, E.F., Mumford, S.L., Chen, Z., Browne, R.W., Barr, D.B., Kim, S. & Louis, G.M.B. 2014. Lipid Concentrations and Semen Quality: The LIFE Study. *Andrology*. 2(3):408–415.

Scribner, A.W., Loscalzo, J. & Napoli, C. 2003. The effect of angiotensin-converting enzyme inhibition on endothelial function and oxidant stress. *European Journal of Pharmacology*. 482(1–3):95–99.

Sermondade, N., Faure, C., Fezeu, L., Shayeb, A.G., Bonde, J.P., Jensen, T.K,…Van Wely, M. 2013. BMI in relation to sperm count: An updated systematic review and collaborative meta-analysis. *Human Reproduction Update*. 19(3):221–231.

Shi, G.J., Li, Z.M., Zheng, J., Chen, J., Han, X.X., Wu, J… Chang, Q. 2017. Diabetes associated with male reproductive system damages: Onset of presentation, pathophysiological mechanisms and drug intervention. *Biomedicine and Pharmacotherapy*. 90:562–574.

Siegel, J.A., Young, L.A., Neiss, M.B., Samuels, M.H., Roselli, C.E. & Janowsky, J.S. 2008. Estrogen, Testosterone, and Sequential Movement in Men. *Behavioral Neuroscience*. 122(5):955–962.

Siems, W.E., Maul, B., Wiesner, B., Becker, M., Walther, T., Rothe, L. & Winkler, A. 2003. Effects of kinins on mammalian spermatozoa and the impact of peptidolytic enzymes. *Andrologia*. 35:44–54.

Silverman, M.N. & Deuster, P.A. 2014. Biological mechanisms underlying the role of physical fitness in health and resilience. *Interface Focus*. 4(5):20140040.

Simon, A. 2014. Cholesterol Metabolism and Immunity. *The New England Journal of Medicine*. 371(20):1933-1935.

Sishi, B., Loos, B., Ellis, B., Smith, W., Du Toit, E.F. & Engelbrecht, A.M. 2011. Diet-induced obesity alters signalling pathways and induces atrophy and apoptosis in skeletal muscle in a prediabetic rat model. *Experimental Physiology*. 96(2):179–193.

Skakkebaek, N.E., Rajpert-De Meyts, E., Buck Louis, G.M., Toppari, J., Andersson, A.-M., Eisenberg, M.L…, Jorgensen, N. 2015. Male Reproductive Disorders and Fertility Trends: Influences of Environment and Genetic Susceptibility. *Physiological Reviews*. 96(1):55–97.

Smith, G.D. 2016. A fatter, healthier but more unequal world. *The Lancet*. 387(10026):1349–1350.

Son, M.J., Minakawa, M., Miura, Y. & Yagasaki, K. 2013. Aspalathin improves hyperglycemia and glucose intolerance in obese diabetic ob/ob mice. *European Journal of Nutrition*. 52(6):1607–1619.

Stern, M.P., Williams, K. & Haffner, S.M. 2002. Identification of persons at high risk for type 2 diabetes mellitus: do we need the oral glucose tolerance test? *Annals of Internal Medicine*.136(8):575–581.

Svartberg, J., von Muhlen, D., Schirmer, H., Barrett-Connor, E., Sundfjord, J. & Jorde, R. 2004. Association of endogenous testosterone with blood pressure and left ventricular mass in men. The Tromso Study. *European Journal of Endocrinology*. 150(1):65–71.

Taheri, E., Djalali, M., Saedisomeolia, A., Moghadam, A.M., Djazayeri, A. & Qorbani, M. 2012. The relationship between the activates of antioxidant enzymes in red blood cells and body mass

index in Iranian type 2 diabetes and healthy subjects. *Journal of Diabetes and Metabolic Disorders*. 11(1):1–5.

Traish, A.M., Saad, F., Feeley, R.J. & Guay, A. 2009. The dark side of testosterone deficiency: III. Cardiovascular disease. *Journal of Andrology*. 30(5):477–494.

Tremellen, K. 2008. Oxidative Stress and Male Infertility – A Clinical Perspective. *Human Reproduction Update*. 14(3):1–16.

Treml, J. & Šmejkal, K. 2016. Flavonoids as Potent Scavengers of Hydroxyl Radicals. *Comprehensive Reviews in Food Science and Food Safety*. 15(4):720–738.

Tsatsanis, C., Dermitzaki, E., Avgoustinaki, P., Malliaraki, N., Mytaras, V. & Margioris, A.N. 2015. The impact of adipose tissue-derived factors on the hypothalamic-pituitary-gonadal (HPG) axis. *Hormones*. 14(4):549–562.

Vauzour, D., Rodriguez-Mateos, A., Corona, G., Oruna-Concha, M.J. & Spencer, J.P.E. 2010. Polyphenols and human health: Prevention of disease and mechanisms of action. *Nutrients*. 2(11):1106–1131.

Verma, K. & Baniya, G.C. 2016. A comparative study of depression among infertile and fertile women. *International Journal of Research in Medical Sciences*. 4(8):3459–3465.

Vihma, V., Naukkarinen, J., Turpeinen, U., Hämäläinen, E., Kaprio, J., Rissanen, A.,…Hakkarainen, A. 2017. Metabolism of sex steroids is influenced by acquired adiposity—A study of young adult male monozygotic twin pairs. *Journal of Steroid Biochemistry and Molecular Biology*. 172:98–105.

Villaño, D., Pecorari, M., Testa, M.F., Raguzzini, A., Stalmach, A., Crozier, A., Tubili, C. & Serafini, M. 2010. Unfermented and fermented rooibos teas (Aspalathus linearis) increase plasma total antioxidant capacity in healthy humans. *Food Chemistry*. 123(3):679–683.

Van Vuuren, S. & Viljoen, A. 2011. Plant-based antimicrobial studies methods and approaches to study the interaction between natural products. *Planta Medica*. 77(11):1168–1182.

Wahlberg, A. 2016. The birth and routinization of IVF in China. *Reproductive Biomedicine and Society Online*. 2:97–107.

Walker, C.G., Zariwala, M.G., Holness, M.J. & Sugden, M.C. 2006. Diet, obesity and diabetes: a current update. *Clinical Science*. 112(2):93-111.

Weissheimer, K.V., Franci, C.R., Lucion, A.B. & Sanvitto, G.L. 2012. The role of AT1 receptor-

mediated reproductive function in renovascular hypertension in male rats. *Hormones and Behavior*. 62(1):43–49.

WHO. 2010. *WHO Laboratory Mannual for Examination and processing of human semen*. Available at : https://www.who.int/reproductivehealth/publications/infertility/9789241547789/en/.

WHO. 2017. *Non Communicable Diseases Progress Monitor 2017*. Available at: https://www.who.int/nmh/publications/ncd-progress-monitor-2017/en/.

Wiesner, J., Henschker, D., Hutchinson, D.B., Beck, E. & Jomaa, H. 2002. In vitro and in vivo synergy of fosmidomycin, a novel antimalarial drug, with clindamycin. *Antimicrobial Agents and Chemotherapy*. 46(9):2889–2894.

Wyk, B. Van & Gorelik, B. 2017. South African Journal of Botany The history and ethnobotany of Cape herbal teas. *South African Journal of Botany*. 110:18–38.

Yan, W., Mu, Y., Yu, N., Yi, T., Zhang, Y., Pang, X., Cheng, D. & Yang, J. 2015. Protective effects of metformin on reproductive function in obese male rats induced by high-fat diet. *Journal of Assisted Reproduction and Genetics*. 32(7):1097–1104.

Yanai, H., Tomono, Y., Ito, K., Furutani, N., Yoshida, H. & Tada, N. 2008. The underlying mechanisms for development of hypertension in the metabolic syndrome. *Nutrition Journal*. 7(1):1–6.

Ye, L., Li, X., Li, L., Chen, H. & Ge, R.S. 2017. Insights into the development of the adult Leydig cell lineage from stem Leydig cells. *Frontiers in Physiology*. 8:1–18.

Yoon, B.H., Kim, C.J., Romero, R., Jun, J.K., Park, K.H., Choi, S.T., Chi, J.G. & Sengupta, P. 2014. The Laboratory Rat : Relating Its Age With Human. *American journal of obstetrics and gynecology*. 4(6):624–630.

Yu, J.S.L. & Cui, W. 2016. Proliferation, survival and metabolism: the role of PI3K/AKT/mTOR signalling in pluripotency and cell fate determination. *Development*. 143(17):3050–3060.

Zegers-Hochschild, F., Adamson, G.D., Dyer, S., Racowsky, C., de Mouzon, J., Sokol, R.&Sunde, A. 2017. The International Glossary on Infertility and Fertility Care. Fertility and Sterility. 108(3):393–406.

Zhang, D.M., Jiao, R.Q. & Kong, L.D. 2017. High dietary fructose: Direct or indirect dangerous factors disturbing tissue and organ functions. *Nutrients*. 9(4):E332-E335.

Zhou, X., Seto, S.W., Chang, D., Kiat, H., Razmovski-Naumovski, V., Chan, K. & Bensoussan, A.

2016. Synergistic effects of Chinese herbal medicine: A comprehensive review of methodology and current research. *Frontiers in Pharmacology*. 7:1–16.